Department of Physics and Astronomy

An Ecosystem Approach, the Acoustic Assessment of the Northern Demersal Scalefish Fishery – Distribution, Habitat and Abundance

Sven Gastauer

**This thesis is presented for the Degree of
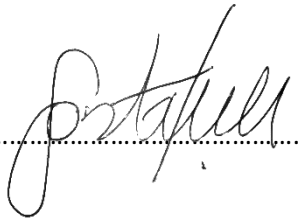Doctor of Philosophy
of
Curtin University**

July 2017

Declaration

To the best of my knowledge and belief this thesis contains no material previously published by any other person except where due acknowledgment has been made.

This thesis contains no material which has been accepted for the award of any other degree or diploma in any university.

All data collection and experiments conducted in relation to this PhD were performed according to the Australian Code of Practice for the care and use of animals for scientific purposes.

Signature   ....

Date   30/06/2017

Funk, I don't think I have anything to do with funk. I've never considered myself funky.

- *David Bowie*

I have never let my schooling interfere with my education.

- *Mark Twain*

Abstract

In order to progress towards a more ecosystem based approach in fisheries management (EBFM), it is important to develop holistic monitoring protocols. Fisheries acoustics is recognised as one of the most promising marine monitoring tools, to be used in conjunction with more traditional sampling methods, such as trawls or other biological sampling methods, to fulfil the data needs of EBFM. To work towards an improved understanding of the ecosystem, there is a need for large scale sampling programs on a temporal and spatial basis, monitoring the entire water column and habitat characteristics. Given the cost involved in running dedicated scientific survey, such a large scale data collection program is often impractical. As an alternative, fishing vessels, with acoustic equipment of scientific standards available or easily mounted can be used as opportunistic or chartered sampling platforms. Opportunistic data collection programs, take advantage of the time spent at sea by fishers. Such an undertaking bears the possibility to continuously collect data over a prolonged period of time, covering areas of commercial interest.

The present thesis can be seen as one of the first attempts to describe tropical, demersal habitats based on opportunistically collected acoustic data and catch information aboard a small (15 m) trap fishing vessel in the Northern Demersal Scalefish Fishery (NDSF). The NDSF is classified as a mixed fishery, targeting a multitude of demersal species, with two main indicator species, goldband snapper (*Pristipomoides multidens)* and red emperor (*Lutjanus sebae*). The main goal for this study was to derive indices, within selected fishing regions (where sufficient data was available), which could be of relevance to EBFM. Three fishing regions with simultaneously collected catch and acoustic data were identified. Optical recordings of the catch, facilitated the extraction of species group-specific composition and length frequency distributions for each recorded trap. Length estimates were based on pixel counting, referenced to the five cm steel meshes of the traps. Calibrated acoustic data was logged twenty-four hours a day at 38 and 120 kHz.

Abundance and biomass indices are the most common indices used in EBFM. In order to translate acoustic densities into biologically meaningful abundance or biomass estimates, a good understanding of the relationship between the acoustic reflection of an individual fish (*TS*) of a given species at a given length L *(TS-L)* is necessary. Given the sparsity of acoustic studies focusing on tropical demersal habitats, *TS-L* relationships for the observed groups had to be established. *TS-L* of red emperor was established through a combination of *ex situ*

measurements and a modelling approach. Model parameters were calibrated by the *ex situ* measurements, using a Bayesian approach. For goldband snapper, *in situ* collected ˆ value could be used in combination with catch information to establish a robust *TS-L* relationship. For the other species groups Kirchhoff Ray mode models, based on computational tomography scans of fish samples, were used to model *TS*. In a following step, the distribution, abundance and biomass of key species groups were estimated. Through the application of geostatistical methods, associated estimates of variance were described.

Other indices, which can be used to describe the distribution patterns of species groups within the selected fishing groups were proposed. Acoustic density hotspots were described through geostatistical methods. Hotspots can help us better understand key areas of biological density. Bottom habitat types were detected through clustering of acoustic bottom descriptors, providing an acoustic habitat classification indicator. Indicator species associated with each habitat cluster were detected and described. Energetic, geometric and bathymetric characteristics of fish schools were described and clustered together, to form an indicator of acoustic diversity. All of these indicators have the potential, if collected over multiple years, to track changes in resource distributions and to link those to changes in environmental or anthropogenic factors. Further, they all contain information on the spatio-temporal structure of the monitored regions, providing valuable information for improved planning and timing of dedicated survey.

As such, the present thesis has shown that useful indices can be derived from acoustic and catch information collected opportunistically aboard a small trap fishing vessel during routine operations. The major outcomes of the thesis are a novel technique to estimate *in situ TS-L* relationships, using the distribution of length and *TS* measurements, rather than grouped frequencies. Robust methods for the combination of catch information and acoustic densities in situations where no directed sampling is available have been established. Variance estimates observed within three focus fishing regions were comparable with those observed in dedicated acoustic surveys conducted in other fisheries. This similarity in variance is an indicator that the quality of biomass and abundance estimates was satisfactory. Goldband snapper has been observed in single species schools and, as a result, improved variance estimates could be established. In a final step, through the use of unsupervised statistical methods, simple indicators with the potential to gain improved insights into the distribution and structure of the fish resources and associated habitats were gained and developed.

The presented methods hold the possibility to be applied to a wide range of habitats and ecosystems. The use of fishing vessels as sampling platforms not only generates useful information, but also strengthens the mutual understanding between scientists and fishers, working together towards more stakeholder involvement in data collection programs and higher acceptance of resulting policies. If data collection programs are to be continued and the presented methods applied, the true value of the latter could be explored in more detail.

Acknowledgments

List of publications included as part of the thesis

Gastauer, S., Scoulding, B., Fässler, S.M., Benden, D.P., Parsons, M., 2016. Target strength estimates of red emperor (Lutjanus sebae) with Bayesian parameter calibration. Aquat. Living Resour. 29, 301. doi: 10.1051/alr/2016024

Gastauer, S., Scoulding, B., Parsons, M., 2017. Estimates of variability of goldband snapper target strength and biomass in three fishing regions within the Northern Demersal Scalefish Fishery (Western Australia). Fisheries Research 193, 250–262. doi:10.1016/j.fishres.2017.05.001

Gastauer, S., Scoulding, B. and Parsons, M., 2017. Towards acoustic monitoring of a mixed demersal fishery based on commercial data: The case of the Northern Demersal Scalefish Fishery (Western Australia). Fisheries Research, 195, pp.91-104. Doi:10.1016/j.fishres.2017.07.008

Gastauer S, Scoulding B, Parsons M. An Unsupervised Acoustic Description of Fish Schools and the Seabed in Three Fishing Regions Within the Northern Demersal Scalefish Fishery (NDSF, Western Australia). Acoustics Australia. 2017:1-8. doi:10.1007/s40857-017-0100-0
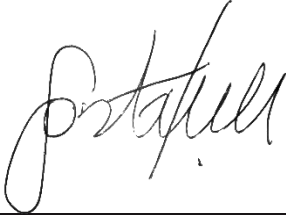
I warrant that I have obtained, where necessary, permission from the copyright owners to use any third- party copyright material reproduced in the thesis (e.g. questionnaires, artwork, unpublished letters), or to use any of my own published work (e.g. journal articles) in which the copyright is held by another party (e.g. publisher, co-author).

Statement of Contribution of Others

Gastauer, S., Scoulding, B., Fässler, S.M., Benden, D.P., Parsons, M., 2016. Target strength estimates of red emperor (Lutjanus sebae) with Bayesian parameter calibration. Aquat. Living Resour. 29, 301. doi: 10.1051/alr/2016024

Contributor	Statement of contribution*
Sven Gastauer Signature Date: 25/04/2017	Wrote the manuscript, designed the experiment, conducted experiments, developed software and conducted data analysis
Miles Parsons Signature Date: 1/06/2017	Aided experimental design, supervised development of work, helped in manuscript evaluation
Daniel P. Benden Signature	Helped in software development
Ben Scoulding Signature	Helped in data analysis and manuscript evaluation
Sascha Faessler Signature	Helped in data analysis and manuscript evaluation

Gastauer, S., Scoulding, B., Parsons, M., 2017. Estimates of variability of goldband snapper target strength and biomass in three fishing regions within the Northern Demersal Scalefish Fishery (Western Australia). Fisheries Research 193, 250–262. doi:10.1016/j.fishres.2017.05.001

Contributor	Statement of contribution*
Sven Gastauer Signature Date: 25/04/2017	Wrote the manuscript, collected data, developed software, conducted data analysis and interpretation
Miles Parsons Signature	Supervised development of work and helped in manuscript evaluation
Ben Scoulding Signature	Helped in data interpretation and manuscript evaluation

Gastauer, S., Scoulding, B. and Parsons, M., 2017. Towards acoustic monitoring of a mixed demersal fishery based on commercial data: The case of the Northern Demersal Scalefish Fishery (Western Australia). Fisheries Research, 195, pp.91-104. Doi:10.1016/j.fishres.2017.07.008

Contributor		Statement of contribution*
Sven Gastauer Signature Date: 25/04/2017		Wrote the manuscript, collected data, developed software, conducted data analysis and interpretation
Miles Parsons Signature		Supervised development of work and helped in manuscript evaluation
Ben Scoulding Signature		Helped in data interpretation and manuscript evaluation

Contributor		Statement of contribution*
Sven Gastauer Signature Date: 25/04/2017		Wrote the manuscript, collected data, developed software, conducted data analysis and interpretation
Miles Parsons Signature		Supervised development of work and helped in manuscript evaluation
Ben Scoulding Signature		Helped in data interpretation and manuscript evaluation

List of additional relevant publications by the candidate

Gastauer, S., Fässler, S.M., O'Donnell, C., Høines, Å., Jakobsen, J.A., Krysov, A.I., Smith, L., Tangen, Ø., Anthonypillai, V., Mortensen, E. Armstrong, E., Scoulding, B. 2016. The distribution of blue whiting west of the British Isles and Ireland. *Fisheries Research*, *183*, pp.32-43.

Couperus, B., **Gastauer, S.**, Fässler, S.M., Tulp, I., van der Veer, H.W. and Poos, J.J., 2016. Abundance and tidal behaviour of pelagic fish in the gateway to the Wadden Sea. *Journal of Sea Research*, *109*, pp.42-51.

Fässler, S.M., Brunel, T., **Gastauer, S**. and Burggraaf, D., 2016. Acoustic data collected on pelagic fishing vessels throughout an annual cycle: Operational framework, interpretation of observations, and future perspectives. *Fisheries Research*, *178*, pp.39-46.

Scoulding, B., **Gastauer, S.**, MacLennan, D.N., Fässler, S.M., Copland, P. and Fernandes, P.G., 2016. Effects of variable mean target strength on estimates of abundance: the case of Atlantic mackerel (Scomber scombrus). *ICES Journal of Marine Science: Journal du Conseil*, p.fsw212.

Table of Contents

Table of Figures

Table of Tables

Chapter 1

General Introduction

In recent years, there has been a transition from single stock management towards a more ecosystem based approach in fisheries management (EBFM) (Pikitch *et al.*, 2004; Trenkel *et al.*, 2011; Handegard *et al.*, 2013; Kupschus *et al.*, 2016). Any fisheries management plan, that is successful in the long-term, requires high-resolution data on the distribution and abundance of the encompassed resources (Rivoirard *et al.*, 2000; Latour *et al.*, 2003; Piet and Quirijns, 2009; Handegard *et al.*, 2013; Godø *et al.*, 2014). This can then support a sound decision making process regarding stock assessments, the definition of total allowable catch (TAC) and effort quotas (Latour *et al.*, 2003; Pikitch *et al.*, 2004; Smith *et al.*, 2007). For many remote offshore fisheries, covering extensive areas, this is a notoriously difficult task. Dedicated scientific surveys of such broad areas are often labour and financially expensive (Piet and Quirijns, 2009; Barbeaux *et al.*, 2013; Fässler *et al.*, 2016). Adequate funding for such undertakings is often limited, especially if the economic power of the fishery is low, making large-scale scientific surveys impractical. Consequently, data deficient or low-data stocks mainly rely on fisheries dependent information (e.g. market samples, catch-per-unit effort (CPUE)), sometimes complemented by small-scale scientific surveys or comparative studies (Chen *et al.*, 2003; Marko *et al.*, 2004; Sadovy and Domeier, 2005).

Following this transition towards EBFM, fisheries acoustics have been identified as one of the most promising tools to fulfil requirements of EBFM (Koslow, 2009; Trenkel *et al.*, 2011; Handegard *et al.*, 2013; Godø *et al.*, 2014; Melvin *et al.*, 2016). Fisheries acoustics have been applied routinely as a single fish species abundance estimation and monitoring tool for over four decades (Voglis and Cook, 1966; Forbes and Nakken, 1972; Nakken and Olsen, 1977; Misund, 1997). These methods have the ability to sample across a wide range of trophic levels and allow for simultaneous sampling of organisms and their habitat (Trenkel *et al.*, 2011; Godø *et al.*, 2014). Fisheries acoustics techniques are most commonly used to monitor pelagic marine fish (Kloser, 1996; Barange and Hampton, 1997; Coetzee, 2000; Kloser *et al.*, 2009;

Fässler, 2010; ICES, 2015; Fässler *et al.*, 2016; Gastauer *et al.*, 2016; Scoulding *et al.*, 2016) or to describe marine seabed habitats (Bax and Williams, 2001; Hamilton, 2001; Siwabessy, 2001; von Szalay and McConnaughey, 2002; Anderson *et al.*, 2007b; Cutter and Demer, 2013) and have been shown capable of monitoring a wide range of other marine organisms including marine mammals (e.g. various whale species (Bernasconi *et al.*, 2013a, 2013b) and seals (Geoffroy *et al.*, 2015; Pyć *et al.*, 2016)), jellyfish (Båmstedt *et al.*, 2003; Brierley *et al.*, 2004; Colombo *et al.*, 2009), phytoplankton (Selivanovsky *et al.*, 1996), zooplankton (Demer and Martin, 1995; Stanton *et al.*, 1996; Stanton and Chu, 2000; Andersen *et al.*, 2013; Lezama-Ochoa *et al.*, 2014), krill (Everson *et al.*, 1990; Demer, 2004; Demer and Conti, 2005; Cox *et al.*, 2010; Fallon *et al.*, 2016) or mesopelagic fish (O'Driscoll *et al.*, 2009; Davison *et al.*, 2015; Scoulding *et al.*, 2015; Peña and Calise, 2016; Proud *et al.*, 2017).

Conventional fisheries sampling techniques and data sources such as CPUE (Quinn and Deriso, 1999), yield or egg per recruit models (YPRM and EPRM, respectively) (Haddon and Hodgson, 2001) and biological sampling of age structure offer good assessments of overall productivity and relative abundance variations. Nonetheless, they are often subject to inherent limitations (e.g. CPUE not directly proportional to abundance in highly aggregating species, bias towards smaller sizes in YPRM) (Mackie *et al.*, 2009). Depending on the conditions, sampling area, and targeted species, they can be labour intensive, and may not be appropriate for use over vast regions of differing habitat and environmental types (Monk, 2014). Fisheries acoustics can help mitigate against these short-comings, and are able to deliver information at a high spatio-temporal resolution over wide scales (Trenkel *et al.*, 2011; Godø *et al.*, 2014), and sample almost the entire water column.

As an alternative to traditional scientific research vessels, fishing vessels can be used as vessels of opportunity (ICES, 2007), for either chartered (Godø and Wespestad, 1993; Melvin *et al.*, 2002; Massé *et al.*, 2016; Nøttestad *et al.*, 2016) or opportunistic data collection programmes (Melvin *et al.*, 2001, 2016; Barbeaux *et al.*, 2013; Fässler *et al.*, 2016). In some cases, chartering commercial vessels (typically fishing vessels, *FV*) for scientific purposes has become an attractive alternative compared to the use of scientific research vessels (*RV*). Depending on the vessel size needed and available, the compensation and size of the crew, running costs of fishing vessels are often lower than those of research vessels. A prerequisite for a fishing vessel to be considered as scientific sampling platforms is that they are, or can be, equipped with sensors providing data of scientific quality (Simmonds and MacLennan, 2005; ICES, 2007). During times of inactivity, when routine operations do not require a task for the

vessel (e.g. while sorting the catch), it can be used to conduct small-scale scientific surveys (O'Driscoll and Macaulay, 2005). Another option is to use the time fishers spend at sea during their normal operations to collect high resolution data, both on a temporal and spatial scale (Barbeaux *et al.*, 2013; Fässler *et al.*, 2016). Opportunistic acoustic data can be collected at a high resolution (over an entire fishing season (Barbeaux, 2012)) which allows for the analysis of behavioural and distributional patterns over a range of spatial and temporal resolutions (Barbeaux *et al.*, 2013). All data used within the present study was collected during routine operations, aboard a commercial trap fishing vessel within the Northern Demersal Scalefish Fishery (NDSF).

1.1 The Northern Demersal Scalefish Fishery (NDSF)

The NDSF extends over a vast area, covering a total area of 408,400 km^2 (Newman *et al.*, 2008). It stretches from southwest of Broome to the Northern Territory border in waters off the northwest coast of Western Australia, extending out to the edge of the Australian fishing zone (200 nautical miles zone) (Figure 1.1). In 2012-13, 1,228 tonnes (t) of fish were landed in the NDSF. Landings were mainly comprised of the two indicator species red emperor (*Lutjanus sebae*) (131 t) and goldband snapper (*Pristipomoides multidens*) (493 t) which equated to a first sale commercial harvest value of seven million AUD (Newman *et al.*, 2015). The remaining target species in the fishery include other snappers (Lutjanidae), emperors (Lethrinidae) and cods (Epinephilidae). These species are typically demersal fish species, forming assemblages of varying species composition (Newman *et al.*, 2015). Red emperor, goldband snapper and cod/grouper are considered fully fished (DEHWA, 2010), however, overall landings have gradually increased since 2004 (Newman *et al.*, 2015) to a near consistent level in recent years (Fletcher and Santoro, 2013; Fletcher, W.J. and Santoro, K. (eds)., 2014; Newman *et al.*, 2014, 2015). The fishery is considered to have a limited quantity of non-retained bycatch, due to the catching capacity of the gear and the high marketability of the caught species (DEHWA, 2010). One of the most common bycatch species is the starry triggerfish (*Abalistes stellaris*), but the numbers taken are not considered to be significant with most of them released alive (Williams *et al.*, 1997; Newman *et al.*, 2012). Other than triggerfish, in the 1,431 traps recorded in 2014, two sharks, two snakes and 8 crabs were observed and released alive.
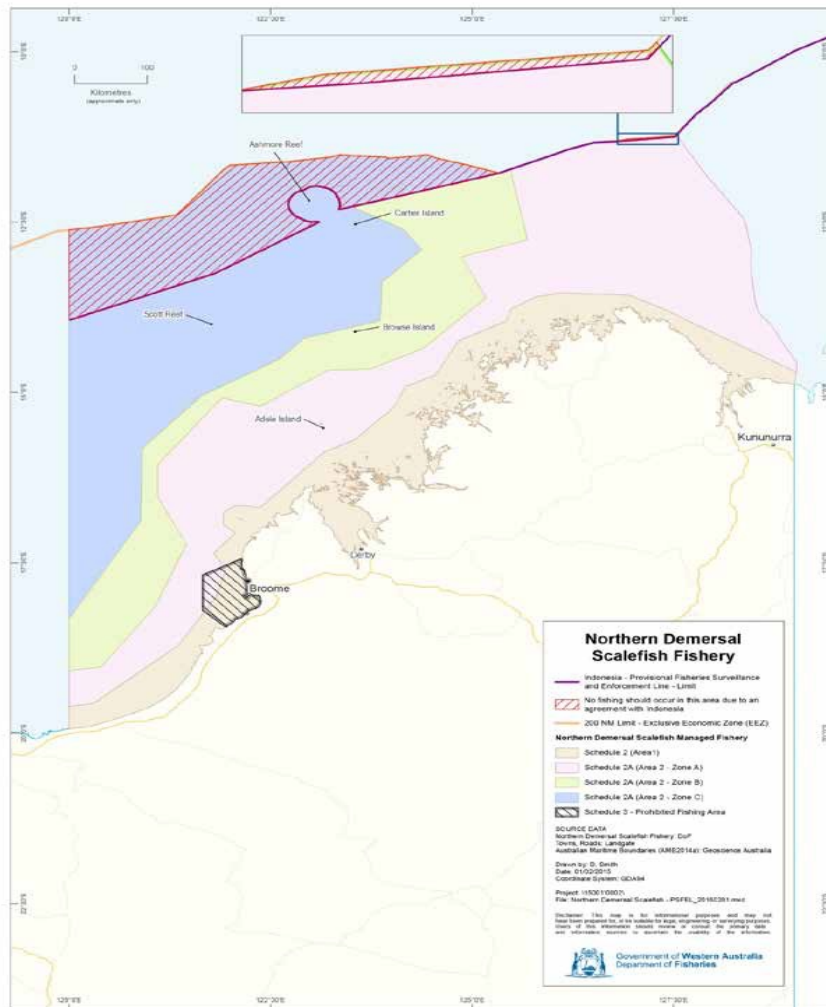
Figure 1.1 Map of the Northern Demersal Scalefish Fishery with an indication of the different three commercial fishing zones: A = pink, the inshore area of the commercially exploited part of the NDSF; B = green, the main fishing area, C = blue, the experimental fishing area; the areas closed to fishing: Area 1 = brown, the inshore area closed to commercial fishing operations; black lines – Broome local waters closed to fishing; red lines – no take zone in agreement with Indonesia; purple line – Fisheries surveillance and enforcement limit line

A normal fishing trip aboard Carolina M., commences by travelling towards a preselected fishing area. Initial steaming can be completed with up to thirty steel fishing traps (1.5 x 1.5 x 0.9 m, five cm steel mesh) aboard (Steam, Figure 1.2). Once at a suitable location, the first 'line' of traps is set (Set Traps, Figure 1.2). A 'line' typically consist of ten baited traps placed in close proximity to each other. The exact deployment location is decided by the fishermen, based on the seafloor characteristics read from the echosounders, availability of fish resources observed as schools on the echogram and other factors taken into account, which are best summarised as fisher's experience or knowledge. Traps are thrown overboard, while the vessel is continuing its course. All traps are marked by buoys, to facilitate an easier retrieval later on. After the traps are all deployed, the vessel moves away from the fishing location (Rest, Figure 1.2). The traps are said to be 'soaking', waiting for the fish to enter. Duration of the soaking
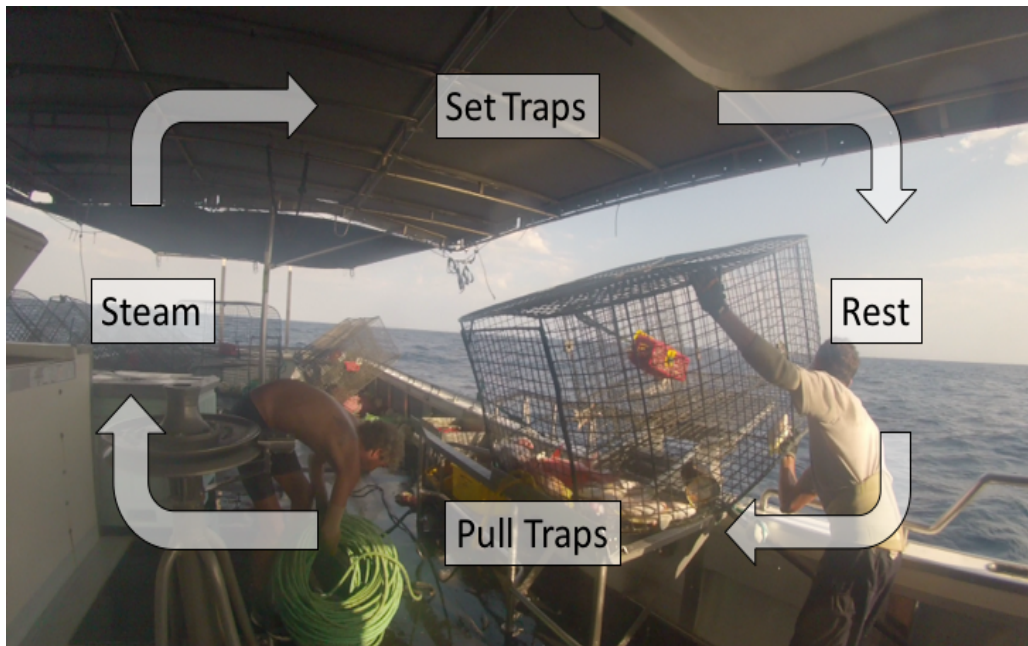
Figure 1.2 Schematic of the normal operation procedures aboard the trap fishing vessel Carolina M

period can vary, but is largely determined by the prevailing tidal regime (mean 7.21 hours, max = 16.62, min = 1.3, n=1431). Generally, at least one tidal phase shift is awaited prior to trap retrieval. Once the fisher judges that sufficient time has passed, the vessel steams back to the locations of trap deployment to pull the traps back aboard (Pull traps, Figure 1.2). Fish contained in the traps are sorted immediately into species of commercial interest and bycatch. Bycatch species or undersized fish are released back into the sea as quickly as possible. Individuals that are retained for landing, are put into an ice slurry, quickly stunning the fish and keeping the produce fresh. Depending on time availability, productivity of the surrounding grounds and observed catch rate, it might be decided to place the next round of traps at a close-by location, further away or to finish the fishing trip and travel back to Broome. At the end of each trip, it might be decided to leave the last line of traps in the water, unbaited. Traps that are left unbaited or that are lost are considered to be ghost fishing, but the impact of ghost fishing on the resources of the NDSF has been judged as being negligible (Newman *et al.*, 2014).

1.2 Fisheries acoustics

1.2.1 Principles

In general terms, traditional echosounders, such as the Simrad ES70 system, consist of a transceiver and a transducer (Urick, 1983; Simmonds and MacLennan, 2005), as illustrated in

Figure 1.3. The transceiver generates electrical energy (voltage) which is converted to mechanical sound energy at discrete frequencies by a downwards pointing transducer. Typically, transducers are mounted in the hull, or in modern research vessels in one or multiple drop-keels. These transducers generally operate at frequencies ranging from 12 to 364 kHz. The transducer has a two-fold function, emitting sound and receiving echoes. They are composed of arrays of piezoelectric or magnetostrictive elements, of which piezoelectric elements are most commonly used, taking advantage of the piezoelectric effect (Urick, 1983; Simmonds and MacLennan, 2005). The prefix piezo, is derived from the Greek word *piezin*, meaning to squeeze. Piezoelectric materials generate electric energy when stressed (signal reception) and are stressed when an electrical field is applied (signal emission) to them (Urick,
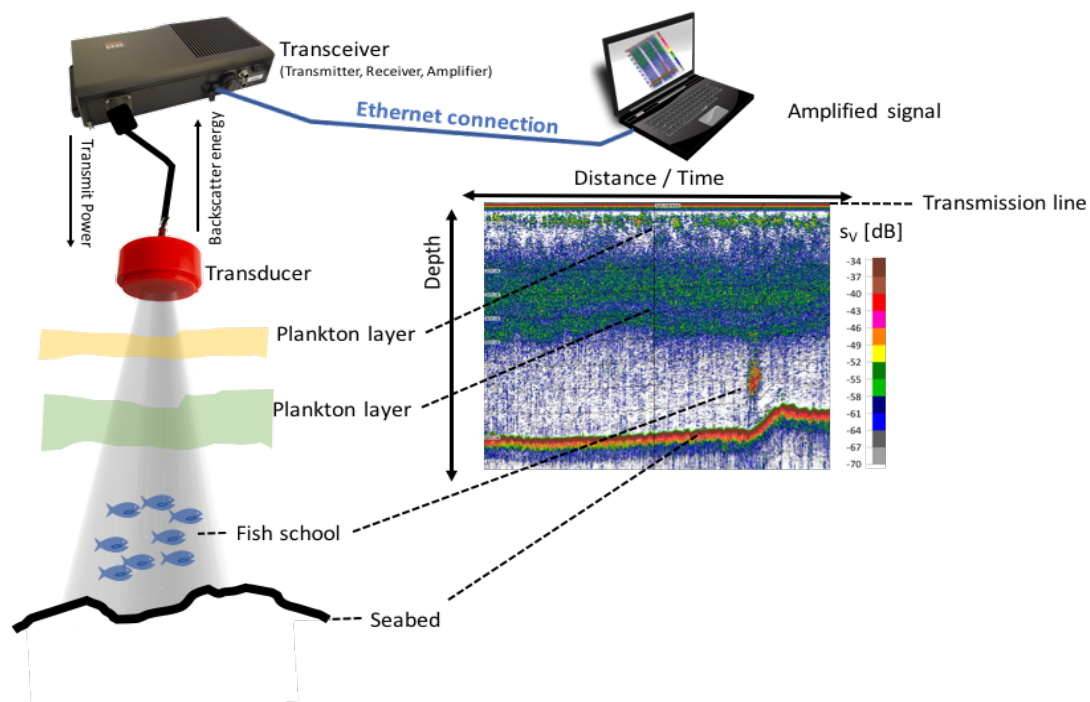
Figure 1.3 Schematic representation of an echosounder system, such as the Simrad ES70. The emitted acoustic pulse is reflected by targets in the water column (in the example are two different weak scattering plankton layers, a fish school and the seabed

1983).

The emitted acoustic signal is directional, typically taking the form of a main lobe, oriented directly below the transducers, and multiple sidelobes of significantly lower intensity. Of the main lobe, the resulting ensonified volume takes the shape of a cone, similar to the light beam produced by a torch, hereafter referred to as acoustic beam, with its respective volume, the beam volume. The beam volume and beamwidth is a function of the transducer size and layout of the internal ceramic pistons, and varies with range from the transducer. Any
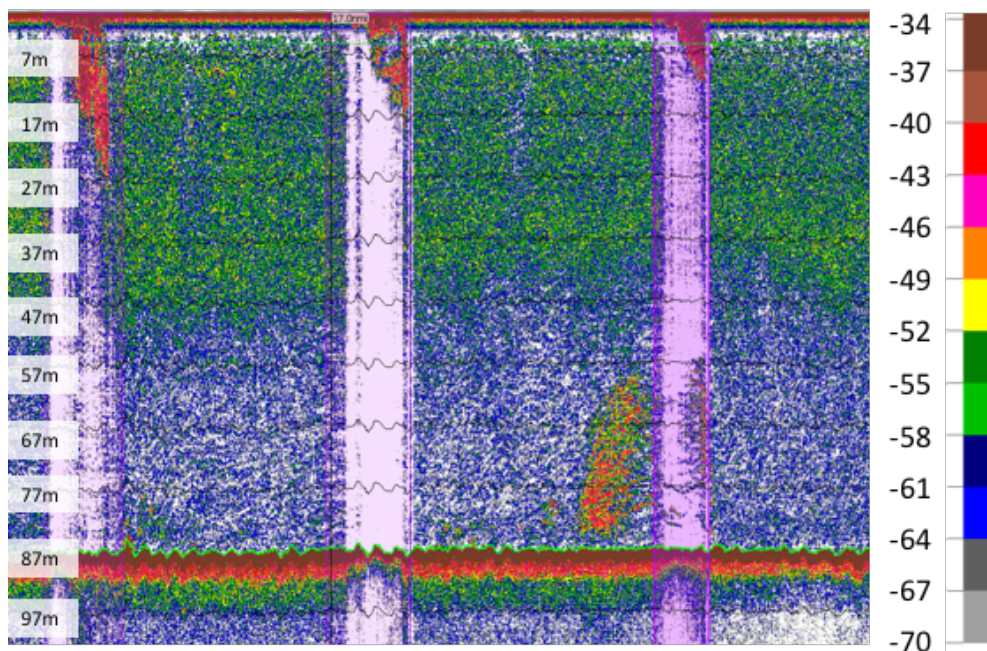
Figure 1.4 Example of an echogram from the NDSF area. The pixel colours indicate the sv values in dB as indicated by the colour scale on the right. Depth in m is shown on the y-axis, travelled distance is shown on the x-axis. Horizontal black lines represent 10 m intervals of altitude off the seabed. The detected seabed is represented by a green line, Purple areas are excluded from further analysis due to a large number of bad pings, as a result of bubble attenuation under the hull of the vessel due to abrupt changes in heading direction. The layer in the upper 50 m is mainly composed of fluid-like weak scatterers, such as plankton. Close to the bottom, indicated by a cluster of red pixels, is a fish school with a height of almost 20 m

ensonified object with an acoustic impedance, i.e. the acoustic resistance of an object when exposed to an acoustic pressure wave, different to the surrounding medium, will cause some kind of backscatter (echo). The reflected energy will then be detected by the transducer. The recorded backscattered acoustic signals are amplified and converted into electrical energy as the received signal (Figure 1.4, 1.5). The two-way distance (*2R*) at which a sound-scattering object has been detected is obtained through the temporal delay between emitting and receiving of the sound signal by the transducer (Δt), multiplied by the sound velocity at ambient seawater conditions (*c*), *R = 0.5 Δtc*. The location of the objects within the beam can be resolved more precisely using split beam echosounders. Split beam echosounders have their emitting and receiving elements arranged on copper plates, divided in four quadrants (or three sectors in more modern transducers). The geometrical displacement of the listening elements makes it possible to detect the position of the target within the beam using a time-of-arrival difference method for the signal received by each sector. The intensity or strength of the received signal provides insights into the density or, in the case of resolvable individual targets, the size and type (e.g. gas bearing or non gas-bearing) of the scattering object.

Visualisation of the recorded data is done as a two-dimensional representation (echogram) of the recorded data with a distance or time variable defining the x-axis and a measure of depth or range on the y-axis (Figure 1.5). The backscatter intensity (backscattering volume, Sv dB re m^2m^{-3}) defines the colour code (Figure 1.5).

1.2.2 Quantification of acoustic backscatter

Acoustic backscatter is generally quantified in the linear domain as the backscattering cross-section $(\sigma_{bs}, [m^2])$ or in the logarithmic domain as target strength (TS, [dB re $1m^2$]. The logarithmic measure in dB, i.e. the ratio to a reference value (m^2 for TS) expressed in the logarithmic domain, is more commonly used as log transformed numbers are easier to work with when compared to very small numbers. The σ_{bs} is the proportion of backscattered intensity (I_{bs}) from the transmitted incident energy (I_i), measured at a distance from the target (R, [m]):

$$\sigma_{bs} = R^2 \, I_{bs} \, I_i^{-1}.$$

TS describes the same physical measurement in the logarithmic space:

$$TS = 10 \, log_{10}(\sigma_{bs}).$$

Acoustic backscatter can consist of discrete resolvable targets (e.g. individual fish) or a convolution of non-resolvable targets, depending in part on the physical separation distance of the targets in the water. The short burst of sound emitted by an echosounder is called a pulse or a ping. A ping consists of multiple pressure waves transmitted at a given frequency (f, [Hz]). Each wave has a wavelength (λ, [m]), defined by the sound velocity [c, ms^{-1}] divided by f. Each ping has a pulse duration (τ, [s]), equalling the wave number (k) divided by f ($\tau = k \, f^1$). Consequently, the length of the pulse (L_p, [m]) is $c\tau$. In order for two targets to be resolvable, the difference between the target ranges, measured from the transducer, has to be greater than half the L_p or $c\tau/2$. This precludes the resulting echoes from overlapping. If individual targets occur closer to each other (typical for schools or shoals), the resulting echoes form a combined (constructive – additive or destructive – subtracting) backscattered signal. In such a scenario, individual fish can't be isolated from the backscatter, but the backscatter intensity remains a proportional measure of biomass in the water column. The sum of all targets contributing to the backscatter over the integrated volume or the sampling volume (V_0) is expressed as volume backscattering coefficient (s_v [m^{-1}]):

$$s_v = \frac{\sum \sigma_{bs}}{V_0}$$

where V_0 is calculated as:

$$V_0 = \psi R^2 \frac{L_p}{2}$$

with ψ being the equivalent beam angle of the transducer in steradians. Analogous to TS, s_v can also be expressed in the logarithmic domain as:

$$S_v = 10 \, log_{10} \, (s_v).$$

Measurements of S_v are defined for small volumes, i.e. pulse volume. If backscattering volume strength is integrated over a larger domain, covering multiple pings and a large range interval, it is expressed as mean volume backscattering strength $(\widehat{S_v})$.

The most common measure of backscattered energy, used in acoustic surveys and most biomass or abundance estimates is the area backscattering coefficient (s_a, sometimes referred to as ABC). s_a is s_v integrated over a given depth range (limited by an upper and lower depth and a start and stop position in a geographical sense). Conventionally, in a survey situation, s_a is integrated over one nautical mile and named s_A (nautical area scattering coefficient, sometimes referred to as NASC), defined as:

$$s_A = 4\pi(1852)^2 s_a$$

The density of individuals contained within a region with a measured s_A can be determined as:

$$\rho = \frac{s_A}{4\pi(\sigma_{bs})}$$

To derive any quantitative information from acoustic backscatter (e.g. abundance or biomass of a given fish species or group), it is crucial to allocate appropriate proportions of s_A to the given species or group and to have good knowledge about the species or groups TS or σ_{bs} (McClatchie $et\ al.$, 1996; Simmonds and MacLennan, 2005). Given the unstable nature of TS it is also important to understand and account for its variability (Everson $et\ al.$, 1990; Ona, 2003; Demer and Conti, 2005; Coetzee $et\ al.$, 2008; Fässler, 2010; Scoulding $et\ al.$, 2016).

1.3 Target strength estimates

TS can be estimated theoretically or empirically. Empirically *TS* can either be measured under natural conditions (*in situ*) or in a controlled environment (*ex situ*) (Simmonds and MacLennan, 2005; Jech *et al.*, 2015). Empirical methods for *TS* estimation are described, discussed and reviewed by Love (1971a), Ehrenberg (1972, 1979), Foote *et al.* (1986), MacLennan (1990), MacLennan and Menz (1996). Conditions for good quality *TS* measurements are discussed by Sawada *et al.* (1993) and Gauthier and Rose (2001a). Theoretically *TS* can be estimated by numerical or analytical scattering models based on information of the physiological and/or morphological features of the target species. Ten currently used models for *TS* estimation have recently been reviewed and compared by Jech *et al.* (2015).

Empirical approaches to *TS* estimates have the advantage that the influence of different biological and physical parameters can be quantified (Hazen and Horne, 2003). In order to get a thorough understanding of the scattering properties of aquatic organisms, a combination of theoretical and empirical methods is required (Henderson and Horne, 2007; Jech *et al.*, 2015). It is important to understand that *TS* is not a point measurement or estimate, but a probability density function (PDF). *TS* can vary depending on external (e.g. fish orientation, depth of occurrence, sound velocity of the surrounding water body, etc.), and internal conditions (e.g. fish size, swimbladder volume, sound speed in the swimbladder, sound speed in the fish flesh, etc.) (Ona, 1999). In order to derive precise biomass or abundance estimates from acoustic measurements it is vital to have an understanding of these effects and the consequent variability of *TS* (Simmonds and MacLennan, 2005; Fässler, 2010).

Generally, *TS* is expressed as a function of fish length (*L*) for a given frequency. The linear relationship between *TS* and *L* was first described by (Nakken and Olsen, 1977). (Nakken and Olsen, 1977) conducted *ex situ TS* experiments, fixing dead herring inside the beams of a 38 kHz and a 120 kHz transducer. Plotting the *TS* measurements against the fish length led to the establishment of the now standard *TS-L* equation:

$$TS = a \ log_{10}(L) + b$$

where *a* and *b* are constants determined by least-mean-squares regression analysis. Soon after those experiments, (Love, 1977) found σ_{bs} to be approximately proportional to L^2, which led to the commonly used:

$$TS = 20 \log_{10}(L) + b_{20}$$

This linear relationship has been described as questionable in certain situations (especially for zooplankton) (Demer and Martin, 1995), but remains the standard form of *TS-L* relationships.

1.3.1 Ex situ estimates

Empirical *ex situ TS* measurements are generally conducted either using tethered or caged fish (Simmonds and MacLennan, 2005). Measurements of *TS* of immobilised (stunned or dead) fish held by a wire represent the earliest estimates of *TS* (Midttun and Hoff, 1962; Love, 1971a, 1971b; Shibata, 1971). For the purpose of such experiments, generally a single fish is fixed upside down below the transducer, in the centre of the beam. Influence of tilt angle can be adjusted through repositioning of the fish (Nakken and Olsen, 1977). The main caveat of this method is that fish are unable to behave naturally. *A priori* knowledge of orientation changes in their normal environment to accurately determine the variability of *TS* expected in the field is needed, but rarely available (Foote, 1980). As an alternative, cage experiments have been designed, assuming that experiments involving living animals are more likely to reproduce the measurements as they would occur in the wild. The first cage experiments involved a lot of individual fish, completed by Johannesson and Losse (1977). The first modern experiments were accomplished and later refined by Edwards and Armstrong (1983, 1984). The design by Edwards and Armstrong (1983, 1984) included two transducers mounted on a gimbal, adjustable to align the acoustic beams with the fish cage (2m in diameter, 1 m deep) and upwards looking cameras. All equipment was mounted on a frame suspended below a moored raft. Additionally, a sphere of known *TS* was suspended below the gimbal, to calibrate the echosounder. Optical recordings facilitated the extraction of fish orientation. Even though the material of the cage should be chosen such as to minimise its reflection, the backscatter of the cage has to be extracted from the recorded fish *TS*. This can be done through measurements of the empty cage. Alternatively this can be avoided by using a cage larger than the acoustic beam (Ona, 2003).

1.3.2 In situ measurements

Empirical *in situ TS* measurements have the potential to deliver the most representative measures of *TS* (Simmonds and MacLennan, 2005), as observations are based on fish behaving "naturally" in their normal environment. If *in situ* measurements are to be undertaken, some factors in terms of equipment selection, target density and biological sampling have to be considered. To achieve good quality *TS* measurements, targets have to be

recorded with calibrated split-beam or dual beam systems (Ehrenberg, 1974). All targets have to be located in the far-field of the transducer and the target (Ona, 1999; Simmonds and MacLennan, 2005), be clearly isolatable, and be attributed to a single fish (Sawada *et al.*, 1993; Soule *et al.*, 1995; Foote, 1996):

- The usage of split-beam or dual-beam echosounders allows for the positioning of the single target in the acoustic beam and *TS* can be measured directly (Ehrenberg, 1974; Traynor and Ehrenberg, 1979, 1990; Foote, 1987). If a target is detected multiple times, within the acoustic beam, its speed and directivity can be tracked through a combination of the targets (Ehrenberg and Torkelson, 1990; Ona, 2001; McQuinn and Winger, 2003).

- The farfield is any distance greater than the nearfield (Ona, 1999), where wave-fronts are close to parallel and the intensity of the wave varies proportionally to the range squared, under the inverse-pressure rule (Simmonds and MacLennan, 2005). The nearfield of a transducer is defined as d^2/λ, where d is the diameter of the transducer. Similarly, the nearfield of a target is l^2/λ, with l the maximum linear dimension of the target (Ona, 1999; Simmonds and MacLennan, 2005).

- Individual echoes can be detected with single echo detectors (SED), in an attempt to remove targets resulting from multiple scatterers. SEDs include a range of algorithms such as phase coherence, amplitude stability and echo duration (Ona, 1999). SEDs generally work well for well spaced targets, but can occasionally include accumulated echoes, especially in areas where targets are packed densely (Sawada *et al.*, 1993; Soule *et al.*, 1995; Barange *et al.*, 1996; Foote, 1996).

- It is important to collect alternative evidence of the acoustically observed targets. Alternative sampling is generally done indirectly through trawling (e.g. pelagic trawls (Nero *et al.*, 2004), purse seines (Misund and Beltestad, 1996), long lines (Bertrand *et al.*, 2002), rod and line (Knudsen *et al.*, 2009), gill-nets (Kubecka *et al.*, 1994)) or directly through optical recordings (Kloser *et al.*, 2011; Macaulay *et al.*, 2012; Fernandes *et al.*, 2016). Alternative sampling should be taken closely to the acoustically observed targets and where possible, other targets should be excluded (Ona, 1999). To determine a *TS-L* relationship, *TS* distributions have to be related to the length distributions of the alternative sampling (MacLennan and Menz, 1996).

Another way of conducting *in situ TS* estimates is through the so-called comparison method. The comparison is made directly between observed acoustic backscatter and catch.

For this method, the entire school has to be ensonified and the entire school has to be caught (Misund and Beltestad, 1996).

1.3.3   Theoretical target strength estimates

With increased computational power, the development of numerical and analytical approaches has improved in recent years. However, choosing which model is the most appropriate for a given task is not a trivial matter, given the availability of diverse approaches, each with specific constraints and advantages (Jech *et al.*, 2015). The following provides a brief description of three commonly used modelling approaches:

Kirchhoff-Ray Mode approximation

The Kirchhoff-Ray Mode (KRM) approximation, estimates the backscatter of targets by simplifying their shape as a set of cylinders of finite length (Clay and Horne, 1994). Using, the Helmholtz-Kirchhoff integral (Foote and Traynor, 1988), the model assumes that every point of the surface reflects as if it was of an infinite plane wave from an infinitive tangential interface (Medwin and Clay, 1998). The total backscatter is computed through summation of the combined contributions of each cylinder element. Morphological components of the fish, generally its body and swimbladder, are commonly extracted from X-rays (Clay and Horne, 1994; Hazen and Horne, 2003), computational tomography scans (CT) (Macaulay, 2002; Sawada, 2002) or magnetic resonance scans (MRI) (Peña and Foote, 2008; Fässler *et al.*, 2013). KRM is relatively easy to compute when compared to other methods such as boundary element methods (BEM) (Simmonds and MacLennan, 2005). KRM has been shown to be a useful tool for analysing the effects of length, frequency, tilt angle, ontogeny, physiology and behaviour on *TS* (Hazen and Horne, 2003; Horne, 2003). The main issue with this method is its lack of accuracy at low frequencies and high tilt angles (Simmonds and MacLennan, 2005).

Boundary Element Model

Similar to the KRM, BEM can be used to compute the backscatter from complex surfaces, simplified by elemental areas, defined by nodal points (Francis, 1993). The backscatter is modelled through the wave equation converted to Helmholtz integrals, considering the pressures and particle velocities at each element (Simmonds and MacLennan, 2005). BEM requires much more computational power than the simpler KRM, but enables, unlike KRM, the integration of different acoustic properties for the interior of the three-dimensional structures (Foote and Francis, 2002b). Further, it takes into account the diffracted

energy in the shadow zone (the part of the body not facing the transducer) (Simmonds and MacLennan, 2005). Foote and Francis (2002) found good agreement between KRM and BEM for gadoids.

Distorted Wave Born Approximation

The distorted wave Born approximation (DWBA), expresses backscatter as a three-dimensional integral over the entire body. DWBA is mainly applied to weak scatterers, such as plankton (Stanton *et al.*, 1993, 1996; Stanton and Chu, 2000) or non-swimbladdered fish (Gorska *et al.*, 2005) or parts of the fish body (Fässler *et al.*, 2008).

1.4 Target classification

Target classification is an important step when analysing echograms. Classification is the process of segregating an echogram into different functional groups with the aim of converting acoustic backscatter measurements to biologically relevant quantities, such as species or group specific abundance or biomass. Target classification is defined here as all data manipulation processes after the data has been calibrated (Demer *et al.*, 2015) and cleaned from noise, working towards the extraction of species- or group-specific backscatter
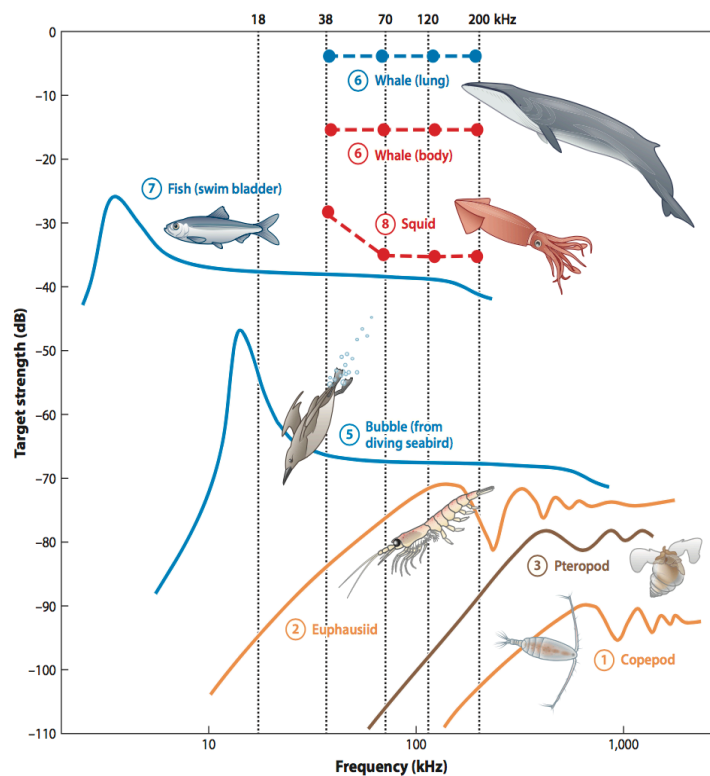
Figure 1.5 Target strength of diverse marine organisms at a range of frequencies, taken from Benoit-Bird and Lawson (2016)

information.

Prior to target classification, it is important to remove noise from echograms. Noise can be caused by different sources. Generally, three categories of noise are differentiated: background noise, transient noise and impulse noise (Ryan *et al.*, 2015). Background noise is a combination of time varied gain (TVG), caused by acoustic transmission loss, and noise originating from various sources, such as vessel noise (Mitson, 2003; Robertis and Higginbottom, 2007). Transient noise is mainly caused by poor weather conditions (Ryan *et al.*, 2015) and vessel movement. Impulse noise generally manifests itself as noise spikes, mainly caused by unsynchronized, simultaneously operated acoustic instruments (Ryan *et al.*, 2015).

Empirical approaches are most commonly chosen for the classification of acoustic targets. They mainly rely on the presence of multi-frequency data, taking advantage of the different scattering properties (frequency responses) of organisms at different frequencies (Figure 1.6). The definition of one reference frequency to produce relative frequency curves is a common application of this method (Fernandes *et al.*, 2006; Korneliussen *et al.*, 2008; De Robertis *et al.*, 2010). Alternatively, frequency response curves can be used to be compared to a feature library, helping the classification of acoustic targets (Korneliussen *et al.*, 2009, 2016). While an empirical approach to target classification remains predominant, several studies have investigated the use of supervised and unsupervised models to classify acoustic targets. Supervised approaches to target classification include the use of support vector machines and neural networks (Robotham *et al.*, 2010) and unsupervised methods, such as clustering (Anderson *et al.*, 2007a; Campanella and Taylor, 2016), random forest classification (Fernandes, 2009; Fallon *et al.*, 2016) and self-organising maps (Peña and Calise, 2016).

1.5 Geostatistics and fisheries acoustics

The main goal of most fisheries acoustics surveys is the estimation of the abundance of a particular fish stock, as well as the description of its distribution, structure and associated estimates of uncertainty (Rivoirard *et al.*, 2000; Fernandes *et al.*, 2002; Simmonds and MacLennan, 2005). The main purpose of geostatistics is to estimate a variable at given locations (regionalised variables), based on a model of spatial variability of the given variable (Matheron, 1971). Geostatistics have been shown to be a useful tool to investigate the distribution and abundance of fish stocks, with the associated sampling error, based on acoustic surveys (Rivoirard *et al.*, 2000; Petitgas, 2001; Woillez *et al.*, 2007, 2016).

Traditionally, fisheries acoustics data used to estimate stock distribution, abundance or biomass, are collected during dedicated acoustic trawl (AT) surveys (Maravelias *et al.*, 1996; Simmonds and MacLennan, 2005; ICES, 2015). Such surveys generally follow predefined stratified parallel, stratified random, or zig-zag survey transects (Jolly and Hampton, 1990; Simmonds *et al.*, 1992; Guillard and Vergès, 2007). In the case of fishers collecting opportunistic data, the underlying design can best be described as preferential or directed (Diggle *et al.*, 2010; Barbeaux, 2012; Barbeaux *et al.*, 2013; Fässler *et al.*, 2016), due to their inherent bias towards promising fishing grounds. All of these designs do not typically satisfy the random sampling theory, which would allow for a direct extraction of the sampling variance (precision) (Petitgas, 2001). Estimates of sampling variance under these scenarios require a model of spatial covariance to estimate survey precision (Rivoirard *et al.*, 2000; Petitgas, 2001).

In general terms, there are two approaches used in geostatistics. Firstly, a transitive approach where the population is looked upon as a whole, without domain delimitation. The structure of the population at each variable point *z(x)* can be described by the transitive covariogram (*g*) at a distance *h* as:

$$g(h) = \int z(x)z(x+h)\,dx.$$

In an ecological context, this is rarely the case, as populations generally are separated and need a finer scale investigation. Therefore, more commonly the second, an intrinsic approach, is used, describing the behaviour of a variable (e.g. fish density or acoustic density) within a defined domain. In the context of intrinsic geostatistics, the regionalised variable *z(x)* is described by a random function *Z(x)*. The variogram can then be computed by the classical estimator (Matheron, 1971), defined as half the variance of *Z(x)* and *Z(x+h)*, with the variance depending on *h* not *x*:

$$\gamma(h) = 0.5\,E((Z(x+h) - Z(x)^2).$$

In practical terms, a variogram is computed based on data and fitted by a model, which can be a simple structure (e.g. nugget, spherical, exponential, linear, etc.) or a combination of multiple structures. If the direction of h influences the behaviour of the variogram behaviour, there is anisotropy, if it is independent of the direction, there is isotropy.

A common interpolation tool in geostatistics is kriging, as the best linear estimator. The most common form of kriging is ordinary kriging, conforming with the intrinsic hypothesis and requiring a variogram. The kriging estimator within a given domain *V* is obtained through variance minimisation with weights *w*. The weights are obtained by resolving:

$$\begin{cases} \sum_i w_i \gamma (x_i - x_j) + \phi = \bar{\gamma}(x, V) \ whatever \ i \\ \sum_j w_j = 1 \end{cases}$$

where ϕ is the Lagrange parameter introduced to satisfy $\sum_j \lambda_j = 1$.

Alternatives to the linear kriging estimator are nonlinear geostatistics, based on multivariate hypotheses (e.g. normality after transformation) (Petitgas, 1993; Petitgas *et al.*, 2016, p 201). Given that kriging has a tendency to smooth data, conditional (honouring the data) or non-conditional simulations are often more suitable as they are representations of the process *Z(x)* over a domain and facilitate better representation of the characteristics of the spatial distribution. They can reproduce the data at a much finer grid than the collected reality (Gimona, 2003; Walline, 2007; Chiles and Delfiner, 2009; Woillez *et al.*, 2009a).

Geostatistics remains a young field, with the theoretical background being established in the mid-1960s by Matheron (Matheron and others, 1965; Matheron, 1967). A detailed description of the use of geostatistics for abundance and variance estimates in fisheries acoustics is given by Rivoirard et al. (2000) and a review of geostatistics for different survey designs is given by Petitgas (2001). A detailed description of the use of Gaussian simulations for the estimation of sampling variance is given by Woillez et al. (2009, 2016). With indicators and indices identified as a main information input into EBFM, in recent years studies have explored the use of geostatistical indices to describe distributions and track inter-annual changes (Woillez *et al.*, 2007, 2009b; Gastauer *et al.*, 2016), or to define hotspot regions (Petitgas *et al.*, 2016).

1.6 Aims and objectives of the thesis

This thesis is composed of four chapters, in the format of scientific papers. All chapters have been submitted to scientific journals and have now been published (Chapter 2 and 3) or are accepted for publication with comments (Chapter 4 and 5). Each chapter therefore consists of an own Introduction, Methods, Results and Discussion section. Effort has been made to reduce overlap between the provided general introduction and the introductions, as well as the method sections provided within each chapter. However, some overlap has been inevitable, given each chapter constitutes a full research paper.

The main objective of the study was to analyse the potential of opportunistically collected acoustic data in conjunction with optical catch recordings from a commercial trap fishing vessel in the NDSF, which could be used as a complimentary data source to traditional monitoring techniques. The purpose of the thesis was the development of standardised methods for data processing, rather than to assess the current management of the NDSF. The following is a summary of the main aims and achievements of the individual chapters:

Chapter 2: Target strength estimates of red emperor with Bayesian parameter calibration

The main motivation of this chapter was a *TS* estimation for red emperor at 38 and 120 kHz. Through Bayesian parameter calibration, *ex situ* experiments were used to fine tune a KRM model based on CT scans of red emperor. Information on *TS* is a crucial step towards acoustic abundance or biomass estimates.

Chapter 3: Variability estimates of the target strength and abundance of goldband snapper in three fishing regions

The main aim of this chapter was to estimate *TS* of the second indicator species, goldband snapper, based on *in situ* recordings and to assess the variability of acoustic abundance estimates of goldband snapper in three selected fishing regions. A good understanding of the expected precision of acoustic density, abundance or biomass estimates is crucial when it comes to judging the value of the collected data or potential future data collection programmes.

Chapter 4: Precision estimates of the abundance of nine key species groups within three fishing regions using geostatistical conditional simulations

The goal of this chapter was the development of methods to provide precision estimates of acoustic abundance and biomass estimates of key species groups within three fishing regions of the NDSF. For species groups where no *a priori TS* information was available, these are provided through a KRM model. Acoustic information and species composition information (based on optical catch information) are combined through GCS.

Chapter 5: An unsupervised approach to the acoustical description of three fishing regions

Classification of echograms is a notoriously difficult task in areas of high species richness. In this chapter, an unsupervised approach to analyse acoustic data in combination with catch information to derive indices which could be useful for EBFM, is being proposed. Acoustic density hotspots are defined, based on a geostatistical definition of hotspots. Acoustic habitat categories, are extracted and indicator species groups are identified. Acoustic school descriptors are clustered and the existence of indicator species groups is explored.

Chapter 6: General discussion

The thesis concludes with a general discussion, putting the entire thesis into a broader context and discussing key findings as well as remaining challenges.

1.7 References

Andersen, L. N., Ona, E., and Macaulay, G. 2013. Measuring fish and zooplankton with a broadband split beam echo sounder. *In* OCEANS-Bergen, 2013 M*TS*/IEEE, pp. 1–4. IEEE. http://ieeexplore.ieee.org/abstract/document/6850133/ (Accessed 25 May 2017).

Anderson, C. I. H., Horne, J. K., and Boyle, J. 2007a. Classifying multi-frequency fisheries acoustic data using a robust probabilistic classification technique. The Journal of the Acoustical Society of America, 121: EL230-EL237.

Anderson, J. T., Holliday, V., Kloser, R., Reid, D., and Simard, Y. 2007b. Acoustic seabed classification of marine physical and biological landscapes. International Council for the Exploration of the Sea.

Båmstedt, U., Kaartvedt, S., and Youngbluth, M. 2003. An evaluation of acoustic and video methods to estimate the abundance and vertical distribution of jellyfish. Journal of Plankton Research, 25: 1307–1318.

Barange, M., Hampton, I., and Soule, M. 1996. Empirical determination of in situ target strengths of three loosely aggregated pelagic fish species. ICES Journal of Marine Science, 53: 225–232.

Barange, M., and Hampton, I. 1997. Spatial structure of co-occurring anchovy and sardine populations from acoustic data: implications for survey design. Fisheries Oceanography, 6: 94–108.

Barbeaux, S. J. 2012. Scientific acoustic data from commercial fishing vessels: Eastern Bering Sea walleye pollock (*Theragra chalcogramma*). University of Washington, United States -- Washington. 227 pp. http://search.proquest.com.dbgw.lis.curtin.edu.au/docview/1013759483/abstract/3E AE09E9E2FC462CPQ/1 (Accessed 6 September 2016).

Barbeaux, S. J., Horne, J. K., and Dorn, M. W. 2013. Characterizing walleye pollock (Theragra chalcogramma) winter distribution from opportunistic acoustic data. ICES Journal of Marine Science, 70: 1162–1173.

Bax, N. J., and Williams, A. 2001. Seabed habitat on the south-eastern Australian continental shelf: context, vulnerability and monitoring. Marine and Freshwater Research, 52: 491–512.

Bernasconi, M., Patel, R., Nøttestad, L., Pedersen, G., and Brierley, A. S. 2013a. The effect of depth on the target strength of a humpback whale (Megaptera novaeangliae). The Journal of the Acoustical Society of America, 134: 4316–4322.

Bernasconi, M., Patel, R., Nøttestad, L., and Brierley, A. S. 2013b. Fin whale (Balaenoptera physalus) target strength measurements. Marine Mammal Science, 29: 371–388.

Bertrand, A., Josse, E., Bach, P., Gros, P., and Dagorn, L. 2002. Hydrological and trophic characteristics of tuna habitat: consequences on tuna distribution and longline catchability. Canadian Journal of Fisheries and Aquatic Sciences, 59: 1002–1013.

Brierley, A. S., Axelsen, B. E., Boyer, D. C., Lynam, C. P., Didcock, C. A., Boyer, H. J., Sparks, C. A., *et al.* 2004. Single-target echo detections of jellyfish. ICES Journal of Marine Science: Journal du Conseil, 61: 383–393.

Campanella, F., and Taylor, J. C. 2016. Investigating acoustic diversity of fish aggregations in coral reef ecosystems from multifrequency fishery sonar surveys. Fisheries Research, 181: 63–76.

Chen, Y., Chen, L., and Stergiou, K. I. 2003. Impacts of data quantity on fisheries stock assessment. Aquatic Sciences, 65: 92–98.

Chiles, J.-P., and Delfiner, P. 2009. Geostatistics: modeling spatial uncertainty. John Wiley & Sons. https://books.google.nl/books?hl=en&lr=&id=tZl07WdjYHgC&oi=fnd&pg=PP1&dq=del

finer+1999+uncertainty+geostatistics&ots=kKIFSS5LOl&sig=JDJOnlgcAD_-PYJWQrpYnY3UJKU (Accessed 23 May 2017).

Clay, C. S., and Horne, J. K. 1994. Acoustic models of fish: The Atlantic cod (Gadus morhua). The Journal of the Acoustical Society of America, 96: 1661–1668.

Coetzee, J. 2000. Use of a shoal analysis and patch estimation system (SHAPES) to characterise sardine schools. Aquatic Living Resources, 13: 1–10.

Coetzee, J. C., Merkle, D., De Moor, C. L., Twatwa, N. M., Barange, M., and Butterworth, D. S. 2008. Refined estimates of South African pelagic fish biomass from hydro-acoustic surveys: quantifying the effects of target strength, signal attenuation and receiver saturation. African Journal of Marine Science, 30: 205–217.

Colombo, G. A., Benović, A., Malej, A., Lučić, D., Makovec, T., Onofri, V., Acha, M., *et al.* 2009. Acoustic survey of a jellyfish-dominated ecosystem (Mljet Island, Croatia). Hydrobiologia, 616: 99–111.

Cox, M. J., Warren, J. D., Demer, D. A., Cutter, G. R., and Brierley, A. S. 2010. Three-dimensional observations of swarms of Antarctic krill (Euphausia superba) made using a multi-beam echosounder. Deep Sea Research Part II: Topical Studies in Oceanography, 57: 508–518.

Cutter, G. R., and Demer, D. A. 2013. Seabed classification using surface backscattering strength versus acoustic frequency and incidence angle measured with vertical, split-beam echosounders. ICES Journal of Marine Science: Journal du Conseil: fst177.

Davison, P. C., Koslow, J. A., and Kloser, R. J. 2015. Acoustic biomass estimation of mesopelagic fish: backscattering from individuals, populations, and communities. ICES Journal of Marine Science, 72: 1413–1424.

De Robertis, A., McKelvey, D. R., and Ressler, P. H. 2010. Development and application of an empirical multifrequency method for backscatter classification. Canadian Journal of Fisheries and Aquatic Sciences, 67: 1459–1474.

DEHWA. 2010. Assessment of the Northern Demersal Scalefish Fishery.

Demer, D. A., and Martin, L. V. 1995. Zooplankton target strength: Volumetric or areal dependence? The Journal of the Acoustical Society of America, 98: 1111–1118.

Demer, D. A. 2004. An estimate of error for the CCAMLR 2000 survey estimate of krill biomass. Deep Sea Research Part II: Topical Studies in Oceanography, 51: 1237–1251.

Demer, D. A., and Conti, S. G. 2005. New target-strength model indicates more krill in the Southern Ocean. ICES Journal of Marine Science: Journal du Conseil, 62: 25–32.

Demer, D.A., Berger, L., Bernasconi, M., Bethke, E., Boswell, K., Chu, D., Domokos, R., et al., 2015. Calibration of acoustic instruments. ICES Cooperative Research Report No. 326.

Diggle, P. J., Menezes, R., and Su, T. 2010. Geostatistical inference under preferential sampling. Journal of the Royal Statistical Society: Series C (Applied Statistics), 59: 191–232.

Edwards, J. I., and Armstrong, F. 1983. Measurements of the target strength of live herring and mackerel.

Edwards, J. I., and Armstrong, F. 1984. Target strength experiments on caged fish. Scottish Fisheries Bulletin, 48: 12–20.

Ehrenberg, J. 1972. A method for extracting the fish target strength distribution from acoustic echoes. *In* Ocean 72 - IEEE International Conference on Engineering in the Ocean Environment, pp. 61–64.

Ehrenberg, J. 1974. Two applications for a dual-beam transducer in hydroacoustic fish assessment systems. *In* Engineering in the Ocean Environment, Ocean'74-IEEE International Conference on, pp. 152–155. IEEE. http://ieeexplore.ieee.org/abstract/document/1161349/ (Accessed 17 May 2017).

Ehrenberg, J. 1979. A comparative analysis of in situ methods for directly measuring the acoustic target strength of individual fish. IEEE Journal of Oceanic Engineering, 4: 141–152.

Ehrenberg, J. E., and Torkelson, T. C. 1990. Application of dual-beam and split-beam target tracking in fisheries acoustics. Representation, 29: 329–334.

Everson, I., Watkins, J. L., Bone, D. G., and Foote, K. G. 1990. Implications of a new acoustic target strength for abundance estimates of Antarctic krill. Nature, 345: 338–340.

Fallon, N. G., Fielding, S., and Fernandes, P. G. 2016. Classification of Southern Ocean krill and icefish echoes using random forests. ICES Journal of Marine Science, 73: 1998–2008.

Fässler, S. M. 2010. Target strength variability in Atlantic herring (Clupea harengus) and its effect on acoustic abundance estimates. University of St Andrews. https://research-repository.st-andrews.ac.uk/handle/10023/1703 (Accessed 9 March 2017).

Fässler, S. M., Brunel, T., Gastauer, S., and Burggraaf, D. 2016. Acoustic data collected on pelagic fishing vessels throughout an annual cycle: Operational framework, interpretation of observations, and future perspectives. Fisheries Research, 178: 39–46.

Fässler, S. M. M., Gorska, N., Ona, E., and Fernandes, P. G. 2008. Differences in swimbladder volume between Baltic and Norwegian spring-spawning herring: Consequences for mean target strength. Fisheries Research, 92: 314–321.

Fässler, S. M. M., O'Donnell, C., and Jech, J. M. 2013. Boarfish (Capros aper) target strength modelled from magnetic resonance imaging (MRI) scans of its swimbladder. ICES Journal of Marine Science: Journal du Conseil, 70: 1451–1459.

Fernandes, P. G., Gerlotto, F., Holliday, D. V., Nakken, O., and Simmonds, E. J. 2002. Acoustic applications in fisheries science: the ICES contribution. *In* ICES Marine Science Symposia, pp. 483–492. http://www.ices.dk/sites/pub/Publication%20Reports/Marine%20Science%20Symposia/Phase%202/ICES%20Marine%20Science%20Symposia%20-%20Volume%20215%20-%202002%20-%20Part%2056%20of%2070.pdf (Accessed 15 March 2017).

Fernandes, P. G., Korneliussen, R. J., Lebourges-Dhaussy, A., Masse, J., Iglesias, M., Diner, N., Ona, E., *et al.* 2006. The SIMFAMI project: species identification methods from acoustic multifrequency information. Final Report to the EC No. Q5RS-2001-02054.

Fernandes, P. G. 2009. Classification trees for species identification of fish-school echotraces. ICES Journal of Marine Science, 66: 1073–1080.

Fernandes, P. G., Copland, P., Garcia, R., Nicosevici, T., and Scoulding, B. 2016. Additional evidence for fisheries acoustics: small cameras and angling gear provide tilt angle distributions and other relevant data for mackerel surveys.

Fletcher, W. J., and Santoro, K. 2013. Status reports of the fisheries and aquatic resources of Western Australia 2012/13: the state of the fisheries. Department of Fisheries, Western Australia, Perth.

Fletcher, W.J., and Santoro, K. (eds). 2014. Status Reports of the Fisheries and Aquatic Resources of Western Australia 2013/14: The State of the Fisheries. Department of Fisheries, Western Australia.

Foote, K. G. 1980. Effect of fish behaviour on echo energy: the need for measurements of orientation distributions. Journal Du Conseil, 39: 193–201.

Foote, K. G., Aglen, A., and Nakken, O. 1986. Measurement of fish target strength with a split-beam echo sounder. The Journal of the Acoustical Society of America, 80: 612–621.

Foote, K. G. 1987. Fish target strengths for use in echo integrator surveys. The Journal of the Acoustical Society of America, 82: 981–987.

Foote, K. G., and Traynor, J. J. 1988. Comparison of walleye pollock target strength estimates determined from insitu measurements and calculations based on swimbladder form. The Journal of the Acoustical Society of America, 83: 9–17.

Foote, K. G. 1996. Coincidence echo statistics. The Journal of the Acoustical Society of America, 99: 266–271.

Foote, K. G., and Francis, D. T. I. 2002a. Acoustic scattering by swimbladdered fish: a review. Bioacoustics, 12: 262–265.

Foote, K. G., and Francis, D. T. I. 2002b. Comparing Kirchhoff-approximation and boundary-element models for computing gadoid target strengths. The Journal of the Acoustical Society of America, 111: 1644–1654.

Forbes, S. T., and Nakken, O. 1972. Manual of methods for fisheries resource survey and appraisal. Part 2. The use of acoustic instruments for fish detection and abundance estimation. FAO Man. Fish. Sci, 5: 38.

Francis, D. T. 1993. A gradient formulation of the Helmholtz integral equation for acoustic radiation and scattering. The Journal of the Acoustical Society of America, 93: 1700–1709.

Gastauer, S., Fässler, S. M. M., O'Donnell, C., Høines, Å., Jakobsen, J. A., Krysov, A. I., Smith, L., et al. 2016. The distribution of blue whiting west of the British Isles and Ireland. Fisheries Research, 183: 32–43.

Gauthier, S., and Rose, G. A. 2001a. Diagnostic tools for unbiased in situ target strength estimation. Canadian Journal of Fisheries and Aquatic Sciences, 58: 2149–2155.

Gauthier, S., and Rose, G. A. 2001b. Target Strength of encaged Atlantic redfish (Sebastes spp.). ICES Journal of Marine Science: Journal du Conseil, 58: 562–568.

Geoffroy, M., Rousseau, S., Knudsen, F. R., and Fortier, L. 2015. Target strengths and echotraces of whales and seals in the Canadian Beaufort Sea. ICES Journal of Marine Science: Journal du Conseil: fsv182.

Gimona, A. 2003. A conditional simulation of acoustic survey data: advantages and potential pitfalls. Aquatic Living Resources, 16: 123–129.

Godø, O. R., and Wespestad, V. G. 1993. Monitoring changes in abundance of gadoids with varying availability to trawl and acoustic surveys. ICES Journal of Marine Science, 50: 39–51.

Godø, O. R., Handegard, N. O., Browman, H. I., Macaulay, G. J., Kaartvedt, S., Giske, J., Ona, E., et al. 2014. Marine ecosystem acoustics (MEA): quantifying processes in the sea at the spatio-temporal scales on which they occur. ICES Journal of Marine Science: Journal du Conseil: fsu116.

Gorska, N., Ona, E., and Korneliussen, R. 2005. Acoustic backscattering by Atlantic mackerel as being representative of fish that lack a swimbladder. Backscattering by individual fish. ICES Journal of Marine Science, 62: 984–995.

Guillard, J., and Vergès, C. 2007. The repeatability of fish biomass and size distribution estimates obtained by hydroacoustic surveys using various sampling strategies and statistical analyses. International Review of Hydrobiology, 92: 605–617.

Haddon, M., and Hodgson, K. 2001. Spatial and seasonal stock dynamics of Northern Tiger prawns using fine-scale commercial catch-effort data. Tasmanian Aquaculture and Fisheries Institute. http://frdc.com.au/research/Documents/Final_reports/1999-100-DLD.pdf (Accessed 6 September 2016).

Hamilton, L. J. 2001. Acoustic seabed classification systems. DTIC Document.

Handegard, N. O., Buisson, L. du, Brehmer, P., Chalmers, S. J., Robertis, A., Huse, G., Kloser, R., et al. 2013. Towards an acoustic-based coupled observation and modelling system for monitoring and predicting ecosystem dynamics of the open ocean. Fish and Fisheries, 14: 605–615.

Hazen, E. L., and Horne, J. K. 2003. A method for evaluating the effects of biological factors on fish target strength. ICES Journal of Marine Science: Journal du Conseil, 60: 555–562.

Henderson, M. J., and Horne, J. K. 2007. Comparison of in situ, ex situ, and backscatter model estimates of Pacific hake (Merluccius productus) target strength. Canadian Journal of Fisheries and Aquatic Sciences, 64: 1781–1794.

Horne, J. K. 2003. The influence of ontogeny, physiology, and behaviour on the target strength of walleye pollock (Theragra chalcogramma). ICES Journal of Marine Science: Journal du Conseil, 60: 1063–1074.

ICES. 2007. Collection of acoustic data from fishing vessels. ICES Cooperative Research Report No. 287. 83 pp. International Council for the Exploration of the Sea.

ICES. 2015. Manual for International Pelagic Surveys (IPS). Series of ICES Survey Protocols, SISP 9. International Council for the Exploration of the Sea - IPS.

Jech, J. M., Horne, J. K., Chu, D., Demer, D. A., Francis, D. T., Gorska, N., Jones, B., *et al.* 2015. Comparisons among ten models of acoustic backscattering used in aquatic ecosystem research. The Journal of the Acoustical Society of America, 138: 3742–3764.

Johannesson, K. A., and Losse, G. F. 1977. Methodology of acoustic estimations of fish abundance in some UNDP/FAO resources survey projects.[Conference paper]. Rapports et Proces-Verbaux des Reunions (ICES). v. 170. http://agris.fao.org/agris-search/search.do?recordID=DK19770191755 (Accessed 18 May 2017).

Jolly, G. M., and Hampton, I. 1990. A stratified random transect design for acoustic surveys of fish stocks. Canadian Journal of Fisheries and Aquatic Sciences, 47: 1282–1291.

Kloser, R. J. 1996. Improved precision of acoustic surveys of benthopelagic fish by means of a deep-towed transducer. ICES Journal of Marine Science: Journal du Conseil, 53: 407–413.

Kloser, R. J., Ryan, T. E., Young, J. W., and Lewis, M. E. 2009. Acoustic observations of micronekton fish on the scale of an ocean basin: potential and challenges. ICES Journal of Marine Science: Journal du Conseil: fsp077.

Kloser, R. J., Ryan, T. E., Macaulay, G. J., and Lewis, M. E. 2011. In situ measurements of target strength with optical and model verification: a case study for blue grenadier, Macruronus novaezelandiae. ICES Journal of Marine Science: Journal du Conseil, 68: 1986–1995.

Knudsen, F. R., Hawkins, A., McAllen, R., and Sand, O. 2009. Diel interactions between sprat and mackerel in a marine lough and their effects upon acoustic measurements of fish abundance. Fisheries Research, 100: 140–147.

Korneliussen, R. J., Diner, N., Ona, E., Berger, L., and Fernandes, P. G. 2008. Proposals for the collection of multifrequency acoustic data. ICES Journal of Marine Science: Journal du Conseil, 65: 982–994.

Korneliussen, R. J., Heggelund, Y., Eliassen, I. K., and Johansen, G. O. 2009. Acoustic species identification of schooling fish. ICES Journal of Marine Science: Journal du Conseil, 66: 1111–1118.

Korneliussen, R. J., Heggelund, Y., Macaulay, G. J., Patel, D., Johnsen, E., and Eliassen, I. K. 2016. Acoustic identification of marine species using a feature library. Methods in Oceanography, 17: 187–205.

Koslow, J. A. 2009. The role of acoustics in ecosystem-based fishery management. ICES Journal of Marine Science: Journal du Conseil: fsp082.

Kubecka, J., Duncan, A., Duncan, W. M., Sinclair, D., and Butterworth, A. J. 1994. Brown trout populations of three Scottish lochs estimated by horizontal sonar and multimesh gill nets. Fisheries Research, 20: 29–48.

Kupschus, S., Schratzberger, M., and Righton, D. 2016. Practical implementation of ecosystem monitoring for the ecosystem approach to management. Journal of Applied Ecology, 53: 1236–1247.

Latour, R. J., Brush, M. J., and Bonzek, C. F. 2003. Toward Ecosystem-Based Fisheries Management. Fisheries, 28: 10–22.

Lezama-Ochoa, A., Irigoien, X., Chaigneau, A., Quiroz, Z., Lebourges-Dhaussy, A., and Bertrand, A. 2014. Acoustics Reveals the Presence of a Macrozooplankton Biocline in the Bay of

Biscay in Response to Hydrological Conditions and Predator-Prey Relationships. PLoS ONE, 9: e88054.

Love, R. H. 1971a. Measurements of fish target strength: a review. Fish. Bull, 69: 703–715.

Love, R. H. 1971b. Dorsal-aspect target strength of an individual fish. The Journal of the Acoustical Society of America, 49: 816–823.

Love, R. H. 1977. Target strength of an individual fish at any aspect. The Journal of the Acoustical Society of America, 62: 1397–1403.

Macaulay, G. J. 2002. Anatomically detailed acoustic scattering models of fish. Bioacoustics, 12: 275–277.

Macaulay, G. J., Kloser, R. J., and Ryan, T. E. 2012. In situ target strength estimates of visually verified orange roughy. ICES Journal of Marine Science: Journal du Conseil: fss154.

Mackie, M. C., McCauley, R. D., Gill, R. H., and Gaughan, D. J. 2009. Management and monitoring of fish spawning aggregations within the west coast bio-region of Western Australia. Fisheries Research Report: 42–56.

MacLennan, D. N. 1990. Acoustical measurement of fish abundance. The Journal of the Acoustical Society of America, 87: 1–15.

MacLennan, D. N., and Menz, A. 1996. Interpretation of in situ target-strength data. ICES Journal of Marine Science: Journal du Conseil, 53: 233–236.

Maravelias, C. D., Reid, D. G., Simmonds, E. J., and Haralabous, J. 1996. Spatial analysis and mapping of acoustic survey data in the presence of high local variability: geostatistical application to North Sea herring (Clupea harengus). Canadian Journal of Fisheries and Aquatic Sciences, 53: 1497–1505.

Marko, P. B., Lee, S. C., Rice, A. M., Gramling, J. M., Fitzhenry, T. M., McAlister, J. S., Harper, G. R., *et al.* 2004. Fisheries: Mislabelling of a depleted reef fish. Nature, 430: 309–310.

Massé, J., Sanchez, F., Delaunay, D., Robert, J. M., and Petitgas, P. 2016. A partnership between science and industry for a monitoring of anchovy & sardine in the Bay of Biscay: When fishermen are actors of science. Fisheries Research, 178: 26–38.

Matheron, G., and others. 1965. Les variables régionalisées et leur estimation. http://imb-biblio.u-bourgogne.fr/Record.htm?record=064312488259&idlist=1 (Accessed 23 May 2017).

Matheron, G. 1967. Kriging or polynomial interpolation procedures. CIMM Transactions, 70: 240–244.

Matheron, G. 1971. The theory of regionalised variables and its applications.

McClatchie, S., Alsop, J., and Coombs, R. F. 1996. A re-evaluation of relationships between fish size, acoustic frequency, and target strength. ICES Journal of Marine Science: Journal du Conseil, 53: 780–791.

McQuinn, I. H., and Winger, P. D. 2003. Tilt angle and target strength: target tracking of Atlantic cod (Gadus morhua) during trawling. ICES Journal of Marine Science: Journal du Conseil, 60: 575–583.

Medwin, H., and Clay, C. S. 1998. Fundamentals of Acoustical Oceanography Academic. New York: 11–12.

Melvin, G., Stephenson, R. L., Power, M. J., Fife, F. J., Clark, K. J., and et al. 2001. Industryacoustic surveys as the basis for in-season decisions in a co-managementregime.

Melvin, G., Li, Y. C., Mayer, L., and Clay, A. 2002. Commercial fishing vessels, automaticacoustic logging systems and 3D data visualization: 179–189.

Melvin, G. D., Kloser, R., and Honkalehto, T. 2016. The adaptation of acoustic data from commercial fishing vessels in resource assessment and ecosystem monitoring. Fisheries Research, 178: 13–25.

Midttun, L., and Hoff, I. 1962. Measurements of the reflection of sound by fish. https://brage.bibsys.no/xmlui/bitstream/handle/11250/114638/sh_vol13_03_1962.pdf?sequence=1 (Accessed 17 May 2017).

Misund, O. A., and Beltestad, A. K. 1996. Target-strength estimates of schooling herring and mackerel using the comparison method. ICES Journal of Marine Science: Journal du Conseil, 53: 281–284.

Misund, O. A. 1997. Underwater acoustics in marine fisheries and fisheries research. Reviews in Fish Biology and Fisheries, 7: 1–34.

Mitson, R. 2003. Causes and effects of underwater noise on fish abundance estimation. Aquatic Living Resources, 16: 255–263.

Monk, J. 2014. How long should we ignore imperfect detection of species in the marine environment when modelling their distribution? Fish and fisheries, 15: 352–358.

Nakken, O., and Olsen, K. 1977. Target strength measurements of fish. ICES.

Nero, R. W., Thompson, C. H., and Jech, J. M. 2004. In situ acoustic estimates of the swimbladder volume of Atlantic herring (Clupea harengus). ICES Journal of Marine Science: Journal du Conseil, 61: 323–337.

Newman, S. J., Smith, K. A., and Skepper, C. L. 2008. Northern demersal scalefish managed fishery. Department of Fisheries, Western Australian Fisheries & Marine Research Laboratories.

Newman, S. J., Harvey, E.S., Rome, B.M., McLean, D.L., and Skepper, C.L. 2012. Relative efficiency of fishing gears and investigation of resource availability in tropical demersal scalefish fisheries. . Final Report FRDC Project No. 2006/031. Fisheries Research Report No. 231. Department of Fisheries, Western Australia, Western Australia.

Newman, S. J., Wakefield, C., Skepper, C., Boddington, D., Blay, N., Jones, R., and Wallis, D. 2014. North Coast Demersal Fisheries Status Report. *In* Status Reports of the Fisheries and Aquatic Resources of Western Australia 2013/14: The State of the Fisheries; eds.: W.J. Fletcher and K. Santoro. Department of Fisheries, Western Australia.

Newman, S. J., Wakefield, C., Skepper, C., Boddington, D., Blay, N., Jones, R., and Dobson, P. 2015. North Coast Demersal Fisheries Status Report In: Status Reports of the Fisheries and Aquatic Resources of Western Australia 2014/15: The State of the Fisheries eds. W.J. Fletcher and K. Santoro, Department of Fisheries, Western Australia, pp. 39-48.

Nøttestad, L., Diaz, J., Penã, H., Søiland, H., Huse, G., and Fernö, A. 2016. Feeding strategy of mackerel in the Norwegian Sea relative to currents, temperature, and prey. ICES Journal of Marine Science, 73: 1127–1137.

O'Driscoll, R. L., and Macaulay, G. J. 2005. Using fish-processing time to carry out acoustic surveys from commercial vessels. ICES Journal of Marine Science: Journal du Conseil, 62: 295–305.

O'Driscoll, R. L., Gauthier, S., and Devine, J. A. 2009. Acoustic estimates of mesopelagic fish: as clear as day and night? ICES Journal of Marine Science, 66: 1310–1317.

Ona, E. 1999. Methodology for target strength measurements. ICES Cooperative research report, 235: 59.

Ona, E. 2001. Herring tilt angles, measured through target tracking. http://brage.bibsys.no/xmlui/handle/11250/108201 (Accessed 9 August 2016).

Ona, E. 2003. An expanded target-strength relationship for herring. ICES Journal of Marine Science: Journal du Conseil, 60: 493–499.

Peña, H., and Foote, K. G. 2008. Modelling the target strength of Trachurus symmetricus murphyi based on high-resolution swimbladder morphometry using an MRI scanner. ICES Journal of Marine Science: Journal du Conseil, 65: 1751–1761.

Peña, M., and Calise, L. 2016. Use of SDWBA predictions for acoustic volume backscattering and the Self-Organizing Map to discern frequencies identifying Meganyctiphanes

norvegica from mesopelagic fish species. Deep Sea Research Part I: Oceanographic Research Papers, 110: 50–64.

Petitgas, P. 1993. Use of a disjunctive kriging to model areas of high pelagic fish density in acoustic fisheries surveys. Aquatic Living Resources, 6: 201–209.

Petitgas, P. 2001. Geostatistics in fisheries survey design and stock assessment: models, variances and applications. Fish and Fisheries, 2: 231–249.

Petitgas, P., Woillez, M., Doray, M., and Rivoirard, J. 2016. A Geostatistical Definition of Hotspots for Fish Spatial Distributions. Mathematical Geosciences, 48: 65–77.

Piet, G. J., and Quirijns, F. J. 2009. The importance of scale for fishing impact estimations. Canadian Journal of Fisheries and Aquatic Sciences, 66: 829–835.

Pikitch, E. K., Santora, C., Babcock, E. A., Bakun, A., Bonfil, R., Conover, D. O., Dayton, P., *et al.* 2004. Ecosystem-Based Fishery Management. Science, 305: 346–347.

Proud, R., Cox, M. J., and Brierley, A. S. 2017. Biogeography of the Global Ocean's Mesopelagic Zone. Current Biology, 27: 113–119.

Pyć, C. D., Geoffroy, M., and Knudsen, F. R. 2016. An evaluation of active acoustic methods for detection of marine mammals in the Canadian Beaufort Sea. Marine Mammal Science, 32: 202–219.

Quinn, T. J., and Deriso, R. B. 1999. Quantitative fish dynamics. Oxford University Press. https://books.google.com.au/books?hl=en&lr=&id=5FVBj8jnh6sC&oi=fnd&pg=PR11& dq=Quinn+and+Deriso+CPUE&ots=tTcKaV9cTm&sig=WNg196KuuMA0kXo4M0tQ09V4 Co4 (Accessed 6 September 2016).

Rivoirard, J., Simmonds, J., Foote, K. G., Fernandes, P., and Bez, N. 2000. Geostatistics for Estimating Fish Abundance. Blackwell Science Ltd, Oxford. 216 pp.

Robertis, A. D., and Higginbottom, I. 2007. A post-processing technique to estimate the signal-to-noise ratio and remove echosounder background noise. ICES Journal of Marine Science: Journal du Conseil, 64: 1282–1291.

Robotham, H., Bosch, P., Gutiérrez-Estrada, J. C., Castillo, J., and Pulido-Calvo, I. 2010. Acoustic identification of small pelagic fish species in Chile using support vector machines and neural networks. Fisheries Research, 102: 115–122.

Ryan, T. E., Downie, R. A., Kloser, R. J., and Keith, G. 2015. Reducing bias due to noise and attenuation in open-ocean echo integration data. ICES Journal of Marine Science: Journal du Conseil, 72: 2482–2493.

Sadovy, Y., and Domeier, M. 2005. Are aggregation-fisheries sustainable? Reef fish fisheries as a case study. Coral Reefs, 24: 254–262.

Sawada, K., Furusawa, M., and Williamson, N. J. 1993. Conditions for the precise measurement of fish target strength *in situ*. The Journal of the Marine Acoustics Society of Japan, 20: 73–79.

Sawada, K. 2002. Study on the precise estimation of the target strength of fish. Bulletin of Fisheries Research Agency (Japan). http://agris.fao.org/agris-search/search.do?recordID=JP2002005603 (Accessed 18 May 2017).

Scoulding, B., Chu, D., Ona, E., and Fernandes, P. G. 2015. Target strengths of two abundant mesopelagic fish species. The Journal of the Acoustical Society of America, 137: 989–1000.

Scoulding, B., Gastauer, S., MacLennan, D. N., Fässler, S. M. M., Copland, P., and Fernandes, P. G. 2016. Effects of variable mean target strength on estimates of abundance: the case of Atlantic mackerel (Scomber scombrus).

Selivanovsky, D. A., Stunzhas, P. A., and Didenkulov, I. N. 1996. Acoustical investigation of phytoplankton. ICES Journal of Marine Science: Journal du Conseil, 53: 313–316.

Shibata, K. 1971. Experimental measurement of target strength of fish. Modern fishing gear of the world, 3: 104–108.

Simmonds, E. J., Williamson, N. J., Gerlotto, F., Aglen, A., and others. 1992. Acoustic survey design and analysis procedure: a comprehensive review of current practice. Internat. Council for the Exploration of the Sea. http://www.ices.dk/sites/pub/Publication%20Reports/Cooperative%20Research%20R eport%20(CRR)/crr187/CRR187.pdf (Accessed 13 May 2017).

Simmonds, J., and MacLennan, D. N. 2005. Fisheries acoustics: theory and practice. John Wiley & Sons. https://books.google.nl/books?hl=en&lr=&id=ktUOvnfzB-QC&oi=fnd&pg=PR5&dq=simmonds+and+maclennan+2005+fisheries+acoustics&ots=K hFAju0IKm&sig=AqqX84hCs6CvysUa4fnhtcEgrc0 (Accessed 9 March 2017).

Siwabessy, P. J. W. 2001. An investigation of the relationship between seabed type and benthic and bentho-pelagic biota using acoustic techniques. http://espace.library.curtin.edu.au/R?func=dbin-jump-full&object_id=12197 (Accessed 6 September 2016).

Smith, A. D. M., Fulton, E. J., Hobday, A. J., Smith, D. C., and Shoulder, P. 2007. Scientific tools to support the practical implementation of ecosystem-based fisheries management. ICES Journal of Marine Science, 64: 633–639.

Soule, M., Barange, M., and Hampton, I. 1995. Evidence of bias in estimates of target strength obtained with a split-beam echo-sounder. ICES Journal of Marine Science: Journal du Conseil, 52: 139–144.

Stanton, T. K., Chu, D., Wiebe, P. H., and Clay, C. S. 1993. Average echoes from randomly oriented random-length finite cylinders: Zooplankton models. The Journal of the Acoustical Society of America, 94: 3463–3472.

Stanton, T. K., Chu, D., and Wiebe, P. H. 1996. Acoustic scattering characteristics of several zooplankton groups. ICES Journal of Marine Science: Journal du Conseil, 53: 289–295.

Stanton, T. K., and Chu, D. 2000. Review and recommendations for the modelling of acoustic scattering by fluid-like elongated zooplankton: euphausiids and copepods. ICES Journal of Marine Science: Journal du Conseil, 57: 793–807.

Traynor, J. J., and Ehrenberg, J. E. 1979. Evaluation of the dual beam acoustic fish target strength measurement method. Journal of the Fisheries Board of Canada, 36: 1065–1071.

Traynor, J. J., and Ehrenberg, J. E. 1990. Fish and standard-sphere target-strength measurements obtained with a dual-beam and split-beam echo-sounding system. Rapp Pv Reun Cons int Explor Mer, 189: 325–335.

Trenkel, V., Ressler, P. H., Jech, M., Giannoulaki, M., and Taylor, C. 2011. Underwater acoustics for ecosystem-based management: state of the science and proposals for ecosystem indicators. Marine Ecology-Progress Series, 442: 285–301.

Urick, R. J. 1983. Principles of underwater sound. http://library.wur.nl/WebQuery/clc/1854688 (Accessed 12 May 2017).

Voglis, G. M., and Cook, J. C. 1966. Underwater applications of an advanced acoustic scanning equipment. Ultrasonics, 4: 1–9.

von Szalay, P. G., and McConnaughey, R. A. 2002. The effect of slope and vessel speed on the performance of a single beam acoustic seabed classification system. Fisheries Research, 56: 99–112.

Walline, P. D. 2007. Geostatistical simulations of eastern Bering Sea walleye pollock spatial distributions, to estimate sampling precision. ICES Journal of Marine Science: Journal du Conseil, 64: 559–569.

Williams, D. M., Fowler, A. J., and Newman, S. J. 1997. Development of trap and drop-line sampling techniques for reef fishes: a report to the Great Barrier Reef Marine Park Authority. http://elibrary.gbrmpa.gov.au/jspui/handle/11017/299 (Accessed 6 September 2016).

Woillez, M., Poulard, J.-C., Rivoirard, J., Petitgas, P., and Bez, N. 2007. Indices for capturing spatial patterns and their evolution in time, with application to European hake (Merluccius merluccius) in the Bay of Biscay. ICES Journal of Marine Science: Journal du Conseil, 64: 537–550.

Woillez, M., Rivoirard, J., and Fernandes, P. G. 2009a. Evaluating the uncertainty of abundance estimates from acoustic surveys using geostatistical simulations. ICES Journal of Marine Science: Journal du Conseil: fsp137.

Woillez, M., Rivoirard, J., and Petitgas, P. 2009b. Notes on survey-based spatial indicators for monitoring fish populations. Aquatic Living Resources, 22: 155–164.

Woillez, M., Walline, P. D., Ianelli, J. N., Dorn, M. W., Wilson, C. D., and Punt, A. E. 2016. Evaluating total uncertainty for biomass-and abundance-at-age estimates from eastern Bering Sea walleye pollock acoustic-trawl surveys. ICES Journal of Marine Science: Journal du Conseil, 73: 2208–2226.

Chapter 2

Target strength estimates of red emperor (*Lutjanus sebae*) with Bayesian parameter calibration

Sven Gastauer[1,2,*], Ben Scoulding[2], Sascha M. M. Fässler[2], Daniel P. L. D. Benden[2], and Miles Parsons[1]

[1]Centre for Marine Science and Technology, Curtin University, GPO Box U1987, Perth, WA 6845, Australia

[2]Wageningen Institute for Marine Resources and Ecosystem Studies (IMARES), PO Box 68, 1970 AB IJmuiden, The Netherlands

* Corresponding author.: sven.gastauer@postgrad.curtin.edu.au

2.1 Abstract

Red emperor (*Lutjanus sebae*) is a long-lived tropical demersal snapper which is widely distributed in the Western Pacific and Indian Ocean. Despite the commercial and recreational importance of the species for the Northern Demersal Scalefish Fishery off the Northwest coast of Western Australia, we still lack a thorough understanding of its distribution and abundance in the area. To better understand the acoustic scattering properties of red emperor its acoustic backscattering characteristics were modelled based on swimbladder and body morphology, determined using computed tomography scans. A Kirchhoff-ray mode approximation was coupled with empirical (*ex situ*) measurements of target strength (*TS*) obtained from a 38 and 120 kHz split-beam echosounder on board a fishing vessel. Bayesian methods were used for model parameter calibration, which provided uncertainty estimates for some of the *TS*-model parameters. The derived *TS*-length relationships were $19.7 \log_{10}(L) - 75.5$ (C.I. 5.9 dB) at 120 kHz and $14.6 \log_{10}(L) - 64.9$ (C.I. 5.8 dB) at 38 kHz. The study demonstrated that small commercial fishing vessels can be used to conduct *ex situ* experiments and target strength modelling can be effectively based on computer tomography scans. This relatively low cost approach could be applied to other species.

Keywords: Target Strength; Bayesian inference; KRM; vessel of opportunity; Fisheries acoustics; Lutjanus sebae

2.2 Introduction

Operating in a large and dynamic environment, offshore fisheries, such as the Northern Demersal Scalefish Fishery (NDSF) in Western Australia, generally require expensive scientific surveys to support stock management. Recording calibrated multifrequency acoustic data on board vessels of opportunity could be an effective alternative to provide data on fish stock size (ICES 2007; Barbeaux et al. 2013). Red emperor (*Lutjanus sebae*) is a long-lived tropical demersal snapper of the Lutjanidae family. It is generally observed in reef environments, epibenthic communities, limestone sand flats and gravel patches from very shallow (1 m) to deeper waters (> 180 m) (Newman and Dunk, 2002). It is widely distributed throughout the Western Pacific and the Indian Ocean and made up almost half (40.15 – 46.96 %) of the total catches of the NDSF between 2005 - 2014 (Newman *et al.*, 2014). Further, it is a popular game fishing species (Newman and Dunk, 2002). To better understand its population dynamics, close collaboration with commercial stakeholders is a beneficial option.

Echo-integration can be used to estimate fish densities within an area and thus contribute to the development of an improved sustainable management plan (ICES, 2007). If acoustic echo-integration techniques (MacLennan 1990) are to be used to estimate the abundance of red emperor, an understanding of their acoustic properties is required. To convert acoustic backscatter into fish abundance or biomass, a target strength (*TS*, in dB) to length (L, in cm) or weight (W, in grams) relationship is needed. *TS* is a logarithmic description of the proportion of incident acoustic energy backscattered from an individual target, such as a fish (Simmonds and MacLennan, 2005). *TS* values are available for numerous commercially important and routinely surveyed pelagic species (Gauthier and Rose, 2001b; Ona, 2003; Kloser *et al.*, 2013). The values are determined by various methods including: empirical measurements of tethered (dead or alive) (Nakken and Olsen, 1977) or caged fish (alive) (Edwards and Armstrong 1981), fish measured *in situ* (Soule et al. 1995), and estimates derived from mathematical models (Clay and Horne 1994; Ye 1997). *In situ* measurements on free-swimming individuals are deemed to provide the most representative estimates of *TS*. However, these are not always practicable and have limitations in species identification, target separation (Soule et al. 1995) and uncertainty in the acoustic (MacLennan and Menz 1996) and biological (MacLennan 1990) representation. Advances in computational power have enabled the development of complex theoretical scattering models that have been used to validate empirical *TS* measurements, based on morphological information of a given species in their

environment (Horne *et al.*, 2000; Foote and Francis, 2002a; Fässler *et al.*, 2009, 2013). Still, the stochastic nature of *TS* has to be acknowledged and the resulting variance and its influence on biomass estimates have to be taken into account.

This paper describes the *TS* of red emperor estimated using the Kirchhoff-ray mode approximation (KRM) (Clay and Horne, 1994) with a Bayesian estimation approach (Fässler *et al.*, 2009). Computed tomography (CT) scans were conducted to measure swimbladder and fish body morphology for use in the KRM model. The empirical *ex situ TS* data were used to validate and fit the model. The model includes a Bayesian estimation component to deal with variability in orientation - one of the main factors influencing the backscatter of a fish (Hazen and Horne, 2003). Few studies have utilised a Bayesian approach to model *TS* before, even though its benefits, including improved variance estimates by being informed by data and expert judgement, are widely recognised (Hammond, 1997; Fässler *et al.*, 2009).

2.3 Material and Methods

2.3.1 Fish samples

Specimens of red emperor were collected on the 7th and 8th of March 2015, between 14.46° and 17.57° S, and 121.47° and 121.52° E, at depths around 70 m, during a dedicated research trip on the chartered trap fishing vessel 'Carolina M' (≈15 m in length). All samples were caught using standard commercial steel trap cages, with a mesh size of 5 cm. Traps were pulled on board as slowly as possible to avoid potential damage to the swimbladder that can occur from rapid pressure changes in water. Red emperor is known to be very robust against barotrauma and swimbladder ruptures, and can acclimatise to depth very quickly (Brown et al. 2010). Once on deck the fish were acclimated in a well oxygenated tank for 24 hours which allowed the swimbladder to adjust to water pressure at the surface. Some specimens were used for cage experiments and others for fish scans.

2.3.2 Ex situ cage experiments

All *ex situ* measurements were made with a hull-mounted 38 kHz and 120 kHz split-beam SIMRAD ES70 echosounder. The echosounders were calibrated using a 38.1 mm tungsten carbide (WC) sphere prior to the investigation period, following standard sphere procedures (Demer, D.A. *et al.*, 2015). A pulse duration of 1.024 ms with a power of 2000 W was used for the 38 kHz transducer, whilst a pulse duration of 0.064 ms and a power of 1000 W was used for the 120 kHz transducer. The pulse durations and power inputs were kept at

the settings normally used by the fishermen, to allow for best compatibility with acoustic data collected during routine operations. Given the power settings were above the recommended settings (Korneliussen et al. 2008), tank calibration experiments were conducted to test for potential bias in the recorded data, but no abnormalities could be detected. The ping rate was set to the maximum. *TS* of individual red emperors were measured in a custom built 1.5 x 1.5 x 1.5 m monofilament cage suspended > 7 m below the transducer, which is outside the near-field zone (near-field at 38 kHz and 120 kHz, with 7° nominal beam widths, were 2.75 m and 0.89 m, respectively). The cage could be manually manoeuvred to maintain its position within the acoustic beam by four point attachments using hand-lines on the deck (Figure 2.1). The cage was held together at the top and bottom by hollow water-filled PVC tubes. To prevent the fish from resting in the cage corners, the mesh was knitted together so that a dent was left in the centre of the cage. This made the edges harder to access. Multiple 500 gram diving weights were attached to the cage bottom. This aided in sinking and provided improved stability once at depth. This was of particular importance, given the strong tidal currents that can be found in the research area. A 38.1 mm WC sphere was attached 2 m below the cage to provide reference values and to measure the performance of the system. After the *ex situ* measurements, the fish were placed in an ice slurry and then frozen for radiographic imagery. Total length (TL, to the nearest 0.5 cm) and total weight (TW, in grams) of each specimen were measured. Five experiments containing one fish each were conducted.
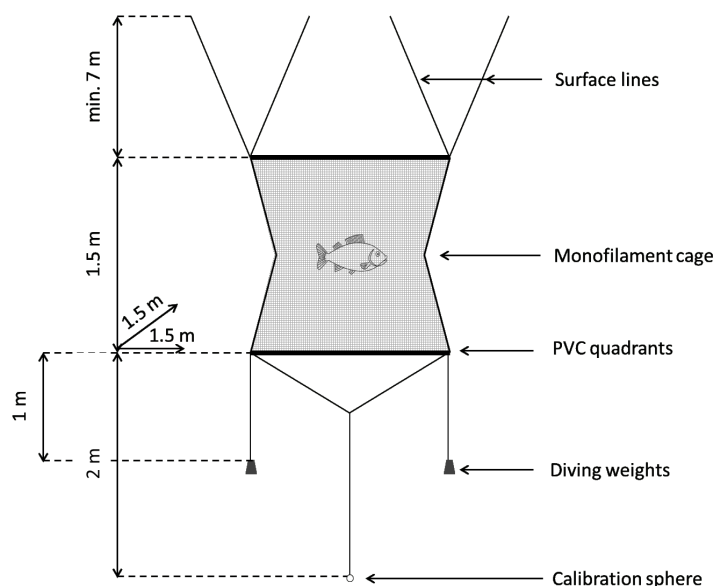
Figure 2.1 Monofilament experimental cage setup used for measuring target strength ex situ with indication of the attached weights, calibration sphere and cameras.

All acoustic data were corrected for triangular wave error (Ryan and Kloser, 2004) and calibration settings were applied prior to the post-processing procedure in Echoview 6.1 (Echoview Software Pty Ltd 2015). Firstly, a single target detection algorithm (e.g. Soule et al. 1997) was used to isolate single fish targets within the cage boundaries. Next, an alpha-beta target tracking algorithm (Blackman 1986) was used to assign individual targets to tracks based on user-defined criteria (*TS* Threshold = -50 dB; Maximum beam compensation = 6 dB; Maximum standard deviation of Minor- or Major-axis = 0.6°). The algorithm predicted target locations based on position (the alpha parameter) and velocity (the beta parameter) of targets at previous ping(s), following a set of acceptance rules. Target tracking allowed investigation of the *TS* variation associated with individual fish.

The bootstrapped mean *TS*, standard deviation (SD) and confidence intervals at 95% of all tracks was used to solve the *TS-L* equation of the form $TS = m \log_{10}(L) + b_{20}$, where b_{20} is a species-specific intercept value, *m* describes the slope and *L* is the total length of the fish (in cm) (Simmonds and MacLennan 2005). To understand the tilt angle distribution of the *ex situ* recordings, the tilt angle (θ) of the fish tracks was approximated using the change in height ($\delta(h)$) and distance, observed in 3D space (z_{3D}), with $\theta = cosine\left(\frac{\delta(h)}{z_{3D}}\right)$ (Ona 2001).

2.3.3 Fish scans

A CT scanner (Siemens SOMATOM Dual Energy 64 slices) was used to measure the dimensions and shapes of the fish body and swimbladder, which are used as inputs to the KRM backscatter model. Prior to scanning, specimens were placed on a styrofoam pedestal (invisible to the scanner), resting on the dorsoventral axis. Data were stored in the standard DICOM format with an in-plane resolution of 0.3 - 0.52 mm and slice spacing of 0.6 mm. Fish and swimbladder shapes were extracted using a purpose built software tool, developed in Python 2.7 (Python Software Foundation, https://www.python.org/). The software allowed DICOM files or folders to be read in and displayed in the available coronal and sagittal planes, with an additional axial view. Various filters (i.e. mean, median, erosion, inversion and binary transformation) were applied to improve the contour extraction algorithm. The software outputs .csv files containing the vertical extreme points of the fish and swimbladder on each slice (x_{upper} and x_{lower}) and the corresponding width. The resulting extremes of fish body and swimbladder dimensions on each slice were used to approximate these 3D shapes respectively as a series of fluid- and gas-filled cylinders. These shape approximations were then used as input for the KRM, modelling *TS* for each of the fish individually. The software also produces a

3D-mesh STL file. This mesh was used to construct a 3D representation of the swimbladder and to determine the respective volume and length coordinates of the entire swimbladder surface.

2.3.4 Kirchhoff-ray-mode model

The KRM model (Clay and Horne, 1994) calculates the combined backscatter of an object as the summed contributions of consecutive short, gas- or fluid-filled cylinders (Clay and Horne 1994). The fish body and the gas-bearing swimbladder were modelled as respective sets of fluid- and gas-filled cylinders. The backscatter was expressed as Reduced Scattering Length (RSL). RSL refers to the estimated scattering length, normalised by the fish caudal length (L). In other words, the RSL is the cumulative sum of backscattering cross-sections (σ_{bs}) of each finite cylinder. RSL relates to TS by:

$$TS = 10 \log_{10}(RSL^2 \times L^2).$$

(1)

Sound speed and density contrasts of sea water, swimbladder and fish body were assumed to be fixed (Table 2.1). Using the information from the fish scans and changing the tilt angle parameter in the KRM model, RSL and subsequently TS were computed over a range of tilt angles (ϑ; 50 to 130 °) to represent the potential orientation range exhibited by the fish. Total fish backscatter was calculated as the combined summation of backscatter contributions of both swimbladder and fish body cylindrical elements (Clay and Horne 1994).

Table 2.1 Constant parameter values used for Kirchhoff-Ray model of red emperor target strength.

Description	Symbol	Value	Unit	Source
Density of sea water	ρ_w	1026	kg/m^3	Gauthier and Horne (2004)
Density of fish body	ρ_{fb}	1071	kg/m^3	Fassler et al. (2009b)
Density of swimbladder gas	ρ_{sb}	2.64	kg/m^3	Clay et al. (1991)
Sound speed of sea water	c_w	1541.2	ms^{-1}	CTD measurements
Sound speed in fish body	c_{fb}	1570	ms^{-1}	Gauthier and Horne (2004)
Sound speed in swimbladder	c_{sb}	340	ms^{-1}	Yasuma et al. (2010)
Echosounder frequency	F	38, 120	kHz	-

| Tilt angle | Θ | [50,130] | ° | - |
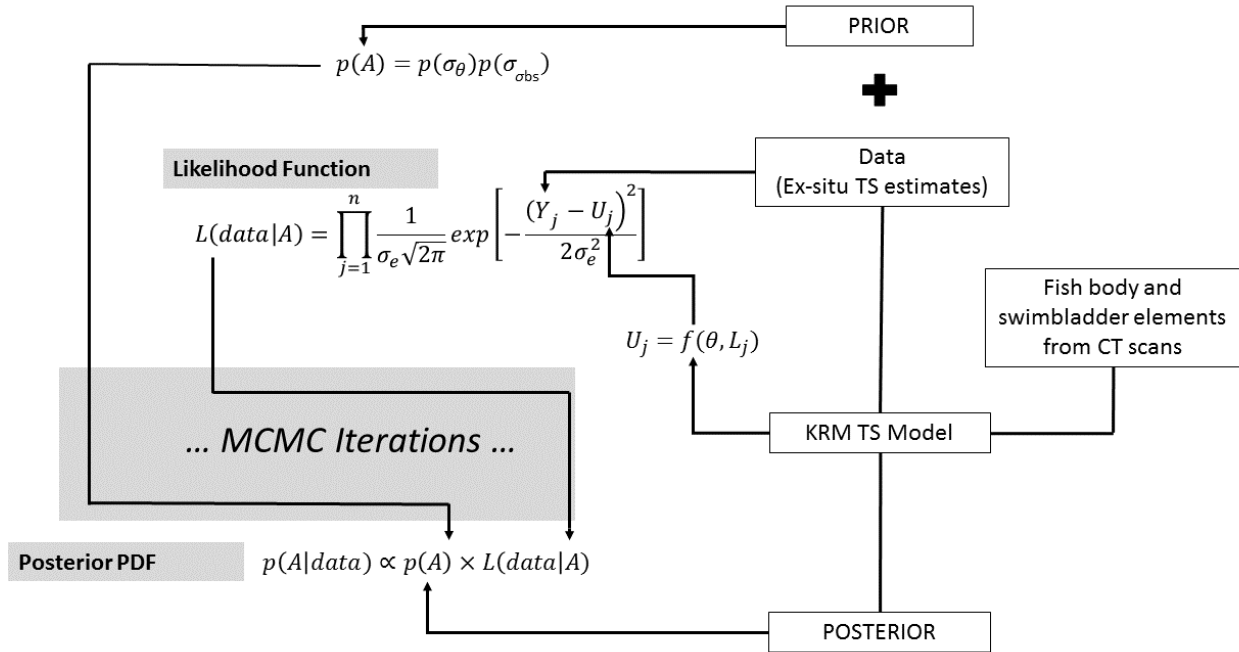
Figure 2.2 Flow chart illustrating the Bayesian parameter estimation process; the posterior PDF with the parameters (A) given the data (based on ex situ experiments) is computed based on uniform prior information (standard deviation of tilt angle (σ_θ) and the standard deviation of mean backscattering cross-sections (σ_{obs})) and the likelihood of the data, given the parameters A, estimated based on length dependent TS (Y_j) from the data and modelled tilt angle and length dependent TS estimates (U_j) from the KRM model where σ_e is the standard deviation of the error

2.3.5 Bayesian estimation of model parameters

A flowchart of the Bayesian parameter estimation process can be found in Figure 2.2. Model parameter estimation can be achieved with different methods. An advantage of using Bayesian inference is that it provides an unambiguous way to combine observations with prior knowledge about model parameters (Hartig *et al.*, 2012). The resulting joint conditional posterior probability distribution $p(A|data)$ for model parameters *A*, given the data, is calculated using Bayes' theorem

$$p(A|data) = \frac{p(data|A) \times p(A)}{p(data)},$$ (2)

where p(data|A) denotes the likelihood function and describes the probability of obtaining the data with the given model parameters *A*. Here, the "data" were the *ex situ TS* measurements

obtained from the caged fish, and "model" was the KRM *TS* model. Uniform distributions were used as priors for the two non-fixed parameters, as little information on these parameters was available beforehand. The term *p*(data) is a normalising constant.

Assuming normality, the likelihood function is

$$L(data|A) = \prod_{j=1}^{n} \frac{1}{\sigma_e \sqrt{2\pi}} exp\left[-\frac{(Y_j - U_j)^2}{2\sigma_e^2}\right], \tag{3}$$

with Y_j the jth observed *TS* value and U_j the *TS* value predicted with the KRM model using parameters values *A* together with fixed values for sound speed and density contrasts of sea water, swimbladder and fish bodies (Table 2.1).

Two model parameters (*A*) were estimated: the standard deviation of the tilt angle distribution (SD_θ) for which a uniform prior distribution (SD_θ ~ Uniform (0.01,1)) was used, and the standard deviation of mean backscattering cross-sections ($SD_{\sigma bs}$), again a uniform prior distribution ($SD_{\sigma bs}$ ~ Uniform (0.001,1)) was used (Hazen and Horne, 2003). Both priors were defined independently, as well as independent from fish length (*L*), standard deviation of fish length (SD_L), and all density and sound speed contrasts.

Bayesian computation was carried out through Metropolis-Hastings Markov chain Monte Carlo sampling (MCMC) (Metropolis *et al.*, 1953) using R 3.2.5 (R Core Team 2016). Posterior distributions converged prior to 200 iterations; however, the first 2,000 samples were conservatively discarded as burn in phase. The subsequent 10,000 samples from the joint posterior distribution were then retained.

As the samples from the posterior distributions of the two parameters were independent for all fishes, separate parametric distributions were fitted to the marginal posterior parameter values. The marginal posterior distribution of SD_θ was best described by a normal distribution of the shape:

$$f(x) = \frac{1}{\sqrt{(2\pi)}\sigma} e^{\frac{(x-u)^2}{2\sigma^2}}, \tag{5}$$

where μ is the mean of the distribution and σ the standard deviation. The posterior distribution of $SD_{\sigma bs}$ was described by a gamma distribution of the shape:

$$f(x) = \frac{1}{s_{sc} y(s_{sh}) x^{(s_{sh}-1)} e^{-(x/s_{sc})}}, \tag{6}$$

with s_{sh} being the shape and s_{sc} the scale parameter.

2.4 Results

2.4.1 Ex situ TS measurements

Three out of a total of five cage experiments, each containing a different fish, were used for further analyses based on data quality and quantity. The three fish measured 45, 52 and 53 cm (Table 2.2). Even if the number of fish measured is low, they still represent a relatively good coverage of the most typically observed size classes in the area (mean length = 51.97 cm; SD± 8.51 cm, based on 751 commercially caught red emperor). Unsuccessful experiment runs were mostly characterised by fish resting in corners or very close to the bottom of the cage for considerable amounts of time. The three analysed experiments delivered recordings of 33 tracks comprising 268 positively identified fish targets at 38 kHz and 48 tracks with 258 targets at 120 kHz (Table 2.2). Mean *ex situ TS* values were based on 10,000 non-parametric bootstrap samples from the recorded data. Mean *TS*, SD and parameter b_{20} of the *TS-L* relationship were computed for each of the three fish (Table 2.2). Calculating the mean b_{20} parameter for the combined measurements gave:

$$\mathrm{TS}_{38} = 20 \log_{10}(L) - 73.9$$

$$\mathrm{TS}_{120} = 20 \log_{10}(L) - 79.4 \ .$$

Tilt angles of individuals measured in the cage at 38 kHz ranged from 80.2 – 97.9 ° with a mean of 89.4° (SD ± 3.8°). At 120 kHz, tilt angles varied between 78.4 – 98.6° with a mean of 90.5° (SD ± 4.43°).

Table 2.2 Mean TS at 38 and 120 kHz for three ex situ measured red emperors, based on detected fish tracks with an indication of the number of fish tracks and targets identified for each specimen.

Fish size [cm]	38 kHz				120 kHz			
	No tracks	No targets	Mean *TS* [dB]	SD	Tracks	Targets	Mean *TS* [dB]	SD
45	19	176	-42.5	1.3	12	53	-47.8	0.8
52	8	38	-38.8	1.4	27	105	-44.9	1.8
53	6	54	-37.4	1.6	9	100	-43.7	1.9

2.4.2 Morphology of the swimbladder

Nine red emperor were scanned in total, but only three fish had intact swimbladders that were deemed in good condition (no rupture to the outline of the swimbladder or complete deflation of the swimbladder). The other six fish all showed signs of swimbladder rupture   that   were
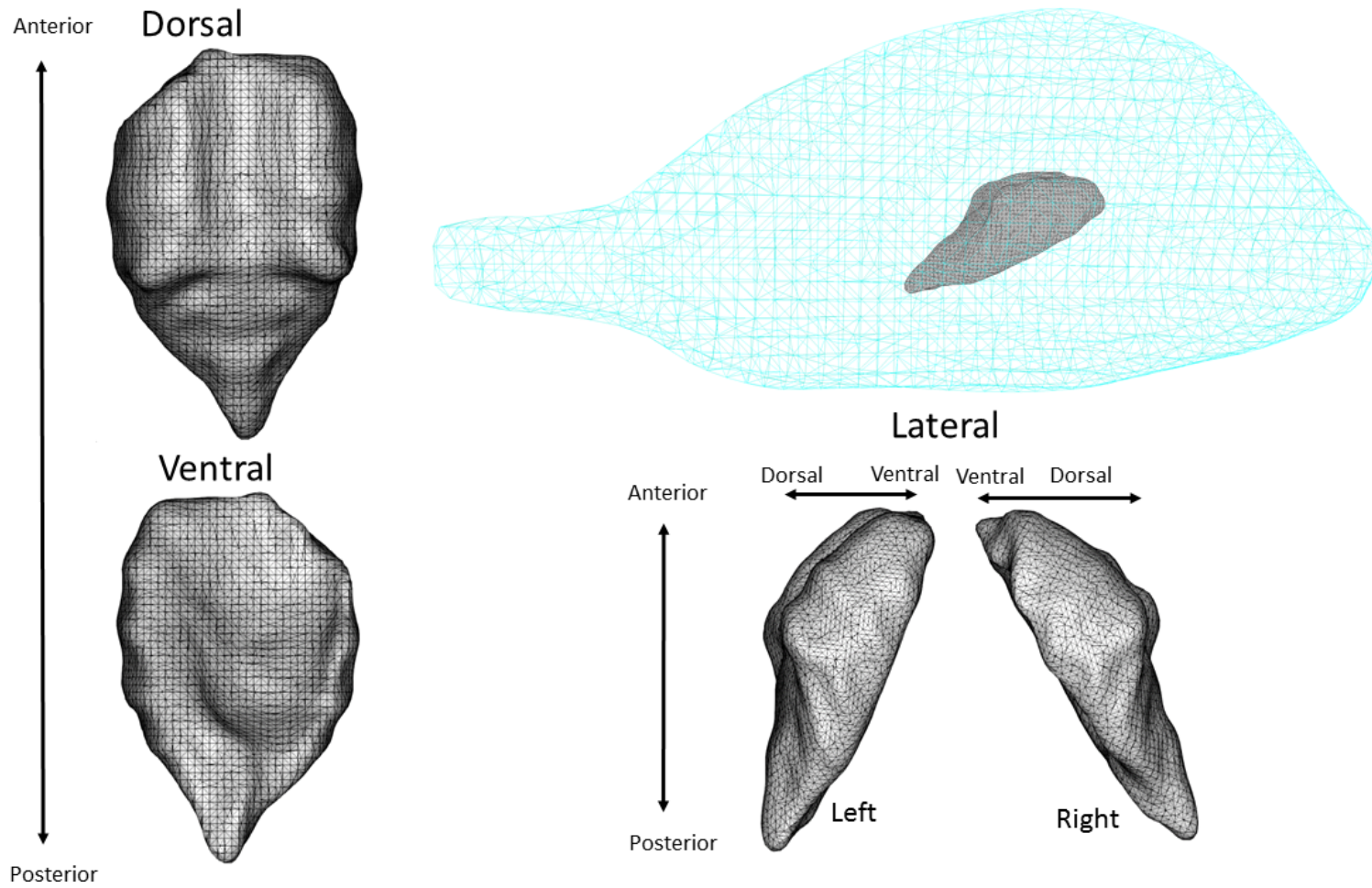
Figure 2.3 Example of a red emperor swimbladder reconstructed from computer tomography measurements shown from different perspectives and a mesh of the fish body with an indication of the swimbladder location.

possibly caused during capture, handling or preparation. The scanned fish had TLs of 41, 43 and 54 cm, with TWs of 1054, 1159 and 2373 g, and swimbladder lengths of 7.1, 6.6 and 7.3 cm, respectively. The swimbladders were dorsoventrally compressed and rostrocaudally elongated. The front section appeared concave with two fairly symmetrical humps on the underside of the swimbladder (Figure 2.3). The overall shape of the front was approximately cube-like, while the back part was almost triangular. The swimbladder was inclined at an angle of approximately 20 − 30° head-up relative to the fish axis (Figure 2.3).

2.4.3 TS estimation

Mean $SD\sigma_{bs}$ at 38 kHz was estimated to be 6.1 dB and 6.0 dB at 120 kHz. Mean SD_{θ} at 38 kHz was 5.8° and 5.9° at 120 kHz. Fitting the TS − L equation to the KRM model outcome resulted in (Figure 2.4):

$$TS_{38} = 14.6 \log_{10}(L) - 64.9 \text{ (S.E. = 1.47, R}^2 = 0.60)$$

$$TS_{120} = 19.7 \log_{10}(L) - 75.5 \text{ (S.E.= 1.70, R}^2\text{=0.65).}$$

Estimated TS and confidence intervals over the entire range of tilt angles for the three scanned fish at 38 kHz were -41.4 ± 5.5 dB, -41.4 ± 5.4 dB and 39.6 ± 5.2 dB for fish sizes 41, 43, 54 cm respectively. At 120 kHz estimated TS and confidence intervals were -43.7 ± 5.8 dB, -43.4 ± 5.7 dB and 41.4 ± 5.4 dB. Based on these three measurements TS was 2.1 dB higher at 38 kHz compared to 120 kHz. Comparing predicted TS for fish of size 30 − 60 cm resulted in a mean dB difference of 2.2 dB, stronger at 38 kHz than at 120 kHz. Tilt angle-specific TS were computed based on different values of ϑ (Figure 2.5). All three fish displayed a slightly different pattern, but troughs and peaks were generally found at similar tilt angles, with troughs located around 60°, 80-90° and 95-110°. This pattern was prominent at 38 kHz, while a similar pattern with more complexity was observed at 120 kHz. Figure 2.5a and 2.5b illustrate this pattern, modelled for two hypothetical fish of length 40 and 50 cm respectively.
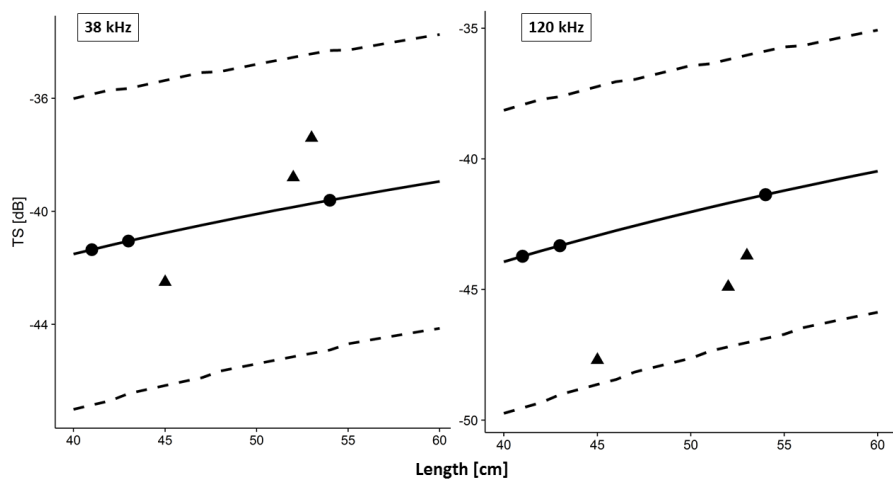
Figure 2.4 Red emperor estimated TS at length relationship with 95% confidence intervals estimated using KRM model parameter values estimated by a Bayesian approach at 38 kHz (a) and 120 kHz (b). Filled circles indicate the total length of fishes for which swimbladder and body measurements were available. Ex situ TS measurements of three fishes are indicated as triangles.
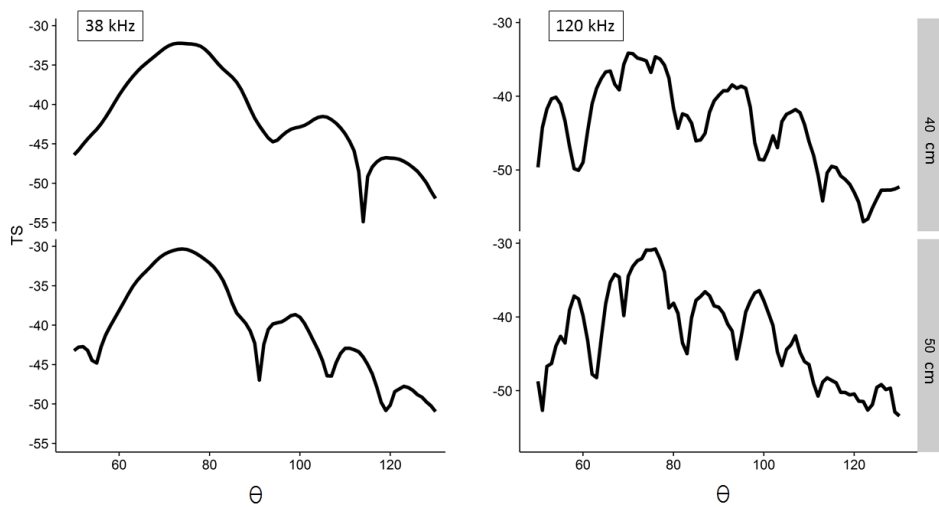
Figure 2.5 Estimated TS for red emperor for tilt angle ϑ ranging from 50 to 130° modelled for hypothetical fish of size 40 and 50 cm at 38 kHz (a) and 120 kHz (b).

2.5 Discussion

The experimental technique used to estimate *TS* can have an influence on the outcome. Empirical *in situ TS* measurements should deliver the most representative measures of *TS* (Simmonds and MacLennan 2005) as observations are based on fish behaving "naturally" in their normal environment. *In situ TS* measurements were impracticable in the given situation, as red emperor is generally found within dense, mixed schools, close to the seabed. In comparison, *ex situ* measurements can be made, allowing for easier target discrimination, and a more controlled environment. Nonetheless, differences have been observed between *TS* of living, dead, and stunned fish (McClatchie *et al.*, 1996). The setup of the *ex situ* measurements probably limited the movement of the fish. For the majority of the time fish were moving in a rather horizontal manner with the observed range of tilt angles ranging from approximately 80° to 100°. They would typically move slowly upwards from the trap and then swim around for a little while, before resting on the bottom of the trap again. Even though all specimens appeared to be swimming freely when put into the cage, the depth at which they were measured could have influenced their behaviour, just as the fact that they were kept in a cage. Only three fish could be measured successfully, due to the prevailing difficult conditions with very strong currents, limited time available at sea and the low number of good condition fish samples available. Despite the limited number of fish, we propose that as the first *TS* measures of a data poor species our results are a valuable starting point upon which future studies may build.

The main contributor to the amplitude of the species-specific acoustic backscatter of fish is the swimbladder, when present (Foote 1980b; Ona 1990; Foote and Francis 2002). For a given species, however, *TS* is predominantly influenced by fish length (Love, 1977; Foote, 1979) and orientation (Nakken and Olsen, 1977; Foote, 1980b). Most empirical *TS* measurements have traditionally been derived from *in situ* or *ex situ* measurements. However, with advancements in computational power, modelling techniques have become widely used (Horne et al. 2000; Fässler et al. 2013; Scoulding et al. 2015). Previous studies have successfully used CT scans to derive morphological representations of swimbladders as an alternative to time consuming and more expensive methods such as microtoming or MRI scans (Reeder *et al.*, 2004; Peña, 2008; Fässler *et al.*, 2013; Scoulding *et al.*, 2015). CT scanning provides high resolution data to reconstruct detailed 3D images of the swimbladder and the fish body for use

in backscatter modelling (Macaulay, 2002; Reeder *et al.*, 2004). It also provides a non-invasive method to describe the position of the swimbladder within the fish body.

One of the main advantages of a modelling approach is the ability to investigate the effects of various factors (e.g. orientation and size) on *TS* estimates. Inherently, these are difficult to control in empirically derived estimates of *TS* (Clay and Horne, 1994; Foote and Francis, 2002c; Fässler *et al.*, 2009). The model approach selected here may not be universally suitable to all species or frequencies. Approximated shapes of the swimbladder and fish body were used in combination. Whilst this is applicable for the acoustic frequencies and species investigated here, other body parts or fine-scale details of the swimbladder or the fish shape may have a greater influence on backscatter. Model choice can have a significant effect on *TS* estimates (Macaulay *et al.*, 2013). Backscatter modelling remains a trade-off between computational power and model complexity. This results in a compromise between simplicity and the need to capture the true anatomical complexity and material properties that contribute to *TS* variation of a fish.

Further, models can assist in uncertainty estimation (Kloser and Horne 2003; Demer 2004; Fässler et al. 2009). The Bayesian model parameter estimation applied here, which essentially 'calibrated' the KRM model on the basis of *ex situ TS* measurements, facilitated the estimation of uncertainty in unknown parameters or parameters that are notoriously difficult to estimate. Combining these estimates in a *TS* model allowed for uncertainty associated with the resultant *TS* distribution. Nonetheless, the approach may still introduce bias in some situations. A potential shortcoming of the applied Bayesian approach for model parameter estimation is the need to select (objective) priors for the parameters. A potentially unrealistic prior may have a severe impact on model outcomes (McAllister and Kirkwood, 1998). Informative priors therefore, should only be used if the *a priori* knowledge about a parameter to be estimated is deemed reliable. In the present study, vaguely informative priors, i.e. lower and upper plausible values, were chosen for the parameters to be estimated, as adequate knowledge about their expected values was absent.

Other studies that have compared modelled estimates of *TS* with empirical measurements (i.e. *in situ* or *ex situ*) found good agreement (Peña and Foote, 2008). Measured $SD_{\log(obs)}$ and SD_θ were very similar for all fish used in the cage experiment at both frequencies (Table 2.2). Comparing the modelled estimates to *ex situ* measurements, we found reasonable agreement at 38 kHz and *ex situ* values spread around the modelled relationship (Figure 2.4).

Modelled TS_{38} values were on average -0.2 dB (SD ± 0.3 dB) lower than those estimated by the *ex situ* experiments. For 120 kHz the shape of the fitted *TS* model relationship was very similar for both modelled and *ex situ* values, but were in general estimated to be stronger (mean 3.4 dB, SD ± 0.02 dB). A possible explanation for the differences between modelled and measured values could be the spread of tilt angles. As mentioned previously, the entire range of tilt angles could not be measured during the *ex situ* measurements. *TS* measured *ex situ,* only detected tilt angles close to 90°, which coincides with a trough in the estimated tilt angle dependent *TS* (Figure 2.5). The higher resolution of the 120 kHz data, due to the much lower pulse duration, could possibly pick up minor details in the physiological characteristics of the swimbladder. This effect could have had a stronger impact at some tilt angles. Generally, the larger the ratio of the target length to acoustic wavelength, the greater the influence of directivity (McCartney and Stubbs, 1971). The potential effect is illustrated by the estimated *TS* for different tilt angles (Figure 2.5). Fluctuations were more pronounced at the higher frequency. While the 38 kHz estimates showed a maximum of five peaks and troughs, a multitude were observed at 120 kHz, hence the effect of the recorded tilt angle was much stronger at 120 kHz.

Previous studies have analysed the *TS* for other Lutjanid species (Au and Benoit-Bird 2003; Benoit-Bird and Au 2003). These studies used different frequencies but found in general higher *TS* values compared to the current study. However, Au and Benoit-Bird (2003) observed troughs in amplitude at around 120 kHz and at the lower frequencies, which might explain part of the dB difference. Another possible explanation could be the different angle at which the swimbladder is positioned in the species, which varied largely.

The use of multifrequency characteristics to identify species or target groups during the scrutinising process is commonplace in fish surveys. In the present study, *TS* for red emperor was estimated at 38 and 120 kHz and a relatively stable dB difference, approximately 2 dB stronger at 38 kHz, was detected. This relationship may become useful to distinguish different species occurring in the same area once there are more measurements available. Multi-frequency discrimination of species will be enhanced if backscatter was measured simultaneously at more than two frequencies. At the time of the *ex situ* experiments 38 and 120 kHz were the only two frequencies available in the field with split-beam capabilities. Nonetheless, the presented data remains highly valuable in a data poor area such as the Northern Demersal Scalefish Fishery.

The 38 kHz data provided more stable *TS* measures that varied less with tilt angle, and showed a better agreement between modelled and measured *TS*. Therefore, it would be recommended to base any acoustic biomass or abundance estimates for red emperors on 38 kHz data rather than using a higher frequency.

The study showed that a Bayesian calibration of *TS* model parameters can be used to describe the joint parameter distribution that contributes to the total precision of the *TS* estimate. The present study demonstrated how relatively low cost, small-scale commercial fishing vessels can be used to carry out *ex situ TS* experiments. Such an approach could be applied to a multitude of species and could improve the general understanding of scattering properties of species that do not have the benefits of regular acoustic survey coverage.

2.6 Acknowledgments

2.7 References

Au W.W., Benoit-Bird K.J., 2003, Acoustic backscattering by Hawaiian lutjanid snappers. II. Broadband temporal and spectral structure. J. Acoust. Soc. Am. 114, 2767–2774.

Barbeaux S.J., Horne J.K., Dorn M.W., 2013, Characterizing walleye pollock (*Theragra chalcogramma*) winter distribution from opportunistic acoustic data. ICES J. Mar. Sci. 70, 1162–1173.

Benoit-Bird K.J., Au W.W., Kelley C.D., 2003, Acoustic backscatter- ing by Hawaiian lutjanid snappers. I. Target strength and swim- bladder characteristics. J. Acoust. Soc. Am., 114, 2757–2766.

Blackman S.S., Norwood, Massachusetts: Artech House Inc., 1986, Multiple-Target Tracking with Radar Applications, 464 pp.

Brown I., Sumpton W., McLennan M., Mayer D., Campbell M., Kirkwood J., Butcher A., Halliday I., Mapleston A., Welch D., Begg G.A., Sawynok B., 2010, An improved technique for es- timating short-term survival of released line-caught fish, and an application comparing barotrauma-relief methods in red emperor (*Lutjanus sebae* Cuvier 1816), J. Exp. Mar. Biol. Ecol. 385, 1–7.

Clay C.S., Horne J.K. 1994, Acoustic models of fish: The Atlantic cod (*Gadus morhua*). J. Acoust. Soc. Am. 96, 1661–1668.

Demer D.A., 2004, An estimate of error for the CCAMLR 2000 sur- vey estimate of krill biomass. Deep Sea Res. Part II Top. Stud. Oceanogr. 51, 1237–1251.

Demer D.A., et al. 2015, Calibration of acoustic instruments. ICES CRR No. 326. 133 p.

Echoview Software Pty Ltd, 2015, Echoview software, version 6.1.44. Echoview Software Pty Ltd, Hobart, Australia

Edwards J.I., Armstrong F., 1981, Measurements of the target strength of live herring and mackerel. ICES CM/ B:26, pp. 5–11. Fässler S.M.M., Brierley A.S., Fernandes P.G., 2009, A Bayesian ap- proach to estimating target strength. ICES J. Mar. Sci. 66, 1197–

1204. Fässler S.M.M., O'Donnell C. Jech J.M., 2013, Boarfish (*Capros aper*) target strength modelled from magnetic resonance imag- ing (MRI) scans of its swimbladder. ICES J. Mar. Sci. 70, 1451– 1459.

Foote K.G., 1979, On representing the length dependence of acoustic target strengths of fish. J. Fish. Board Can. 36, 1490–1496.

Foote K.G., 1980a, Averaging of fish target strength functions. J. Acoust. Soc. Am. 67, 504–515.

Foote K.G., 1980b, Importance of the swimbladder in acoustic scat- tering by fish: A comparison of Gadoid and mackerel target strengths. J. Acoust. Soc. Am. 67, 2084– 2089.

Foote K.G., Francis D.T.I., 2002, Comparing Kirchhoff- approximation and boundary-element models for computing gadoid target strengths. J. Acoust. Soc. Am. 111, 1644–1654.

Gauthier S., Rose G.A., 2001, Target Strength of encaged Atlantic redfish (*Sebastes* spp.). ICES J. Mar. Sci. 58, 562–568.

Hammond T., 1997, A Bayesian interpretation of target strength data from the Grand Banks. Can. J. Fish. Aquat. Sci. 54, 2323–2333.

Hartig F., Dyke J., Hickler T., Higgins S.I., O'Hara R.B., Scheiter S., Huth A., 2012, Connecting dynamic vegetation models to data – an inverse perspective. J. Biogeogr. 39, 2240– 2252.

Hazen E.L., Horne J.K., 2003, A method for evaluating the effects of biological factors on fish target strength. ICES J. Mar. Sci. 60, 555–562.

Hazen E.L., Horne J.K., 2004, Comparing the modelled and mea- sured target-strength variability of walleye pollock, *Theragra chalcogramma*. ICES J. Mar. Sci. 61, 363–377.

Henderson M.J., Horne J.K., 2007, Comparison of in situ, ex situ, and backscatter model estimates of Pacific hake (*Merluccius produc- tus*) target strength. Can. J. Fish. Aqua. Sci. 64, 1781–1794.

Horne J.K., Walline P.D., Jech J.M., 2000, Comparing acoustic model predictions to in situ backscatter measurements of fish with dual- chambered swimbladders. J. Fish Biol. 57, 1105–1121.

ICES, 2007, Collection of acoustic data from fishing vessels. ICES CRReport No. 287. 83 pp.

Kloser R.J., Horne J.K., 2003, Characterizing uncertainty in target- strength measurements of a deepwater fish: orange roughy (*Hoplostethus atlanticus*). ICES J. Mar. Sci. 60, 516–523.

Korneliussen R.J., Diner N., Ona E., Berger L., Fernandes P.G., 2008, Proposals for the collection of multifrequency acoustic data. ICES J. Mar. Sci. 65, 982–994.

Love R.H., 1977, Target strength of an individual fish at any aspect. J. Acoust. Soc. Am. 62, 1397–1403.

Macaulay G.J., 2002, Anatomically detailed acoustic scattering mod- els of fish. Bioacoustics 12, 275–277.

Macaulay G.J., Peña H., Fässler S.M.M., Pedersen G., Ona E., 2013, Accuracy of the Kirchhoff-approximation and Kirchhoff-Ray- Mode fish swimbladder acoustic scattering models. PLoS ONE 8, e64055.

MacLennan D.N., 1990, Acoustical measurement of fish abundance. J. Acoust. Soc. Am. 87, 1–15.

MacLennan D.N., Menz A., 1996, Interpretation of in situ target- strength data. ICES J. Mar. Sci. 53, 233–236.

McAllister M.K., Kirkwood G.P., 1998, Bayesian stock assessment: a review and example application using the logistic model. ICES J. Mar. Sci. 55, 1031–1060.

McCartney B.S., Stubbs A.R., 1971, Measurements of the acoustic target strengths of fish in dorsal aspect, including swimbladder resonance. J. Sound Vib. 15, 397–420.

McClatchie S., Alsop J., Coombs R.F., 1996, A re-evaluation of relationships between fish size, acoustic frequency, and target strength. ICES J. Mar. Sci. 53, 780–791.

Metropolis N., Rosenbluth A.W., Rosenbluth M.N., Teller A.H., Teller E., 1953, Equation of state calculations by fast computing machines. J. Chem. Phys. 21, 1087.

Nakken O., Olsen K., 1977, Target strength measurements of fish. Newman S.J., Dunk I.J., 2002, Growth, age validation, mortality, and other population characteristics of the red emperor snapper, *Lutjanus sebae* (Cuvier, 1828), off the Kimberley Coast of North-Western Australia. Estuar. Coast. Shelf Sci. 55, 67–80.

Newman S.J., Wakefield C., Skepper C., Boddington D., Blay N., Jones R., Wallis D. 2014, North coast demersal fisheries status report. In: Status Reports of the Fisheries and Aquatic Resources of Western Australia 2013/14: The State of the Fisheries; Eds.: W.J. Fletcher and K. Santoro, (Department of Fisheries, Western Australia).

Ona E., 1990, Physiological factors causing natural variations in acoustic target strength of fish. J. Mar. Biol. Assoc. U. K. 70, 107–127.

Ona E., 2001, Herring tilt angles, measured through target tracking. In Herring: Expectations for a New Millennium. Ed. by F. Funk, J. Blackburn, D. Hay, A. J. Paul, R. Stephenson, R. Toresen, and D. Witherell. University of Alaska, Sea Grant, AK-SG-01-04. Fairbanks. 800 p.

Ona E., 2003, An expanded target-strength relationship for herring. ICES J. Mar. Sci. 60, 493–499.

Peña H., 2008, In situ target-strength measurements of Chilean jack mackerel (*Trachurus symmetricus murphyi*) collected with a sci- entific echosounder installed on a fishing vessel. ICES J. Mar. Sci. 65, 594–604.

Peña H., Foote K.G., 2008, Modelling the target strength of *Trachurus symmetricus murphyi* based on high-resolution swimbladder morphometry using an MRI scanner. ICES J. Mar. Sci. 65, 1751– 1761.

R Core Team, 2016, R: A language and environment for statisti- cal computing. R Foundation for Statistical Computing, Vienna, Austria. https://www.R-project.org/.

Reeder D.B., Jech J.M., Stanton T.K., 2004, Broadband acous- tic backscatter and high-resolution morphology of fish: Measurement and modeling. J. Acoust. Soc. Am. 116, 747–761.

Ryan T.E., Kloser R.J., 2004, Improving the precision of ES60 and EK60 echosounder applications. Rep. Work. Group Fish. Acoust. Sci. Technol. WGFAST 20–23.

Scoulding B., Chu D., Ona E., Fernandes P.G., 2015, Target strengths of two abundant mesopelagic fish species. J. Acoust. Soc. Am. 137, 989–1000.

Simmonds J., MacLennan D., 2005, Fisheries acoustics: theory and practice. Blackwell Publishing, Oxford. 437 p.

Soule M., Barange M., Hampton J., 1995, Evidence of bias in esti- mates of target strength obtained with a split-beam echo-sounder. ICES J. Mar. Sci. 52, 139–144.

Soule M., Barange M., Solli H., Hampton I., 1997, Performance of a new phase algorithm for discriminating between single and over- lapping echoes in a split-beam echosounder. ICES J. Mar. Sci. 54, 934–938.

Ye Z., 1997, Low-frequency acoustic scattering by gas-filled prolate spheroids in liquids. J. Acoust. Soc. Am. 101, 1945–1952.

Chapter 3

Estimates of variability of goldband snapper target strength and biomass in three fishing regions within the Northern Demersal Scalefish Fishery (Western Australia)

Sven Gastauer[1,2, 3], Ben Scoulding[4], Miles Parsons[1]

[1] *Centre for Marine Science and Technology, Curtin University, GPO Box U1987, Perth, WA 6845, Australia*

[2] *Wageningen Marine Research, P.O. Box 68, 1970 AB IJmuiden, The Netherlands*

[3] *Antarctic Climate and Ecosystems Cooperative Research Centre, University of Tasmania, Private Bag 80, Hobart, Tasmania 7001*

[4] *Echoview Software Pty Ltd, GPO Box 1387, Hobart, 7001, Tasmania, Australia*

Corresponding author: *Sven Gastauer, CMST, Curtin University B301 Hayman Rd, Bentley WA 6102, Australia; email:* sven.gastauer@postgrad.curtin.edu.au

3.1 Abstract

Goldband snapper (*Pristipomoides multidens*) is an ecologically and economically important species in the Northern Demersal Scalefish Fishery (NDSF). The *Carolina M*, a trap fishing vessel operating in the NDSF, was equipped with Simrad ES70 echosounders, operated at 38 and 120 kHz. In 2014 acoustic data, in combination with optical recordings of the catch, were opportunistically collected during routine fishing operations. In December 2014 pure, low density goldband snapper schools were observed on the echograms. *In situ* target strength (*TS*) estimates were derived and linked to length distributions of catch information with the curve fitting method. Estimated *TS-L*ength *(L)* at 38 kHz was $20.1 \log_{10}(L)$-70.5 and $16.4 \log_{10}(L)$-77 at 120 kHz. Three fishing grounds, where near simultaneously recorded acoustic and optical information was available were selected. Fish school densities observed within the 38 kHz acoustic data were disaggregated according to catch proportions using kriging. Goldband snapper density estimates ranged between 9,518 individuals per nmi^2 in the high-density fishing region and 2,512 and 945 individuals per nmi^2 in the two low density fishing regions. Sampling variance was estimated using geostatistics (coefficient of variance, CV = 10-20.9%). Other errors considered were signal-to-noise ratio (CV < 1%), variation in the acoustic signal due to fluctuations in temperature and salinity (CV = 0.5 – 1.15%), effects of diurnal vertical migration and variability of catch information (CV = 1.2 – 2%). A total CV of 28.2 – 50.6 % was estimated for all considered sources, for the three fishing regions.

Keywords: *fisheries acoustics, geostatistics, target strength, NDSF, fishing vessel, goldband snapper, error estimates*

3.2 Introduction

Goldband snapper (*Pristipomoides multidens*), a member of the Lutjanidae family, is widely distributed within the tropical waters of the Indo-Pacific (Allen, 1985; Newman and Dunk, 2003). It is described as long-lived (up to 30 years) and exhibits low levels of natural mortality (M), with M ranging between 0.10 and 0.14 (Newman and Dunk, 2003). It reaches sexual maturity at a relatively late stage, growing rapidly until age 9 and reaching a maximum length of ~80 cm at ~18 years of age (Newman and Dunk, 2003). Given these life history traits goldband snapper are considered vulnerable to overfishing Newman and Dunk, 2003). In Western Australia (WA), goldband snapper occur as far South as Cape Pasley (34°S) and are commercially targeted north of the Ningaloo Reef, around Exmouth (23°30'S) (Kailola, 1993). Goldband snapper, together with red emperor (*Lutjanus sebae*), are considered indicator species (i.e. species that are considered ecologically important and reflective of the ecosystem characteristics and condition) in the Northern Demersal Scalefish Fishery (NDSF), located in waters off the coast of Broome in Northwest Australia around to the WA-Northern Territory border (Marriott *et al.*, 2014). The NDSF is a trap-based mixed fishery, covering a large area of approximately 408,400 km^2, of which the main fishing effort is concentrated over 226,500 km^2 (Newman *et al.*, 2008).

The NDSF is a relatively low value fishery (approximately 7 million AUD in 2013 (Newman *et al.*, 2015b)) covering a vast, remote area. Funds for monitoring this resource are limited, in relation to its size, which restricts the ability to conduct effective fisheries ecosystem monitoring with traditional techniques (e.g. daily egg production method or trawl surveys). Fisheries acoustics is identified as one of the most promising tools for establishing an ecosystem-based approach to fisheries management (EBFM) (Koslow, 2009; Trenkel *et al.*, 2011). Active-acoustic methods are considered standard practice for studying a diverse range of marine animals, e.g. fish, birds and zooplankton(Kloser *et al.*, 2002; Simmonds and MacLennan, 2005; Kloser *et al.*, 2009; ICES, 2015; Campanella and Taylor, 2016). Many commercial fishing vessels are now fitted with scientific echosounders (i.e. echosounders which can be calibrated and can store data). This enables fishers to collect acoustic data continuously whilst at sea. Such vessels are often termed 'vessels of opportunity' (Dalen and Karp, 2007; Ryan *et al.*, 2015; Fässler *et al.*, 2016). Combining acoustic (e.g. density estimates) and catch data (e.g. species, length and weight distributions) collected on board fishing vessels could improve our understanding of the marine resources in the NDSF. This information can

help to optimise survey strategies and deliver abundance indices for use in assessment models (Barbeaux, 2012; Gastauer *et al.*, 2016a)(Barbeaux 2012, Fässler et al. 2016).

To convert acoustic density estimates into fish abundance or biomass, *a priori* or *a posteriori* knowledge of the mean target strength (*TS*, in decibels [dB re 1 m^2]) must be available for the size range and species being studied. *TS* is a logarithmic measure of the amount of acoustic energy backscattered from an individual target, usually related to fish length as *TS-L* (Simmonds and MacLennan 2005). When fish aggregate, echo-integration (Dragesund and Olsen, 1965) can be used to estimate their density (MacLennan *et al.*, 2002). To translate this acoustic density into estimates of biomass or abundance, alternative sampling data (e.g. video footage or hand lining; Fernandes et al. (2016)), to verify acoustic observations, is required. This is typically in the form of biological samples, obtained from trawls in traditional acoustic trawl surveys (AT).

Reductions in total allowable catch (TAC), total allowable effort (TAE) and limitations in the available resources for monitoring creates a need for low cost sampling strategies in multiple fisheries, as an alternative to traditional techniques. Here, we combine opportunistically collected echosounder and catch data, obtained on board the commercial fishing vessel *Carolina M* in the NDSF, in 2014, during routine operations. The aim was to deliver an acoustic assessment of goldband snapper in three fishing regions within the NDSF, with associated error estimates. Sampling error was assessed through the application of geostatistical methods (Rivoirard *et al.*, 2000, p 200; Gimona, 2003; Woillez *et al.*, 2009a; Scoulding *et al.*, 2016). Other sources of error considered were fluctuations in acoustic backscattering properties due to changes in the environment (temperature and salinity), behaviour (diel vertical migration, DVM), detection probability through estimates of signal-to-noise ratio (r_{sn}) and the associated error. Total random error was estimated through bootstrapping.

3.3 Methods

3.3.1 Study area

The NDSF extends over a vast area (Figure 3.1), composed of smaller, spread out, preferred fishing regions. Generally, fishers revisit those fishing grounds, considered to be the most productive areas, on a regular basis. This study focuses on data collected on board a
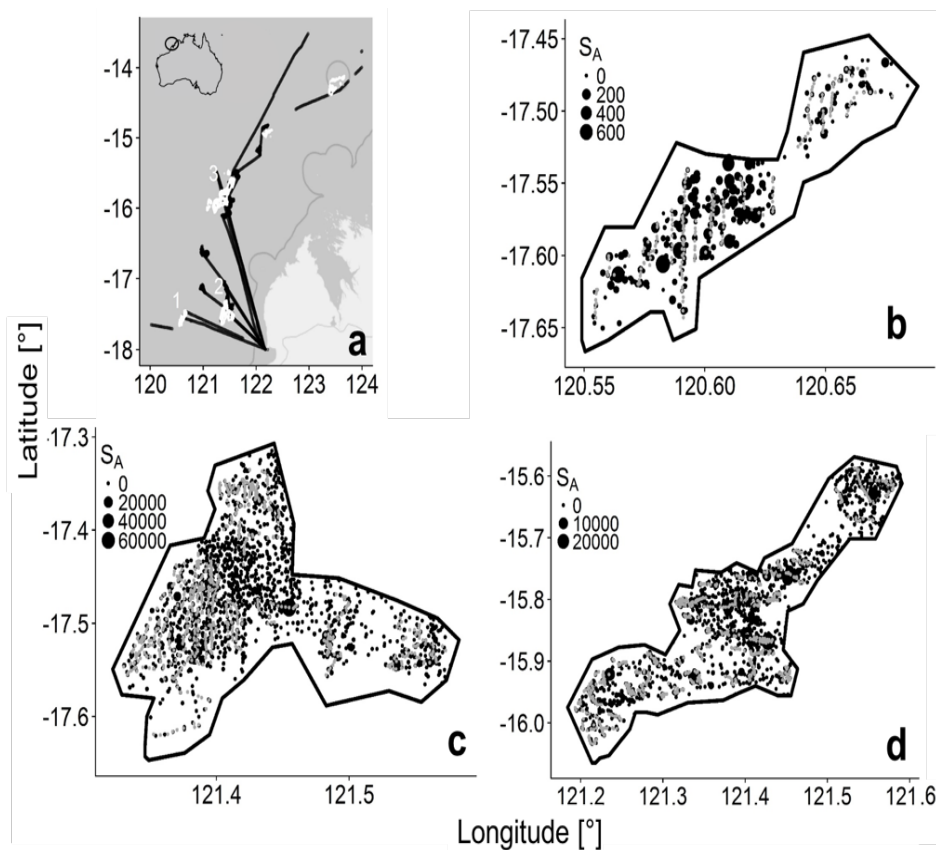
Figure 3.1 a) Map of waters of the Northwest coast of Australia that include the Northern Demersal Scalefish Fishery showing example cruise tracks (black lines) of Carolina M. The white lines show the locations of three fishing regions represented in b) Region 1, c) Region 2 and d) Region 3. The black circles show the acoustic density (Nautical Area Scattering Coefficient, s_A in m^2 nmi^{-1}) and the grey circles show catch locations.

commercial fishing vessel, *Carolina M*, during normal commercial operation. Fishing grounds could easily be recognised through the availability of high density catch and acoustic data. During time of data collection, three such regions could be identified and were delineated through manually drawn polygons. This study, focussed on goldband snapper within these three regions of interest (Figure 3.1b, c, d).

Region 1 was located in the southwest (area (A) = 33 nmi^2, mean depth ($\overline{d_w}$) = 124 m (water depth range (d_r) = 120 − 130 m)) (Figure 3.1b), Region 2 was located in the southeast (A = 129 nmi^2, $\overline{d_w}$ = 78 m (d_r = 61 − 90 m)) (Figure 3.1c), and Region 3 was located in the more central part (A = 211 nmi^2, $\overline{d_w}$ = 91 m (d_r = 76 − 103 m)) (Figure 3.1d) of the NDSF. Data within each region were collected at different times in 2014 (Region 1: 3rd - 7th December, Region 2: 29th October − 8th November and Region 3: 19th − 30th August).

Salinity (s_w) and temperature (t_w) information were retrieved from the CSIRO Atlas of Regional Seas (CARS), an atlas of seasonal ocean water properties, based on research vessel

instrument profiles and autonomous profiling buoys (Ridgway *et al.*, 2002). Data were retrieved for August, November and December at 121.23° E and 15° S. Mean temperatures and salinities fluctuated within the different months of data collection (Table 3.1). In November, the mean t_w at 10 m was 27.47 °C and in August the t_w was 23.51 °C at 100 m. The mean s_w were 34.53 ppt at 10 m in November and 34.62 ppt at 100 m in August.

Table 3.1. Summary of Temperature, salinity, sound speed, expected target strength of the calibration sphere (TS$_{Cal}$) with variation from the original value in brackets and signal to noise ratio (r_{sn}) at depths of 10 m and 100 m for August; November and December

Parameter	Unit	Month					
		August		November		December	
		Depth [m]					
		10	*100*	*10*	*100*	*10*	*100*
Salinity	ppt	34.16	34.42	34.67	34.71	34.77	34.72
Temperature	°C	25.91	24.86	27.73	22.59	28.78	23.07
Water sound speed	ms^{-1}	1535.83	1535.12	1540.56	1529.76	1542.97	1531.00
TS_{cal}	dB re 1 m^2	-42.33 (-0.92%)	-42.33 (-0.92%)	-42.30 (-0.23%)	-42.36 (-1.6%)	-42.28 (+ 0.23%)	-42.35 (-1.37%)
r_{sn} (S_v = -60 dB re 1 m^{2}m^{-3})	Dimensionless	52.03	30.27	52.03	30.26	52.05	30.26
r_{sn} (S_v = -70 dB re 1 m^{2}m^{-3})	Dimensionless	182.03	160.27	182.04	160.26	182.05	160.26
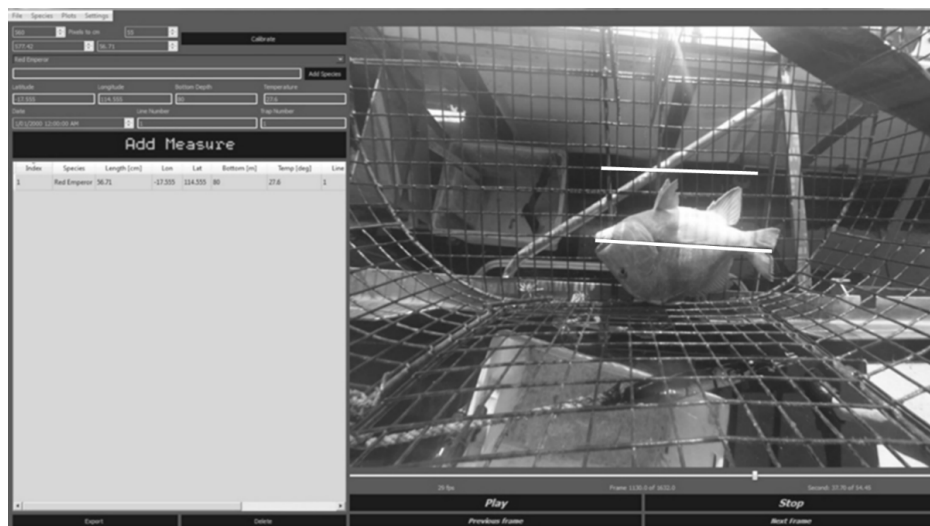
Figure 3.2 Screenshot of FishVid, catch recording analysis tool. Top white line is an example calibration bar to count the number of pixels across 10 of the 5 cm mesh squares, while bottom white line marks the length of a Red Emperor, for measurement. Left hand panel records length and species details for each fish measured.

3.3.2 Biological sampling

Catch information was collected using steel traps of approximate dimensions 1.5 x 1.5 x 0.9 m with a 5 cm mesh throughout. *Carolina M* generally deploys 10 of these traps at a time,

up to 8 times a day. As each trap was brought on board, a GoPro Hero 3 camera was fixed to the top of the trap. The downwards facing GoPro camera was able to record all fish caught within the trap, before the catch was separated as landings or returned to sea. The GoPro was directed down, pointing at fish lying on the bottom of the trap. This enabled direct measures of fish numbers, length and species identification using a custom-built software package ('FishVid v.0.1', developed in Python 2.7, Python Software Foundation, https://www.python.org/) (Figure 3.2). Prior to measuring fish length, the built-in GoPro distortion was removed from the video footage using the GoPro Studio software (gopro.com/software-app/gopro-studio-edit-software). Each video recording was calibrated through comparison of the number of pixels with the known size of the trap mesh and distance from the camera (~0.9 m). Where multiple fish were present in the trap, calibration was repeated in close proximity to the fish, to minimise measurement and parallax error. This facilitated a conversion of pixel size into length [cm]. Thus, providing individual fish were lying flat against the bottom of the cage, their length could be estimated. From these measurements, species group and region-specific length distributions were produced. Based on video recordings, fish were categorised into nine groups of interest: goldband snapper, red emperor, saddletail (*Lutjanus malabaricus*), lutjanids (members of the Lutjanidae family, other than saddletail, red emperor or goldband snapper), lethrinids (members of the Lethrinidae family), rankin cod (*Epinephelus multinotatus*), cods (members of the Epinephelidae family other than rankin cod), triggerfish (members of the Balistidae family, as main by-catch species) and a miscellaneous group containing all other species.

Weight was estimated by fitting a length-weight regression: $W = a_{lw} * L^{b_{lw}}$, where W is weight in grams, L is total length in cm, a_{lw} (0.019 for goldband snapper) and b_{lw} (2.912 for goldband snapper) are constants, extracted from FishBase (Allen, 1985; Froese and Pauly, 2016).

Catch information provided alternative sampling data (Fernandes et al. 2016) to complement information from acoustic recordings. Biological samples collected by traps are not completely representative due to gear selectivity and the unknown catchment area of a single trap. Additionally, as traps are soaked in the water for many hours, schools observed on the echograms do not necessarily reflect the species composition observed within the traps. However, while trap species and length composition may not be directly related to acoustic data from the immediate surrounds, they have been shown to reflect the assemblage in the general area (Newman et al. 2012).

Based on the estimated individual fish weights (determined from *L*), the contribution of goldband snapper, as a proportion of the total weight of the trap catch, could be determined. Kriged maps of goldband snapper proportions were then derived, based on fitted variograms (Matheron 1971):

$$\gamma(h) = 0.5E([Z(x + h) - Z(x)]^2), \tag{1}$$

with *Z(x)* representing the value of the variable at a given point *x* and *Z(x+h)* the value at a model dependent lag (*h*) from *x*. Ordinary kriging acts as the best linear estimator, with weights w_i minimising the kriging variance. The kriging weight across individual elements *i* and *j* has to be defined such that it solves the equation system (Rivoirard et al. 2000):

$$\begin{cases} \sum_j w_j \gamma(x_i - x_j) + \phi = \bar{\gamma}(x_i, V) \; whatever \; i \\ \sum_i w_i = 1 \end{cases}, \tag{2}$$

$$\tag{3}$$

where, *V* is the domain, ϕ is the Lagrange parameter needed to fulfil Equation 3 and γ is the variance. The kriging variance is:

$$\sum_i w_i \bar{\gamma}(x_i, V) - \bar{\gamma}(V, V) + \phi. \tag{4}$$

Coefficients of variance (CV, in %) were derived from the catch proportions and goldband snapper lengths, to estimate the associated random error.

3.3.3 Acoustic data collection

Acoustic data were collected using hull-mounted SIMRAD ES70 split-beam echosounders operating at 38 kHz (beam width: 9.6°, ping rate: maximum, pulse duration (τ): 0.256 ms, transmit electrical power (p_{et}): 1500 W) and 120 kHz (beam width: 7°, ping rate: maximum, τ: 0.064 ms, p_{et}: 1000 W). Settings used during normal commercial operations were maintained. Given the short τ and deviation of the p_{et} settings from those recommended by Korneliussen et al. (2008), the echosounders were calibrated in a tank prior to data collection at sea, to test for non-linear effects. An *in situ* calibration was conducted outside of the fishing grounds in March 2015, following standard sphere procedures, using a 38.1 mm Tungsten-

carbide sphere (WC), with 6% cobalt binder (Demer et al. 2015). Calibration using the sphere method are precise to ±2 - ±7 %, depending on the receiver bandwidth (Simrad, 1993). To assess the variability of measurements caused by changes in t_w and s_w (due to spatial and temporal mismatch), the theoretical TS of a 38.1 mm WC sphere (TS_{cal}) was computed for sound speed in water (c_w) at given t_w and s_w in the three fishing regions (Table 3.1), during data collection. TS_{cal} was calculated according to methods described in Demer et al. (2015). A summary of the fixed parameters can be found in Table 3.2. Sound speed in sea water based on t_w and s_w was calculated following the most commonly used algorithm (Fofonoff and Millard, 1983), proposed by Chen and Millero (1977) and recommended by Demer et al. (2015) (Table 3.1).

Table 3.2 Parameters for calculating the theoretical target strength of a 38.1 mm Tungsten-carbide sphere at various depths and sound speeds.

Parameter	Symbol	Unit	Value
Frequency	F	Hz	38000, 120000
Bandwidth	$\%f$	%	1
Sphere properties			
Diameter	D	mm	38.1
Density	ρ_s	kg m^{-3}	14.9×10^3
Compressional wave speed	c_c	ms^{-1}	6853
Shear wave speed	c_s	ms^{-1}	4171
Depth	d_w	m	0-150
Water properties			
Density	ρ_w	kg m^{-3}	1.027
Temperature	t_w	°C	15-30
Salinity	s_w	ppt	33-36
Sound speed	c_w	ms^{-1}	1450-1550

3.3.4 Acoustic data processing

Raw acoustic data acquired by the SIMRAD ES70 echosounder were corrected for the triangular wave error (Ryan and Kloser 2004, Keith et al. 2005). Further processing of the data, including the application of the calibration settings, was conducted in Echoview 7 (Echoview Software Pty Ltd 2016). Due to the high noise levels (commonly found on commercial vessels) the data were cleaned for impulsive noise (Ryan and Kloser 2004, Vaseghi 2008), caused by non-synchronised pinging between the ES70 and a FURUNO FCV1150 operating at 28/50 kHz; transient noise, caused by poor weather conditions and; background noise, which can be caused by a number of sources, such as vessel engine noise (Mitson and Knudsen 2003, Ryan

et al. 2015). Noise filters, based on Ryan et al. (2015), were adapted and applied to clean the data.

Due to the difference in τ at 38 and 120 kHz, the ping times and geometry were matched and the data were resampled by one ping. This ensured that for the two frequencies, the number of pings and depth bins (matching the horizontal and vertical resolution, respectively) were the same (Demer et al. 1999, Conti et al. 2005).

Table 3.3 Parameters used to compute r_{sn} according to Demer (2004).

Parameter	Symbol	Unit	Value
Frequency	F	Hz	38000
Transmit electrical power	P_{et}	W	1500
(Mean) Volume backscattering strength	S_v	dB re 1 $m^2 m^{-3}$	-30 to -70 (10 dB increments)
Equivalent two-way beam angle	Ψ	dB re 1 steradian	-18
Wavelength	λ	m	c_w/f
Water sound speed	c_w	ms^{-1}	1450-1550
Pulse duration	τ	s	0.256×10^{-3}
Range	R	m	0-250
Absorption coefficient	α_α	dB m^{-1}	0.0097
Ambient noise power	P_n	dB re 1 W	120
On axis system gain	G_0	dB re 1	22.80

3.3.5 School detection

Aggregations (i.e. non-resolvable targets) were classified as fish using a bi-frequency algorithm (38 and 120 kHz) which could separate swimbladdered fish from fluid-like targets or macro-zooplankton, described by Ballón et al. (2011) and Lezama-Ochoa et al. (2011). The algorithm uses the differences in the (mean) volume backscattering strength (S_v [dB re 1 $m^2 m^{-3}$]) at 38 and 120 kHz to discriminate between 'scattering groups'. To be considered as fish, the sum of S_v at 38 and 120 kHz had to be > -127 dB re 1 $m^2 m^{-3}$ and the subtraction of S_v at 38 kHz from S_v at 120 kHz had to be < 3 dB re 1 $m^2 m^{-3}$. Schools were then detected at 38 kHz using the shoal analysis and patch estimate system (SHAPES) algorithm (Coetzee 2000) (threshold = -60 dB re 1 $m^2 m^{-3}$). The echograms were cross-checked manually to ensure the algorithms successfully delineated fish schools of interest. Volume backscattering coefficients (s_v; $m^2 m^{-3}$) of the schools identified as fish were integrated (s_A; $m^2 nmi^{-2}$) and averaged over 1 nmi grid cells, stratified into 10 m range bins. Data were integrated from 10 m depth (outside the near-field) to 1 m above the seabed (to avoid inclusion of seabed echoes). Integration data were exported from the cleaned 38 kHz echograms, masked with detected fish schools, thresholded

at -70 dB re 1 m^2 m^{-3}. Based on depth stratified information, the $\overline{d_w}$ of schools in the water column at a given time could be extracted, to examine the effects of DVM. Time of sunrise and sunset were computed based on Meeus (1991). s_A values of aggregations classified as fish schools were disaggregated according to the kriged, weighted catch proportions.

3.3.6 Detection probability

Performance of echosounders can vary depending on depth and variants in the environment. The signal to noise ratio (r_{sn} [dimensionless]) is defined as the ratio between signal energy and noise energy at the bandwidth of interest and is a common measure to assess the quality of an echosounder (Simmonds and MacLennan 2005)). r_{sn} was calculated for the 38 kHz echosounder according to (Demer 2004):

$$p_{et}r_{sn} = p_{et} + S_v + 2G_0 + \Psi + 10\log_{10}(32\pi^2\lambda^2 c_w\tau) - 20\log_{10}(d_w) - 2\alpha_\alpha d_w - P_{n,,} \quad (5)$$

where, G_0 is the on-axis gain [dB re 1]; Ψ is the equivalent two-way beam angle [dB re 1 sr]; λ is the wavelength [m], calculated as c_w divided by frequency [Hz]; α_α is the absorption coefficient [dB re m^{-1}] and P_n is the ambient noise power [dB re 1 W], taken as a mean based on measurements in the three regions. A summary of the parameter values can be found in Table 3.3. r_{sn} was computed for different values of c_w depending on the environmental conditions. Assuming noise and signal to be coherently additive, r_{sn} can provide bias information for each detection at a given level of S_v (Demer 2004):

$$\frac{Noise}{Signal} = \left(10^{\frac{r_{sn}}{10}}\right)^{-1}\times 100 \text{ [%]}. \quad (6)$$

3.3.7 Single-target detection for target strength estimates

Single-target analysis was limited to data collected in Region 1 on the 4th of December 2014, where low density goldband snapper schools were observed in the acoustic data, and where the catch data contained solely goldband snapper or more than 90% goldband snapper. To avoid inclusion of non-goldband snapper targets, the single-target analysis was limited to a depth range from 90 m to the seafloor (where goldband snapper are most prevalent and tend to form single species aggregations) and only targets associated with schools classified as goldband snapper were considered. Schools were classed as goldband snapper if they were observed near areas where catch was clearly dominated by goldband snapper and matched a

pyramidal or tower-like shape fishermen anecdotally associate with goldband snapper. Detection of single echoes is dependent on the vertical resolution of the echosounder. For narrowband echosounders this is a function of τ and c_w, with the sample resolution being equal to $c_w\tau/2$. When the vertical distance between two targets is less than this, their respective echoes overlap resulting in various combinations of constructive or destructive interference (Soule et al. 1995, Simmonds and MacLennan 2005).

To determine the target density, methods described by Sawada et al. (1993) were applied. Selected schools and surrounding areas were gridded in to cells with a horizontal sampling spacing (HSS) of 20 m and a vertical bin size of 15 m. Fish density within each cell (N_v individuals per reverberation volume) was determined as:

$$N_v = \frac{c_w\tau\Psi d_w{}^2 N_{ei}}{2},$$
(7)

and N_{ei} is the fish density estimated by the echo integrator, as a relation between cellular mean S_v and cellular mean TS ($\overline{TS}$). Only cells with $N_v < 0.04$ and the ratio of multiple echoes when measuring a single-target (M_{ei}) <0.7 were considered for TS estimation (Sawada et al. 1993, Ona 1999). M_{ei} was defined as:

$$M_{ei} = \frac{N_{ei}-N_{ec}}{N_{ei}},$$
(8)

where N_{ec} is the number of single-targets per summed beam volume. A single-target algorithm, taking into account beam compensation and angular information, was applied to the low-density cells (Soule et al. 1997, Ona 1999).

A minimum threshold of -50 dB re 1 m^2 was set for single target detection at 38 and 120 kHz. The pulse length determination level (PLDL) is defined as the number of dB re 1 m^2 below the peak value of a detected pulse at which targets are still considered, when determining the pulse length. This PLDL was set at 6 dB. The maximum standard deviation (σ) of minor and major axis of all samples within a ping during PLDL determination was 1°. The minimum and maximum normalised pulse length, which equals the measured pulse length divided by the transmitted pulse length, were set to 0.7 and 1.5 respectively. Beam compensation, allowing for correction of transducer directivity was set to 6 dB re 1 m^2. Additionally, an intersection filter was applied, whereby only targets detected at both the 38

kHz and 120 kHz frequencies, within 3 m range of each other, were accepted (Demer et al. 1999, Scoulding et al. 2016). Here, vessel speed (0.52 – 2.06 ms^{-1}) was lower than that of other studies, thus the intersection filter was set wider than other studies, as at this speed, fish could move within and between beams. Targets accepted by the algorithm were used as input into an α - β fixed coefficient filtering algorithm ($\alpha_{Major\ axis}$, $\alpha_{Minor\ axis}$, α_{Range} = 0.7; $\beta_{Major\ axis}$, $\beta_{Minor\ axis}$, β_{Range} = 0.5; exclusion distance major and minor axis = 4, range = 0.4; and mixed ping expansion (% of pings without a detection allowed in track) = 0.0) to identify tracks from individual targets (Blackman 1986). A minimum of three single targets from three pings were required to form a fish track. Target tracking provides information on the swimming direction of individual fish which is related to the incidence angle (tilt angle, ϑ). Single-targets and target tracks were treated separately. Only single targets were used to compile *TS* density distributions.
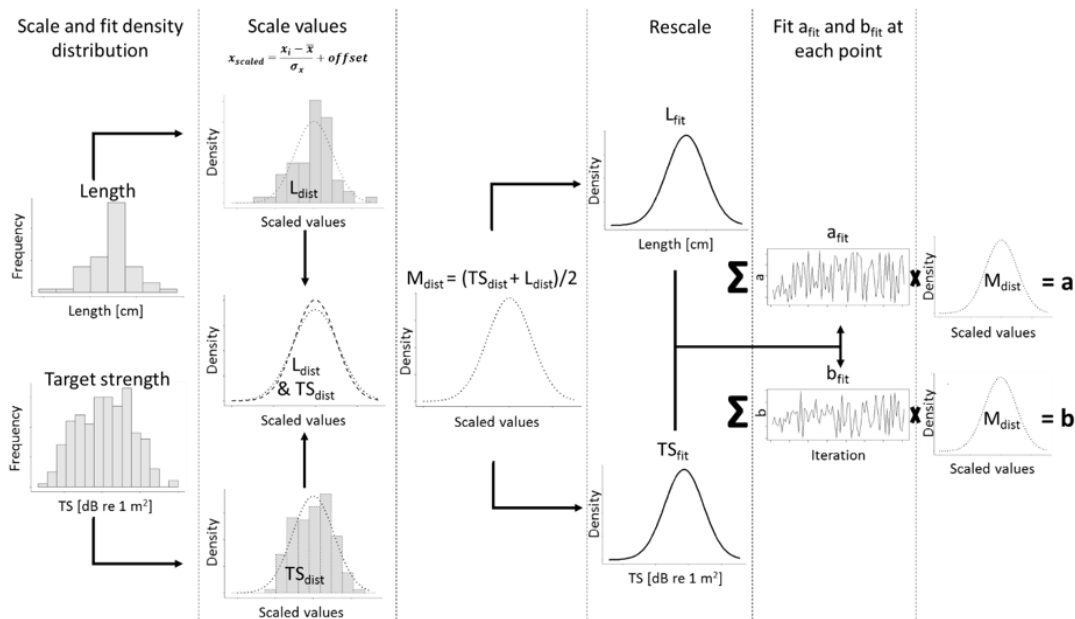
Figure 3.3 Illustration of the curve fitting method to estimate TS-L. In a first step L and TS values are scaled and their density distributions overlaid (TS$_{dist}$, L$_{dist}$). M$_{dist}$ is calculated as the mean of both distributions. L$_{fit}$ and TS$_{fit}$ are generated as the back-transformed raw values based on M$_{dist}$. a$_{fit}$ and b$_{fit}$ are fitted for each pair of TS$_{fit}$ and L$_{fit}$. Summed a$_{fit}$ and b$_{fit}$ weighted by M$_{dist}$ provide the final estimate of a and b

The *TS-L* relationship of goldband snapper was estimated using two different methods. All estimates of *TS-L* were conducted in the linear domain. Therefore, all *TS* values were converted from the logarithmic domain into linear backscattering cross sections (σ_{bs}, [m^2]), according to $\sigma_{bs} = 10^{(TS/10)}$.

Firstly, *TS-L* was estimated by fitting the mean σ_{bs} to the mean length ($\bar{L}$) (mean fitting, *MF*), with an assumed slope (a) of 20, resulting in a *TS-L* equation of the shape:

$$TS = a \, \log_{10}(L)\text{-}b, \qquad\qquad (9)$$

where, b is the intercept. To improve the fit of TS and L, a curve fitting method (curve fitting, CF) (Figure 3.3), similar to MacLennan and Menz (1996), was applied. To make the TS and L distributions directly comparable, they were scaled around their standard deviations:

$$x_{scaled} = \frac{x_i - \bar{x}}{\sigma_x} + \text{offset}, \qquad\qquad (10)$$

where $\bar{x}$ is mean of the data points x_i, σ_x is the standard deviation of x. The offset in each case is defined such that scaled values were strictly positive and the centres of the ranked distribution are at a similar location. To fit the TS distribution to the L distribution, normal or gamma distributions were fitted around the probability density distributions of scaled TS and scaled L. Curve fitting was assessed through the log-likelihood and the Akaike criterion (AIC) (Akaike 1973). At each point along the x-axis a value was taken both from the fitted L and TS density curves. The mean of these two values then provided a new reading for each point along the x-axis. In essence, the culmination of all these new values produced a new probability density $p(x)$ for each value x of the variable. Ranked scaled TS and L values were transformed back ($_{bt}$) into TS_{bt} and L_{bt} values. TS-L constants a and b with a given p were estimated for each TS_{bt} and L_{bt} pair in the linear domain.

3.3.8 Biomass estimates

Biomass and abundance estimates were based on 38 kHz recordings only. s_A were averaged over an Equivalent Distance Sampling Unit (EDSU) of 1 nmi (MacLennan 1990). A $\bar{L}$ was attributed to each fishing region. s_A recordings were gridded into regular sampling cells (30 x 30 m), defined such as to minimise the sampling error. Interpolation of non-sampled cells within each fishing region was achieved through kriging of the $\log_{10}$-transformed s_A values. The $\bar{L}$ was input in to the chosen TS-L relationship to give a $\overline{TS}$ for each fishing region. The mean fish density (ρ, the number of fish per nmi^2) for each fishing region was then calculated according to (MacLennan et al. 2002):

$$\rho = \frac{s_A}{4\pi \, \sigma_{bs}}, \qquad\qquad (11)$$

which was then scaled to the total area of each fishing region, to provide an abundance estimate. Applying a mean weight to these estimates resulted in a biomass estimate for the three fishing regions.

3.3.9 Estimation of sampling variance

Confidence intervals (CI) accounting for sampling error were computed using geostatistical techniques (Rivoirard et al. 2000, Gimona and Fernandes 2003, Woillez et al. 2009, Zwolinski et al. 2009, Scoulding et al. 2016). Due to the high percentage of zero values contained within acoustic data, variograms were based on a scaled, and natural log transformed dataset (Bez and Rivoirard 2001):

$$T = Ln\left(1 + \frac{s_A}{\overline{s_A}}\right). \tag{12}$$

The variogram of *T* was determined using the classical estimator (Matheron 1971) (Equation 1). Back-transformed variograms with a lag *h* $(\hat{v}_x(h))$ (Guiblin et al. 1995) were obtained through:

$$\hat{v}_x(h) = \left((d + \bar{x})^2 + var(x)\right) \cdot \left(1 - e^{\frac{-\sigma^2 v_T(h)}{var(T)}}\right), \tag{13}$$

$$\text{with } \sigma^2 = Ln\left(1 + \frac{var(x)}{(d+\bar{x})^2}\right), \tag{14}$$

where *d* is a constant, *var(x)* is the variance of the data points *x* and $\hat{\gamma}_L(h)$ is the variogram value of *T* at lag *h*.

The back-transformed experimental variograms were fitted by an exponential model. Various discretisation grids were trialled to compute the sampling variance σ_E^2. The number of discretisation steps used to estimate σ_E^2 was varied to minimise σ_E^2. The coefficient of variance (CV [%]) (Rivoirard et al. 2000) was calculated as:

$$CV = \sqrt{\frac{\sigma_E^2}{\bar{x}}}. \tag{15}$$

According to the central limit theorem the precision of estimates based on acoustic surveys generally follow a Gaussian distribution (Woillez et al. 2009). Therefore, CIs of the biomass estimates could be derived as:

$$CI = [est - t * (est * CV), est + t * (est * CV)],\qquad (16)$$

where *est* is the biomass estimate and *t* is 1.96 (at a level of 95%) (Scoulding et al. 2016).

3.4 Results

3.4.1 Biological sampling

A summary of the catch information, including the number of individuals caught by species or species-group within each of the three regions with percentage contributions to the total catch, the $\bar{L}$ for each species or species-group (estimated by fishing region), as well as the respective contribution to the total catch weight, can be found in Table 3.4.
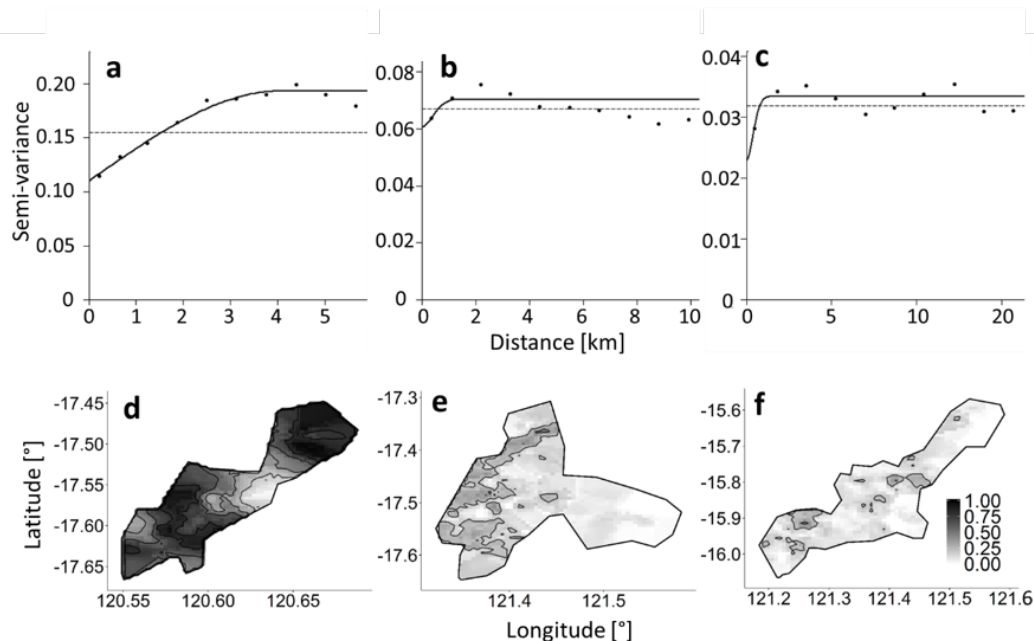
Figure 3.4 Experimental (black dots) and model (solid lines) variograms of the goldband snapper catch proportions, with the sample variance indicated by the dotted line within a) Region 1, b) Region 2 and c) Region 3. Ordinary kriging results for the goldband snapper catch proportions (greyscale gradient from 0 to 1) in Regions 1, 2, and 3 (d, e and f, respectively).

Variograms were fitted automatically (Desassis and Renard, 2013) to the catch proportions attributed to goldband snapper. Region 1 was fitted by a spherical model with range 4.07, sill

0.19 and a nugget effect of 0.11 (Figure 3.4a); Region 2 was fitted by a Gaussian model with a range of 1.04, a theoretical range of 0.60, a sill of 0.07 and a nugget effect of 0.06 (Figure 3.4b); Region 3 was fitted by a Gaussian model with a range of 0.99, a theoretical range of 0.57, a sill of 0.11 and a nugget effect of 0.02 (Figure 3.4c). Distribution of high goldband snapper catch proportions within Region 1 were widely distributed, except for the most central part (Figure 3.4d). In Region 2, the highest concentrations were found in the south-eastern part (Figure 3.3e), while in Region 3 distribution was patchier and in general contained the lowest concentrations (Figure 3.4f). Catch proportions directly influence acoustic density estimates, as they were used to disaggregate s_A. CV's on density estimates were 2.53 %, 2.74 % and 3.65 % for Regions 1, 2 and 3, respectively.

3.4.2 Target Strength estimates

TS estimates were based on a small number of schools that matched the detection criteria, recorded on the 4th December 2014. On this day, 61 goldband snapper were caught ($\bar{L}$ = 56.0 cm, σ = 4.71 cm, range = 43.5 – 68.0 cm). After the application of the Sawada index, a total of 2,564 targets and 311 tracks were detected at 38 kHz. Of these, 279 targets and 43 tracks were retained following the intersection filter. Mean ϑ of fish tracks ranged from -19.12° to 30.53° ($\bar{\theta}$ = 2.38°, σ = 7.79°). No significant correlation between mean TS and mean ϑ was detected at 38 kHz (Pearson correlation, r = 0.11, n = 43, p = 0.53). At 120 kHz, 2,913 targets and 578 tracks were detected prior to the intersection filtering, with 572 targets and 79 tracks remaining after application of the intersection filter. The $\bar{\theta}$ of all tracks was 1.11° (σ = 7.53°), ranging from -28.58° to 14.07°. No significant correlation between ϑ and TS could be found (Pearson correlation r = 0.08, n = 79, p = 0.48).
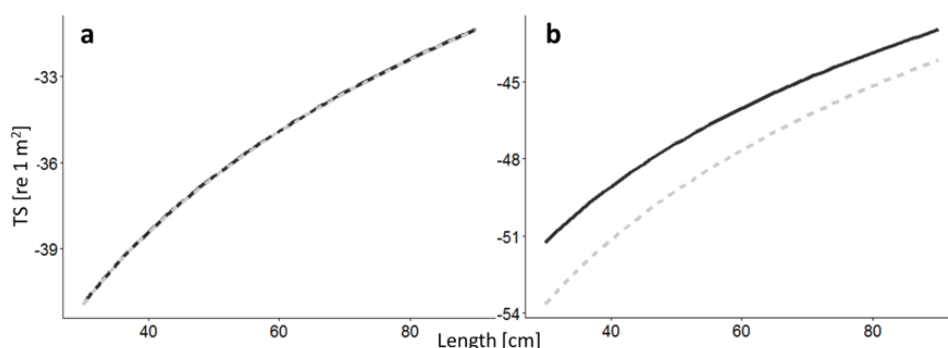
Figure 3.5 TS-L regressions estimated by mean fitting (grey dashed line) and curve fitting (black solid line) at a) 38 and b) 120 kHz for goldband between 30 and 90 cm in length.

Table 3.4 Summary of the catch information for Regions 1, 2 and 3. Mean length information with SD for all species groups and all 3 regions, number (N) of specimens observed with percentage contribution to the total observed catch in the respective region and estimated mean weight for all species groups and regions with percentage contribution to the total catch.

Region	Species group								
	Goldband snapper	Red emperor	Saddletail	Lutjanidae	Lethrinidae	Rankin cod	Cod	Trigger fish	Miscellaneous
	Mean length (± 1 standard deviation) [cm]								
1	56.33 (± 4.59)	56.75 (± 9.01)	57.45 (± 8.30)	30.97 (± 3.72)	30.87 (± 5.84)	NA	34.85 (± 5.27)	36.72 (± 6.61)	37.55 (± 11.1)
2	58.59 (± 7.35)	52.70 (± 8.53)	58.30 (± 14.9)	30.14 (± 5.10)	33.62 (± 6.64)	61.93 (± 8.86)	37.24 (± 10.8)	32.55 (± 4.21)	39.82 (± 15.9)
3	57.10 (± 7.23)	51.11 (± 8.39)	56.83 (± 10.9)	30.53 (± 4.89)	31.78 (± 6.54)	61.76 (± 7.62)	37.24 (± 8.76)	33.58 (± 5.03)	41.86 (± 14.8)
	Number of specimens (% contribution to the total catch by number)								
1	971 (66.05 %)	13 (0.88 %)	29 (1.97 %)	180 (12.24 %)	5 (0.34 %)	0	22 (1.50 %)	18 (1.22 %)	232 (15.78 %)
2	387 (10.22 %)	896 (23.65 %)	54 (1.43 %)	643 (16.97 %)	355 (9.37 %)	303 (8.00 %)	157 (4.14 %)	779 (20.56 %)	214 (5.65 %)
3	383 (5.16 %)	1376 (18.55 %)	293 (3.95 %)	1872 (25.24 %)	972 (13.11 %)	320 (4.31 %)	1220 (16.45 %)	245 (3.30 %)	735 (9.91 %)
	Mean weight [g] (% contribution to the total catch by weight)								
1	2382 (66.02 %)	3057 (1.18 %)	3718 (2.95 %)	692 (7.57 %)	486 (0.18 %)	0	1062 (1.12 %)	1212 (0.97 %)	1049 (13.80 %)
2	2671 (15.01 %)	2439 (28.48 %)	3880 (2.86 %)	640 (8.09 %)	621 (4.08 %)	3481 (11.00 %)	1293 (3.20 %)	852 (15.69 %)	1247 (6.11 %)
3	2478 (9.29 %)	2222 (21.93 %)	3601 (5.51 %)	664 (16.62 %)	528 (6.57 %)	3451 (9.06 %)	1293 (17.42 %)	933 (3.75 %)	1444 (5.55 %)
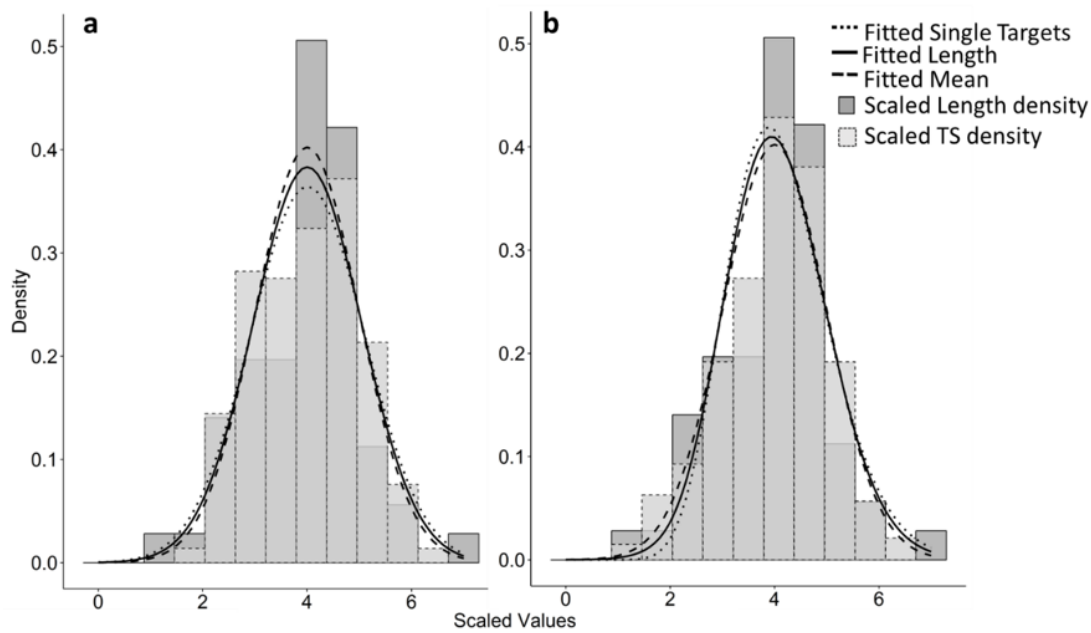
Figure 3.6 Fitted single targets (black dotted line), fitted length (black solid line), and fitted mean (black dashed line) distributions of goldband snapper with length (dark grey) and single-target density (light grey) distribution histograms at a) 38 kHz and b) 120 kHz. The histograms are superimposed on one another for comparison purposes.

Fitting the $\overline{TS}$ with the $\overline{L}$, assuming a slope (a) of 20, resulted in (Figure 3.5):

$$TS_{MF38} = 20\log_{10}(L) - 70.5 \qquad (17)$$

and

$$TS_{MF120} = 20\log_{10}(L) - 83.2 . \qquad (18)$$

The length distribution of the 61 goldband snapper was best described by a normal distribution (Figure 3.6):

$$\frac{1}{\sqrt{(2\pi)}\sigma(x)} e^{\frac{(x-\bar{x})^2}{2\sigma(x)^2}} , \qquad (19)$$

where *x* is the value of the scaled variable (length), $\bar{x}$ = 4.01 and $\sigma(x)$ = 2.83 (log-likelihood = -354.85, *AIC* = 713.70). Similarly, single-targets retained at 38 kHz fitted a normal distribution with $\bar{x}$ = 4.00 and σ = 0.99 (log-likelihood = -86.05, AIC = 176.10) (Figure 3.6). Single-targets at 120 kHz were best fitted by a gamma distribution of the shape (Figure 3.6):

$$\frac{1}{\left(s^q \gamma(k)\right) x^{q-1} e^{\frac{x}{s}}},$$
(20)

where γ is the gamma function, shape (q) = 17.83 and rate (k) = 4.33 (log-likelihood = -861.28, AIC = 1726.57), and scale (s) $= \frac{1}{k}$. Weighting σ_{bs} and L by the probability distribution of the combined mean of the length distribution and single-target distribution curves, resulted in a single *TS-L* equation for each frequency (Figure 3.5 and 3.7):

$$TS_{CF38} = 20.01 \log_{10}(L) - 70.5 \; (\sigma_a = 3.18, \sigma_b = 5.06)$$
(21)

and

$$TS_{CF120} = 16.4 \log_{10}(L) - 77.0 \; (\sigma_a = 1.96, \sigma_b = 2.54) \,.$$
(22)

If applied to the *L* distribution, the modelled $\overline{TS}$ at 38 kHz was -35.7 dB re 1 m^2 (σ = 0.8 dB re 1 m^2) while the computed mean, based on *in situ* recordings was -35.7 dB re 1 m^2 (σ = 2.8 dB re 1 m^2). At 120 kHz the mean TS_{CF} was -48.4 dB re 1 m^2 (σ = 0.6 dB re 1 m^2), compared to a mean of -48.4 dB re 1 m^2 (σ = 3.4 dB re 1 m^2) based on the measured data, with a modelled $\overline{L}$ of 54.80 cm and an observed $\overline{L}$ of 54.92 cm.

Based on TS_{CF} at 38 kHz, σ_{bs} for all *L* contained in the catch data was derived (σ_{bsCF}). Based on σ_{bsCF} the CV of length variations on acoustic density estimates could be derived and was 1.21 % for Region 1; 1.62 % for Region 2; 2.00 % for Region 3.
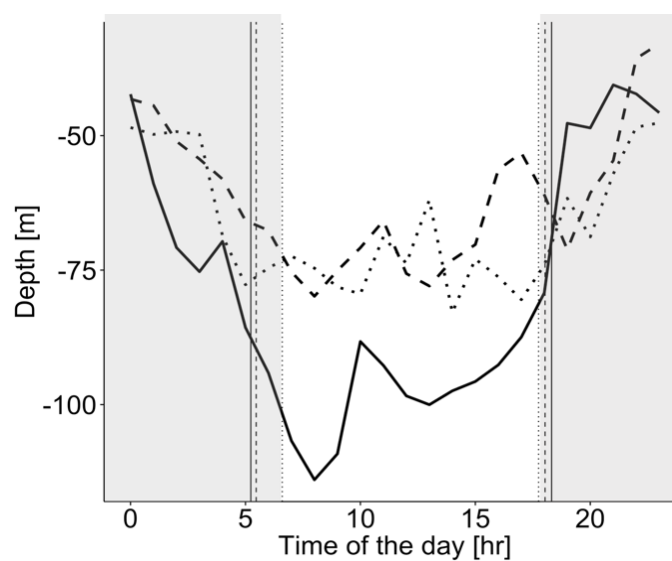
Figure 3.7 Indication of the diurnal vertical migration of goldband snapper schools detected within the three regions with the mean depth [m] of occurrence plotted against the time of the day in hours (black line = Region 1; dashed line = Region 2; dotted line = Region 3).

3.4.3 Diurnal vertical migration

The location of schools in the water column varied with time. Daytime and night time were defined by modelled times of sunrise and sunset (Figure 3.7). On the days of data collection sunrise was at 05:14 (σ = 00:13) in Region 1, 05:28 (σ = 00:15) in Region 2 and 06:06 (σ = 00:16) in Region 3. Sunset was estimated to have occurred at 18:19 (σ = 00:01) in Region 1, at 18:02 (σ = 00:10) in Region 2 and at 17:45 (σ = 00:10) in Region 3. During daylight (time between sunrise and sunset), the mean depth of schools was 95.59 m (σ = 38.84 m) in Region 1; 70.21 m (σ = 23.63 m) in Region 2 and 73.02 m (σ = 23.78 m) in Region 3. During night time (time between sunset and sunrise), schools were generally found higher in the water column. In Region 1 the mean depth of schools during night time was 77.54 m (σ = 39.15 m), 55.20 m (σ = 22.63 m) within Region 2 and 55.39 m (σ = 26.77 m) in Region 3 (Figure 3.7). A higher number of schools were detected during the daytime, 71.4 %, 69.2 % and 71.5 % for Regions 1, 2, and 3 respectively. Peak school detections in all three regions occurred at: 1) around sunrise, 2) about seven hours' post-sunrise and 3) 10 hours after sunrise. The lowest number of detections were observed approximately 13 hours after sunrise, which coincides roughly with the time of sunset. Acoustic analysis of schools and biomass or abundance estimates were based on daytime data only, as all biological sampling was conducted on the bottom and the lower number of schools in the water column indicate that fish were more dispersed during the night.

Region	s_A			Density [individuals/nmi^2]			Abundance [individuals]			Weight [g]	Biomass [t]			CV [%]
	Mean	CI (±95%)		Estimate	CI (±95%)		Estimate	CI (±95%)		Mean	Estimate	CI (±95%)		
		Lower	Upper		Lower	Upper		Lower	Upper			Lower	Upper	
1	33.96	25.35	42.58	9,517.9	7,176.5	11,906.5	314,089	235,179	391,257	2,381	748.1	562.5	933.8	20.9
2	9.70	5.40	14.04	2,511.6	1,383.7	3,649.0	323,998	191,193	468,840	2,670	865.4	477.5	1,266.0	15.4
3	3.46	2.28	4.65	944.7	621.2	1,270.0	199,324	133,240	266.930	2,476	493.7	326.62	670.2	10.2

Table 3.5 Mean sA, abundance, biomass and density estimates (with 95% CI) for Regions 1, 2, and 3 with coefficient of variance (CV in %) based on sampling and confidence intervals at a level of 95 % (CI)

3.4.4 Biomass estimates and sampling variance

The water depth of the three fishing regions was less than 200 m throughout. At these depths, the r_{sn}, estimated from 38 kHz S_v echograms (thresholded at -60 dB re 1 m^2 m^{-3}) was

greater than 30. The resulting estimated error introduced to biomass or abundance estimates would be <0.1%. At a data threshold of -70 dB re 1 m^2 m^{-3} (38 kHz), this r_{sn} introduced a bias would be ≈1 % at 200 m. The calculated CV attributed to fluctuations in temperature and salinity on r_{sn} were < 0.01 % (Figure 3.9) and were therefore deemed not to have a significant impact on the eventual biomass or abundance estimates.

TS of a 38.1 mm WC calibration sphere (TS_{Cal}) varies with c_w. The maximum difference in c_w and therefore TS occurred between the calibration (March, 2015) and November, 2014. During calibration, c_w was 1541 ms^{-1} (at 10 m depth), while in November, it was 1530 ms^{-1} (at 100 m depth) in November. The impact of this fluctuation on TS_{Cal} was a variation between -42.3 and -42.4 dB re 1 m^2. Total variation of TS_{Cal} between August and March was 1.60%, which equals a CV of 1.15 % in the linear domain.
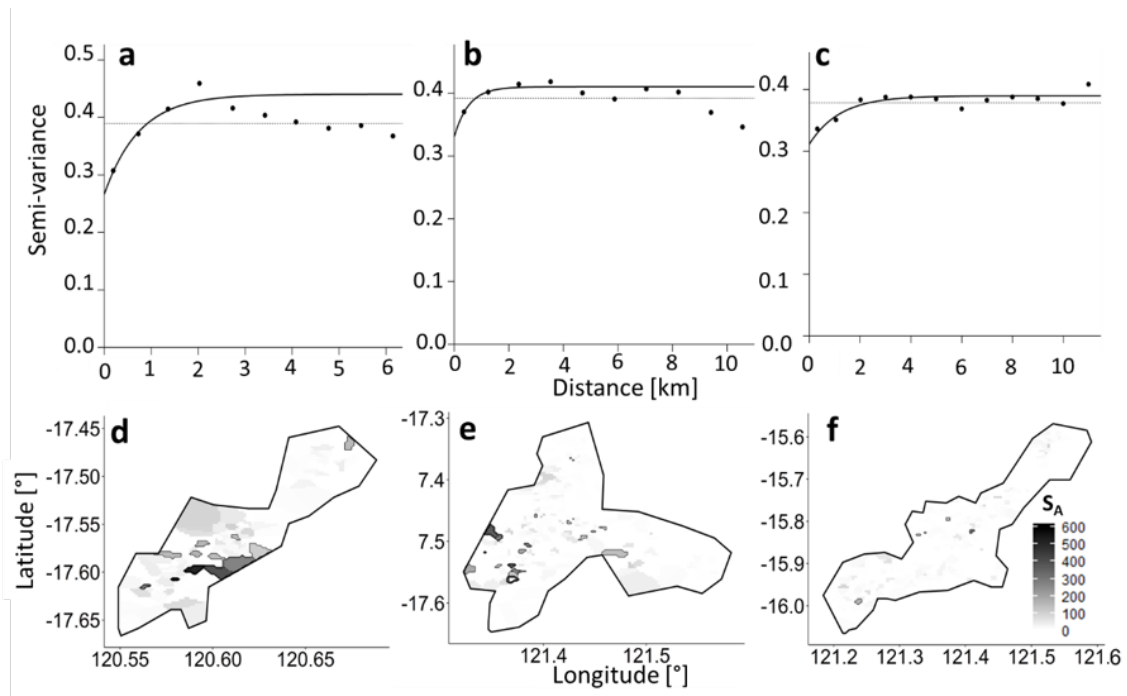
Figure 3.8 Experimental (black dots) and model (solid black lines) variograms, fitting the log transformed s_A [m^2 nmi^{-2}] attributed to goldband snapper with sampling variation (grey dotted lines) for; a) Region 1, fitted by an exponential model (range is 2.23, theoretical range is 0.75, sill is 0.17) with a nugget effect of sill 0.27; b) Region 2 fitted by an exponential model (range is 1.63, theoretical range is 0.54, sill is 0.13) with a nugget effect sill of 0.27 (c); Region 3 fitted by an exponential model (range is 3.62, theoretical range is 1.21 sill is 0.08) with a nugget sill of 0.39.

A summary of density, abundance and biomass estimates with associated CI based on 38 kHz data can be found in Table 3.5. Exponential variograms fitting the log transformed experimental variograms of the s_A in Region 1, 2 and 3 had a range of 2.16, 1.63 and 3.62 km,

respectively. Theoretical range was 0.72, 0.54 and 1.21 km for Regions 1, 2 and 3, respectively. The sill was 0.24, 0.13, 0.08 with a nugget effect of sill 0.23, 0.27, 0.31 for the three regions, respectively (Figure 3.8). Kriging of s_A at 38 kHz revealed a patchy distribution of the detected acoustic density, attributed to goldband snapper within the three regions. Mean acoustic
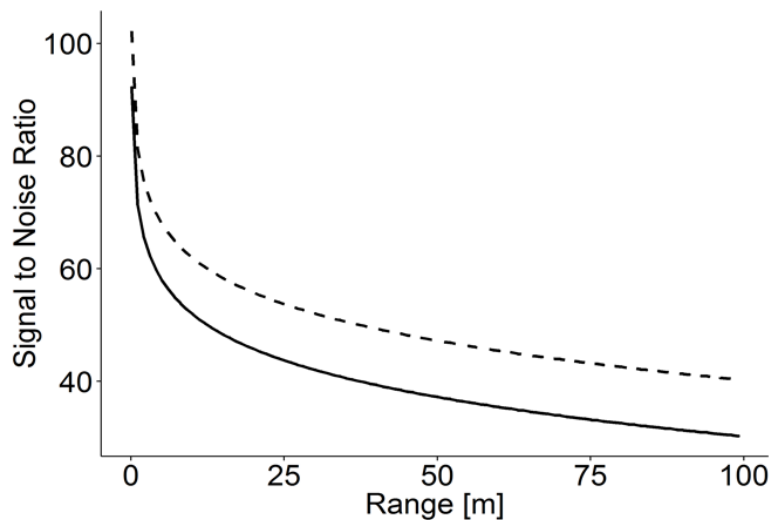
Figure 3.9 Signal to Noise Ratio (rsn) estimates at 38 kHz for depths ranging from 0 to 100 m for Sv of -60 dB re 1 m2m-3 (dashed line) and -70 dB re 1 m2m-3 (black line).

density was highest in Region 1 at 33.96 m^2nmi^{-2} (CI = [25.35, 42.58]) compared to 9.70 m^2nmi^{-2} (CI = [5.40, 14.04]) in Region 2 and 3.46 m^2nmi^{-2} (CI = [2.28, 4.65]) in Region 3. The curve fitting method was selected as it was assumed that the fit would be more accurate, given the method takes into account density variations of TS and L. Applying the TS-L equation based on the curve fitting method (Equation 21), with mean lengths of 56.6, 58.59 and 57.09 cm for Regions 1, 2 and 3, respectively (Table 3.4), gave density estimates for the regions. The estimated goldband snapper density in Region 1 was 9,518 individuals/nmi^2, whilst the density estimate in Region 2 was approximately 1/4rd of this, with 2,512 individuals/nmi^2 (Table 3.5). The lowest density estimate was observed in Region 3, with only 945 individuals/nmi^2 (Table 3.5). The total abundance of goldband snapper in each fishing region is given in Table 3.5. Raising abundance estimates to biomass estimates, with mean weights of 2,138 g for Region 1, 2,670 g for Region 2 and 2,476 g for Region 3 (Table 3.4), resulted in total biomass estimates of 748.1 t, 477.5 t and 326.6 t for the three regions respectively (Table 3.5). Applying either of the TS-L equations (TS_{CF} or TS_{MF}), to estimates of acoustic density at 38 kHz, caused minor differences (less than 0.1 %) in abundance and biomass. Estimation of the sampling error resulted in CV's of 20.9 %; 15.4 % and 10.2 % for Regions 1, 2 and 3, respectively. Bootstrapped CV's of the s_A data were ± 13.8 % for Region 1; ± 22.7 % for Region 2; ± 18.6% in Region 3. The combined errors gave a total CV of 28.2 – 50.6 % for the three regions. A summary of CV's for

the different error estimates and their respective influence on biomass or abundance estimates can be found in Table 3.6.

Table 3.6 . CV estimates for density estimates of goldband snapper based on various analysed sources of error.

Source of error	CV [%]
Random error in acoustic data	13.8 - 22.7
Sampling variance	10.2 – 20.9
Signal to Noise	0 – 0.1
TS variability due to changes in temperature and salinity	0.5 – 1.15
Length estimates	1.2 – 2.0
Catch proportions	2.5 – 3.7
Total	28.2 – 50.6

3.5 Discussion

Most current fisheries resource monitoring programmes are focussed on assessing single species populations. Monitoring is typically carried out under ideal conditions for the chosen sampling method. AT surveys, for example, are generally conducted during the spawning season, when mature fish are known to aggregate in large single-species schools. Such an approach is a valuable tool, which provides a snapshot of the status and distribution of the species being surveyed within defined spatio-temporal boundaries, building up consistent time series over years of survey (Fässler et al. 2016). In order to move towards EBFM there is a need for larger scale monitoring, both temporally and spatially, to allow for improved parametrisation and validation of EBFM (Handegard et al. 2013). Taking advantage of their time at sea, fishing vessels are being considered as alternative sampling platforms, to the traditional research vessel (ICES 2007). Previous studies have investigated the potential of chartered fishing vessels to perform scientific surveys (ICES 2007, Ressler et al. 2009, Barbeaux 2012). This can be successful when such studies are able to take advantage of the catch processing times to conduct surveys (O'Driscoll and Macaulay 2005), though these times are not always available. They can also build a knowledge base by making use of fisheries dependent acoustic data to improve timing and design of AT surveys (Melvin et al. 2001, 2002). Some studies have looked into the utility of uncalibrated acoustic data to gain insights into the distribution of fish aggregations (Barbeaux 2012, Barbeaux et al. 2013), or have explored the potential use of opportunistically collected, calibrated acoustic data (Fässler et al. 2016). Fässler et al. (2016) showed that acoustic densities derived from calibrated fishing vessels are valid proxies for fish densities which could be converted into relatively accurate

biomass estimates, within key fishing regions. The main challenges associated with the large-scale collection of opportunistic acoustic data are the large amount of data collected (acoustic and alternative sampling), which still require manual processing, the need for calibration to derive any quantitative estimates, and the lack of a systematic sampling design. Here, all acoustic data were collected from calibrated systems.

In a multi-species environment, such as the NDSF, acoustic studies generally depend on dedicated groundtruth information, to improve the disaggregation of acoustic data into biologically meaningful categories at species or species group levels (Simmonds and MacLennan 2005). During AT surveys, such information can generally be obtained from dedicated fishing operations (i.e. by trawling on acoustic observations). In the current study, no dedicated catch information could be collected without interruption to routine fishing operations. Alternative sampling methods to verify acoustic observations include optical recordings of the resource (Ryan et al. 2009, Kloser et al. 2011, 2013, Fernandes et al. 2016), which typically collect visual data that is as spatially and temporally co-located as possible (Ryan et al 2009; Fernandes et al 2016). In the current study, fish caught by traps, and measured using a GoPro, were used to collect alternative evidence to verify acoustic observations. Due to the nature of the fishery, where traps typically soak for multiple hours, attracting fish from areas surrounding the trap to varying degrees and distances (Newman et al. 2012), catch information and acoustic recordings were not temporally, or spatially synchronised. Kriging species proportions as a proxy for the relative goldband snapper distributions was assumed to be a valid approximation based on findings by Newman et al. (2012), where species richness and diversity found within traps were described as representative. It is noted here that some species might be underrepresented by traps, however, the dominance of goldband snapper in the selected fishing regions suggest that kriged proportions were acceptable as the best available approximation. It is also noted that, on occasion goldband snapper might have been confused with other species of the *Pristipomoides* genus. However, based on anecdotal information provided by the fisherman, this error is assumed to be low, given that species of this genus, other than goldband snapper are mainly observed on the shelf edge, outside of the three fishing regions.

Mean estimated lengths of goldband snapper (56.33 cm (Region 1); 58.59 cm (Region 2); 57.10 cm (Region 3), Table 3.4) were comparable to measurements made by Lloyd et al. (2000) in Northern Australia, where mean length ranged from 55 to 60 cm. As goldband snapper become sexually mature at around 55 cm (Newman and Dunk 2002) and previous

studies have reported that juvenile and adult goldband snapper do not generally occupy the same habitat (Allen 1985), it is suggestive that the acoustic data in this study represent aggregating adult fish and, as such, can be used as a monitoring tool. Furthermore, adult goldband snapper tend to form large schools, feeding on fish, crustaceans, squid and salps, close to the bottom and within the water column (Allen 1985).

TS-L equations can only be derived from single-targets in combination with length measurements taken from the same population (MacLennan and Menz 1996). Only catch information, obtained near the selected goldband snapper schools were accepted as being biologically relevant and could therefore, be assumed to originate from the same population. To remove unwanted targets and only consider 'clean' single-targets, several filtering methods were applied to the data. Only targets close to the bottom, where adult goldband snapper are most likely to school during the day (Newman et al. 2008), were considered. High density cells were excluded, applying methods described by Sawada et al. (1993). Tilt angle is known to be one of the main sources of variability in *TS* estimates for many fish (Ona 1999, 1990, 2001, Simmonds and MacLennan 2005). Influence of tilt angle could not be investigated within the present study. The majority of recorded targets were orientated between -10° and 10° (92.0 % at 38 kHz; 83.4 % at 120 kHz) and detected fluctuations were masked by the larger stochastic variation in *TS*. Extended recordings or a modelling approach is recommended to further assess this relationship.

Similar to methods described by MacLennan and Menz (1996), we propose a stochastic method to derive a *TS-L* equation from similarly shaped *TS* and *L* distributions (Equations 21 and 22). *TS-L* estimates were applied to length distribution data and were very similar to estimates (<0.1% variation) given by the traditional *TS-L* fitting method (Equations 17 and 18). As with MacLennan and Menz (1996), this new density curve fitting method takes into account the distribution of both, *TS* and *L*. A main difference compared to MacLennan and Menz (1996), is that the *TS-L* equation here is based on a back-transformed, scaled, combined density distribution curve, rather than on histogram based percentiles. An advantage of the proposed method, over that presented by MacLennan and Menz (1996), is that both constants, *a* and *b*, of the *TS-L* equation can be estimated rather than assuming a slope of 20.

Geostatistics have been identified as a viable tool to estimate fish abundance and biomass based on acoustic densities and to derive reliable sampling error estimates (Rivoirard et al. 2000, Petitgas et al. 2003, Gimona and Fernandes 2003, Woillez et al. 2009, Scoulding et

al. 2016). Understanding the effects of survey design is crucial to any biomass, abundance or distribution estimate. This is particularly important if the underlying sampling strategy can, at best, be described as un-stratified and directed. Whereas, traditional AT surveys systematically sample the survey area, generally following parallel line or zig-zag transects (Simmonds and MacLennan 2005), fishing vessels (during normal operation) directly target known fishing grounds, in an attempt to maximise catch or catch opportunities (Fässler et al. 2016). The application of kriging techniques to estimate catch proportion distributions, as well as acoustic fish density estimates, facilitated the estimation of a sampling error (CV = 20.9 % in Region 1, CV = 15.4 % in Region 2 and CV = 10.2 % in Region 3). Given the high density of data points collected within these fishing regions, CV's were similar to age stratified acoustic abundance CV's for herring in the North Sea estimated by Woillez et al. (2009) (10-32 %), and those estimated by Scoulding et al. (2016) for mackerel around the Shetland islands (14-17 %). This suggests that sampling within these fishing regions is of sufficient quality to provide localised abundance, biomass or distribution estimates. These estimates are based on manually drawn polygons around key fishing regions, hence containing high resolution data. Estimates are most likely only valid for those selected fishing regions and are not necessarily representative of the wider stock distribution, nor the remaining area of the fishery.

Demer (2004) identified several sources of error influencing the outcome of biomass estimates, including hydrographic conditions, diurnal vertical migration, species classification, detection probability (i.e. r_{sn}), sound speed and absorption as well as sampling and random error. Here, bias associated with r_{sn} was estimated to be low, at levels <0.1 %, which is comparable to Demer (2004). r_{sn} increases with depth and if deeper areas were considered, the r_{sn} bias would increase exponentially (Figure 3.9). Influence of hydrographic conditions was estimated by Simmonds and MacLennan (2005) to be 0-5%. Fluctuations in environmental conditions within the sampled regions were not extreme, due to the location of the NDSF and the general stability of tropical climates. Total estimated error based on environmental conditions was of 1.15 %. *TS* estimates were based on *in situ* recordings and should therefore minimise the error associated with *TS* estimates.

Simmonds and MacLennan (2005) estimate that an uncertainty of 0-25 % can be linked with diurnal migration of fish. Given that the vessel was mostly stationary or drifting during night time, and the lack of fishing activity in times of darkness only daytime information was used and no error estimates could be derived. Only using data collected during hours of daylight should remove effects of diurnal vertical migration.

Localised hotspots with catch consisting purely of, or dominated by goldband snapper could be easily identified through catch observations. If analysis of catch data was to be extended to all boats operating within the NDSF, key habitats of goldband snapper at given times could be identified. Through direct observations of catch information, improved estimates of catch indices, as proposed by Marriott et al. (2013), could be expanded to include length stratified catch indices and methods presented here could be extended to other species of interest. Taking advantage of such information encompasses the possibility of conducting dedicated surveys, based on a combination of catch information and acoustic recordings. As an alternative to trap catches, alternative methods including optical recordings (Fernandes et al. 2016) could be explored, to overcome the spatio-temporal lag between acoustic observations and biological sampling. Continuous sampling of identified fishing grounds would potentially improve insights into the health of the stock, through the establishment of a relative acoustic biomass index.

3.6 Acknowledgements

3.7 References

Akaike, H. 1973. Information theory and an extension of the maximum likelihood principle. International Symposium on Information Theory, Akadeemiai Kiadi, Budapest, Hungary In B. Petran and F. Csaaki: 267–281.

Allen, G.R. 1985. FAO species catalogue vol. 6 snappers of the world: An annotated and illustrated catalogue of Lutjanid species known to date. Food and Agriculture Organization of the United Nations. Available from http://afrilib.odinafrica.org/handle/0/15796 [accessed 30 November 2016].

Ballón, M., Bertrand, A., Lebourges-Dhaussy, A., Gutiérrez, M., Ayón, P., Grados, D., and Gerlotto, F. 2011. Is there enough zooplankton to feed forage fish populations off Peru? An acoustic (positive) answer. Prog. Oceanogr. **91**(4): 360–381. doi:10.1016/j.pocean.2011.03.001.

Barbeaux, S.J. 2012. Scientific acoustic data from commercial fishing vessels: Eastern Bering Sea walleye pollock (*Theragra chalcogramma*). Ph.D., University of Washington, United States -- Washington. Available from http://search.proquest.com.dbgw.lis.curtin.edu.au/docview/1013759483/abstract/3E AE09E9E2FC462CPQ/1 [accessed 6 September 2016].

Barbeaux, S.J., Horne, J.K., and Dorn, M.W. 2013. Characterizing walleye pollock(Theragra chalcogramma) winter distribution from opportunistic acoustic data. .ICES J. Mar. Sci. **70**: 1162–1173.

Bez, N., and Rivoirard, J. 2001. Transitive geostatistics to characterise spatial aggregations with diffuse limits: an application on mackerel ichtyoplankton. Fish. Res. **50**(1–2): 41–58. doi:10.1016/S0165-7836(00)00241-1.

Blackman, S.S. 1986. Multiple-target tracking with radar applications. Dedham MA Artech House Inc 1986 463 P **1**. Available from http://adsabs.harvard.edu/abs/1986ah...bookQ....B [accessed 9 August 2016].

Campanella, F., and Taylor, J.C. 2016. Investigating acoustic diversity of fish aggregations in coral reef ecosystems from multifrequency fishery sonar surveys. Fish. Res. **181**: 63–76. doi:10.1016/j.fishres.2016.03.027.

Chen, C.T., and Millero, F.J. 1977. Speed of sound in seawater at high-pressures. Journal of the Acoustical Society of America **62**: 1129–1135.

Coetzee, J. 2000. Use of a shoal analysis and patch estimation system (SHAPES) to characterise sardine schools. Aquat. Living Resour. **13**(1): 1–10. doi:10.1016/S0990-7440(00)00139-X.

Conti, S.G., Demer, D.A., Soule, M.A., and Conti, J.H. 2005. An improved multiple-frequency method for measuring in situ target strengths. ICES J. Mar. Sci. J. Cons. **62**(8): 1636–1646.

Dalen, J., and Karp, W.A. 2007. Collection of acoustic data from fishing vessels. International Council for the Exploration of the Sea.

Demer, D.A. 2004. An estimate of error for the CCAMLR 2000 survey estimate of krill biomass. Deep Sea Res. Part II Top. Stud. Oceanogr. **51**(12): 1237–1251.

Demer, D.A., Berger, L., Bernasconi, M, Bethke, E., Boswell, K., Chu, D., Domokos, R., and et al. 2015. Calibration of acoustic instruments. ICES Cooperative Research Report No. 326.

Demer, D.A., Soule, M.A., and Hewitt, R.P. 1999. A multiple-frequency method for potentially improving the accuracy and precision of in situ target strength measurements. J. Acoust. Soc. Am. **105**(4): 2359–2376.

Desassis, N., and Renard, D. (2013) Automatic Variogram Modeling by Iterative Least Squares: Univariate and Multivariate Cases. Mathematical Geosciences 45 (4) pp 453-470.

Dragesund, O., and Olsen, S. 1965. On the possibility of estimating year-class strength by measuring echo-abundance of 0-group fish.

Echoview Software Pty Ltd. 2016. Echoview software. Echoview Software Pty Ltd, Hobart, Australia.

Fässler, S.M.M., Brunel, T., Gastauer, S., and Burggraaf, D. 2016. Acoustic data collected on pelagic fishing vessels throughout an annual cycle: Operational framework, interpretation of observations, and future perspectives. Fish. Res. **178**: 39–46. doi:10.1016/j.fishres.2015.10.020.

Fernandes, P.G., Copland, P., Garcia, R., Nicosevici, T., and Scoulding, B. 2016. Additional evidence for fisheries acoustics: small cameras and angling gear provide tilt angle distributions and other relevant data for mackerel surveys. ICES Journal of Marine Science. doi:10.1093/icesjms/fsw091.

Fofonoff, P., and Millard, R. 1983. Algorithms for computation of fundamental properties of seawater. UNESCO Technical Papers in Marine Science.: 53.

Froese, R., and Pauly, D. 2016. FishBase. World Wide Web electronic publication. Available from www.fishbase.org, (07/2016).

Gimona, A., and Fernandes, P.G. 2003. A conditional simulation of acoustic survey data: advantages and potential pitfalls. Aquat. Living Resour. **16**(3): 123–129. doi:10.1016/S0990-7440(03)00028-7.

Guiblin, P., Rivoirard, J., and Simmonds, E.J. 1995. Analyse structurale de donnees a distribution dissymetrique exemple du hareng ecossais. Cahiers de Geostatistique 5: 137-160.

Handegard, N.O., Buisson, L. d., Brehmer, P., Chalmers, S.J., De Robertis, A., Huse, G., Kloser, R., Macaulay, G., Maury, O., Ressler, P.H., Stenseth, N.C., and Godø, O.R. 2013. Towards an acoustic-based coupled observation and modelling systemfor monitoring and predicting ecosystem dynamics of the open ocean. Fish **14**: 605–615.

ICES. 2007. Collection of acoustic data from fishing vessels. ICES Cooperative Research Report No. 287. 83 pp. International Council for the Exploration of the Sea.

ICES. 2015. Manual for International Pelagic Surveys (IPS). International Council for the Exploration of the Sea - IPS.

Kailola, P.J. 1993. Australian fisheries resources. Bureau of Resource Sciences, Dept. of Primary Industries and Energy; Fisheries Research and Development Corp. Available from http://agris.fao.org/agris-search/search.do?recordID=US201300733922 [accessed 30 November 2016].

Keith, G. J., Ryan, T. E., and Kloser, R. J. 2005. ES60adjust.jar. Java software utility to remove a systematic error in Simrad ES60 data. In CSIRO Marine and Atmospheric Research Hobart. Castray Esplanade, Tasmania, Australia. https://bitbucket.org/gjm/calibration-code/wiki/Home.

Kloser, R.J., Macaulay, G.J., Ryan, T.E., and Lewis, M. 2013. Identification and target strength of orange roughy (Hoplostethus atlanticus) measured in situ. J. Acoust. Soc. Am. **134**(1): 97–108. doi:10.1121/1.4807748.

Kloser, R.J., Ryan, T., Sakov, P., Williams, A., and Koslow, J.A. 2002. Species identification in deep water using multiple acoustic frequencies. Can. J. Fish. Aquat. Sci. **59**(6): 1065–1077. doi:10.1139/f02-076.

Kloser, R.J., Ryan, T.E., Macaulay, G.J., and Lewis, M.E. 2011. In situ measurements of target strength with optical and model verification: a case study for blue grenadier, Macruronus novaezelandiae. ICES J. Mar. Sci. J. Cons. **68**(9): 1986–1995.

Kloser, R.J., Ryan, T.E., Young, J.W., and Lewis, M.E. 2009. Acoustic observations of micronekton fish on the scale of an ocean basin: potential and challenges. ICES J. Mar. Sci. J. Cons. **66**(6): 998–1006. doi:10.1093/icesjms/fsp077.

Korneliussen, R.J., Diner, N., Ona, E., Berger, L., and Fernandes, P.G. 2008. Proposals for the collection of multifrequency acoustic data. ICES J. Mar. Sci. J. Cons. **65**(6): 982–994. doi:10.1093/icesjms/fsn052.

Koslow, J.A. 2009. The role of acoustics in ecosystem-based fishery management. ICES J. Mar. Sci. J. Cons. **66**(6): 966–973. doi:10.1093/icesjms/fsp082.

Lezama-Ochoa, A., Ballón, M., Woillez, M., Grados, D., Irigoien, X., and Bertrand, A. 2011. Spatial patterns and scale-dependent relationships between macrozooplankton and fish in the Bay of Biscay: an acoustic study. Mar. Ecol. Prog. Ser. **439**: 151–168. doi:10.3354/meps09318.

Lloyd, J., Ovenden, J., Newman, S., and Keenan, C. 2000. Stock structure of Pristipomoides multidens resources across northern Australia. NT Fish. Rep. **49**. Available from http://frdc.com.au/research/Documents/Final_reports/1996-131-DLD.pdf [accessed 30 November 2016].

MacLennan, D.N. 1990. Acoustical measurement of fish abundance. J. Acoust. Soc. Am. **87**(1): 1–15.

MacLennan, D.N., Fernandes, P.G., and Dalen, J. 2002. A consistent approach to definitions and symbols in fisheries acoustics. ICES J. Mar. Sci. J. Cons. **59**(2): 365–369. doi:10.1006/jmsc.2001.1158.

MacLennan, D.N., and Menz, A. 1996. Interpretation of in situ target-strength data. ICES J. Mar. Sci. J. Cons. **53**(2): 233–236. doi:10.1006/jmsc.1996.0027.

Marriott, R.J., O'Neill, M.F., Newman, S.J., and Skepper, C.L. 2013. Abundance indices for long-lived tropical snappers: estimating standardized catch rates from spatially and temporally coarse logbook data. ICES J. Mar. Sci. J. Cons.: fst167. doi:10.1093/icesjms/fst167.

Matheron, G. 1971. The theory of regionalised variables and its applications. Cahiers du centre de Morphologie Mathematique, Fontainebleau 5 (Ecole Nationale Superiore des Mines de Paris, Paris, France).

Meeus, J.H. 1991. Astronomical Algorithms. Willmann-Bell, Incorporated.

Melvin, G., Li, Y.C., Mayer, L., and Clay, A. 2002. Commercial fishing vessels, automaticacoustic logging systems and 3D data visualization. ICES J. Mar. Sci. (59): 179–189.

Melvin, G., Stephenson, R.L., Power, M.J., Fife, F.J., Clark, K.J., and et al. 2001. Industryacoustic surveys as the basis for in-season decisions in a co-managementregime. In: Funk, F. (Ed.), Herring Expectations for a New Millennium.University of Alaska Sea Grant, AK-SG-01-04, Fairbanks, Alaska,pp. 675–688.

Mitson, R.B., and Knudsen, H.P. 2003. Causes and effects of underwater noise on fish abundance estimation. Aquat. Living Resour. **16**(3): 255–263. doi:10.1016/S0990-7440(03)00021-4.

Newman, S.J., and Dunk, I.J. 2002. Growth, Age Validation, Mortality, and other Population Characteristics of the Red Emperor Snapper, Lutjanus sebae (Cuvier, 1828), off the Kimberley Coast of North-Western Australia. Estuar. Coast. Shelf Sci. **55**(1): 67–80. doi:10.1006/ecss.2001.0887.

Newman, S.J., and Dunk, I.J. 2003. Age validation, growth, mortality, and additional population parameters of the goldband snapper (Pristipomoides multidens) off the Kimberley coast of northwestern Australia. Fish. Bull. **101**(1): 116–128.

Newman, S.J., Harvey, E.S., Rome, B.M., McLean, D.L., and Skepper, C.L. 2012. Relative efficiency of fishing gears and investigation of resource availability in tropical demersal scalefish fisheries. . Final Report FRDC Project No. 2006/031. Fisheries Research Report No. 231. Department of Fisheries, Western Australia, Western Australia.

Newman, S.J., Smith, K.A., and Skepper, C.L. 2008. Northern demersal scalefish managed fishery. Department of Fisheries, Western Australian Fisheries & Marine Research Laboratories.

Newman, S.J., Wakefield, C., Skepper, C., Boddington, D., Blay, N., Jones, R., and Dobson, P. 2015. North Coast Demersal Fisheries Status Report In: Status Reports of the Fisheries and Aquatic Resources of Western Australia 2014/15: The State of the Fisheries eds. W.J. Fletcher and K. Santoro, Department of Fisheries, Western Australia, pp. 39-48.

O'Driscoll, R.L., and Macaulay, G.J. 2005. Using fish-processing time to carry out acoustic surveys from commercial vessels. ICES J. Mar. Sci. J. Cons. **62**(2): 295–305.

Ona, E. 1990. Physiological factors causing natural variations in acoustic target strength of fish. J. Mar. Biol. Assoc. U. K. **70**(1): 107–127. doi:10.1017/S002531540003424X.

Ona, E. 1999. Methodology for target strength measurements. ICES Coop. Res. Rep. **235**: 59.

Ona, E. 2001. Herring tilt angles, measured through target tracking. In Herring: Expectations for a New Millennium. Ed. by F. Funk, J. Blackburn, D. Hay, A. J. Paul, R. Stephenson, R. Toresen, and D. Witherell. University of Alaska, Sea Grant, AK-SG-01-04. Fairbanks. 800 pp. Available from http://brage.bibsys.no/xmlui/handle/11250/108201 [accessed 9 August 2016].

Petitgas, P., Massé, J., Beillois, P., Lebarbier, E., and Cann, A.L. 2003. Sampling variance of species identification in fisheries acoustic surveys based on automated procedures associating acoustic images and trawl hauls. ICES J. Mar. Sci. J. Cons. **60**(3): 437–445. doi:10.1016/S1054-3139(03)00026-2.

Ressler, P.H., Fleischer, G.W., Wespestad, V.G., and Harms, J. 2009. Developing acommercial-vessel-based stock assessment survey methodology formonitoring the US west coast widow rockfish (Sebastes entomelas) stock. Fish.Res. **99**: 63–73.

Ridgway, K.R., Dunn, J.R., and Wilkin, J.L. 2002. Ocean interpolation by four-dimensional least squares -Application to the waters around Australia. J. Atmos. Ocean. Tech. **19**(9): 1357–1375.

Rivoirard, J., Simmonds, J., Foote, K.G., Fernandes, P., and Bez, N. 2000. Geostatistics for Estimating Fish Abundance. Blackwell Science Ltd, Oxford.

Ryan, T.E., Downie, R.A., Kloser, R.J., and Keith, G. 2015. Reducing bias due to noise and attenuation in open-ocean echo integration data. ICES J. Mar. Sci. J. Cons. **72**(8): 2482–2493. doi:10.1093/icesjms/fsv121.

Ryan, T.E., and Kloser, R.J. 2004. Improving the precision of ES60 and EK60 echosounder applications. Rep. Work. Group Fish. Acoust. Sci. Technol. WGFAST: 20–23.

Ryan, T.E., Kloser, R.J., and Macaulay, G.J. 2009. Measurement and visual verification of fish target strength using an acoustic-optical system attached to a trawlnet. ICES J. Mar. Sci. J. Cons. **66**(6): 1238–1244. doi:10.1093/icesjms/fsp122.

Sawada, K., Furusawa, M., and Williamson, N.J. 1993. Conditions for the precise measurement of fish target strength *in situ*. J. Mar. Acoust. Soc. Jpn. **20**(2): 73–79. doi:10.3135/jmasj.20.73.

Scoulding, B., Gastauer, S., MacLennan, D.N., Fässler, S.M.M., Copland, P., and Fernandes, P.G. 2016. Effects of variable mean target strength on estimates of abundance: the case of Atlantic mackerel (Scomber scombrus). ICES Jour. Mar. Sci. doi:doi:10.1093/icesjms/fsw212.

Simmonds, J., and MacLennan, D. 2005. Fisheries acoustics: theory and practice. Fish Aquat. Resour. Ser.

Simrad. 1993. Simrad EK500 Scientific Echo Sounder Instruction Manual. Simrad Subsea A/S, Horten, Norway.

Soule, M., Barange, M., and Hampton, I. 1995. Evidence of bias in estimates of target strength obtained with a split-beam echo-sounder. ICES J. Mar. Sci. J. Cons. **52**(1): 139–144.

Soule, M., Barange, M., Solli, H., and Hampton, I. 1997. Performance of a new phase algorithm for discriminating between single and overlapping echoes in a split-beam echosounder. ICES J. Mar. Sci. J. Cons. **54**(5): 934–938.

Trenkel, V., Ressler, P.H., Jech, M., Giannoulaki, M., and Taylor, C. 2011. Underwater acoustics for ecosystem-based management: state of the science and proposals for ecosystem indicators. Mar. Ecol.-Prog. Ser. **442**: 285–301.

Vaseghi, S.V. 2008. Advanced digital signal processing and noise reduction. John Wiley & Sons. Available from https://books.google.com.au/books?hl=en&lr=&id=vVgLv0ed3cgC&oi=fnd&pg=PR7&dq=Vaseghi,+S.+V.+(2008).+Advanced+digital+signal+processing+and+noise+reduction,+John+Wiley+%26+Sons.&ots=9INDSQTyAr&sig=vto1t_2Bpx71Wmtt1Zyq3FgVTxY [accessed 8 July 2016].

Woillez, M., Rivoirard, J., and Fernandes, P.G. 2009. Evaluating the uncertainty of abundance estimates from acoustic surveys using geostatistical simulations. ICES J. Mar. Sci. J. Cons.: fsp137.

Zwolinski, J., Fernandes, P.G., Marques, V., and Stratoudakis, Y. 2009. Estimating fish abundance from acoustic surveys: calculating variance due to acoustic backscatter and length distribution error. Can. J. Fish. Aquat. Sci. **66**(12): 2081–2095. doi:10.1139/F09-138.

Chapter 4

Towards acoustic monitoring of a mixed demersal fishery based on commercial data: the case of the Northern Demersal Scalefish Fishery (Western Australia)

Sven Gastauer[1,2,3], Ben Scoulding[4], Miles Parsons[1]

[1] *Centre for Marine Science and Technology, Curtin University, GPO Box U1987, Perth, WA 6845, Australia*

[2] *Wageningen Marine Research, P.O. Box 68, 1970 AB IJmuiden, The Netherlands*

[3] *Antarctic Climate and Ecosystems Cooperative Research Centre, University of Tasmania, Private Bag 80, Hobart, Tasmania 7001*

[4] *Echoview Software Pty Ltd, GPO Box 1387, Hobart, 7001, Tasmania, Australia*

Corresponding author: *Sven Gastauer, CMST, Curtin University B301 Hayman Rd, Bentley WA 6102, Australia; email:* sven.gastauer@postgrad.curtin.edu.au

4.1 Abstract

Ongoing monitoring of complex, mixed species environments is a challenging task. In this study, the potential of acoustic and catch data collected aboard a commercial fishing vessel, in combination with geostatistical variance estimates, are explored as a means to derive information on the distribution and abundance of key species groups within selected fishing regions. The *FV Carolina M*, a trap fishing vessel which operates in waters off Broome, Western Australia, in the Northern Demersal Scalefish Fishery, was equipped with Simrad ES70 echosounders, operated at 38 and 120 kHz. Optical recordings of catch were also obtained, in addition to the acoustic data, during routine fishing operations in 2014. Three regions, where both optical and acoustic datasets were available, were selected for analysis. Geostatistical conditional simulations were used to combine acoustic density information with species composition proportions and length distributions within the catch. For each of the input datasets 250 simulations were conducted, from which individual and combined sampling CVs were derived. Conversion of acoustic densities into abundance estimates was achieved through application of target strength to length relationships (*TS-L*). Where *TS-L* was unavailable in the literature for a particular species it was estimated through a Kirchhoff-ray mode model. *TS-L* equations were estimated for rankin cod (*Epinephelus multinotatus*)(TS_{RC} = 20 $\log_{10}(L)$ − 79.6), triggerfish (*Balistidae*) (TS_{TF} = 20 $\log_{10}(L)$ − 77.7) and spangled emperor (*Lethrinus nebulosus*) (TS_{SE} = 20 $\log_{10}(L)$ − 70.8) at 38 kHz. Sampling error was found to be generally low for catch proportions (<12%) and acoustic densities (<10%). Total sampling error CV for species group abundances within each of the three regions was 9% - 38%, which is similar to typical estimates reported for acoustic surveys.

Keywords: *fisheries acoustics, geostatistics, target strength, NDSF, fishing vessel, error estimates*

4.2 Introduction

Historically, fisheries surveys have focussed on single-species management, and fisheries acoustics has become one of the standard assessment tools for monitoring pelagic fish stocks in temperate waters, where schools generally contain a single species (Horne, 2000; Simmonds and MacLennan, 2005; Koslow, 2009; De Robertis et al., 2010). In warm tropical waters school composition is often more complex due to high levels of species richness (Campanella and Taylor, 2016). While different discrete frequencies allow us to distinguish some functional groups, such as swimbladdered and non-swimbladdered fish, with a high level of confidence, differentiating between fish with similar morphological and physiological characteristics remains challenging (De Robertis et al., 2010; Korneliussen et al., 2008; Woillez et al., 2012). Identification tools remain largely focussed on empirical methods e.g. manual scrutiny, classification libraries or frequency response (Fernandes et al., 2006; Korneliussen et al., 2016, 2009). To verify acoustic observations, these approaches depend on the availability of dedicated alternative sampling, such as trawl samples or optical data (De Robertis et al., 2010; Handegard et al., 2013). Collection of such data is not always practical, especially with regards to a more ecosystem based approach in fisheries management (EBFM), where it is not always possible to collect information on all components of an ecosystem. Fisheries acoustics are now acknowledged as being one of the most promising tools for establishing an EBFM as the methods are capable of delivering information over a wide range of trophic levels and can provide details on environmental descriptors, such as seabed type and bottom depth (Koslow, 2009; Trenkel et al., 2011).

Reductions in dedicated survey budgets and advances in marine technologies have prompted managers to investigate the application of alternative data collection methods capable of providing data at a high spatio-temporal resolution (Handegard et al., 2013). Given the large costs associated with operating marine research vessels, there is a growing trend in looking at alternative sampling platforms (Dalen and Karp, 2007; Fässler et al., 2016; Gastauer et al., 2017). Many commercial fishing vessels are now equipped with scientific echosounders capable of collecting and storing high-quality calibrated acoustic data. As a result, investigators have increasingly been exploring the potential use of active-acoustic data collected opportunistically from vessels of opportunity (e.g. fishing vessels), during normal commercial operations (Dalen and Karp, 2007; Fässler et al., 2016; Gastauer et al., 2017).

While dedicated scientific surveys, such as acoustic trawl (AT) surveys, can deliver spatial and temporal snapshots of population distributions inside a surveyed area, the underlying dynamics (e.g. seasonal migrations) of that population remain largely unknown. This is in part due to the limited spatio-temporal coverage. To date, most studies which have utilised opportunistically collected acoustic data have focussed on the assessment of fish populations already assessed by AT surveys within the context of single-species fisheries (Barbeaux et al., 2013; Fässler et al., 2016; van der Kooij et al., 2016). In this study, we explore the potential of acoustic data, collected in combination with catch information obtained aboard a commercial trap fishing vessel during normal operations, to derive estimates of abundance and biomass with associated sampling error, through the use of geostatistical conditional simulations (GCS), for selected fishing regions of a mixed-species environment.

The existence of spatial structure within the distribution of many fish stocks has been widely recognised (Rivoirard et al., 2000). As a result, most estimates of fish abundance and biomass are based on spatially located data. Geostatistics have been developed as a statistical tool to work on regionalised variables (i.e. variables that are spread in space), with or without an underlying random or regular grid (Matheron, 1971). In fisheries science, they have been established as a suitable tool to provide abundance and biomass estimates from spatial data (Rivoirard et al., 2000). A major strength of geostatistics is that it can be used to explicitly account for spatial autocorrelation. In reality it is rarely possible to fully survey a given area in its entirety, i.e. conduct a survey fully representative of the underlying complexity. Limitations arise either through areas deficient in sampling density or an inability to reach the extents of the survey area. In order to understand the validity of derived estimates, an important part of any biomass or abundance estimate is the computation of uncertainty arising from the spatially explicit sampling (Woillez et al., 2009a, 2016). Geostatistics have been shown to be an effective tool to derive abundance estimates from acoustic data, to estimate the precision of acoustic estimates, and to make precision estimates of acoustic datasets, explicitly taking into account the spatial variance (Petitgas et al., 2003; Scoulding et al., 2016; Tugores et al., 2016; Woillez et al., 2009a, 2016).

4.3 Methods

Study area

All data were collected during normal fishing operations on board the *FV Carolina M*, a trap fishing vessel based out of Broome, Western Australia (WA), that fishes at various sites throughout the Northern Demersal Scalefish Fishery (NDSF) (Figure 4.1). The NDSF is a mixed, demersal, trap based fishery which covers an area of 408,400 km^2. The NDSF extends up to the shelf edge towards the Indonesian border with depths down to 200 m. In this study, we focus on regions where catch and acoustic data were simultaneously available. Three regions met these criteria (Regions 1, 2 and 3) and were delimited by manually drawn polygons (Figure 4.1b, c, d). Data from the three regions were collected at different times in 2014: Region 1 from 3rd to 7th December (area (A) = 33 nautical miles (nmi)^2, mean depth ($\bar{z}$) = 124 m, depth range (r = 120 – 130 m), Region 2 from 29th October to 8th November (A = 129 nmi^2, $\bar{z}$ = 78 m, r = 61 – 90 m) and Region 3 from 19th to 30th August (A = 211 nmi^2, $\bar{z}$ = 91 m, r = 76 – 103 m).
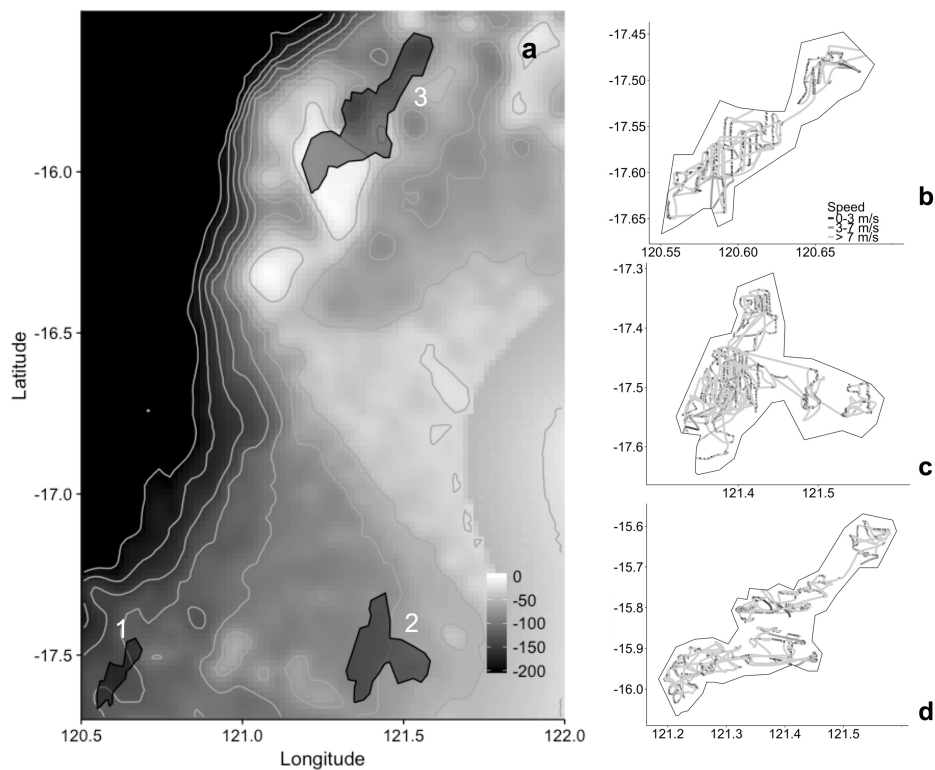
Figure 4.1 Bathymetric map of the part of the NDSF containing the three fishing Regions (1, 2, 3) indicated by the shaded areas; detailed map of acoustic data collection locations, with an indication of vessel speed with light colouring for slow speeds and dark colouring for high speeds, for Region 1 (a), Region 2 (b) and Region 3 (c)

4.3.1 Sampling strategy
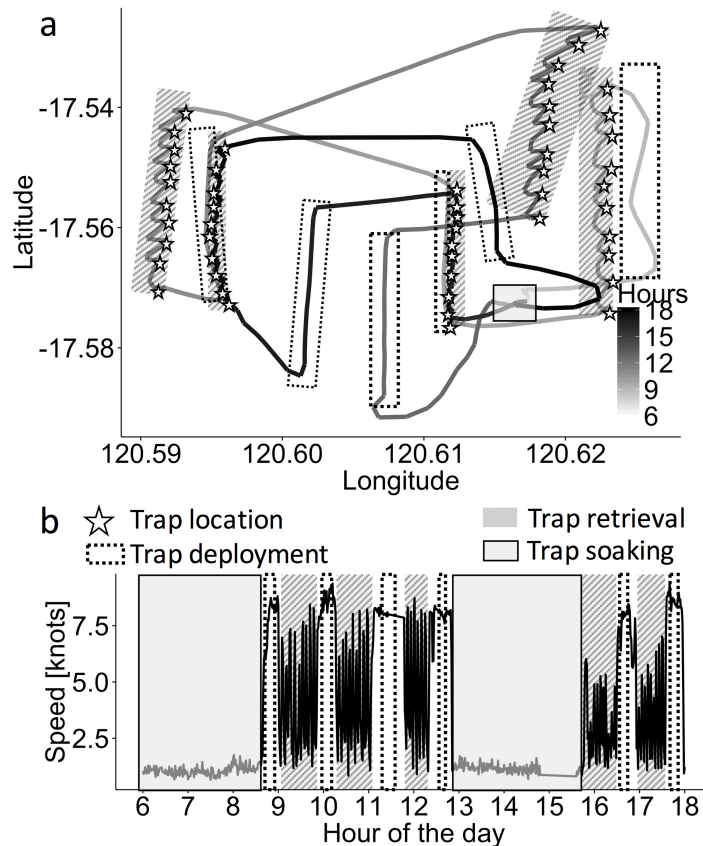
Figure 4.2 One day of sampling in Region 1; a) GPS positions of Carolina M visualised as a coloured line, from 6 in the morning (light coloring) until 6 in the evening (dark colouring). The different activities at a given time are indicated by shaded areas and the location of traps is indicated by a star symbol; b) the travelling speed over time averaged by one minute intervals with an indication of the different activites at a given time by shaded areas.

With up to 30 steel fish traps (1.5 x 1.5 x 0.9 m) on board, the general sampling strategy of the fisher is to commence a fishing trip from Broome, travelling at high speed (7-12 knots) towards a predetermined fishing area. Fishing areas are chosen based on historic catch information and the expert knowledge of the fisher. Once at the desired fishing ground, the traps are deployed at suitable sites. Suitability is judged by the fisher, based on the seabed structure, the availability of fish schools (determined from on board acoustic systems) and other factors which are best summarised as experience. Generally, so called 'lines', consisting of ten traps placed close to each other (Figure 4.2a), are deployed whilst the vessel is moving at about 7 knots (Figure 4.2b). Three to eight lines were set and retrieved per day. Once deployed a line is deployed, the vessel moves away from the region (to avoid any negative behaviour response) and the traps are left to 'soak' for at least one tidal phase shift. While the traps are in the water ('soaking') the vessel remains at anchor or drifts (depending on the prevailing coniditons) several nautical miles from the site of trap deployement (Figure 4.2a, b).

After an allotted amount of time has passed (mean 7.21 hours; max = 16.62 h; min = 1.3 h, n=1431), based on the fishers expert judgement, the vessel moves back to the location of deployment to retrieve the traps (Figure 4.2a, b). Once aboard, all fish are immediately removed from the trap and fish of commercial interest are placed into an ice slurry before storage. Undersized or non-commercial species are returned alive into the ocean as quickly and as careful as possible. If fishing conditions and yields are promising, the fisher might decide to put the traps back into the water in close proximity to the previous location. Otherwise the traps will be redeployed elsewhere or vessel will return to Broome.

4.3.2 Biological sampling

Biological information was obtained from catch. A GoPro wide-angle camera was placed on top of the traps to record the catch as they were being hauled on deck. Based on the optical information, fish were identified and measured (total length) using FishVid (Gastauer et al., 2017). Catch was divided into nine biological and commercially relevant groups. These were goldband snapper (GB, *Pristipomoides multidens*), red emperor (RE, *Lutjanus sebae*), saddletail (ST, *Lutjanus malabaricus*), lutjanids (LJ, members of the Lutjanidae family, other than saddletail, red emperor or goldband snapper), lethrinids (LT, members of the Lethrinidae family), rankin cod (RC, *Epinephelus multinotatus*), cods (Cod, members of the Epinephelidae family other than rankin cod), triggerfish (TF, members of the Balistidae family, as the main by-catch species) and a miscellaneous group (MISC) containing all other species or unidentified individuals. Specimens outside of these nine groups consisted of two sharks, two snakes and eight crabs, which were excluded from further analysis.

Length (*L*, in cm) to weight (*W*, in grams) relationship constants (a_{LW} and b_{LW}), fitting the *LW* equation $W = a_{LW} * L^{b_{LW}}$, were taken from FishBase (Froese et al., 2016). As the LT, LJ, and Cod groups may have contained varying proportions of different species within them, the two constants were averaged based on the proportions present in the assemblage reported by Newman et al. (2012). For the MISC group, which may have contained an ensemble of all other groups with additional species, the mean a_{LW} and b_{LW} of all other groups was used.

Similar to other sampling methods (e.g. trawling), traps are not always fully reflective of the local fish community composition. This is due to gear selectivity and a lack of information about the catchment area of a single trap. Furthermore, direct sampling of schools is often not possible and those observed on the echogram are not necessarily sampled by the

traps. Despite these limitations traps are shown to be reasonably representative of the community (species richness) in the general area (Newman et al., 2012).

4.3.3 Acoustic data collection and processing

Acoustic data were collected from hull-mounted SIMRAD ES70 split-beam echosounders, operating at 38 and 120 kHz. Settings were the same as those used during normal commercial operations; 38 kHz (beam width: 9.6°, ping rate: maximum, pulse duration (τ): 0.256 ms, transmit electrical power (p_{et}): 1500 W) and 120 kHz (beam width: 7°, ping rate: maximum, τ: 0.064 ms, p_{et}: 1000 W). Tank calibrations were conducted to test for effects of non-linearity, due to the short pulse duration and high power settings (Korneliussen et al., 2008), but no effects were found. Standard sphere calibration using a 38.1 mm Tungsten-carbide sphere (WC), with 6% cobalt binder (Demer et al., 2015) was carried out in March 2016 within the NDSF. Methods to deal with this temporal and spatial mismatch are described by Gastauer et al. (2017).

Raw acoustic data were firstly corrected for the built-in triangular wave error (Ryan and Kloser 2004). Subsequent analysis was conducted in Echoview 7.0 (Echoview Software Pty Ltd, 2015), including application of calibration settings. Various algorithms were applied to the data to deal with impulse, transient and background noise (Ryan et al., 2015). Ping times and geometry were matched and data were resampled by one ping (Demer et al., 1999; Conti et al., 2005). Schools (i.e. non-resolvable targets) were classified as fish using a bi-frequency algorithm which could separate swimbladdered fish from fluid-like targets or macro-zooplankton (Ballón et al., 2011; Lezama-Ochoa et al., 2015; Gastauer et al., 2017). Differences in the (mean) volume backscattering strength (S_v; dB re 1 m^2 m^{-3}) at 38 and 120 kHz were used to discriminate between 'scattering groups'. Volume backscattering coefficients (s_v; m^2 m^{-3}) of the schools identified as fish were integrated as nautical area scattering coefficents (s_A; m^2 nmi^{-2}), averaged over 1 nmi grid cells. Integration was done from 10 m below the surface to 1 m above the seafloor, thereby avoiding the nearfield close to the transducer face and integration of bottom echoes close to the seabed, respectively. Night-time data were excluded as diurnal vertical migration (DVM) was observed with fish being more dispersed during times of darkness and becoming aggregated during daylight (Gastauer et al., 2017). Interpretation of acoustic data at times of trap removal is non-trivial, due to drastic changes speed and heading. Sudden changes in direction to locate traps for retrieval are common and cause signal loss due to bubble attenuation (Figure 4.1 b,c,d, Figure 4.2). These events were excluded manually and cross-checked with available logbook information. Information at similar locations could be

extracted easier at times when the traps were deployed. Deployment generally occurs at more stable speeds and headings (Figure 4.1 b, c, d , Figure 4.2a, b).

4.3.4 Target strength estimates

Target strength (TS; dB re 1 m^2) to length (L; cm) or weight (W; grams) relationships are needed to derive abundance or biomass estimates from s_v (Simmonds and MacLennan, 2005). TS-L is generally formulated as a linear regression under the shape of:

$$TS = a_{TS} \, log(L) + b_{TS} \, , \tag{1}$$

where a_{TS} and b_{TS} are constants, with a_{TS} commonly assumed to be 20 (Foote, 1979). TS-W can easily be derived when combined with the LW equation. All presented TS relationships and biomass estimates were based on 38 kHz data. Information provided by the 120 kHz echosounder was used for classification purposes only.

TS-L equations were available for red emperor (Gastauer et al., 2016b) and goldband snapper (Gastauer et al., 2017), but not for the other groups. Available TS-L for red emperor was assumed to be valid for the lutjanids group and saddletail, given their close biological relation and similar morphological features.

A Kirchhoff-ray mode (KRM) model (Clay and Horne, 1994) was used to model the theoretical TS of triggerfish (representative of the TF group), rankin cod (representative of the RC and Cod groups) and spangled emperor (*Lethrinus nebulosus*) (representative of the LT group). Constants used in the model can be found in Table 4.1. Biological samples used as model inputs were all taken from within the NDSF during one fishing trip in November 2014. Fish and swimbladder shapes used as inputs for the KRM were taken from computational tomography scans (CT). All CT scans were acquired by a Siemens SOMATOM Dual Energy scanner, producing standard DICOM files (Gastauer et al., 2016b). Swimbladder shape and fish body shape were extracted using region of interest (ROI) definitions within ImageJ (Schindelin et al., 2015). Exported ROI's were read into R (R Core Team, 2016) to produce simplified shapes, defined by the upper position, lower position and width for each slice. The resulting simplified shapes were then used within the KRM model. CT scans were also used to estimate fish body density and sound speed within the fish body. Pixel values were transformed into Hounsfield (HU) units through application of a linear correction factor read from the DICOM header files (pixel value * rescale slope + rescale intercept). Sound speed (c_{fb} in ms^{-1}) within the fish body was calculated following Au and Fay (2012). The density of fish flesh was found to be

within the thresholds of soft tissue (138 – 150 HU) (Au and Fay, 2012), where c_{fb} is defined empirically as 1.24 x pixel value in HU + 1544. Seawater density (ρ_w) was computed following the UNESCO equation of state for seawater (Fofonoff and Millard Jr, 1983), using average salinity and temperatures from CARS (CSIRO Atlas of Regional Seas) (Ridgway et al., 2002) (Table 4.1).

Table 4.1 Constant parameters input for the KRM model to compute the theoretical TS of triggerfish, Rankin Cod and Spangled Emperor.

Description	Species	Symbol	Value	Unit	Source
Salinity	All	S	34.4	ppt	CSIRO Atlas of Regional Seas (Ridgway et al., 2002)
Temperature	All	T	24.9	˚C	
Density of sea water	All	ρ_w	1023	kg/m3	(Fofonoff and Millard Jr, 1983)
Density of swimbladder gas	All	ρ_{sb}	2.64	kg/m3	(Clay, 1991)
Sound speed of sea water	All	c_w	1541.2	m/s	CTD measurements
Sound speed in swimbladder	All	c_{sb}	340	m/s	(Yasuma et al., 2010)
Density of fish body	Triggerfish	ρ_{fb}	1693	kg/m3	CT scans
	Rankin cod		1631		
	Spangled emperor		1680		
Sound speed in fish body	Triggerfish	c_{fb}	1144	m/s	
	Rankin cod		1094		
	Spangled emperor		1139		
Echosounder frequency	All	f	38	kHz	-
Tilt angle	All	ϑ	[50,130]	°	-

KRM outputs were tilt-angle (θ) dependent backscattering cross section values (σ_{bs} in m^2). θ ranged between 50° and 130°, where 90° was defined as swimming horizontally, largely following recommendations by McClatchie et al. (1996b). *TS-L* was computed in the linear domain, assuming a slope (a_{TS}) of 20 and with σ_{bs} being weighted by the probability of θ. Probability of θ was assumed to follow a normal distribution (mean 90°), giving more weight to small deviations from swimming horizontally and less weight to extreme values.

4.3.5 Geostatistical conditional simulations
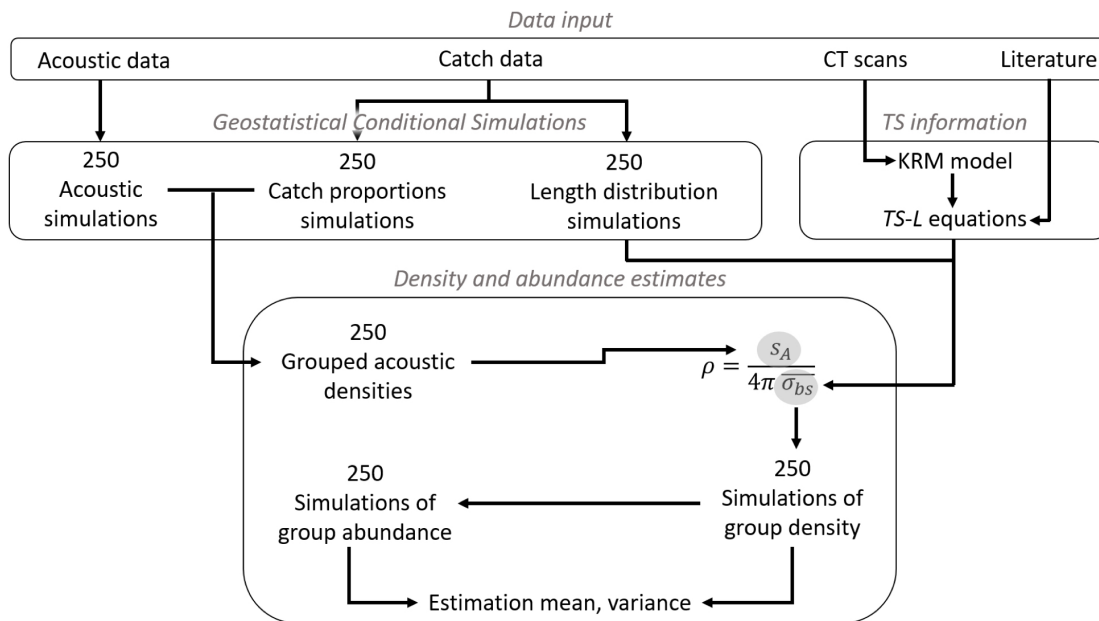
Figure 4.3 Schematic of the workflow from acoustic data, catch and literature information through geostatistical conditional simulations to group abundance and density estimates with estimation means and variances

Geostatistical conditional simulations (GCS) were used to combine catch information with acoustic data to derive combined sampling uncertainty estimates (Rivoirard et al., 2000). To get from fish-only s_A to group-specific abundance or biomass, 250 conditional simulations of s_A were combined with 250 conditional simulations of group-specific catch proportions, weighted by estimated fish weights at observed lengths (Figure 4.3). In the following step, the resulting simulations of the group-specific s_A (s_{Agroup}) were combined with conditional simulations of the group-specific length distributions, from which absolute density, biomass or abundance estimates could be derived, based on specific *TS-L* (Table 4.1, Table 4.2) or *TS-W* equations.

GCS are a geostatistical concept, generating numerous realisations (simulations) of the Gaussian random function, which in contrast to non-conditional simulations honour the data. GCS are replicates of the Gaussian random function model, following the variability of the data, based on the histogram and the variogram (Rivoirard et al., 2000). The main benefit of conditional simulations for acoustic data is that they allow for the combination of different data sources, generating a combined variability estimate. The different variables (i.e. acoustic backscatter and proportion of the catch and length distributions) are simulated individually, but multiple times (250 replicates), and then combined to generate simulations of fish density within the domain (each of the three regions). Uncertainty can be derived through the

computation of basic statistics such as variance, standard deviation (s.d.) or coefficients of variation (CV in %) of the final realisations (Woillez et al., 2009a, 2016). The resulting uncertainty represents the sampling error associated with the abundance estimates, which should not be confused with the measurement error, which is derived from Monte Carlo simulations (Woillez et al., 2009a).

Table 4.2 TS-L equations at 38 kHz with information for which species the relationship was originally estimated (Species), the method used to develop the equation, the group to which it was applied, the slope (a_{TS}) and intercept (b_{TS}) of the TS-L equation and a reference to the paper where the estimates were originally published, if not developed within this study

Species	Estimates method	Group	a_{TS}	b_{TS}	Reference
Red emperor	KRM with Bayesian parameter estimation	Red Emperor; Lutjanids; Saddletail	14.6	-64.9	(Gastauer et al., 2016b)
Goldband snapper	*In situ*	Goldband snapper	20.1	-70.5	(Gastauer et al., 2017)
Triggerfish	KRM	Triggerfish	20.0	-77.7	-
Rankin cod	KRM	Cods; Rankin cod	20.0	-82.9	-
Spangled emperor	KRM	Lethrinids	20.0	-70.8	-

Two main properties of the Gaussian model make it especially suitable for simulations. Due to the central limit theorem, results from the simulation of many independent variables converge towards a normal distribution making it relatively easy to condition the data points. In the present study, the spatial structure of fish density is represented numerically through the variogram and covariogram. Kriging is used as the best linear, unbiased estimation of point values at any location or region within the domain. The hypothetical error map is the difference between the kriged map and the unknown reality. Given the stochastic independence of the error map from the kriged map, in the Gaussian case, an error map is simulated from a non-conditional simulation. Adding the error map to the kriged map results in a conditional simulation. This provides a new map where at locations where data are available, the variance between the kriged values and actual values equals to zero, hence the simulated value is the same as the actual data value (Rivoirard et al., 2000; Woillez et al., 2009a, 2016).

An important prerequisite for the random function in the stationary case is for the variable $Z(x)$ to be derived from a Gaussian field $Y(x)$ using Gaussian anamorphosis (Φ) as $Z= \Phi$

(Y). This requires a transformation from the data values *Z* to normal scores. Gaussian values can be directly determined for positive *z,* but not for *z* = 0 (i.e. *Y* < some threshold or cut off value y_c determined by the proportion of zero values). A Gibbs sampler was used to iteratively simulate *Y* at the points where *z* = 0, conditional on them being lower than the cut off value y_c and on the other data points. This is an iterative process, where *Y* is simulated using the modelled variogram of *Y*. A detailed description of GCS can be found in Woillez et al. (2016).

4.3.6 Habitat overlap

Based on the resulting estimated spatial densities for the nine groups within the three regions, geostatistical indices were extracted. Geostatistical indices can be used to characterise the spatial distribution of target variables (Gastauer et al., 2016a; Spedicato et al., 2007; Woillez et al., 2007, 2009b). For each simulation of group densities, the centre of gravity CG (the mean location) (Bez, 2007), isotropy (the roundness of the distribution) (Bez et al., 1997), inertia (measure of dispersion) and the global index of colocation (GIC) were extracted (Woillez et al., 2007). GIC is a measure to describe how geographically distinct two populations are through comparison of their respective CGs and the distance between individual samples taken at random and individually.

4.4 Results

4.4.1 Target strength to length estimates

TS-L equations found in literature were used where possible (Gastauer et al. 2016b; Gastauer et al 2017). A summary of the *TS-L* equations used can be found in Table 4.2. Constants used in the KRM model to estimate *TS-L* of TF, RC and SE are summarised in Table 4.1.

To estimate *TS-L* for *TF*, three members of the balistidae family with intact swimbladders were scanned. Standard lengths of the three fish were 20.1, 24.7 and 26.9 cm. *TS* at 90º (horizontal) fluctuated around -50 dB for all three fishes ($L_{20.1 \, cm}$ = -50.0 dB re 1 m^2; $L_{24.7 \, cm}$ = -50.5 dB re 1 m^2; $L_{26.9 \, cm}$ = -49.7 dB re 1 m^2) (Figure 4.4a). KRM, computed for 38 kHz, revealed a generally increasing trend of *TS* with ϑ for Triggerfish. Maximum *TS* was observed at 130º for all three triggerfish (Figure 4.4a). Fitting the *TS-L* equation with an assumed slope of 20 and a mean *TS* weighted by the probability of ϑ (assuming a normal distribution) resulted in:

$$TS_{TF} = 20 \log_{10}(L) - 77.7 \text{ (Figure 4.5a).} \tag{2}$$

Two *RC* with intact swimbladders were scanned (L_{RC1}= 40.1 cm; L_{RC2}= 50.0 cm) to estimate a *TS-L* relationship for rankin cod and the cod group. The larger *RC* model exhibited maximum *TS* at $\theta \approx 102$ º (max $TS_{\theta=94º}$ = -42.7 dB re 1 m²), fluctuating around -47 dB re 1 m² for all analysed θ. *TS* for the smaller *RC* showed more pronounced maxima and minima, with highest *TS* of -44.5 dB re 1 m² at 77º and 94º. *TS* was lowest within the range of 90º to 110º (mean $TS_{\theta[90,110]}$ = -61.4 dB re 1 m²) (Figure 4.4b). Weighted with an assumed normal distribution of θ between 50º and 130º and accepting a slope of 20, *TS-L* for *RC* was estimated as:

$$TS_{RC} = 20\log_{10}(L) - 79.6 \text{ (Figure 4.5b).} \tag{3}$$

TS-L for lethrinids was estimated through two scans of *SE* of similar size (L_{SE1} = 29.1 cm; L_{SE2} = 29.7 cm). Both followed a very similar pattern over the range of modelled θ. Two local maxima were detected for both examples at 88º (TS_{SE1} = -37.6 dB re 1 m²; TS_{SE2}= 39.6 dB re 1 m²) and 105º (TS_{SE1} = -39.8 dB re 1 m²; TS_{SE2} = -39.2 dB re 1 m²) (Figure 4.4c). Fitting a *TS-L* with a slope of 20 resulted in:

$$TS_{SE} = 20\log_{10}(L)\text{-}70.8 \text{ (Figure 4.5c).} \tag{4}$$
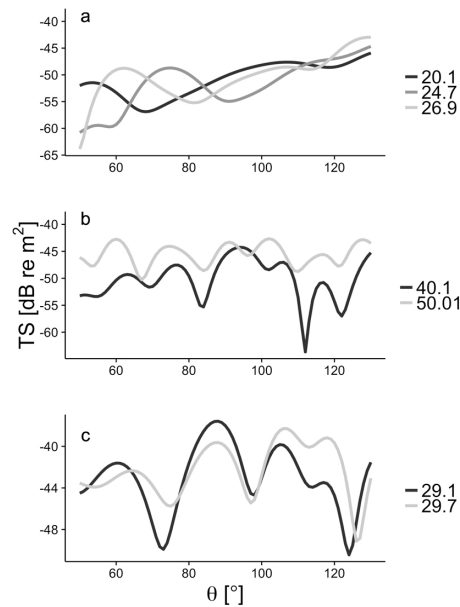
Figure 4.4 Target strength [dB re 1 m²] at 38 kHz, modelled through a Kirchhoff-Ray Mode model for triggerfish (a), rankin cod (b) and spangled emperor (c), over a range of tilt angles (ϑ) [º], based on CT scans, each estimate of fish length [in cm] at different sizes coloured in greyscale
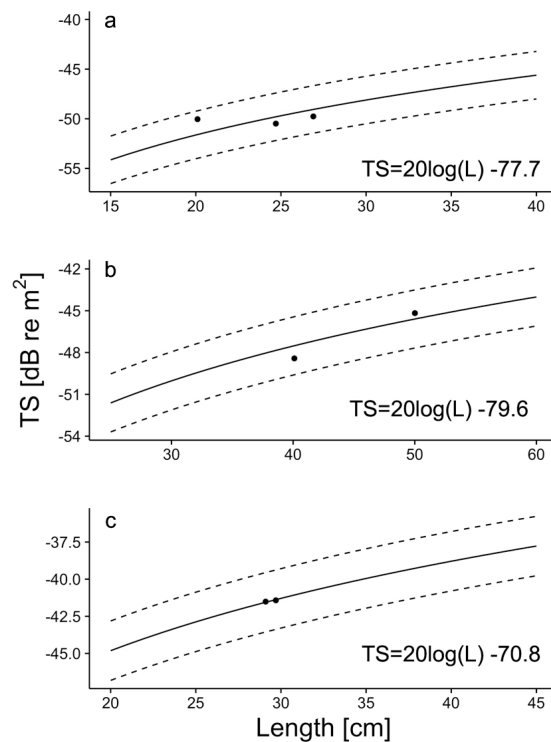
Figure 4.5 TS-L relationship for triggerfish (a), rankin cod (b) and spangled emperor (c), based on estimates modelled through Kirchhoff-Ray Mode model (black dots).

Geostatistical conditional simulation of acoustic backscatter

For each of the three regions 250 realisations of acoustic data were produced. All three regions were characterised by a high number of zero values (25 – 51%), with few high s_A values (maximum 1172 – 2547 m^2 nmi^{-2}) (Table 4.3). The values below the cut off value (determined by the proportion of zero values) in Region 1 and 2 were fitted by a nested structure, with a high nugget and a spherical component (Table 4.4). Transformed s_A values contained within Region 3 were fitted by an exponential structure (Table 4.4). In accordance with the central limit theorem, the histograms of the simulated mean s_A approximated normal distributions (Figure 4.6). The relative number of zeros in the original data and the simulations were similar, with a maximum variation of 8.9% in Region 1 (Table 4.3). Similarly, the estimation mean and standard deviations based on simulations and data were comparable (Table 4.3). Highest mean s_A was found in Region 2 (73.6 m^2 nmi^{-2}) (Figure 4.7). At the same time, the highest s_A (1943.9 m^2 nmi^{-2}) value and the highest percentage of zero values (51%) was observed within this region (Figure 4.7). Computing the mean s_A for each of the 250 simulations and deriving a CV estimate, delivers the CV_{sam} attributed to sampling error for s_A estimates. CV_{sam} was 8.0% for Region 1, 7.0% for Region 2 and 10.0% for Region 3.

Bootstrapping the s_A data (10,000 replicates of 10,000 random samples) provides an estimate of random error (CV_{ran}) which was estimated to be 2.2%, 3.1% and 3.2% for Region 1, 2, 3 respectively.
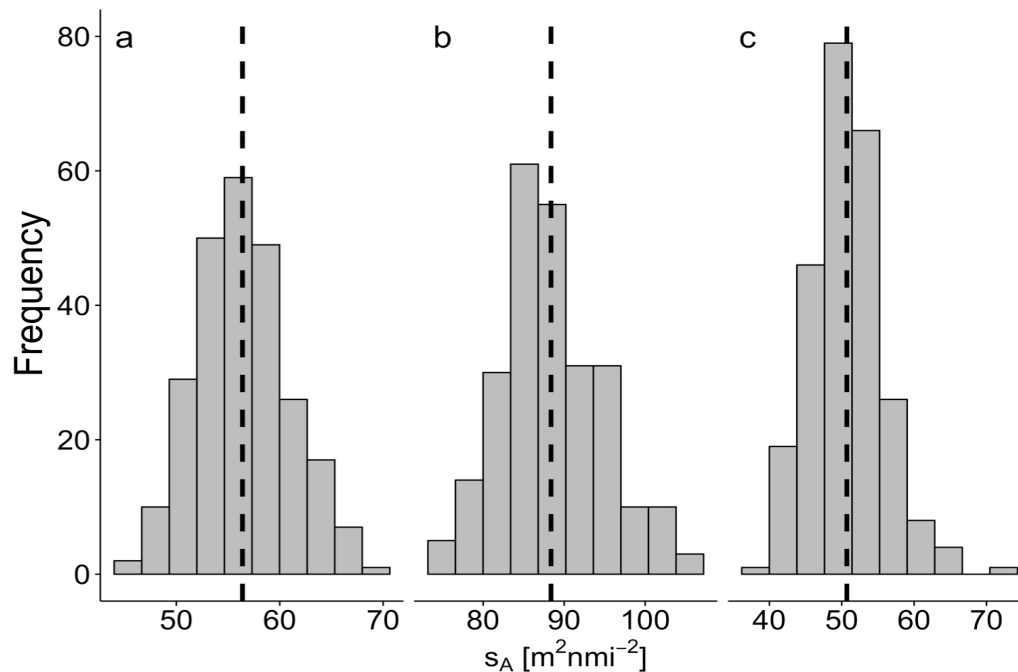
Figure 4.6. Histograms of the frequency (N) of estimated mean s_A based on 250 geostastical conditional simulations, for the three regions (a, b, c) with an indication of the global estimation mean (dashed vertical line).

Table 4.3 Summary statistics (mean, standard deviation (s.d.), maximum, percent of zero values and number of data samples (N)) of raw and simulated s_A for the three analysed regions.

Region	Mean		s.d.		Maximum		% zeros		N	
	Data	Simu	Data	Simu	Data	Simu	Data	Simu	Data	Simu
1	53.97	56.40	120.50	123.59	797.53	1172.91	22.91	25.15	167	6636
2	73.58	88.37	228.24	246.65	1943.86	1981.13	50.91	49.04	834	8576
3	51.75	50.70	165.69	172.14	1805.37	2547.34	45.15	44.37	746	5924

Table 4.4 Model fit parameters of the experimental variogram, fitting the transformed s_A values in Regions 1, 2 and 3 (sph=spherical, exp = exponential).

Region	Structure 1	Structure 2		
	Nugget	Type	Partial Sill	Range
1	0.84	sph	0.37	7.12
2	0.92	sph	0.20	5.14
3	/	exp	0.99	1.22

Table 4.5 Summary statistics (mean, standard deviation (s.d.), maximum, percent zeros and number of data samples (N)) of raw (Data) and simulated (Simu) group proportions by weight for each group within the three analysed regions.

Group	Region	Mean		s.d.		Maximum		% zeros		Sampling	Random
		Data	Simu	Data	Simu	Data	Simu	Data	Simu	CV [%]	CV [%]
Cod	1	0.01	0.02	0.08	0.1	0.7	0.81	96.17	94.57	19.11	5.76
	2	0.04	0.04	0.13	0.26	1	1	85.76	88.09	<0.1	3.43
	3	0.16	0.24	0.22	0	1	1	43.05	47.32	5.25	1.38
Goldband	1	0.63	0.55	0.38	0.14	1	1	18.18	23.27	4.22	0.60
	2	0.16	0.23	0.26	0.22	1	1	65.7	61.74	8.32	1.62
	3	0.11	0.17	0.19	0.14	1	1	70.03	60.45	<0.1	1.78
Lethrinid	1	0	0	0.02	0.14	0.19	0.25	98.09	98.16	6.72	7.44
	2	0.04	0.06	0.1	0.14	1	1	75.4	70.52	<0.1	2.65
	3	0.06	0.13	0.12	0.14	1	1	51.49	50.2	7.68	1.88
Lutjanid	1	0.08	0.11	0.18	0.2	1	1	70.33	70.85	6.81	2.32
	2	0.07	0.13	0.16	0.14	1	1	66.02	65.37	11.70	2.46
	3	0.11	0.19	0.18	0.14	1	1	41.39	42.79	6.92	1.61
Misc	1	0.14	0.21	0.26	0.17	1	1	63.16	52.52	7.72	1.83
	2	0.07	0.17	0.18	0.17	1	1	76.38	65	9.27	2.45
	3	0.07	0.11	0.15	0.26	0.84	1	73.01	68.3	3.81	2.11
Rankin cod	2	0.12	0.17	0.21	0.1	1	1	72.17	68.43	7.30	1.79
	3	0.1	0.18	0.2	0.22	1	1	74.01	63.89	6.87	1.94
Red Emperor	1	0.02	0.05	0.1	0.17	0.76	0.87	95.69	89.13	10.38	5.05
	2	0.27	0.36	0.29	0.24	1	1	39.32	40.29	2.39	1.05
	3	0.23	0.3	0.25	0.1	1	1	39.24	42.74	4.82	1.11
Saddletail	1	0.04	0.09	0.14	0.14	0.67	0.75	92.82	81.52	9.62	3.67
	2	0.04	0.02	0.14	0.14	1	1	92.07	93.46	2.75	3.77
	3	0.07	0.14	0.17	0.14	1	1	82.28	72.17	4.04	2.42
Triggerfish	1	0.02	0.04	0.09	0.2	0.94	1	95.22	90.67	16.58	5.69
	2	0.15	0.23	0.25	0.14	1	1	48.22	43.12	3.54	1.68
	3	0.05	0.11	0.12	0.1	1	1	74.17	66.71	8.79	2.42
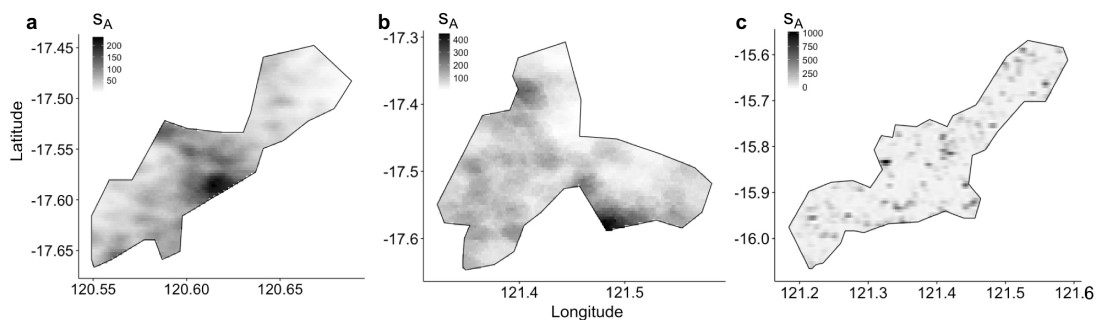
Figure 4.7 Kriged sA values based on one simulation for Region 1 (a), Region 2 (b) and Region 3 (c)
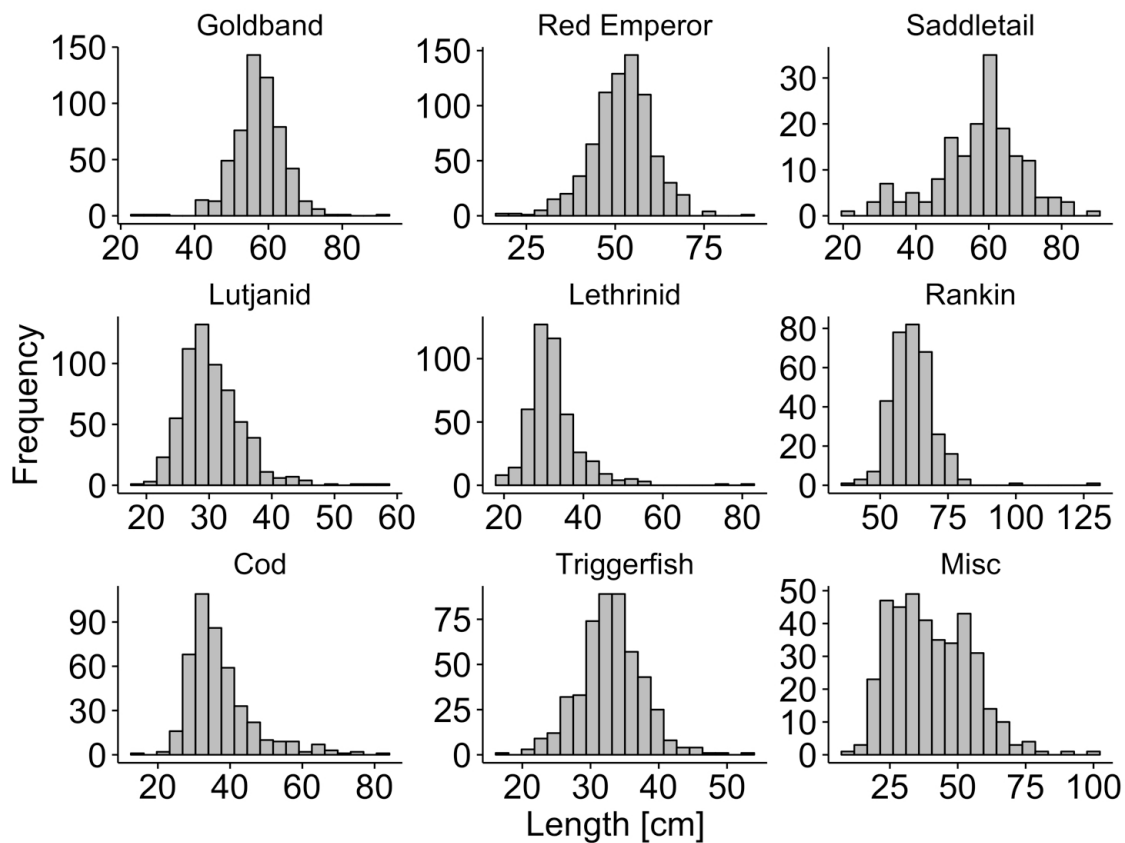
Figure 4.8 Length Frequency histograms of the length distributions for the nine groups.

4.4.2 Simulations of the group proportions

To attribute acoustic backscatter to groups, 250 realisations of weight-weighted catch proportions were computed (Table 4.5). A total of 1431 traps where recorded and analysed (Region 1: 209, Region 2: 618, Region 3: 604). A summary of descriptive statistics of the group-specific length measurements (estimates of mean, maximum, minimum), disaggregated by regions based on recorded data, can be found in Table 4.5. Length histograms for all groups, combined over the three regions are presented in Figure 4.8. All length-frequency histograms were unimodal, with the exception of the miscellaneous group which was closer to a bimodal distribution. Generally, catches were mixed (Figure 4.9). In Region 1, goldband snapper was present in 171 traps and absent in 78 traps. In Region 2, red emperor and triggerfish were present in more traps than absent and in Region 3, lutjanids, cods and red emperor were present (354, 530, 367 traps respectively) in more traps than absent (250, 260, 237 traps respectively) (Figure 4.9). Samples for all groups were influenced by a high number of zeros (no recorded specimens in the group). The lowest percentage of zeros was observed for goldband snapper in Region 1 (18.2%). No rankin cod were observed in Region 1. Differences

in mean proportions for any of the groups based on simulations and data was lower than 0.1. Mean proportion of the total catch was highest for goldband snapper in Region 1 (0.6). All other proportions were less than 0.3 (red emperor in Region 2) (Table 4.5). Most groups in Regions 1, 2 and 3 were fitted by a nested structure with a nugget and one or two exponential or spherical structures (Table 4.6). The proportion of cod in Region 1 and lethrinids in Region 2 were fitted by a pure nugget (Table 4.6). A summary of the variogram parameters can be found in Table 4.6. CV for the mean sampling error was highest for cod in Region 1 (19.1%), and for the random error it was was (5.8%). Mean sampling error attributed CV was 6.7% (s.d. 4.5%) and mean random error was 2.7% (s.d. 1.6%).

Table 4.6 Variogram parameters fitting the ranked group proportions for the nine groups within the three regions, where exp = exponential structure and sph = spherical structure.

Group	Region	Structure 1	Structure 2			Structure 3		
		Nugget	Type	Sill	Range	Type	Sill	Range
Cod	1	<0.01	exp	0.05	0.35	sph	10.33	<0.01
	2	0.29						
	3		exp	0.93	0.23			
Goldband	1	0.09	sph	0.29	1.16			
	2		exp	1.13	1.08			
	3	0.86						
Lethrinid	1	<0.01	exp	<0.01	0.91	sph	0.03	0.65
	2	0.96						
	3		exp	0.88	0.31	sph	0.16	3.39
Lutjanid	1	0.06	exp	0.30	0.81			
	2		exp	1.21	0.95			
	3		exp	0.84	0.08	sph	0.10	2.42
Misc	1	0.30	sph	0.33	1.56			
	2		exp	0.51	0.43	sph	0.12	1.09
	3	0.98	sph	0.18	5.69			
Rankin cod	2	0.30	exp	0.60	0.54	sph	0.35	1.60
	3		exp	0.78	0.43			
Red emperor	1		sph	0.10	5.15			
	2	0.56	sph	0.27	5.28			
	3	0.19	exp	0.41	0.03	sph	0.47	0.79
Saddletail	1	0.10	sph	0.28	4.43			
	2	0.04	exp	<0.01	0.07	sph	0.01	6.67
	3	0.89	exp	0.15	1.46			
Triggerfish	1		sph	0.12	1.65			
	2	0.65	sph	0.16	2.61			
	3	0.54	exp	0.80	1.21			
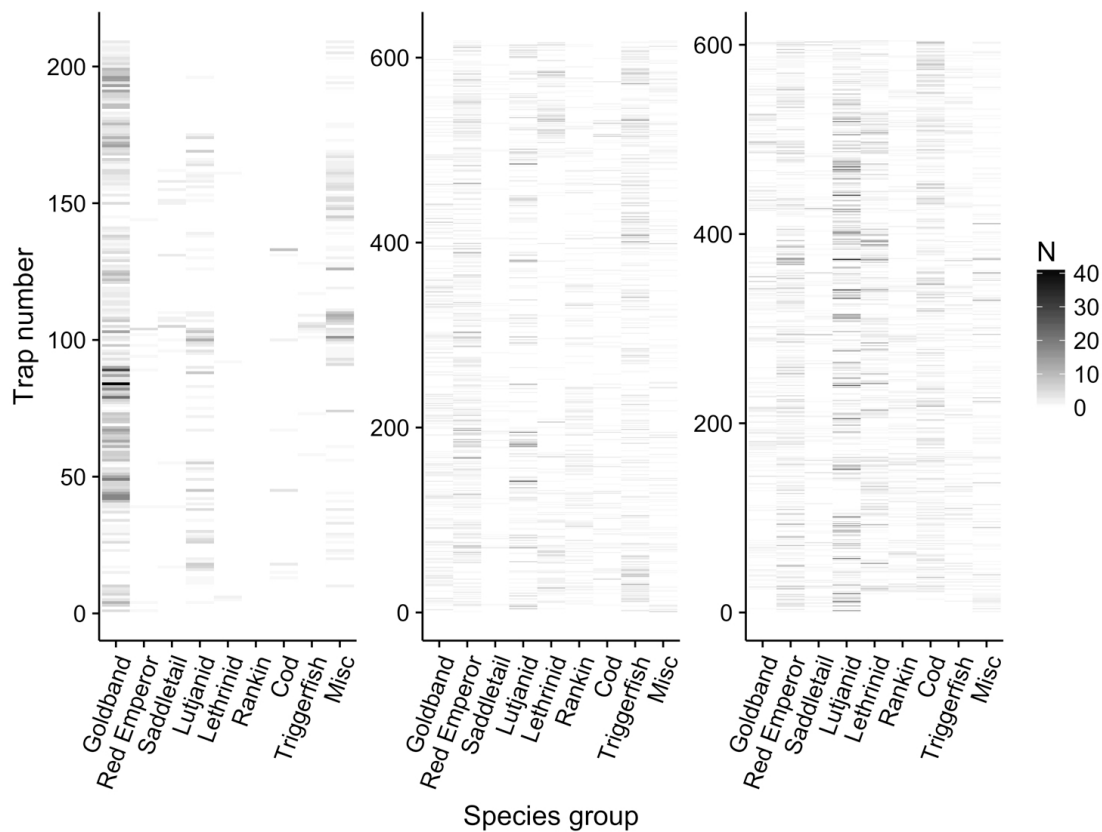
Figure 4.9 Catch summary, split up by species group, as recorded in Region 1 (a), Region 2 (b) and Region 3 (c). The number (N) of individual fish present in each trap is coloured from white (N=0) to black (N=40).

4.4.3 Simulations of fish lengths

A summary of mean lengths for each of the nine groups contained within the three regions can be found in Table 4.7 and are shown in Figure 4.10. A summary of the structures describing the variograms for the groups is given in Table 4.8. Most variograms contained a nugget effect and one or two additional spherical or exponential structures (Table 4.8). Cod in Region 1 and 2, as well as rankin cod in Region 2 were fitted by a pure nugget (Table 4.8). Lethrinids in Region 1 and 2, lutjanids in Region 1, saddletail in Region 1 and triggerfish in Region 1 did not contain any nugget sill (Table 4.8). Mean lengths of the data and the averaged simulated data fluctuated for the different groups by less than 1 cm with the exceptions of lethrinids in Region 1 (4.4 cm), red emperor in Region 2 (1.4 cm), saddletail in Region 3 (1.6 cm) and triggerfish in Region 1 (2.1 cm) (Figure 4.10, Table 4.7). Mean CV attributed to sampling for length distributions was 1.8% (s.d. 1.7%) (Table 4.9). CV attributed to random error for length distributions was on average 2.1% (s.d. 1.6%) (Table 4.9).

Table 4.7 Summary statistics (mean, standard deviation (s.d.), number of data samples (N) and range) of raw and simulated group lengths for each group within the 3 analysed regions and the combined length-weight (L-W) constants a and b taken from FishBase (Froese et al., 2016).

Group	Region	N		Mean [cm]		s.d. [cm]		Range [cm]		L-W constants	
		Data	Simu	Data	Simu	Data	Simu	Min	Max	a	b
Cod	1	8	5314	34.85	32.69	5.27	5.98	27.63	42.37		
	2	88	8576	37.24	37.82	10.80	12.01	24.08	76.67	0.028	2.969
	3	344	5924	37.24	38.99	8.76	11.29	15.10	83.11		
Goldband	1	171	6636	56.33	56.65	4.59	3.98	42.31	70.59		
	2	212	8576	58.59	58.12	7.35	6.74	25.86	79.83	0.019	2.912
	3	181	5924	57.10	57.16	7.23	6.94	40.53	92.38		
Lethrinid	1	4	6636	30.87	32.88	5.84	1.98	25.19	38.66		
	2	152	8564	33.62	33.59	6.64	5.15	18.90	76.21	0.027	2.857
	3	293	5924	31.78	33.27	6.54	7.18	18.33	80.18		
Lutjanid	1	62	6636	30.97	31.64	3.72	4.94	22.11	45.23		
	2	210	8565	30.14	31.37	5.10	5.29	19.57	56.10	0.031	2.917
	3	354	5924	30.53	30.70	4.89	4.98	21.16	58.74		
Misc	1	77	6636	37.55	38.23	11.05	10.35	21.73	65.50		
	2	146	8576	39.82	39.70	15.48	14.75	12.98	101.38	0.017	2.964
	3	163	5924	41.86	41.25	14.82	15.25	10.92	81.16		
Rankin cod	2	172	8576	61.93	61.01	8.86	10.73	41.99	128.35	0.014	3.044
	3	157	5924	61.76	59.99	7.62	7.09	37.86	100.65		
Red Emperor	1	9	5801	56.75	53.56	9.01	10.43	38.33	69.29		
	2	375	8576	52.70	54.18	8.53	8.18	18.29	87.40	0.028	2.912
	3	367	5924	51.11	51.79	8.39	8.27	23.38	70.26		
Saddletail	1	15	6636	57.45	57.02	8.30	9.51	38.63	70.50		
	2	49	8446	58.30	58.19	14.98	12.14	21.64	89.08	0.033	2.917
	3	107	5924	56.83	58.24	10.99	10.71	29.47	80.97		
Triggerfish	1	10	4870	36.72	40.32	6.61	5.43	29.93	52.24		
	2	320	8576	32.55	33.01	4.21	5.18	20.19	46.49	0.025	2.936
	3	156	5924	33.58	34.56	5.03	5.75	16.25	49.40		

Table 4.8 Summary of the structures describing the variograms of the length distributions for the different groups within the three regions, where exp = exponential structure and sph = spherical structure.

Group	Region		
	1	2	3
Cod	Nugget	Nugget	Nugget , exp , sph
Goldband snapper	Nugget , exp , sph	Nugget , sph	Nugget , exp , sph
Lethrinid	exp , sph	exp , sph	Nugget , sph
Lutjanid	sph	Nugget , exp , sph	Nugget , sph
Misc	Nugget , sph	Nugget , sph	Nugget , sph
Rankin cod	/	Nugget	Nugget , sph
Red emperor	Nugget , sph	Nugget , exp	Nugget , exp , sph
Saddletail	sph	Nugget , sph	Nugget , exp
Triggerfish	sph	Nugget , sph	Nugget , sph

Table 4.9 Sampling (CV_{sam}) and random CV (CV_{rand}) of lengths for the nine groups within the three regions based on 250 simulations.

Group	Region	CV_{sam}	CV_{rand}
Cod	1	0.00	5.10
	2	0.00	2.57
	3	1.89	0.91
Goldband	1	0.56	0.48
	2	0.54	1.41
	3	0.75	1.54
Lethrinid	1	7.97	7.32
	2	1.98	1.78
	3	1.29	1.08
Lutjanid	1	1.90	1.57
	2	1.41	1.42
	3	1.01	0.87
Misc	1	2.09	1.39
	2	2.73	1.97
	3	2.48	1.77
Rankin cod	2	0.00	1.65
	3	0.73	1.72
Red Emperor	1	4.32	4.72
	2	0.78	0.82
	3	1.07	0.84
Saddletail	1	4.15	3.66
	2	1.90	3.51
	3	1.94	2.18
Triggerfish	1	3.25	4.55
	2	0.70	0.99
	3	0.99	1.72
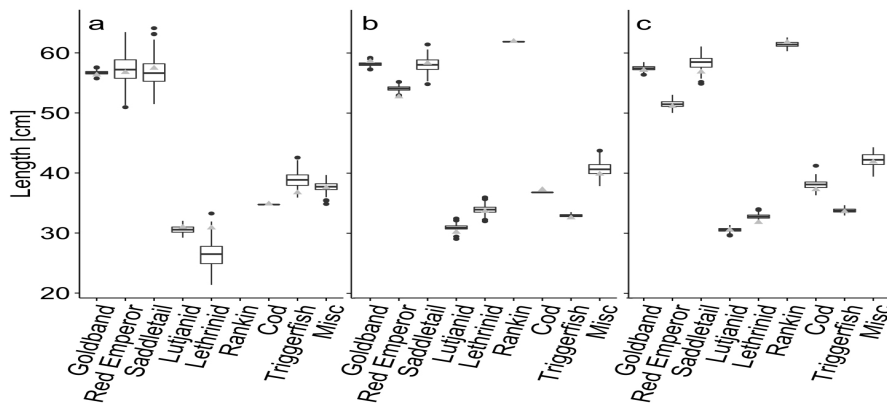
Figure 4.10 Boxplot of 250 simulated mean length estimates for the nine groups within the three regions (a, b, c), with the mean of the data (grey triangles).

4.4.4 Biomass and abundance simulations

Realisations of absolute density, abundance and biomass were obtained through combination of s_A group portions, length simulations and *LW*-equations (Figure 4.11, Table 4.7, 10). Each combined realisation explicitly contains the combined sampling error of the simulations it is based on. Lowest CVs were observed for species occurring most commonly and highest CVs for the least frequently observed groups (Table 4.10). Lowest combined sampling CV was modelled for goldband snapper in Region 1 (CVs_A = 9.0%; $CV_{density}$ = 9.1%; $CV_{abundance}$ = 9.1%; $CV_{biomass}$ = 9.1%). Highest overall CV for s_A, density, abundance and biomass (24.07%) was observed for cods in Region 1 (Table 4.10). Given that abundance estimates are simply density estimates raised by the area of the integration region, CVs are the same. CVs for biomass are different due to the application of a *LW* relationship, but as the mean length of each simulation was an input into the applied *LW* relationship, variation was minimal. Of all simulated estimates, triggerfish showed highest density in Region 2 with 82,550 individuals nmi^{-2}. This would equate to over 10 million triggerfish contained within Region 2, which would equal to one triggerfish every 41.6 m^2. Cods and rankin cod were estimated to have the highest total biomass within the three regions combined (both > 20,000 tonnes), followed by red emperor with a total of 16,413 tonnes (Table 4.10). Triggerfish showed a high overall biomass with a total of 10,959 tonnes. Lethrinids had the lowest biomass with only 1,106 tonness across all regions. Similarly, the miscellaneous group had a low biomass with only 1,617 tonnes (Table 4.10).

Table 4.10 Acoustic density, absolute density, abundance and biomass estimates with corresponding CVs attributed to sampling design and s.d. for the nine groups in the three regions.

Group	Region	sₐ [m2nmi-2]		Abundance [in 1000 x individuals]		Density	Biomass [tonnes]	
		Mean	CV [%]	Mean	CV [%]	Mean	Mean	CV [%]
Cod	1	0.94	34.07	187.49	34.07	1.21	197.1	34.07
	2	3.54	21.64	2454.87	21.64	4.07	3053.6	21.64
	3	12.65	14.09	13397.18	14.26	13.57	18440.6	14.37
Goldband snapper	1	28.96	9.04	254.99	9.11	7.73	618.9	9.06
	2	20.85	12.65	682.75	12.72	5.29	1781.3	12.65
	3	8.28	13.3	454.39	13.37	2.15	1145.4	13.32
Lethrinid	1	0.18	32.37	8.17	38.02	0.25	2.5	32.32
	2	5.04	23.23	542.34	23.59	4.2	343.9	23.28
	3	7.01	18.01	1318.67	17.91	6.25	759.4	18.16
Lutjanid	1	6.53	17.99	194.18	17.64	5.88	129.6	18.63
	2	11.5	18.69	1313.19	18.71	10.18	905	18.89
	3	9.37	16	1787.43	15.93	8.47	1186.4	16.19
Misc	1	12.11	16.59	224.31	17.4	6.8	178.9	16.58
	2	14.05	13.84	875.17	14.37	6.78	872.7	14.33
	3	5.34	14.83	504.14	15.29	2.39	562.3	15.19
Rankin cod	2	14.69	12.64	3594.45	12.64	5.96	14279.9	12.64
	3	9.51	14.43	2443.89	14.56	3.91	15019	14.42
Red Emperor	1	3.62	31.17	118.54	31.78	2.43	295	32.00
	2	32.65	11.88	3056.6	11.87	23.69	9518.9	11.99
	3	14.85	13.81	2443.89	13.89	11.58	6598.8	13.91
Saddletail	1	5.3	19.32	118.54	20.6	3.59	513.1	20.02
	2	2.32	21.75	195.92	21.21	1.52	903.6	22.68
	3	6.75	15.76	923.04	15.8	4.37	4333	16.24
Triggerfish	1	1.81	25.24	185.7	25.41	5.63	214.8	25.79
	2	19.06	13.42	10649.3	13.45	82.55	7574.6	13.46
	3	4.76	16.71	4134.16	16.88	19.59	3170.1	16.71
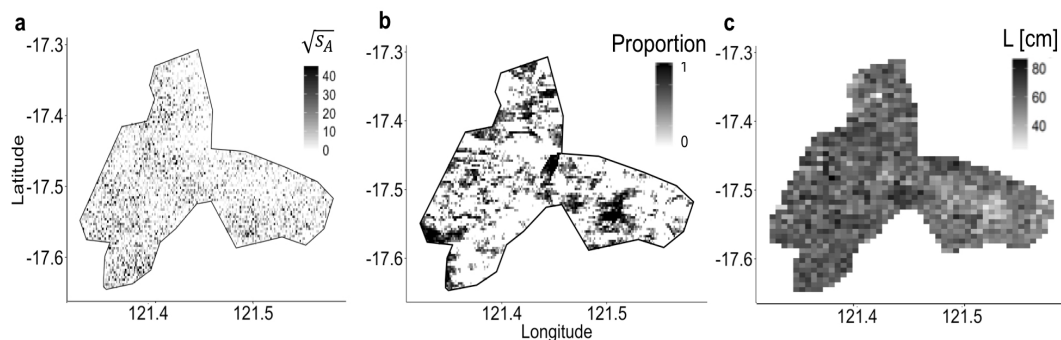
Figure 4.11 One simulation of acoustic backscatter (a), catch proportions (b) and mean length (c) for goldband snapper in region 2

4.4.5 Spatial distribution

The collection of alternative biological information, in conjunction with acoustic data, within mixed species environments can be challenging. Geostatistical indices can describe spatial distribution patterns of marine species. Globel index of colocation (GIC) and centre of gravities (CGs) indicated that most groups co-occurred at very similar locations within the selected fishing grounds (Figure 4.12, Figure 4.13), suggesting no clear habitat segregation, but rather a truly mixed environment, with the exception of goldband snapper in Region 1. In Region 1, theCG of lutjanids, goldband snapper, saddletail and miscellaneous were grouped closely together in the centre of the region, while the mean location for lethrinids and red emperor were located in the northern part of the centre (Figure 4.12). Triggerfish, as well as, cods were more likely to occur in the southern part of Region 1. In Region 2, all CGs were distributed around the centre of the region (Figure 4.12). In Region 3, all CGs were clustered together very closely in the centre of the region (Figure 4.12). Isotropy and inertia were low throughout all three regions for all groups, with a maximal isotropy observed for red emperor in Region 1 (0.12), and maximal inertia observed for triggerfish in Region 3 (<0.01). This suggests that the distribution of the different groups is elongated and localised. Isotropy was lower in Region 3 (mean = 0.02), compared to Region 2 (mean = 0.08) and Region 1 (mean = 0.05), while inertia was maximal in Region 3 (mean = 0.04) and very low in Region 1 and 2 (mean < 0.01). GIC confirmed these findings (Figure 4.13). In Regions 2 and 3, all groups were packed closely together, with highly overlapping distributions (GIC > 0.9, Figure 4.13b, c). In Region 1 all groups showed overlapping distributions, with the exception of triggerfish and cods (GIC 0.3 – 0.6, Figure 4.13a),
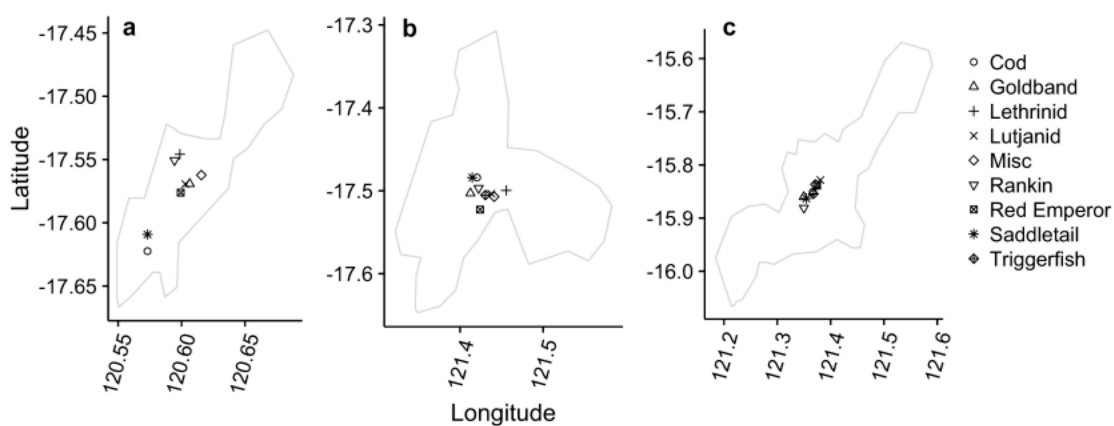
Figure 4.12 Centre of gravity for the nine groups within the three regions (TF = triggerfish, ST = saddletail, RE = red emperor, MISC = miscellaneous, LJ = lutjanid, LT =lethrinids, GB = goldband snapper, Cod = Cod, RC = rankin cod).
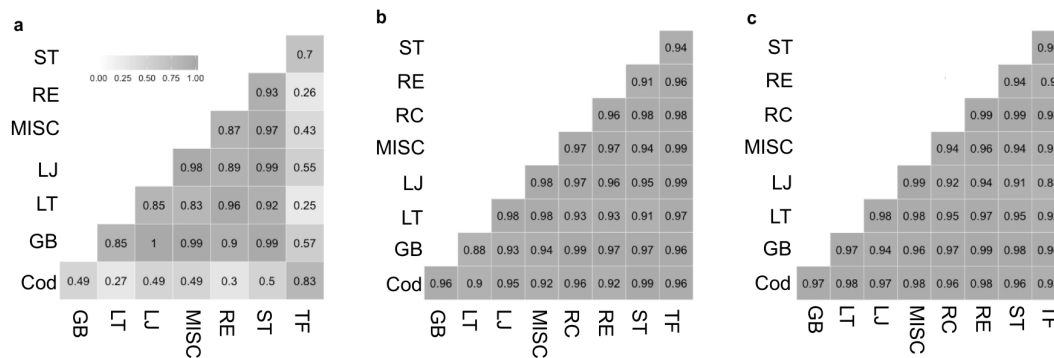
Figure 4.13 Global Index of Collocation for all groups in the three regions (TF = triggerfish, ST = saddletail, RE = red emperor, MISC = miscellaneous, LJ = lutjanid, LT =lethrinids, GB = goldband snapper, Cod = Cod, RC = rankin cod) , based on Geostatistical conditional simulations.

4.5 Discussion

The present study is one of the first attempts to estimate density, abundance and biomass of key resources for a given area, including estimates of sampling variation based exclusively on information collected from a commercial fishing vessel during normal operation without dedicated biological information from a multi-species environment.

Geostatistics have widely been shown to be a viable tool to describe the spatial distribution, abundance and variability of fish resources based on acoustic measurements (Rivoirard et al., 2000 ; Petitgas et al., 2003; Spedicato et al., 2007; Doray et al., 2008; Woillez et al., 2009a; Gastauer et al., 2016a; Petitgas et al., 2016; Scoulding et al., 2016). A major benefit for spatial modelling using geostatistical techniques is that it explicitly takes into account spatial autocorrelation (Bez, 2007; Rivoirard et al., 2000). This is especially valid when dealing with non-stratified, non-random but directed survey designs, such as fishing tracks (Fässler et al., 2016).

This paper has demonstrated that GCS can be used to derive estimates of density, abundance and biomass with associated sampling error based on acoustic and catch information obtained from a commercial trap fishing vessel. While traps may not reflect directly what can be seen on the acoustic recordings, they provide valid information on species richness and composition within the NDSF (Newman et al., 2012). In the present study, regions were delimited manually, closely around areas of high fishing density, where simultaneously

collected acoustic data was available. Consequently, a relatively high coverage of these areas could be realised, with numerous trap samples and high density acoustic information. Even though traps can contain highly variable species compositions a spatial structure could be detected in most cases, with the exception of cods and lethrinids in Region 2, as well as goldband snapper in Region 3. For those, the variograms were described by a pure nugget effect, suggesting random distribution of the data, or with a spatial structure that can't be detected at the given resolution (Rivoirard et al., 2000).

Generally, error associated with sampling design was low for catch proportions (<12%), except for cods in Region 1 (19.1%) and triggerfish in Region 1 (16.6%). Both species comprised on average of 1 or 2% of the total catch and therefore they were considered rare within Region 1, making adequate sampling difficult. Random error of catch proportions was very low overall (<6%). These low sampling errors suggest that catch samples were taken adequately for the chosen regions. Sampling error found in the acoustic data was less than 10% in all three regions. Overall CVs fluctuated between 9.0 and 34.1% for density, 9.1 and 38.0% for abundance and 9.0 and 34.0% for biomass. These values are comparable to findings by Woillez et al. (2016) who found CV estimates of abundance to fluctuate between 12.0 and48.0% and 3.0 and 22.0% for biomass, depending on the year of the survey and the age group of Bering sea-walleye being analysed. Where Woillez et al. (2016) used age classes of one species to split up the abundance estimates, here we split up the final estimates by species groups in a similar fashion. In agreement with Woillez et al. (2016) and Woillez et al. (2007) lowest CVs were determined for the most abundant groups while higher CVs were observed for the rarer groups. With CVs estimated within this study being comparable to CVs estimated from dedicated survey data, it can be assumed that sampling within the given regions during the time of recording was adequate. It should be noted, however, that the covered areas are relatively small and estimates only provide a snapshot of the situation at the time of recording. A much longer time series with repeated coverage over larger areas would be needed to derive valid abundance or biomass estimates for the entire NDSF.

Another challenge associated with the estimation of abundance or biomass derived from acoustic recordings is the influence of *TS* and associated *TS-L* equations. Woillez et al. (2016) found that *TS-L* equations can contribute >80% to the total CV of biomass estimates. In order to convert acoustic estimates into absolute abundance or biomass estimates, a thorough understanding of the *TS* properties of the target species is essential. Small variations in *TS* can have a significant effect on the absolute estimates of abundance or biomass (Everson et al.,

1990; Foote, 1980; McClatchie et al., 1996a; Scoulding et al., 2016). While *TS-L* equations were available for red emperor and goldband snapper (Gastauer et al 2016b; 2017) there were no published *TS-L* equations available for the other groups. Given the close biological relation and similarities in the morphology and physiology of saddletail, other lutjanids and red emperor, using the same *TS-L* for all three groups was assumed to be an acceptable approximation. To gain some insights into abundance and biomass estimates of the other groups, we have presented estimates of *TS-L* for rankin cod, triggerfish and spangled emperor over a range of tilt angles using a KRM model, similar to Gastauer et al (2017), calculated without Bayesian parametrisation.

Previous studies found good agreement between KRM based *TS* estimates and *in situ* or *ex situ* empirical measurements (Hazen and Horne, 2003; Henderson and Horne, 2007; Peña and Foote, 2008; Gastauer et al., 2016b). Based on information obtained from CT scans, tilt angle dependent *TS-L* relationships for rankin cod, triggerfish and spangled emperor could be estimated, although it should be noted that only a limited amount of good quality specimens with intact swimbladders were available (3 triggerfish, 2 spangled emperors, 2 rankin cods). Biological samples taken from the NDSF are mostly caught at depths greater than 100m. Retrieval of specimens from this depth can cause damage to the swimbladder (Rudershausen et al., 2007). It is therefore recommended that the exercise should be repeated with more samples. Nonetheless, the authors consider the established *TS-L* relationships suitable for providing estimates of abundance and biomass. The *TS-L* constant intercept (b_{TS} = -70.5) for spangled emperor, which in physiological and morphological terms is closely related to the lutjanidae family, was very similar to the intercept for goldband snapper (b_{TS} = -70.8, a_{TS} = 20.1), based on *in situ* data (Gastauer *et* al., 2017). Estimated *TS-L* for rankin cod was low. This value can be explained by the deflated swimbladder. Rankin cod and other cods are known to regularly suffer from barotrauma when taken from great depths (Rudershausen et al., 2007; Sadovy de Mitcheson et al., 2013). Given the ability of these fish to inflate and deflate their swimbladders estimating *TS* based on deflated swimbladders will result in an overestimation of total abundance and biomass.

The methods presented here could be applied to a wide range of ecosystems and fisheries where mixed species are encountered and some information, representative of species richness or species composition groups, is available. Continuation of data collection, over a larger area and an extended time period would allow for improved mapping of resource distributions and abundances contained within the NDSF. In areas where time series data are

available, indices could be extracted, to track changes in the resource structure and distribution. If such a long-term monitoring programme were employed, it is recommended that *in situ* calibrations are conducted seasonally, to test the stability of the acoustic equipment. Such information is of high value in regions where funds for scientific surveys are limited and some/many of the targeted resources are described as data deficient.

4.6 Acknowledgements

4.7 References

Au, W.W.L., Fay, R.R., 2012. Hearing by Whales and Dolphins. Springer Science & Business Media.

Ballón, M., Bertrand, A., Lebourges-Dhaussy, A., Gutiérrez, M., Ayón, P., Grados, D., Gerlotto, F., 2011. Is there enough zooplankton to feed forage fish populations off Peru? An acoustic (positive) answer. Prog. Oceanogr. 91, 360–381. doi:10.1016/j.pocean.2011.03.001

Barbeaux, S.J., Horne, J.K., Dorn, M.W., 2013. Characterizing walleye pollock (Theragra chalcogramma) winter distribution from opportunistic acoustic data. ICES J. Mar. Sci. J. Cons. fst052.

Bez, N., 2007. Transitive geostatistics and statistics per individual : a relevant framework for assessing resources with diffuse limits. J. Société Fr. Stat. 148, 53–75.

Bez, N., Rivoirard, J., Guiblin, P., Walsh, M., 1997. Covariogram and related tools for structural analysis of fish survey data. Geostat. Wollongong 96, 1316–1327.

Campanella, F., Taylor, J.C., 2016. Investigating acoustic diversity of fish aggregations in coral reef ecosystems from multifrequency fishery sonar surveys. Fish. Res. 181, 63–76.

Clay, C.S., 1991. Low-resolution acoustic scattering models: Fluid-filled cylinders and fish with swim bladders. J. Acoust. Soc. Am. 89, 2168–2179. doi:10.1121/1.400910

Clay, C.S., Horne, J.K., 1994. Acoustic models of fish: the Atlantic cod (Gadus morhua). J. Acoust. Soc. Am. 96, 1661–1668.

Conti, S.G., Demer, D.A., Soule, M.A., Conti, J.H., 2005. An improved multiple-frequency method for measuring in situ target strengths. ICES J. Mar. Sci. J. Cons. 62, 1636–1646.

Dalen, J., Karp, W.A., 2007. Collection of acoustic data from fishing vessels. International Council for the Exploration of the Sea.

De Robertis, A., McKelvey, D.R., Ressler, P.H., 2010. Development and application of an empirical multifrequency method for backscatter classification. Can. J. Fish. Aquat. Sci. 67, 1459–1474.

Demer, D.A., Berger, L., Bernasconi, M., Bethke, E., Boswell, K., Chu, D., Domokos, R., et al., 2015. Calibration of acoustic instruments. ICES Cooperative Research Report No. 326.

Demer, D.A., Soule, M.A., Hewitt, R.P., 1999. A multiple-frequency method for potentially improving the accuracy and precision of in situ target strength measurements. J. Acoust. Soc. Am. 105, 2359–2376.

Doray, M., Petitgas, P., Josse, E., 2008. A geostatistical method for assessing biomassof tuna aggregations around moored fish aggregating devices with star acoustic surveys. Can. J. Fish. Aquat. Sci. 65, 1193–1205. doi:10.1139/F08-050

Echoview Software Pty Ltd, 2015. Echoview software 6.1.44. Hobart, Australia.

Everson, I., Watkins, J.L., Bone, D.G., Foote, K.G., 1990. Implications of a new acoustic target strength for abundance estimates of Antarctic krill. Nature 345, 338–340. doi:10.1038/345338a0

Fässler, S.M.M., Brunel, T., Gastauer, S., Burggraaf, D., 2016. Acoustic data collected on pelagic fishing vessels throughout an annual cycle: Operational framework, interpretation of observations, and future perspectives. Fish. Res., The use of fishing vessels as scientific platforms 178, 39–46. doi:10.1016/j.fishres.2015.10.020

Fernandes, P.G., Korneliussen, R.J., Lebourges-Dhaussy, A., Masse, J., Iglesias, M., Diner, N., Ona, E., Knutsen, T., Gajate, J., Ponce, R., 2006. The SIMFAMI project: species identification methods from acoustic multifrequency information. Final Report to the EC No. Q5RS-2001-02054.

Fofonoff, N.P., Millard Jr, R.C., 1983. Algorithms for the computation of fundamental properties of seawater.

Foote, K.G., 1979. On representing the length dependence of acoustic target strengths of fish. *Journal of the Fisheries Board of Canada*, *36*(12), pp.1490-1496.

Foote, K.G., 1980. Importance of the swimbladder in acoustic scattering by fish: A comparison of gadoid and mackerel target strengths. J. Acoust. Soc. Am. 67, 2084–2089. doi:10.1121/1.384452

Froese, R., and Pauly, D. 2016. FishBase. World Wide Web electronic publication. Available from www.fishbase.org, (07/2016).

Gastauer, S., Fässler, S.M.M., O'Donnell, C., Høines, Å., Jakobsen, J.A., Krysov, A.I., Smith, L., Tangen, Ø., Anthonypillai, V., Mortensen, E., Armstrong, E., Schaber, M., Scoulding, B., 2016a. The distribution of blue whiting west of the British Isles and Ireland. Fish. Res. 183, 32–43. doi:10.1016/j.fishres.2016.05.012

Gastauer, S., Scoulding, B., Fässler, S.M., Benden, D.P., Parsons, M., 2016b. Target strength estimates of red emperor (Lutjanus sebae) with Bayesian parameter calibration. Aquat. Living Resour. 29, 301.

Gastauer, S., Scoulding, B., Parsons, M. 2017 "Estimates of variability of goldband snapper target strength and biomass in three fishing regions within the Northern Demersal Scalefish Fishery (Western Australia)." *Fisheries Research* 193 (2017): 250-262.

Handegard, N.O., Buisson, L. du, Brehmer, P., Chalmers, S.J., Robertis, A., Huse, G., Kloser, R., Macaulay, G., Maury, O., Ressler, P.H., others, 2013. Towards an acoustic-based coupled observation and modelling system for monitoring and predicting ecosystem dynamics of the open ocean. Fish Fish. 14, 605–615.

Hazen, E.L., Horne, J.K., 2003. A method for evaluating the effects of biological factors on fish target strength. ICES J. Mar. Sci. J. Cons. 60, 555–562. doi:10.1016/S1054-3139(03)00053-5

Henderson, M.J., Horne, J.K., 2007. Comparison of in situ, ex situ, and backscatter model estimates of Pacific hake (Merluccius productus) target strength. Can. J. Fish. Aquat. Sci. 64, 1781–1794. doi:10.1139/f07-134

Horne, J.K., 2000. Acoustic approaches to remote species identification: a review. Fish. Oceanogr. 9, 356–371.

Korneliussen, R.J., Diner, N., Ona, E., Berger, L., Fernandes, P.G., 2008. Proposals for the collection of multifrequency acoustic data. ICES J. Mar. Sci. J. Cons. 65, 982–994. doi:10.1093/icesjms/fsn052

Korneliussen, R.J., Heggelund, Y., Eliassen, I.K., Johansen, G.O., 2009. Acoustic species identification of schooling fish. ICES J. Mar. Sci. 66, 1111–1118. doi:10.1093/icesjms/fsp119

Korneliussen, R.J., Heggelund, Y., Macaulay, G.J., Patel, D., Johnsen, E., Eliassen, I.K., 2016. Acoustic identification of marine species using a feature library. Methods Oceanogr., Special section on Novel instrumentation in Oceanography: a dedication to Rob Pinkel 17, 187–205. doi:10.1016/j.mio.2016.09.002

Koslow, J.A., 2009. The role of acoustics in ecosystem-based fishery management. ICES J. Mar. Sci. J. Cons. fsp082.

Lezama-Ochoa, A., Grados, D., Lebourges-Dhaussy, A., Irigoien, X., Chaigneau, A., Bertrand, A., 2015. Biological characteristics of the hydrological landscapes in the Bay of Biscay in spring 2009. Fish. Oceanogr. 24, 26–41. doi:10.1111/fog.12090

Matheron, G., 1971. The theory of regionalised variables and its applications. Cahiers du centre de Morphologie Mathematique, Fontainebleau 5 (Ecole Nationale Superiore des Mines de Paris, Paris, France).

McClatchie, S., Alsop, J., Coombs, R.F., 1996a. A re-evaluation of relationships between fish size, acoustic frequency, and target strength. ICES J. Mar. Sci. J. Cons. 53, 780–791. doi:10.1006/jmsc.1996.0099

McClatchie, S., Alsop, J., Ye, Z., Coombs, R.F., 1996b. Consequence of swimbladder model choice and fish orientation to target strength of three New Zealand fish species. ICES J. Mar. Sci. J. Cons. 53, 847–862.

Newman, S.J., Harvey, E.S., Rome, B.M., McLean, D.L., Skepper, C.L, 2012. Relative efficiency of fishing gears and investigation of resource availability in tropical demersal scalefish fisheries. . Final Report FRDC Project No. 2006/031. Fisheries Research Report No. 231. Department of Fisheries, Western Australia, Western Australia.

Peña, H., Foote, K.G., 2008. Modelling the target strength of Trachurus symmetricus murphyi based on high-resolution swimbladder morphometry using an MRI scanner. ICES J. Mar. Sci. J. Cons. 65, 1751–1761. doi:10.1093/icesjms/fsn190

Petitgas, P., Massé, J., Beillois, P., Lebarbier, E., Cann, A.L., 2003. Sampling variance of species identification in fisheries acoustic surveys based on automated procedures associating acoustic images and trawl hauls. ICES J. Mar. Sci. J. Cons. 60, 437–445. doi:10.1016/S1054-3139(03)00026-2

Petitgas, P., Woillez, M., Doray, M., Rivoirard, J., 2016. A Geostatistical Definition of Hotspots for Fish Spatial Distributions. Math. Geosci. 48, 65–77.

R Core Team, 2016. R: A language and environment for statistical computing. R Foundation for Statistical Computing, Vienna, Austria. URL https://www.R-project.org/.

Reeder, D.B., Jech, J.M., Stanton, T.K., 2004. Broadband acoustic backscatter and high-resolution morphology of fish: Measurement and modeling. J. Acoust. Soc. Am. 116, 747–761. doi:10.1121/1.1648318

Ridgway, K.R., Dunn, J.R., Wilkin, J.L., 2002. Ocean interpolation by four-dimensional least squares -Application to the waters around Australia. J. Atmos. Ocean. Tech. 19, 1357–1375.

Rivoirard, J., Simmonds, J., Foote, K.G., Fernandes, P., Bez, N., 2000. Geostatistics for Estimating Fish Abundance. Blackwell Science Ltd, Oxford.

Rose, G.A., 1992. A review of problems and new directions in the application of fisheries acoustics on the Canadian East Coast. Fish. Res. 14, 105–128.

Rudershausen, P.J., Buckel, J.A., Williams, E.H., 2007. Discard composition and release fate in the snapper and grouper commercial hook-and-line fishery in North Carolina, USA. Fish. Manag. Ecol. 14, 103–113. doi:10.1111/j.1365-2400.2007.00530.x

Ryan, T.E., Downie, R.A., Kloser, R.J., Keith, G., 2015. Reducing bias due to noise and attenuation in open-ocean echo integration data. ICES J. Mar. Sci. J. Cons. 72, 2482–2493. doi:10.1093/icesjms/fsv121

Sadovy de Mitcheson, Y., Craig, M.T., Bertoncini, A.A., Carpenter, K.E., Cheung, W.W.L., Choat, J.H., Cornish, A.S., Fennessy, S.T., Ferreira, B.P., Heemstra, P.C., Liu, M., Myers, R.F., Pollard, D.A., Rhodes, K.L., Rocha, L.A., Russell, B.C., Samoilys, M.A., Sanciangco, J., 2013. Fishing groupers towards extinction: a global assessment of threats and extinction risks in a billion dollar fishery. Fish Fish. 14, 119–136. doi:10.1111/j.1467-2979.2011.00455.x

Schindelin, J., Rueden, C.T., Hiner, M.C., Eliceiri, K.W., 2015. The ImageJ ecosystem: An open platform for biomedical image analysis. Mol. Reprod. Dev. 82, 518–529. doi:10.1002/mrd.22489

Scoulding, B., Gastauer, S., MacLennan, D.N., Fässler, S.M.M., Copland, P., Fernandes, P.G., 2016. Effects of variable mean target strength on estimates of abundance: the case of Atlantic mackerel (Scomber scombrus). ICES Jour. Mar. Sci. doi:doi:10.1093/icesjms/fsw212

Simmonds, J., MacLennan, D., 2005. Fisheries acoustics: theory and practice. Fish Aquat. Resour. Ser.

Spedicato, M.T., Woillez, M., Rivoirard, J., Petitgas, P., Carbonara, P., Lembo, G., 2007. Usefulness of the spatial indices to define the distribution pattern of key life stages: an application to the red mullet (Mullus barbatus) population in the south Tyrrhenian sea. ICES CM.

Stanton, T.K., Chu, D., Jech, J.M., Irish, J.D., 2010. New broadband methods for resonance classification and high-resolution imagery of fish with swimbladders using a modified commercial broadband echosounder. ICES J. Mar. Sci. J. Cons. 67, 365–378. doi:10.1093/icesjms/fsp262

Trenkel, V., Ressler, P.H., Jech, M., Giannoulaki, M., Taylor, C., 2011. Underwater acoustics for ecosystem-based management: state of the science and proposals for ecosystem indicators. Mar. Ecol.-Prog. Ser. 442, 285–301.

Tugores, M.P., Iglesias, M., Oñate, D., Miquel, J., 2016. Spatial distribution, sampling precision and survey design optimisation with non-normal variables: The case of anchovy (Engraulis encrasicolus) recruitment in Spanish Mediterranean waters. Prog. Oceanogr. 141, 168–178.

van der Kooij, J., Fässler, S.M.M., Stephens, D., Readdy, L., Scott, B.E., Roel, B.A., 2016. Opportunistically recorded acoustic data support Northeast Atlantic mackerel expansion theory. ICES J. Mar. Sci. J. Cons. 73, 1115–1126. doi:10.1093/icesjms/fsv243

Woillez, M., Poulard, J.-C., Rivoirard, J., Petitgas, P., Bez, N., 2007. Indices for capturing spatial patterns and their evolution in time, with application to European hake (Merluccius merluccius) in the Bay of Biscay. ICES J. Mar. Sci. J. Cons. 64, 537–550. doi:10.1093/icesjms/fsm025

Woillez, M., Ressler, P.H., Wilson, C.D., Horne, J.K., 2012. Multifrequency species classification of acoustic-trawl survey data using semi-supervised learning with class discovery. J. Acoust. Soc. Am. 131, EL184–EL190.

Woillez, M., Rivoirard, J., Fernandes, P.G., 2009a. Evaluating the uncertainty of abundance estimates from acoustic surveys using geostatistical simulations. ICES J. Mar. Sci. J. Cons. fsp137.

Woillez, M., Rivoirard, J., Petitgas, P., 2009b. Notes on survey-based spatial indicators for monitoring fish populations. Aquat. Living Resour. 22, 155–164.

Woillez, M., Walline, P.D., Ianelli, J.N., Dorn, M.W., Wilson, C.D., Punt, A.E., 2016. Evaluating total uncertainty for biomass-and abundance-at-age estimates from eastern Bering Sea walleye pollock acoustic-trawl surveys. ICES J. Mar. Sci. J. Cons. 73, 2208–2226.

Yasuma, H., Sawada, K., Takao, Y., Miyashita, K., Aoki, I., 2010. Swimbladder condition and target strength of myctophid fish in the temperate zone of the Northwest Pacific. ICES J. Mar. Sci. J. Cons. 67, 135–144. doi:10.1093/icesjms/fsp218

Chapter 5

An unsupervised acoustic description of fish schools and the seabed in three fishing regions within the Northern Demersal Scalefish Fishery (NDSF, Western Australia)

Sven Gastauer[1,2,3], Ben Scoulding[4], Miles Parsons[1]

[1] Centre for Marine Science and Technology, Curtin University, GPO Box U1987, Perth, WA 6845, Australia

[2] Wageningen Marine Research, P.O. Box 68, 1970 AB IJmuiden, The Netherlands

[3] Antarctic Climate and Ecosystems Cooperative Research Centre, University of Tasmania, Private Bag 80, Hobart, Tasmania 7001

[4] Echoview Software Pty Ltd, GPO Box 1387, Hobart, 7001, Tasmania, Australia

Corresponding author: *Sven Gastauer, CMST, Curtin University B301 Hayman Rd, Bentley WA 6102, Australia; email:* sven.gastauer@postgrad.curtin.edu.au

5.1 Abstract

Fisheries acoustics is now a standard tool for monitoring marine organisms. Another use of active-acoustics techniques is the potential to qualitatively describe fish school and seafloor characteristics or the distribution of fish density hotspots. Here, we use a geostatistical approach to describe the distribution of acoustic density hotspots within three fishing regions of the Northern Demersal Scalefish Fishery in Western Australia. This revealed a patchy distribution of hotspots within the three regions, covering almost half of the total areas. Energetic, geometric and bathymetric descriptors of acoustically identified fish schools were clustered using Robust Sparse K-Means clustering with a Clest algorithm to determine the ideal number of clusters. Identified clusters were mainly defined by the energetic component of the school. Seabed descriptors considered were depth, roughness, first bottom length, maximum S_v, kurtosis, skewness and bottom rise time. The ideal number of bottom clusters (maximisation rule with D-Index, Hubert Score and Weighted Sum of Squares), following the majority rule, was three. Cluster 1 (mainly driven by depth) was the sole type present in Region 1, Cluster 2 (mainly driven by roughness and maximum S_v) dominated Region 3, while Region 2 was split up almost equally between Cluster 2 and 3. Detection of indicator species for the three seabed clusters revealed that the selected clusters could be related to biological information. Goldband snapper and miscellaneous fish were indicators for Cluster 1; Cods, Lethrinids, Red Emperor and other Lutjanids were linked with Cluster 2, while Rankin Cod and Triggerfish were indicators for Cluster 3.

Keywords: *Fisheries acoustics, acoustic habitat descriptors, unsupervised target classification, geostatistical hotspots, indicator species*

5.2 Introduction

Fisheries acoustics is a tool used by scientists and fishermen alike (Dalen and Karp, 2007; Melvin et al., 2016; Ressler et al., 2009). Fishermen often use active-acoustic instruments (e.g. echosounders) to support their search for high-quality fishing grounds, to determine bottom depth, and in some situations to derive information about the seabed structure (Fässler et al., 2016). Fisheries scientists commonly use active-acoustics to estimate stock abundance and biomass of marine fish species (ICES, 2015; Kloser et al., 2009, 2002; Simmonds and MacLennan, 2005). Due to the growing interest of fishers and scientists in active-acoustic technology, it is unsurprising that many modern fishing vessels are equipped with scientifically rated echosounders (Barbeaux, 2012; Barbeaux et al., 2013; Dalen and Karp, 2007; Fässler et al., 2016; Gastauer et al., 2017). Such echosounders can be calibrated and are capable of recording raw acoustic data with a minimal amount of internal data manipulation (Barbeaux et al., 2013; Dalen and Karp, 2007; Fässler et al., 2016). Due to their time at sea and distances travelled, opportunistic recording of acoustic data by fishers at sea can deliver new insights into the distribution and structure of the targeted fish species in the area. Such data can be used to compliment data collected during existing scientific monitoring programmes, to improve the spatial and temporal effectiveness of these surveys (Fässler et al., 2016). Where dedicated scientific surveys provide good snapshots of the presence and abundance of fish contained within the surveyed region at the time of the survey, data collected on vessels of opportunity (e.g. fishing vessels) can give a broader picture on a wider temporal and spatial scale (Fässler et al., 2016). Deriving information such as density hotspots (Petitgas et al., 2016) or geostatistical indices (Gastauer et al., 2016; Woillez et al., 2009, 2007) of this data can then support an informed decision process on surveying strategies.

In the higher latitudes (north and south), in temperate climate regimes, fisheries acoustics have become a standard tool for monitoring many pelagic fish stocks (Simmonds and MacLennan, 2005). These fish species generally form single-species aggregations, making them ideal for acoustic monitoring. In contrast, in tropical ecosystems, fish often occur in mixed-species schools with a much higher species diversity and, as such, species-specific acoustic assessment is more difficult (Campanella and Taylor, 2016; De Robertis et al., 2010; Horne, 2000; Koslow, 2009). While post-processing techniques based on multi-frequency acoustic data are able to distinguish between different functional groups, such as phytoplankton, zooplankton, swimbladder and non-swimbladder fish, distinguishing between similar species in

mixed schools is more challenging (De Robertis et al., 2010; Korneliussen et al., 2008; Woillez et al., 2012). Although supervised (e.g. feed forward neural networks (Cabreira et al., 2009; Haralabous and Georgakarakos, 1996)) and unsupervised (e.g. clustering (Campanella and Taylor, 2016; Legendre and Legendre, 2012), random forest classification (Fernandes, 2009) and self-organising maps (Peña et al., 2015; Peña and Calise, 2016)) methods for acoustic target classification exist, their application remains limited. Most classification methods used in fisheries acoustics are empirical, for example, the use of classification feature libraries (Korneliussen et al., 2009a) or frequency response characteristics (De Robertis et al., 2010; Fernandes et al., 2006). These methods are both, data-driven and dependent on expert judgement (Korneliussen et al., 2016). They generally require data collected by additional sampling methods (Fernandes et al., 2016). Unsupervised or supervised modelling approaches to target classification are advantageous in situations where no, or limited, dedicated alternative sampling observations are available (Campanella and Taylor, 2016).

Moving towards an ecosystem approach in fisheries management (EBFM), the identification of different habitats and their association with different marine species is important (Handegard et al., 2013; Trenkel et al., 2011). Fisheries acoustics is considered as being one of the main tools to provide the basis for EBFM (Handegard et al., 2013; Koslow, 2009; Trenkel et al., 2011). In addition to the detection of fish, active-acoustics can be used to derive information about seabed characteristics (Anderson et al., 2007; Cutter and Demer, 2013; Hamilton, 2001; Siwabessy et al., 2004a). Seabed properties have been shown to play an important role in the habitat description of demersal and semi-demersal fish species (Bax and Williams, 2001; Collins and McConnaughey, 1998; Greenstreet et al., 1997; Lazzari and Tupper, 2002; Maravelias, 1999). An enhanced understanding of the distribution of acoustic density hotspots and fish school characteristics, in conjunction with habitat characteristics, has the potential to improve the monitoring and management of mixed-species fisheries in tropical environments (Hall and Mainprize, 2004; Link, 2005). Here, we use acoustic and catch information collected on a commercially operating trap fishing vessel to identify density hotspots, describe acoustic diversity of fish schools and identify different acoustic seabed habitats within three fishing regions. Defined clusters of school and seabed descriptors were then linked to catch information to investigate the ecological meaning of the clusters.

5.3 Methods

5.3.1 Study area

Table 5.1 Summary of the three fishing regions.

Region	Area [nmi²]	Mean depth [m]	Depth range [m]	Period of data collection in 2014
1	33	124	120-130	03/12 - 07/12
2	129	78	61-90	29/10 - 08/11
3	211	91	76-103	19/08 - 30/08

The Northern Demersal Scalefish Fishery (NDSF) is a mixed-demersal trap fishery which encompasses an area of 408,400 km². In the northwest of Australia, off the coast of Broome, the NDSF extends to the shelf edge close to the Indonesian border. All data were collected on board *FV Carolina M*, a 15 m trap fishing boat, during normal commercial operations. In this study, we focussed on three fishing regions where simultaneously collected acoustic and biological information was available. Details on the total area of the three fishing regions, delimited by manually drawn polygons, and the period of data collection are given in Table 5.1, with additional information found in (Gastauer et al., 2017a; Gastauer et al., 2017b). Fishing regions were defined as areas where high densities of fishing and acoustic data were available. An overview of the locations of the three fishing regions and acoustic recordings are given in Figure 5.1.
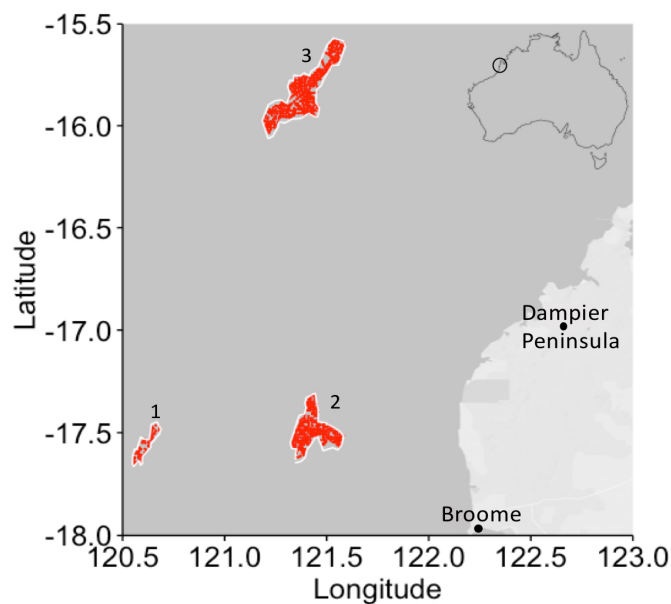
Figure 5.1 Map of a part of the NDSF area off Broome in Western Australia. The location and extents of the three selected fishing regions are indicated by the three white polygons. Locations of acoustic recordings are shown as red dots.

5.3.2 Biological sampling

Catch information on all specimens was obtained by a GoPro Hero 3 camera mounted on each trap as it was hauled on board (see (S. Gastauer et al., 2017; Sven Gastauer et al., 2017) for details). The downwards looking camera, facilitated recording of all fish caught within the trap before the catch was split into commercially relevant species or returned to sea. The optical recordings of the catch facilitated counting of fish per species group. Length measurements of the individual fish was based on pixel counting, calibrated through the known, constant mesh size of the traps. Calibrated video recordings were corrected for the built-in wide angle distortion and subsequent processing was performed using a custom built software package, FishVid (S. Gastauer et al., 2017; Sven Gastauer et al., 2017). Specimens were categorised into nine groups (S. Gastauer et al., 2017; Sven Gastauer et al., 2017) (for simplicity referred to as species groups): Goldband snapper (*Pristipomoides multidens*), Red Emperor (*Lutjanus sebae*), Saddletail (*Lutjanus malabaricus*), Lutjanids (members of the Lutjanidae family, other than Saddletail, Red Emperor or Goldband snapper), Lethrinids (members of the Lethrinidae family), Rankin Cod (*Epinephelus multinotatus*), Cods (members of the Epinephelidae family other than Rankin Cod), Triggerfish (members of the Balistidae family) and a miscellaneous group containing all other species.

5.3.3 Acoustic data processing

All acoustic data were collected (Figure 5.1) using calibrated (Demer et al., 2015) hull-mounted SIMRAD ES-70 split-beam echosounders operating at 38 and 120 kHz. All settings were the same as those used during normal commercial operations. A detailed description of these settings and the acoustic processing steps can be found in (S. Gastauer et al., 2017; Sven Gastauer et al., 2017). All acoustic processing was conducted in Echoview 7.0 (Echoview Software Pty Ltd, 2015). Ping geometry and times were matched for 38 and 120 kHz (Conti et al., 2005; Demer et al., 1999). Effects of impulse noise (mainly caused by non-synchronised echosounders), transient noise (mainly caused by poor weather conditions) and background noise (mainly caused by the vessels engine and bad weather (Mitson, 2003; Ryan et al., 2015)), were minimised through adaptation of filters described by (Ryan et al., 2015).

All fish observed in the catch possessed a swimbladder. This allowed for the application of a simple bi-frequency algorithm to differentiate between fish and fluid-like (e.g. plankton) targets (Ballón et al., 2011; Sven Gastauer et al., 2017; Lezama-Ochoa et al., 2011). Volume backscattering coefficients (sv; m2 m−3) of acoustically detected fish schools were

integrated (s_A; m^2 nmi^{-2}) and averaged over 1 nmi by 10 m grid cells, starting at a depth of 10 m (outside the near-field) to 1 m above the seabed (to avoid inclusion of seabed echoes). Effects of the acoustic deadzone were compensated through the application of methods described by (Ona and Mitson, 1996).

5.3.4 Acoustic density hotspots – a geostatistical approach

In this study, acoustic density hotspots (hereafter referred to as hotspots) are defined as areas with high concentrations of s_A. These hotspots are considered as proxies for areas of higher than average fish densities. Generally, hotspots are identified through the application of a subjective threshold (Nelson and Boots, 2008) which are mostly based on the cumulative distribution function of the data (Bartolino et al., 2011) or defined through a kernel (Kenchington et al., 2014). Here we apply a local, non-linear rule for identifying hotspots (Petitgas et al., 2016). Thresholds are based on the spatial relationship between data points above a cut-off value and those below the cut-off value (Petitgas et al., 2016). Cut-off values are based on local transition probabilities, which can be temporally and spatially variable (Petitgas et al., 2016).

Seven s_A cut-off values (0.01, 10, 50, 100, 200, 400 and 600 m^2 nmi^{-2}), ranked from one to seven, were used. For each of the s_A cut-off values binary indicator sets (1 if above s_A cut-off; 0 if below s_A cut-off) and variograms were generated. The ratio between two indicator variograms of a lower first s_A cut-off value and a higher second s_A cut-off value provides the transition probability of moving from the indicator set defined by the lower s_A cut-off value into the indicator set defined by the higher s_A cut-off value. The variogram ratio is defined over the distance described within the variogram models. If the variogram ratio increases with distance, the indicator set defined by the higher s_A cut-off value tends to be positioned in the central part of the indicator set defined by the lower s_A cut-off value. If the variogram ratio is flat (pure nugget), the data points contained within the indicator set of the higher s_A cut-off value are randomly distributed within the indicator set of the s_A lower cut-off value, the geometries of both indicator sets are spatially uncorrelated (no edge effect). If the s_A cut-off is high, the variograms tend to be described by a pure nugget effect (unstructured data), due to destructuration (Matheron, 1982). The s_A cut-off is defined as the lower value of the pair where no edge effect is observed and above which the residuals are ideally pure nugget. This s_A cut-off value becomes the top cut in the model described in detail by (Rivoirard et al., 2013). Ordinary kriging was used to map the hotspot probabilities and indicator kriging was used to clearly differentiate the hotspots.

Table 5.2 Description of the eleven acoustic school descriptors used as inputs into the robust sparse k-mean clustering algorithm used to define school clusters.

Descriptor	Unit	Definition
		Geometric
Height mean	m	The extent of the school in the vertical direction.
Corrected length	m	The horizontal dimension of the school in the plane of an echogram, corrected for beam geometry.
Corrected thickness	m	The vertical dimension of the school in the plane of an echogram, corrected for beam geometry.
Corrected area	m^2	The cross-sectional area of the school in the plane of the echogram, corrected for beam geometry.
Corrected perimeter	m	The length of the perimeter of the school, in the plane of an echogram, equivalent to the distance around each sample at the edge of the region, corrected for beam geometry.
Image compactness		Indicator of roundness of the school. It is the dimensionless ratio between the squared perimeter of the school and the area of the school. A perfect circular school will have an image compactness of 1.
		Energetic
S_v mean	dB re 1 m^{2}m^{-3}	The mean volume backscattering volume is the sum of the backscattering cross-section divided by the sampling volume.
Corrected MVBS	dB re 1 m^{2}m^{-3}	The mean volume backscattering volume corrected for known beam geometry based on the corrected mean amplitude in the school.
S_v max	dB re 1 m^{2}m^{-3}	S_v max is analogous to S_v mean the maximum S_v value within the school, above the defined minimum threshold and below the minimum threshold.
Skewness		A statistical measure of how skewed the distribution of the samples within the school are.
		Bathymetric
Mean depth	m	Mean depth of the school where depth is the linear distance from the surface along the vessel axis to the centre of the school.

5.3.5 Acoustic school descriptors

A set of eleven school descriptors (six geometric, four energetic (for both frequencies 38 kHz and 120 kHz) and one bathymetric) were extracted for each school from the acoustic data, largely following the methods described in (Campanella and Taylor, 2016) (Table 5.2). The geometric descriptors were mean height (height mean [m]), length (corrected length [m]), area (corrected area [m^2]), perimeter (corrected perimeter [m]) and roundness of the school (Image compactness) (Table 5.2). Energetic descriptors were mean backscattering volume (S_v mean [dB re 1 m^{-1}]), beam geometry corrected S_v mean (corrected MVBS [dB re 1 m^{-1}]),

maximum S_v (S_v max [dB re 1 m^{-1}]) and skewness (skewness) (Table 5.2). The bathymetric descriptor was mean depth of the school (mean depth [m]) (Table 5.2). These descriptors were used to describe the characteristics of the fish schools to categorise them into different clusters.

5.3.6 Clustering

Clustering of acoustically detected fish schools, using school descriptors, was applied to each of the three fishing regions separately, as they were spatially and temporally disconnected. Only schools observed at an altitude of less than 20 m from the seabed were considered. This allowed for improved comparison with biological information and omitted analysis of pelagic fish species. Schools observed during night-time were excluded from clustering as diurnal migration patterns have been observed within the study area (Sven Gastauer et al., 2017). Times of sunrise and sunset within the study area were around 06:00 and 18:00 respectively (S. Gastauer et al., 2017) at the time of data collection.

An unsupervised clustering algorithm, Robust Sparse k-means Clustering (RSKC) (Kondo et al., 2012a), was used to label the different school clusters based on the energetic, geometric and bathymetric descriptors. Ideally, clustered groups should represent biologically meaningful categories, for example, group together species that have similar morphology and which show similarities in their aggregation structure (Campanella and Taylor, 2016). RSKC is a relatively new clustering algorithm which combines the trimmed k-means (Gordaliza, 1991) and the sparse k-means (Witten and Tibshirani, 2010) algorithms, which are both derivatives of the k-means algorithm. The main strength of the RSKC, compared to other k-means algorithms is its robustness against noisy data containing outliers. This is useful for acoustic data where sudden large variations are not uncommon. Maximisation of dissimilarities is based on the squared Euclidean distance, rather than the normal Euclidean distance, giving more weight to points at a greater distance (Kondo et al., 2012a). The algorithm assumes that the dissimilarity between clusters is additive, depending on the contribution of each descriptor. Using the Lasso method (Tibshirani, 1996), a weight w, constrained to a tuning parameter I_1 [1:$\sqrt{N_{features}}$] is attributed to each descriptor in order to maximise the separation of clusters. Here I_1 was kept at a maximum, giving non-zero weights to all descriptors.

Any k-means algorithm requires the number of clusters to be defined *a priori* (Legendre and Legendre, 2012). The number of clusters was selected using the "Clest" algorithm (Dudoit and Fridlyand, 2002; Kondo et al., 2012a). The optimal number of clusters is

based on the maximisation of the predictive power of the model, which is based on random subsamples of the data (random validation was executed 15 times). Validation of the predictive power is based on the Classification Error Rate (CER) (Chipman and Tibshirani, 2006). The accepted optimal number of clusters is obtained through minimisation of the subtraction of the median CER for different numbers of clusters (CER_{Obs}) and the median expected CER under the null hypothesis, where the number of clusters equals one. The expected CER was computed using five different datasets generated through Monte Carlo sampling.

The similarities of the schools and the cluster they were attributed to were tested through revised silhouette values (Rousseeuw, 1987). The revised silhouette plot and value represent a measure of cohesion, i.e. they describe how similar a school is to the cluster it is contained in compared to the other clusters. Revised silhouette values range from -1 to +1, where a value close to +1 has a high similarity with the cluster (Rousseeuw, 1987). The influence of the different descriptors on the clustering was shown through Principal Component Analysis (PCA) (Zuur et al., 2007). The characteristics of the different clusters are illustrated through a parallel coordinate plot (Huh and Park, 2008). Indicator kriging was used to produce maps of the most dominant clusters within the three regions. Catch information was linked with school descriptor clusters through distance minimisation.

5.3.7 Habitat description

To describe the habitat associated with the fish schools, seafloor characteristics were assessed using acoustic techniques. Seabed characteristics were determined based on the scattering properties of the first bottom echo on the recorded echograms. The seabed features exported from Echoview (Echoview Software Pty Ltd, 2015) were bottom depth, bottom roughness, first bottom length, maximum S_v, bottom rise time, skewness and kurtosis (see below for details on each seabed feature). All seabed features, except for bottom depth, which was exported for every ping, were based on intervals of 15 pings to minimise measurement variability (Anderson et al., 2007; Siwabessy et al., 2004b).

Bottom depth was detected using the "best bottom candidate" algorithm in Echoview. The algorithm searches for peaks (i.e. the shallowest detections) within a ping window, containing eight pings in this study. If no peak is found, the average of the peaks in the surrounding ping windows is used. The maxima of the different retained peaks are summed and the highest (i.e. shallowest) value is considered representative of the bottom response for

that ping window. These points are connected to form the final bottom line which is then shifted towards the transducer until the detected value at individual points drops below the discrimination level (-50 dB re m^{-1}). Finally, a backstep of 0.2 m is added.

The first bottom length refers to the total duration of the first bottom echo. Firstly, for a bottom echo to be considered valid, a minimum of three consecutive sample values above a given threshold (here -60 dB re m^{-1}) are required. These consecutive sample values determine the beginning of the first bottom echo (i.e. bottom depth). The end of the first bottom echo is then determined using a bottom echo threshold at 1 m (dB). The first of three consecutive sample values below this threshold indicate the end of the first bottom echo.

Bottom roughness is determined from an integration of the tail energy of the first bottom echo (Chivers et al., 1990; Chivers and Burns, 1992) as it is assumed that the energy contained in the first echo is mainly (Hamilton, 2001) dependent on the bottom roughness. A rough bottom will have an increased, more complex surface and therefore an increased integration interval (longer tail due to the delayed arrival of energy packets at the transducer face), resulting in an increased bottom acoustic roughness index. Smoother seabeds act more like acoustic mirrors, reflecting the incident energy directly to the transducer, resulting in a steep, sharp peak, with a small or no tail.

Kurtosis and skewness describe the shape of the probability distribution of sample values. Kurtosis sometimes referred to as "peakedness", is a measure of the variability in sample values in the first bottom echo and is defined by the "tailedness" of the data. This means that the higher the kurtosis, the higher the proportion of variance which is explained by extreme deviations. Skewness describes the asymmetry, i.e. how unbalanced the sample values are, or how the distribution of sample values deviates from a normal distribution towards either tail.

Maximum S_v is the maximum energy reflected by the bottom and can, to a certain extent, be considered as a proxy for density. For example, a dense substrate such as bedrock is likely to reflect more energy than a less dense substrate like sand and therefore have a higher maximum S_v.

Bottom rise time is the rise time of the first bottom echo in the integration interval. Bottom rise time is mainly influenced by sudden drops or rises of the seabed.

Maps of the different seabed descriptors were generated using ordinary kriging. Seabed types were defined and classified using PCA analysis with k-means clustering. The ideal number of clusters (k) was determined using a combination of the Hubert score (Hubert and Arabie, 1985), D-Index (Lebart et al., 2000) and Weighted Sum of Squares (WSS) (Hothorn and Everitt, 2014). For WSS, the number of clusters was determined through comparison of WSS against the number of clusters. The ideal number of clusters was located where WSS was minimised or a larger number of clusters contributed very little to the minimisation of WSS (Hothorn and Everitt, 2014). For the Hubert score (correlation coefficient between two matrices) (Hubert and Arabie, 1985) and the D-index (Lebart et al., 2000), a knee point, that corresponds to a significant increase of the measurement value was identified. The final number of clusters was defined through the majority rule, where the most frequently detected ideal number of clusters was accepted as the final number. Maps of the resulting seabed clusters were produced using indicator kriging.

The clusters were related to biological information (derived from catch data) through indicator species analysis (De Cáceres et al., 2012), where the nine species groups were treated as potential indicators. Significance of the relationship was tested through a permutation test (Dufrêne and Legendre, 1997). Indicator values are a statistical tool used to define which species can be seen as indicators of a given cluster (Dufrêne and Legendre, 1997) or a group of habitat clusters (De Cáceres et al., 2010). A significant benefit of the indicator values approach is that it combines mean abundance and occurrence frequencies of a given species within a cluster (Cáceres and Legendre, 2009; De Cáceres et al., 2010; Dufrêne and Legendre, 1997; Legendre and Legendre, 2012). Indicator values are a combination of two components called A and B (Legendre and Legendre, 2012). A is the probability that a given cluster belongs to the target cluster, since the selected species group was detected (also known as specificity or positive predictive value). B is the fidelity or sensitivity, which is the probability of encountering the species group within a given cluster (Legendre and Legendre, 2012). In order to assess the validity of indicator species for a given cluster, proportion coverage was computed (De Cáceres et al., 2012). Proportion coverage or quantity coverage is the proportion of sites where one of the indicators is found (De Cáceres et al., 2012).
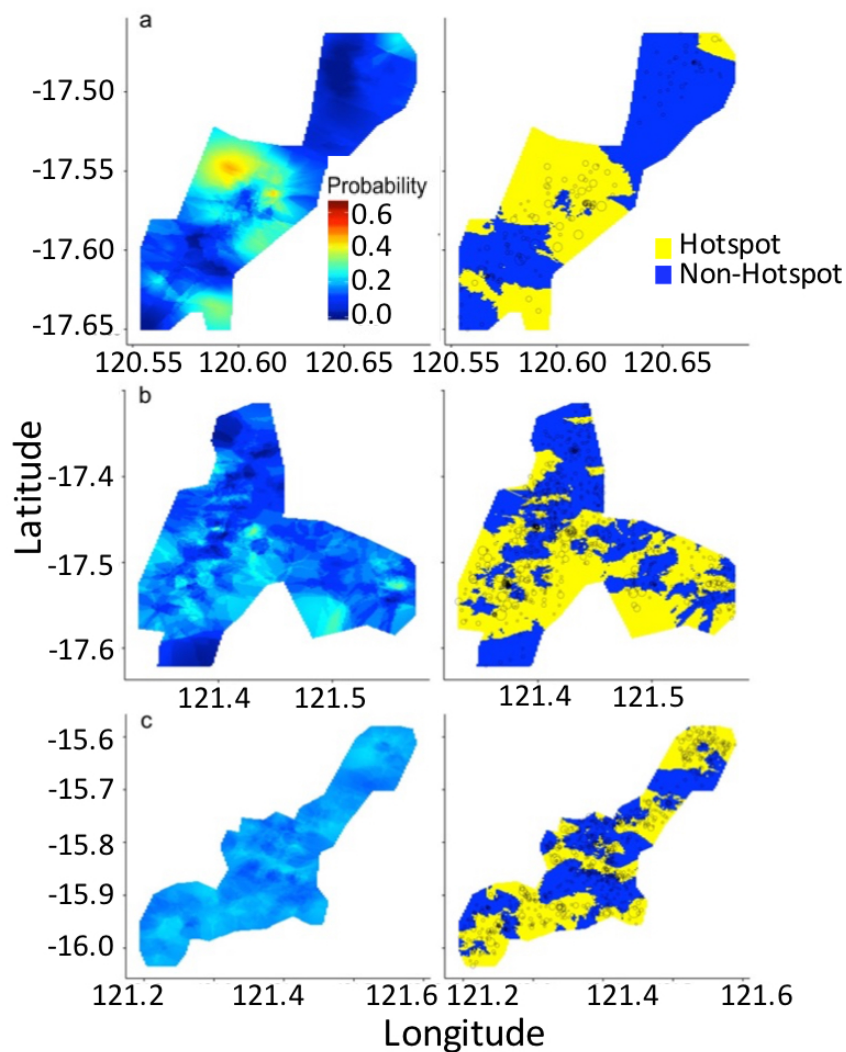
Figure 5.2 Geostatistical hotspots of acoustic density within the three regions (a = Region 1, b = Region 2, c = Region 3), with the probability maps on the left and the identified hotspots on the right (light = hotspot, dark = no hotspot), relative s_A is indicated by size of black circles

5.4 Results

5.4.1 Acoustic hotspots

The highest mean s_A of 73.6 m^2 nmi^{-2} (standard deviation (s.d.) 228.24 m^2 nmi^{-2}) and highest percentage of zero values (50.9%) were observed in Region 2. Lower mean s_A were observed in Region 1 (54.0 m^2 nmi^{-2}, s.d. 120.5 m^2 nmi^{-2}) and Region 3 (51.8 m^2 nmi^{-2}, s.d. 165.7 m^2 nmi^{-2}). Region 3 had a percentage of zero values (45.2%) comparable to Region 2, whilst this percentage was much lower in Region 1 (25.2%). Within Region 1 and Region 2 the s_A cut-off value was 100 m^2 nmi^{-2} which corresponded to the fourth hotspot indicator value. In Region 3, the region with the lowest mean s_A, the s_A cut-off value was detected at the third hotspot indicator value with an s_A cut-off of 50 m^2 nmi^{-2}. In all three regions about half of the total

areas were identified as hotspots (44% in Region 1, 52% in Region 2 and 51% in Region 3). The hotspot indicator, in all regions, was the last structured indicator defined by the selected s_A cut-off. For higher s_A cut-offs no structure was detected and the variograms were described by a pure nugget. Hotspots were patchily distributed in the three regions (Figure 5.2). The central part of Region 1 contained the main density hotspot with smaller patches observed in the north and south of the region (Figure 5.2a). In Region 2, hotspots were mainly concentrated in the south of the region whilst they were largely absent in the north (Figure 5.2b). In Region 3 hotspots were distributed as patches throughout the region (Figure 5.2c).

Table 5.3 Results of the Clest algorithm which identified three as the optimal number of school clusters (bold row), with k = number of clusters, d_k = test statistic, CER_{obs} and CER_{ref} = observational and reference Classification Error Rates respectively, p = probability of the absolute CER being higher than the CER under the null hypothesis.

k	Region 1				Region 2				Region 3			
	d_k	CER_{obs}	CER_{ref}	p	d_k	CER_{obs}	CER_{ref}	p	d_k	CER_{obs}	CER_{ref}	p
2	**-0.31**	**0.03**	**0.34**	**0.00**	0.17	0.24	0.06	1.00	**-0.08**	**0.08**	**0.15**	**0.00**
3	-0.07	0.24	0.30	0.00	0.21	0.34	0.13	1.00	-0.09	0.16	0.25	0.20
4	0.04	0.13	0.09	0.80	0.00	0.20	0.21	0.40	0.07	0.27	0.20	1.00
5	0.00	0.18	0.18	0.40	**-0.05**	**0.12**	**0.17**	**0.00**	-0.02	0.17	0.18	0.20
6	-0.01	0.16	0.17	0.20	-0.03	0.11	0.14	0.20	-0.01	0.15	0.17	0.20
7	0.01	0.16	0.15	0.80	0.00	0.12	0.13	0.40	0.01	0.15	0.14	0.60
8	0.01	0.17	0.15	0.60	0.00	0.11	0.12	0.60	0.02	0.14	0.12	1.00
9	0.04	0.17	0.12	1.00	0.00	0.11	0.11	0.60	0.01	0.13	0.11	0.80

5.4.2 Acoustic school descriptors

The optimal number of clusters determined by the Clest algorithm was two in Regions 1 and 3, and five in Region 2 (Table 5.3). The median observed Classification Error Rate (CER_{Obs}) was low in all three regions (0.03, 0.12 and 0.08 in Regions 1, 2, and 3, respectively; Table 5.3). During clustering, the energetic descriptors were the most important for all clusters in all three regions (Figure 5.3, Table 5.4).

The first two principal components of the PCA explained 63.9% of the variation contained within the data in Region 1; 66.0% in Region 2 and 66.2% in Region 3 (Figure 5.3). Principal component 1 (PC1) accounted for 44.5% of the variance in Region 1, 50.9% in Region 2 and 44.3% in Region 3. PC1 was predominantly driven by the energetic descriptors (Table 5.4). Principal component 2 (PC2) explained 19.4% of the total variance in Region 1, 15.1% in Region 2 and 21.9% in Region 3 and was mainly influenced by geometric features (Table 5.4, Figure 5.3). All three clusters were mainly separated by PC1, hence mostly determined by

energetic features. High agreement was found in Regions 1 and 3 with average silhouette values of 0.83 and 0.71, respectively (Figure 5.4). The highest agreement was found for Cluster 1 in Region 1, with a silhouette value of 0.89. In Region 2, moderate to high agreement was found, with an average silhouette value of 0.57. The highest agreement in Region 2 was found for Cluster 2 with a silhouette value of 0.70 and lowest for Cluster 4 (0.44) (Figure 5.4).
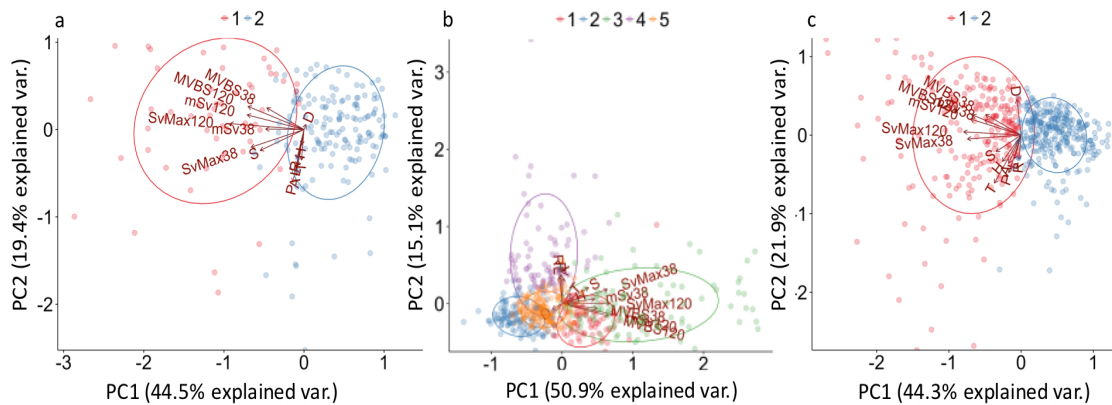
Figure 5.3 Biplot of the first (PC1) and second (PC2) principal components of the school clusters with circles indicating the 68% confidence intervals of the clusters obtained from Robust Sparse k-means clustering for the three regions (a, b, c), with an indication of the pulling direction of the school descriptors, where mSv38 = mean Sv at 38 kHz, mSv120 = mean Sv at 120 kHz, SvMax38 = Maximum Sv at 38 kHz, SvMax120 = Maximum Sv at 120 kHz, MVBS38 = Corrected Sv at 38 kHz, MVBS120 = Corrected Sv at 120 kHz, H = Height, S = Skewness, L = Length, R = Image compactness, P = Perimeter, T = Thickness, A =Area, D = Depth

Table 5.4 Weights of the descriptors within the robust sparse k-means clustering (RSKM weights) defining the school clusters and contributions to the first (PC1) and second (PC2) components of the Principal Component Analysis.

	Region 1			Region 2			Region 3		
	RSKM weights	PC1	PC2	RSKM weights	PC1	PC2	RSKM weights	PC1	PC2
Sv_{mean38}	0.08	-0.27	0.00	0.48	0.29	0.07	0.31	-0.29	0.16
$Sv_{mean120}$	0.47	-0.40	0.15	0.32	0.46	-0.16	0.42	-0.40	0.17
Sv_{max38}	0.19	-0.38	-0.17	0.40	0.40	0.21	0.48	-0.43	-0.04
Sv_{max120}	0.72	-0.53	0.06	0.25	0.43	0.00	0.41	-0.46	0.03
$MVBS_{38}$	0.11	-0.26	0.22	0.44	0.31	-0.07	0.29	-0.28	0.21
$MVBS_{120}$	0.33	-0.40	0.23	0.30	0.42	-0.18	0.36	-0.39	0.21
Height	0.00	-0.02	-0.15	0.02	0.10	0.07	0.21	-0.15	-0.27
Skewness	0.31	-0.31	-0.21	0.06	0.24	0.24	0.14	-0.20	-0.17
Length	0.00	-0.05	-0.36	0.26	-0.02	0.41	0.01	-0.05	-0.24
Image compactness	0.00	-0.05	-0.29	0.26	-0.03	0.53	0.00	-0.02	-0.25
Perimeter	0.00	-0.08	-0.52	0.11	-0.01	0.44	0.04	-0.10	-0.39
Thickness	0.00	-0.02	-0.30	0.01	0.08	0.15	0.24	-0.21	-0.50
Area	0.00	-0.06	-0.45	0.01	0.01	0.38	0.03	-0.10	-0.29
Depth	0.00	0.01	0.05	0.01	-0.09	-0.09	0.00	-0.03	0.37
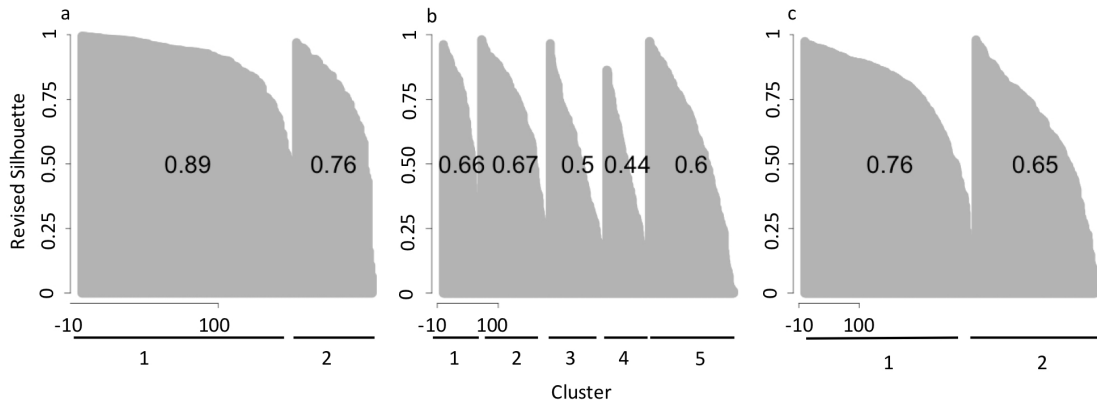
Figure 5.5 Revised silhouette plot for the three regions (a, b, c), where each silhouette represents one cluster, composed of single lines, each representing a school. The y axis represents the revised silhouette value and the printed values are the mean revised silhouette value for each cluster
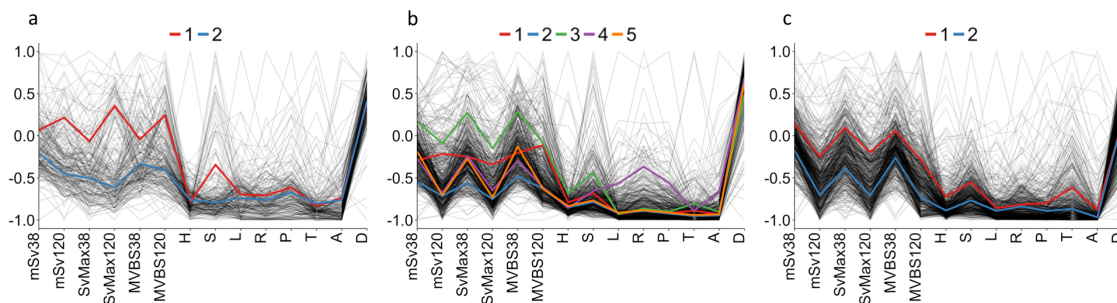
Figure 5.4 Parallel coordinate plot of the descriptors considered in the Robust Sparse k-means clustering for the three regions (a, b, c), with scaled values on the y-axis. Each thin line represents one school and the thick, coloured lines represent the scaled mean descriptor value of each cluster, , where mSv38 = mean Sv at 38 kHz, mSv120 = mean Sv at 120 kHz, SvMax38 = Maximum Sv at 38 kHz, SvMax120 = Maximum Sv at 120 kHz, MVBS38 = Corrected Sv at 38 kHz, MVBS120 = Corrected Sv at 120 kHz, H = Height, S = Skewness, L = Length, R = Image compactness, P = Perimeter, T = Thickness, A =Area, D = Depth

Given the high influence of the energetic descriptors on the cluster separation, the clusters can best be described by mean, max S_v and MVBS at 38 and 120 kHz (Figure 5.5, Table 5.4). In Regions 1 and 3, clustering largely followed the same trends, with Cluster 1 being considered a high-energy cluster, whilst Cluster 2 was regarded as a moderate to low energy cluster (Figure 5.5). In Region 3, schools within Cluster 1 were generally found to occupy a much larger area, with a slightly greater thickness, a larger perimeter and of marginally greater height (Figure 5.5, Table 5.5).

In Region 2, one high energy cluster (Cluster 3) and one low energy cluster (Cluster 2) could be identified (Figure 5.5, Table 5.4). Clusters 1, 4 and 5 were considered moderate energy clusters, with Cluster 1 mainly differentiated through higher energetic values at 120 kHz (Figure 5.5, Table 5.4). Cluster 4 was mainly separated from other clusters due to more elongated and larger schools, with a larger perimeter (Figure 5.5, Table 5.4).

Table 5.5 Summary of the mean, and standard deviation (s.d.) of the considered descriptors within each cluster and region.

Region	Cluster		Sv_{mean} 38	Sv_{mean} 120	Sv_{max} 38	Sv_{max} 120	MVBS 38	MVBS 120	Height	Skewness	Length	Image	Perimeter	Thickness	Area	Depth
1	1	mean	-50.15	-48.63	-36.69	-27.41	-47.62	-47.06	1.33	7.26	24.55	15.20	70.89	3.00	33.53	121.65
		sd	3.33	5.13	6.31	6.76	5.07	5.47	0.64	5.28	21.51	14.64	60.09	2.16	39.98	2.31
	2	mean	-52.66	-60.13	-43.06	-49.88	-51.09	-58.24	1.44	3.05	21.70	12.53	61.40	3.30	30.82	121.84
		sd	2.34	2.94	3.72	4.34	3.87	4.71	0.88	1.82	17.02	9.76	46.54	3.45	34.80	3.44
2	1	mean	-50.08	-58.22	-41.27	-48.64	-48.98	-56.72	1.24	2.87	15.90	10.02	42.25	2.14	18.40	83.14
		sd	1.36	2.68	2.56	3.86	2.33	5.35	0.99	1.36	10.46	7.78	34.73	2.36	24.26	3.19
	2	mean	-53.38	-65.68	-46.57	-58.47	-52.85	-66.15	1.01	2.01	17.69	9.47	40.45	1.51	15.19	83.30
		sd	1.58	2.47	2.49	3.26	2.21	3.79	0.26	0.95	12.42	7.28	26.50	0.63	11.20	3.31
	3	mean	-44.05	-56.33	-32.46	-44.06	-42.13	-56.19	1.70	4.88	16.02	11.20	50.16	2.99	25.18	79.27
		sd	2.79	7.22	5.15	10.65	3.10	7.45	1.14	3.60	15.23	11.18	46.15	2.68	33.80	7.89
	4	mean	-49.80	-65.20	-41.13	-55.97	-50.24	-65.85	0.97	3.12	87.46	46.61	200.11	2.11	81.38	82.88
		sd	2.00	2.54	2.66	4.32	2.36	2.52	0.27	2.55	58.48	23.87	126.42	1.09	77.63	2.85
	5	mean	-48.67	-65.56	-41.69	-58.05	-47.93	-66.19	1.08	2.16	19.23	9.93	44.94	1.62	18.12	81.97
		sd	1.41	2.01	2.33	3.00	2.31	2.15	0.39	1.28	13.42	6.43	30.33	0.71	17.49	4.36
3	1	mean	-46.42	-58.12	-34.01	-44.56	-45.30	-57.26	2.77	4.54	35.42	21.31	152.11	6.97	143.78	83.75
		sd	2.75	4.51	4.05	6.78	3.67	5.58	2.54	2.36	44.42	22.62	213.02	6.36	333.89	6.38
	2	mean	-50.17	-65.28	-41.44	-55.86	-49.72	-65.25	1.39	2.65	27.94	18.82	85.82	3.05	41.60	83.84
		sd	2.35	2.74	3.27	3.75	3.04	3.70	0.66	1.40	38.82	21.55	116.03	2.20	94.97	5.61

The percentage of traps taken and the percentage of schools observed, generally agreed well (Table 5.6). In Region 1, the low-energy Cluster 2 was dominant in terms of area coverage (76.8%) (Figure 5.6), amount of schools (73.6%) and traps (66.0%) (Table 5.6). In Region 2, almost half of the area was dominated by the high-energy Cluster 3 (49.2%) (Figure 5.6), encompassing 19.4% of the observed schools and 37.7% of the recorded traps within this region (Table 5.6). In Region 3, the two clusters were more evenly spread, with 52.4% of the area covered by the high-energy Cluster 1 (Figure 5.6) (55.6% of the traps, 41.1% of the schools) (Table 5.6).
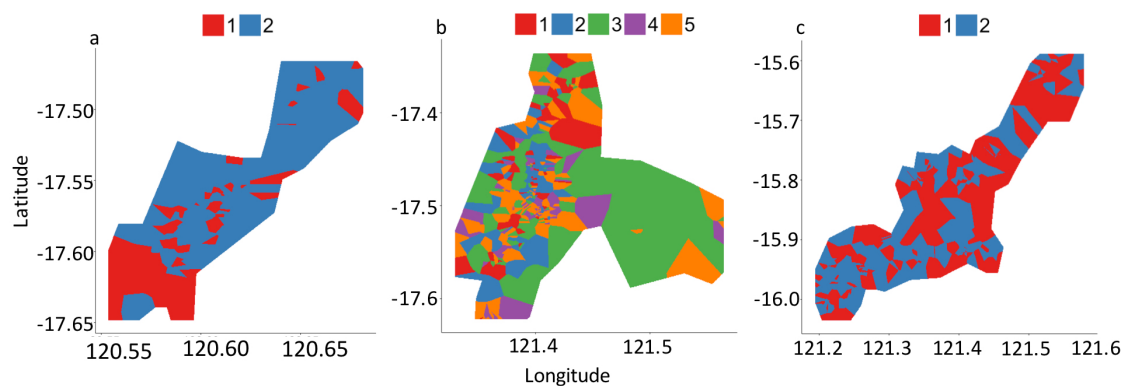
Figure 5.6 Indicator kriging maps of the occurrence of the school clusters in the three regions (a, b, c)

Table 5.6 Total number of eligible acoustic schools and number of traps recorded in each region with the percentage of the area (% area) of dominance of the school clusters and percentage of traps (% traps) taken within each cluster for the three regions.

Region	$N_{schools}$	N_{traps}	Cluster	% area	% traps
1	212	209	1	28.2	34.0
			2	76.8	66.0
2	525	584	1	10.5	12.0
			2	12.9	16.0
			3	49.2	37.7
			4	8.8	10.8
			5	18.7	23.5
3	530	604	1	52.4	55.6
			2	47.6	44.4

Indicator species could be detected for some of the school clusters at a significance level of 5% (Table 5.7). No significant indicator species could be detected for Cluster 2 in Region 1 and Clusters 4 and 5 in Region 2. In general, high *A* values were observed (up to 0.86), while *B* values remained low (<0.45 except for Cod in Cluster 1, Region 3, where *B* = 0.60)

Table 5.7 Indicator species groups associated with the respective school cluster within the three selected regions with the corresponding indicator value (indval), the p-value (p) and the indicator variable A and B

Region	School cluster	Species	indval	*p*	*A*	*B*
1	1	Triggerfish	0.29	0.02	0.86	0.10
		Misc+Triggerfish	0.25	0.02	0.88	0.07
		Goldband+Triggerfish	0.25	0.09	0.84	0.07
2	1	Lutjanid	0.37	0.04	0.31	0.45
	2	Rankin	0.34	0.05	0.27	0.41
		Rankin+Red.Emperor	0.33	0.01	0.32	0.34
		Rankin+Red.Emperor+Triggerfish	0.32	0.00	0.43	0.23
		Rankin+Triggerfish	0.31	0.01	0.38	0.26
		Misc+Rankin+Red.Emperor	0.21	0.04	0.48	0.09
		Misc+Rankin+Triggerfish	0.20	0.03	0.54	0.08
		Rankin+Cod+Triggerfish	0.20	0.01	0.53	0.08
	3	Lethrinid	0.35	0.01	0.33	0.38
		Lethrinid+Red.Emperor	0.34	0.01	0.38	0.31
		Lethrinid+Red.Emperor+Triggerfish	0.26	0.04	0.36	0.19
	5	Rankin+Cod+Saddletail	0.15	0.07	1.00	0.02
3	1	Cod	0.59	0.02	0.58	0.60
		Lutjanid+Misc+Cod	0.29	0.05	0.62	0.13
	2	Goldband+Red.Emperor+Triggerfish	0.26	0.03	0.68	0.10
		Goldband+Saddletail	0.24	0.04	0.70	0.08
		Goldband+Lutjanid+Triggerfish	0.23	0.04	0.66	0.08
		Goldband+Red.Emperor+Saddletail	0.23	0.01	0.74	0.07
		Goldband+Saddletail+Triggerfish	0.14	0.04	0.88	0.02

(Table 5.7). If considering only one species group, Triggerfish were the only indicator species group for Cluster 1 in Region 1. In Region 2, Lutjanids were detected as an indicator species for Cluster 1, Rankin Cod for Cluster 2 and Lethrinids for Cluster 3 (Table 5.7). In Region 3, Cod was detected as an indicator species, while no singular indicator species could be detected for Cluster 2 (Table 5.7). If a combination of up to three species groups was accepted, combinations of Misc, Goldband and Lutjanids with Triggerfish were detected as indicator species (Table 5.7). In Region 2, for Cluster 2, various combinations including Miscellaneous,

Rankin Cod, Red Emperor, Cod and Triggerfish were obtained (Table 5.7). For Cluster 3, Lethrinids and/or Red Emperor, with or without Triggerfish were accepted as indicator species groups. In Region 3, for Cluster 1 a combination of 1) Lutjanids, Miscellaneous and Cod were considered indicative and combinations of Goldband with 2) Red Emperor and Triggerfish; 3) Saddletail, Lutjanids and Triggerfish; 4) Red Emperor and Saddletail or 5) Saddletail and Triggerfish for Cluster 2 (Table 5.7).

5.4.3 Habitat description

Region 1 was the deepest (120-130 m) of the three regions throughout, while Region 2 was the shallowest (61-90m) (Figure 5.7, Table 5.1). In Region 1 the deepest parts were observed in the north, gradually decreasing south- and eastwards (Figure 5.7). Within Region 2 the deeper areas were in the west getting shallower towards the east, while in Region 3 the deepest part was found in the central area (Figure 5.7b and 6c respectively). Regions 2 and 3 showed similar roughness indices with values over 7 for the majority of the areas (Figure 5.8b and 7c respectively). Region 3 contained only a small channel of less rough seabed in the central part (Figure 5.8c). Region 1 appeared to be less rough with maximum roughness values of around 7.5 (Figure 5.8a). First bottom length and maximum S_v showed similar trends and distributions of patches to bottom roughness with lowest values of each seabed feature observed throughout Region 1. Maps for bottom skewness and kurtosis were almost identical to one another for the three regions (Figure 5.9). Like the other seabed features the lowest values for skewness and kurtosis were observed in Region 1 and similar values, with well defined, patchy hotspots found in Region 2 and 3 (Figure 5.9).

According to the majority rule, the ideal number of clusters for the bottom classification within the three regions was three. The first two principal components (PC1 and PC2) of the PCA explained 73.9% of the variance (Figure 5.10). PC1 (explained 46.6% of variance) caused separation between the three clusters with some overlap found between Cluster 1 and Cluster 2. PC2 increased the difference between Cluster 1 and Cluster 2 as well as removing the overlap between Cluster 2 and Cluster 3 (Figure 5.10). Cluster 1 mainly occurred at greater depths, in areas with low roughness, first bottom length, bottom rise time, maximum S_v, kurtosis and skewness (Figure 5.11). In short, Cluster 1 describes a deep, smooth seabed. Cluster 2 was predominantly characterised by high levels of roughness and maximum S_v, but low bottom rise time, skewness and kurtosis (Figure 5.11). This suggests that Cluster 2 describes a rough bottom with low variance within the sample values. Cluster 3 contained high

levels of all descriptors except for depth (Figure 5.11). Cluster 3 describes a rough, complex bottom, with high inter-sample variance.
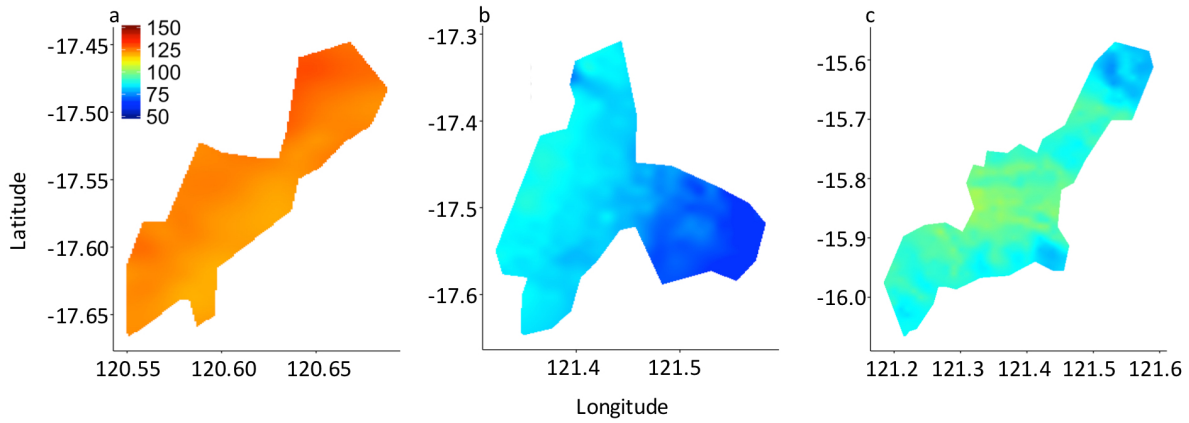
Figure 5.9 Kriged bottom depth maps for the three regions (a, b, c)
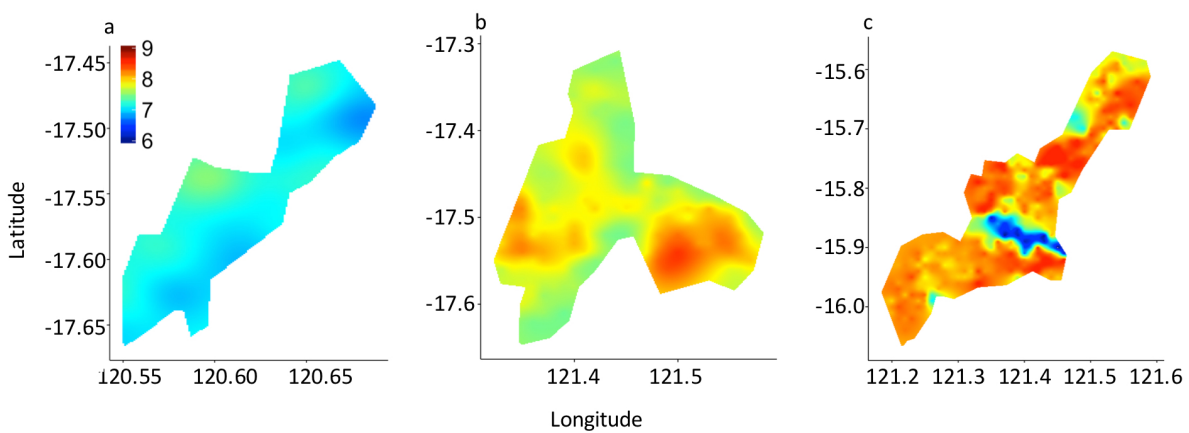
Figure 5.8 Kriged bottom roughness maps for the three regions (a, b, c)
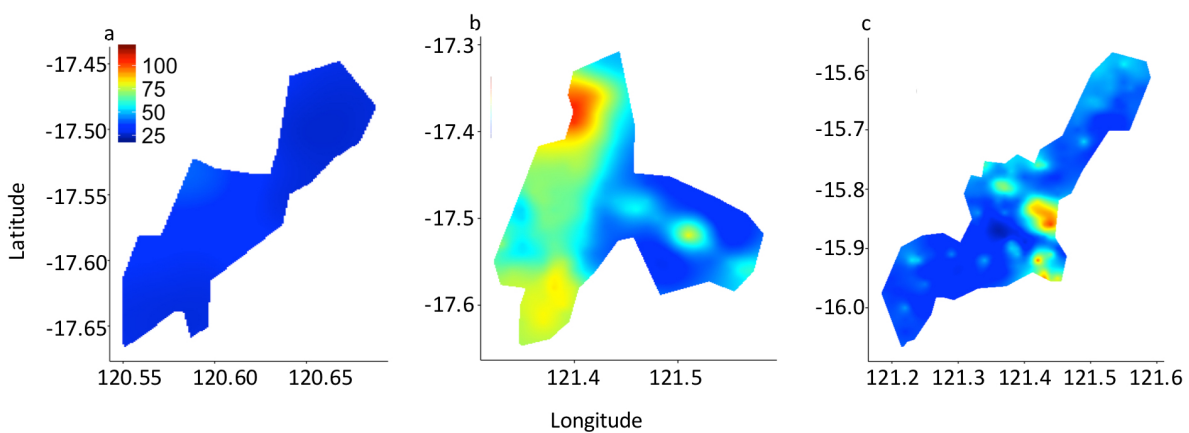
Figure 5.7 Kriged bottom kurtosis maps for the three regions (a, b, c)

In Region 1, only Cluster 1 was found (Figure 5.12a). Almost half of the area of Region 2 was attributed to Cluster 2 (53.4%) and the other half to Cluster 3 (46.6%) (Figure 5.12b). Region 3 contained all three clusters, but was strongly dominated by Cluster 2 (85.6%), with some small areas identified as Cluster 3 (7.8%) and a smaller proportion of the area attributed to Cluster 1 (6.7%) (Figure 5.12c).

If only one species group is considered as an indicator species group at a time, Goldband snapper and the Miscellaneous group was identified as an indicator species group for habitat Cluster 1. Four groups were considered indicator species groups in Cluster 2 (Lethrinids, Red Emperor, Cods and Lutjanids) and two indicator species groups were identified within Cluster 3 (Triggerfish and Rankin Cod). If a combination of up to three species groups are considered, 129 species group combinations present in the data, could be tested. Sixty-nine combinations, each containing up to three species groups were significantly detected as indicator species groups for one of the three habitat clusters. A summary of the most relevant indicator species groups ($A > 0.5$, $B > 0.2$, indicator values > 0.3, $p < 0.01$) can be found in Table 5.8.
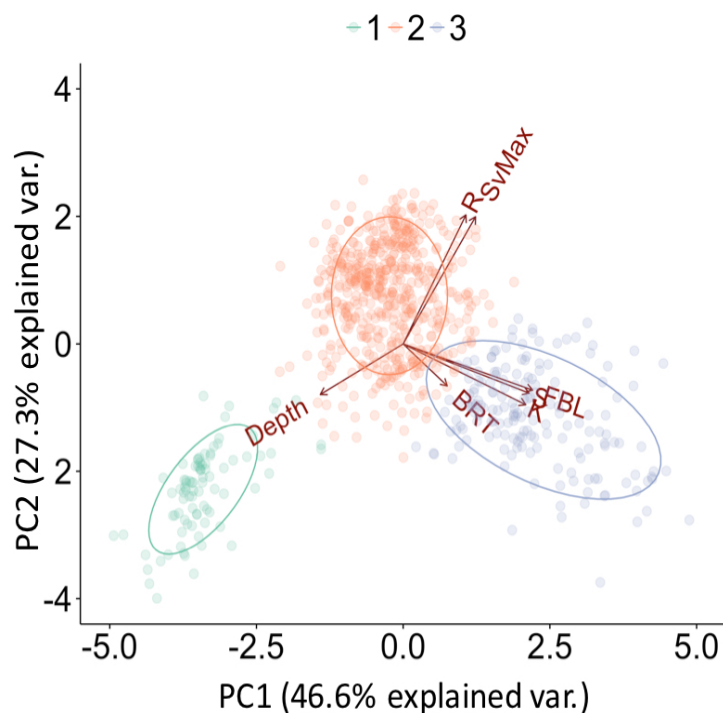
Figure 5.10 Biplot of the first (PC1) and second (PC2) principal components of the bottom clusters, with Depth = Depth, BRT = Bottom Rise Time, K = Kurtosis, S = Skewness, FBL = First Bottom Length, SvMax = Maximum Sv, R = Roughness. with circles indicating the 68% confidence intervals of the clusters obtained from k-means clustering
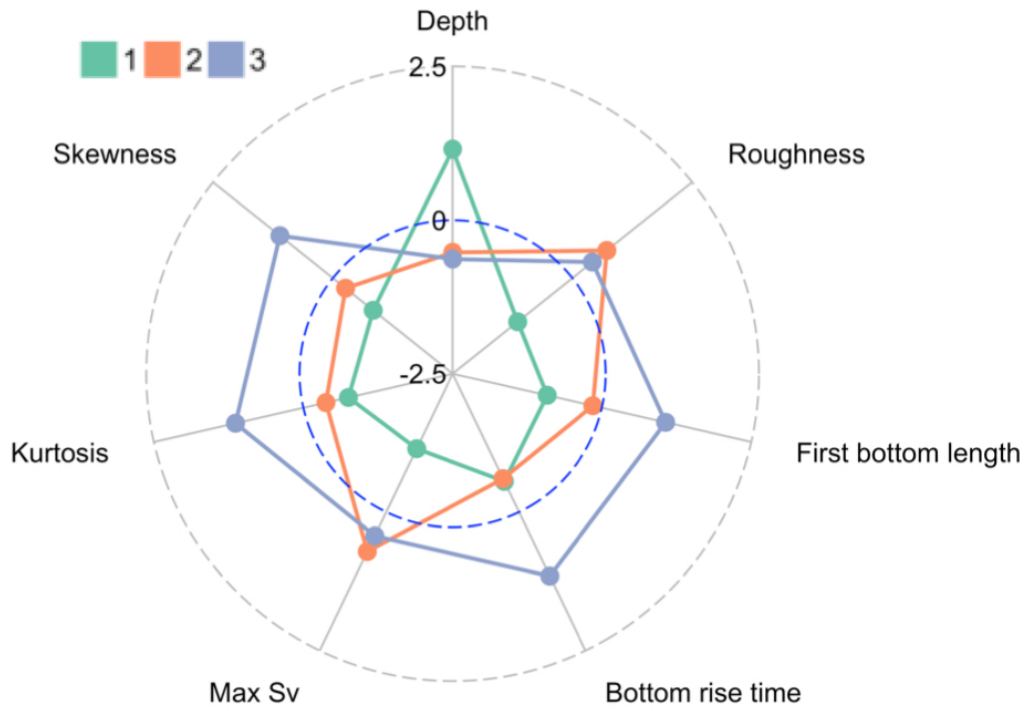
Figure 5.11 Radial plot highlighting the mean value of the bottom descriptors scaled around its own mean for the three bottom clusters, identified by colours.

Figure 5.12 Indicator kriging maps of the three bottom clusters within the three regions.
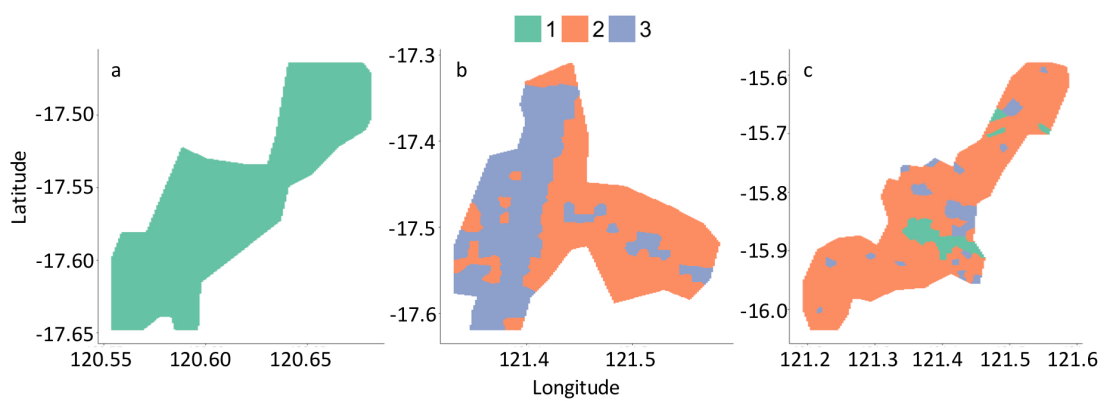
Table 5.8 Most relevant indicator species groups, composed of up to three species groups, with a probability (p) < 0.01, an indicator value (indval) > 0.3, an A value > 0.5 and a B value > 0.2 for the three acoustic habitat clusters.

Seabed Cluster	Species group	indval	p	A	B
1	Goldband	0.75	<0.01	0.76	0.73
	Goldband + Lutjanid	0.35	<0.01	0.56	0.22
	Goldband + Misc	0.43	<0.01	0.76	0.25
	Misc	0.44	<0.01	0.55	0.36
2	Cod	0.52	<0.01	0.62	0.45
	Cod +Red Emperor	0.42	<0.01	0.59	0.29
	Lethrinid	0.54	<0.01	0.64	0.45
	Lethrinid + Cod	0.38	<0.01	0.63	0.23
	Lethrinid + Lutjanid	0.44	<0.01	0.73	0.27
	Lethrinid + Red Emperor	0.43	<0.01	0.60	0.32
	Lutjanid	0.50	<0.01	0.48	0.51
	Lutjanid + Cod	0.40	<0.01	0.61	0.26
	Lutjanid + Red Emperor	0.40	<0.01	0.50	0.32
	Red Emperor	0.53	<0.01	0.45	0.62
3	Goldband + Red Emperor	0.32	<0.01	0.47	0.22
	Rankin	0.39	<0.01	0.50	0.31
	Rankin + Red Emperor	0.34	<0.01	0.52	0.23
	Red Emperor + Triggerfish	0.34	<0.01	0.47	0.25
	Triggerfish	0.51	<0.01	0.56	0.47

5.5 Discussion

The concept of hotspots is an important part of conservation and spatial management strategies (Nelson and Boots, 2008). As acoustic data can be collected over large areas in short time periods, acoustics are a valuable method for detecting hotspots (Petitgas et al., 2016) within large survey areas (Trenkel et al., 2011). Here, it was shown that within the three fishing regions examined the acoustic density hotspots of fish aggregations could be identified. The identification of acoustic hotspots is a relatively easy metric to extract from acoustic data. If this data was repeatedly (e.g. seasonally or annually) collected over very large areas it would be possible to track differences in the spatial structure of fish in the area (Petitgas et al., 2016).

Almost half of the areas in the three regions were considered hotspots, which is unsurprising given they represent fishing regions directly targeted by the fishers. The distribution of acoustic densities revealed that despite the small size of the three fishing regions the distributions of high density areas were patchy rather than uniform. The presence of such spatial structures indicates the presence of different habitat types, which are likely to encompass different organisms with their specific habitat selection criteria (Crowder and Cooper, 1982; Schlosser, 1982). For all three regions, the area of detected hotspots increased for lower s_A cut-off values, an indication for the presence of lower s_A values over significant parts of the regions, i.e. the regions are not solely composed of zero or high s_A values. Region 1 contained the lowest percentage of zero values, and the lowest percentage of hotspots (Figure 5.2, Table 5.1). This suggests that fish schools in Region 1 are distributed more evenly. The main hotspot observed in the central part of the area coincided largely with the area of highest bottom kurtosis and roughness (Figure 5.2, Figure 5.8 and Figure 5.9). In contrast, Region 2 was characterised by the highest mean s_A values and the highest percentage of zero values. Hotspots in Region 2 were patchier compared to Region 1 (Figure 5.2). The seabed descriptor and hotspot maps show that the distribution of hotspots within Region 2 are largely influenced by high bottom roughness (Figure 5.2 and Figure 5.8). This suggests that fish schools are concentrated around the more rugged areas of Regions 1 and 2 (Walker et al., 2009). In coral reef ecosystems, areas of higher roughness are often linked to coral patches, which often have higher species richness and attract more individuals resulting in increased biomass when compared to surrounding areas (Ardron, 2002; Friedlander and Parrish, 1998; Gratwicke and Speight, 2005; Luckhurst and Luckhurst, 1978; Pittman et al., 2007). The distribution of hotspots in Region 3 are patchier than Regions 1 and 2, but at the same time the

differentiation between hotspot areas and non-hotspot areas was not as pronounced in Region 3.

The patchiness of hotspots within such a small area can be seen as an indication for the complexity of the habitat (Walker et al., 2009), at scales smaller than those observed in the clusters. As catches in the NDSF contain a mixture of species, often with similar morphology, the use of traditional acoustic classification methods is not possible (Campanella and Taylor, 2016). Furthermore, the verification of acoustic detections is hindered by the lack of dedicated alternative sampling evidence (Fernandes et al., 2016; Simmonds and MacLennan, 2005). Information obtained from traps typically contains a temporal and spatial lag with the collection of acoustic data. In general the traps are left to soak over a number of hours, whilst the fishing vessel is resting several miles away so not to induce an avoidance behaviour (S. Gastauer et al., 2017; Sven Gastauer et al., 2017). The present study is among the first to describe the acoustic diversity of fish schools within a tropical environment based purely on commercially collected acoustic data.

The acoustic geometric and energetic metrics used in this study are widely used (Cabreira et al., 2009; Campanella and Taylor, 2016; Haralabous and Georgakarakos, 1996; Lawson et al., 2001; Massé et al., 1996; Weill et al., 1993) to classify acoustic targets through ordination techniques or neural networks. Similar to (Campanella and Taylor, 2016), the energetic descriptors contributed more strongly to the classification than the geometric descriptors. Geometric features had less influence on the categorisation of the fish schools (Table 5.3). Geometric descriptors largely followed the trends of the energetic features, but differences were less pronounced (Table 5.5, Figure 5.5). The lack of contribution from the shape related descriptors may be linked to high levels of observed variance (Table 5.5, Figure 5.5). This variability it likely caused by external (e.g. prey-predator interaction, vessel avoidance or fishing pressure) or internal factors (e.g. size distribution or life history traits) which influence the schooling behaviour of the fish (Castillo and Robotham, 2004; Fréon et al., 1992). Furthermore, due to the relatively narrow beam width (38 kHz = 9.6°; 120 kHz = 7°) of the echosounders used, on occasion only the edge of a fish school may have been detected (Korneliussen et al., 2009b; Soria et al., 1996). This error is amplified inversely with depth. Given the smaller beam volume at shallower depths, there is an increased risk of missing parts of a school if the school is occurring in shallow parts of the water column.

The stability of the school descriptor clustering results, given by the Clest algorithm, indicates the presence of patterns (mainly driven by energetic descriptors) that clearly distinguish the three clusters. These may reflect biological patterns, such as species composition (Campanella and Taylor, 2016; Kondo et al., 2012b). Even though significant indicator species groups could be detected for some of the school clusters, the relationships were generally less pronounced than for the habitats. Mainly high A values, indicating a strong association of the given species group with the cluster, could be detected, while B values generally remained low. Low B values are an indication that school compositions of the given clusters are highly variable. For example, in Region 1 for school Cluster 1, if Triggerfish are caught, there is an 86% chance that the surrounding area is dominated by schools of Cluster 1, but if a school which is classified as Cluster 1 is observed, there is only a 10% chance that Triggerfish will be caught. One exception to this pattern is Cod in Region 3. If schools of Cluster 1 are observed in Region 3, there is a 60% chance that Cod will be observed within the catch. Other noteworthy B values were observed for Lutjanids (0.45) and Cluster 1 in Region 2, as well as for Rankin Cod (0.41) and Cluster 2 in the same region. The lack of a clear relationship between the school clusters and species group composition of the catch information, may be an artefact originating from the nature of the data. As previously stated, there is an element of spatial and temporal separation between the detection of fish schools on the echosounder images and the biological sampling process (S. Gastauer et al., 2017). Despite this, it has been demonstrated that distinctive patterns, mainly explained by energetic descriptors, in fish aggregations could be detected (Table 5.5, Figure 5.3, Figure 5.4, Figure 5.5). It is recommended that dedicated simultaneous sampling, such as optical recordings at depth, to complement acoustic recordings should be undertaken (Fernandes et al., 2016; Kloser et al., 2011; Ryan et al., 2009).

The bottom descriptors divided the area into three clusters, within which Cluster 3 (Figure 5.10, Figure 5.11) was mainly driven by depth. To relate these clusters to meaningful measures, require the collection of high resolution physical sampling (e.g. grab samples) (Cutter and Demer, 2013; Siwabessy et al., 2004a). It should be noted that an important component of many bottom classification algorithms is the information contained in the second reflection of the seabed (Anderson et al., 2007; Siwabessy et al., 2004b, 1999). In the present study, information on the second bottom echo, which is used to describe the hardness of the seabed, was unavailable. In broad terms, Cluster 1 and 2 are most likely to represent

sandy bottoms with different degrees of coral or rock cover when compared to maps presented in (Carrigy and Fairbridge, 1954).

The different bottom clusters could be related to indicator species groups. This is a strong indication for habitat selectivity among the different species groups. For Goldband snapper in particular, the high *A* and *B* values within Cluster 1 indicate that the location where Goldband can be found, is likely to be classified within Cluster 1. Furthermore, if the location is categorised as Cluster 1 there is a >70% chance of encountering Goldband. In Cluster 2, indicator species groups were not as prominent, but Lutjanids, Lethrinids and Cod remained strong indicators, with indicator values as well as *A* and *B* values of around 0.5. Similarly, for locations classified within habitat Cluster 3, the chance of encountering Triggerfish is approximately 50%. Once more detailed habitat information has been collected, indicator species can be relatively easily extracted from commercial catch information. The availability of such metrics could help to quickly identify changes in the distribution pattern which might be related to environmental or management changes (Hall and Mainprize, 2004; Link, 2005; Nicholson and Jennings, 2004).

We have shown that acoustic data collected on a small commercial fishing vessel, within a mixed-species environment, can be used to derive meaningful ecological metrics. The methods presented here can be applied to a large variety of environments, but are especially valuable in tropical ecosystems, where complimentary dedicated sampling is often difficult to acquire and the structure of the environment is too complex for currently available acoustic processing techniques. All the metrics used in this study would benefit from long-term data collection programs. If multi-seasonal or multi-annual information from within the same area was available, the metrics would be a useful tool for tracking changes in the ecosystem.

5.6 Acknowledgements

5.7 References

Anderson, J.T., Holliday, V., Kloser, R., Reid, D., Simard, Y., 2007. Acoustic seabed classification of marine physical and biological landscapes. International Council for the Exploration of the Sea.

Ardron, J., 2002. A GIS recipe for determining benthic complexity. Breman J Éditeur Mar. Geogr. GIS Oceans Seas 169–175.

Ballón, M., Bertrand, A., Lebourges-Dhaussy, A., Gutiérrez, M., Ayón, P., Grados, D., Gerlotto, F., 2011. Is there enough zooplankton to feed forage fish populations off Peru? An acoustic (positive) answer. Prog. Oceanogr. 91, 360–381. doi:10.1016/j.pocean.2011.03.001

Barbeaux, S.J., 2012. Scientific acoustic data from commercial fishing vessels: Eastern Bering Sea walleye pollock (*Theragra chalcogramma*) (Ph.D.). University of Washington, United States -- Washington.

Barbeaux, S.J., Horne, J.K., Dorn, M.W., 2013. Characterizing walleye pollock (Theragra chalcogramma) winter distribution from opportunistic acoustic data. ICES J. Mar. Sci. J. Cons. fst052.

Bartolino, V., Maiorano, L., Colloca, F., 2011. A frequency distribution approach to hotspot identification. Popul. Ecol. 53, 351–359. doi:10.1007/s10144-010-0229-2

Bax, N.J., Williams, A., 2001. Seabed habitat on the south-eastern Australian continental shelf: context, vulnerability and monitoring. Mar. Freshw. Res. 52, 491–512.

Cabreira, A.G., Tripode, M., Madirolas, A., 2009. Artificial neural networks for fish-species identification. ICES J. Mar. Sci. J. Cons. 66, 1119–1129. doi:10.1093/icesjms/fsp009

Cáceres, M.D., Legendre, P., 2009. Associations between species and groups of sites: indices and statistical inference. Ecology 90, 3566–3574. doi:10.1890/08-1823.1

Campanella, F., Taylor, J.C., 2016. Investigating acoustic diversity of fish aggregations in coral reef ecosystems from multifrequency fishery sonar surveys. Fish. Res. 181, 63–76. doi:10.1016/j.fishres.2016.03.027

Carrigy, M.A., Fairbridge, R.W., 1954. Recent sedimentation, physiography and structure of the continental shelves of Western Australia. J. R. Soc. West. Aust. 38, 65–95.

Castillo, J., Robotham, H., 2004. Spatial structure and geometry of schools of sardine (Sardinops sagax) in relation to abundance, fishing effort, and catch in northern Chile. ICES J. Mar. Sci. J. Cons. 61, 1113–1119. doi:10.1016/j.icesjms.2004.07.011

Chipman, H., Tibshirani, R., 2006. Hybrid hierarchical clustering with applications to microarray data. Biostatistics 7, 286–301. doi:10.1093/biostatistics/kxj007

Chivers, R.C., Burns, D., 1992. Acoustic surveying of the sea bed. Acoust Bull 17, 5–9.

Chivers, R.C., Emerson, N., Burns, D.R., 1990. New acoustic processing for underway surveying. Hydrogr. J. 56, 9–17.

Collins, W.T., McConnaughey, R.A., 1998. Acoustic classification of the sea floor to address essential fish habitat and marine protected area requirements, in: Proceedings of the Canadian Hydrographic Conference. Citeseer, p. 369e377.

Conti, S.G., Demer, D.A., Soule, M.A., Conti, J.H., 2005. An improved multiple-frequency method for measuring in situ target strengths. ICES J. Mar. Sci. J. Cons. 62, 1636–1646.

Crowder, L.B., Cooper, W.E., 1982. Habitat Structural Complexity and the Interaction Between Bluegills and Their Prey. Ecology 63, 1802–1813. doi:10.2307/1940122

Cutter, G.R., Demer, D.A., 2013. Seabed classification using surface backscattering strength versus acoustic frequency and incidence angle measured with vertical, split-beam echosounders. ICES J. Mar. Sci. J. Cons. fst177. doi:10.1093/icesjms/fst177

Dalen, J., Karp, W.A., 2007. Collection of acoustic data from fishing vessels. International Council for the Exploration of the Sea.

De Cáceres, M., Legendre, P., Moretti, M., 2010. Improving indicator species analysis by combining groups of sites. Oikos 119, 1674–1684. doi:10.1111/j.1600-0706.2010.18334.x

De Cáceres, M., Legendre, P., Wiser, S.K., Brotons, L., 2012. Using species combinations in indicator value analyses. Methods Ecol. Evol. 3, 973–982. doi:10.1111/j.2041-210X.2012.00246.x

De Robertis, A., McKelvey, D.R., Ressler, P.H., 2010. Development and application of an empirical multifrequency method for backscatter classification. Can. J. Fish. Aquat. Sci. 67, 1459–1474.

Demer, D.A., Berger, L., Bernasconi, M., Bethke, E., Boswell, K., Chu, D., Domokos, R., et al., 2015. Calibration of acoustic instruments. ICES Cooperative Research Report No. 326.

Demer, D.A., Soule, M.A., Hewitt, R.P., 1999. A multiple-frequency method for potentially improving the accuracy and precision of in situ target strength measurements. J. Acoust. Soc. Am. 105, 2359–2376.

Dudoit, S., Fridlyand, J., 2002. A prediction-based resampling method for estimating the number of clusters in a dataset. Genome Biol. 3, research0036. doi:10.1186/gb-2002-3-7-research0036

Dufrêne, M., Legendre, P., 1997. Species Assemblages and Indicator Species:the Need for a Flexible Asymmetrical Approach. Ecol. Monogr. 67, 345–366. doi:10.1890/0012-9615(1997)067[0345:SAAIST]2.0.CO;2

Echoview Software Pty Ltd, 2015. Echoview software 6.1.44. Hobart, Australia.

Fässler, S.M., Brunel, T., Gastauer, S., Burggraaf, D., 2016. Acoustic data collected on pelagic fishing vessels throughout an annual cycle: Operational framework, interpretation of observations, and future perspectives. Fish. Res. 178, 39–46.

Fernandes, P.G., 2009. Classification trees for species identification of fish-school echotraces. ICES J. Mar. Sci. J. Cons. 66, 1073–1080. doi:10.1093/icesjms/fsp060

Fernandes, P.G., Copland, P., Garcia, R., Nicosevici, T., Scoulding, B., 2016. Additional evidence for fisheries acoustics: small cameras and angling gear provide tilt angle distributions and other relevant data for mackerel surveys. ICES Journal of Marine Science. doi:10.1093/icesjms/fsw091

Fernandes, P.G., Korneliussen, R.J., Lebourges-Dhaussy, A., Masse, J., Iglesias, M., Diner, N., Ona, E., Knutsen, T., Gajate, J., Ponce, R., 2006. The SIMFAMI project: species identification methods from acoustic multifrequency information. Final Report to the EC No. Q5RS-2001-02054.

Fréon, P., Gerlotto, F., Soria, M., 1992. Changes in school structure according to external stimuli: description and influence on acoustic assessment. Fish. Res. 15, 45–66.

Friedlander, A.M., Parrish, J.D., 1998. Habitat characteristics affecting fish assemblages on a Hawaiian coral reef. J. Exp. Mar. Biol. Ecol. 224, 1–30.

Gastauer, S., Fässler, S.M.M., O'Donnell, C., Høines, Å., Jakobsen, J.A., Krysov, A.I., Smith, L., Tangen, Ø., Anthonypillai, V., Mortensen, E., Armstrong, E., Schaber, M., Scoulding, B., 2016. The distribution of blue whiting west of the British Isles and Ireland. Fish. Res. 183, 32–43. doi:10.1016/j.fishres.2016.05.012

Gastauer, S., Scoulding, B., Parsons, M., 2017. Towards acoustic monitoring of a mixed demersal fishery based on commercial data: the case of the Northern Demersal Scalefish Fishery (Western Australia) - In Review Fisheries Research.

Gastauer, S., Scoulding, B., Parsons, M., 2017. Estimates of variability of goldband snapper target strength and biomass in three fishing regions within the Northern Demersal Scalefish Fishery (Western Australia). Fish. Res. 193, 250–262. doi:10.1016/j.fishres.2017.05.001

Gordaliza, A., 1991. Best approximations to random variables based on trimming procedures. J. Approx. Theory 64, 162–180. doi:10.1016/0021-9045(91)90072-I

Gratwicke, B., Speight, M.R., 2005. The relationship between fish species richness, abundance and habitat complexity in a range of shallow tropical marine habitats. J. Fish Biol. 66, 650–667.

Greenstreet, S.P., Tuck, I.D., Grewar, G.N., Armstrong, E., Reid, D.G., Wright, P.J., 1997. An assessment of the acoustic survey technique, RoxAnn, as a means of mapping seabed habitat. ICES J. Mar. Sci. J. Cons. 54, 939–959.

Hall, S.J., Mainprize, B., 2004. Towards ecosystem-based fisheries management. Fish Fish. 5, 1–20. doi:10.1111/j.1467-2960.2004.00133.x

Hamilton, L.J., 2001. Acoustic seabed classification systems. DTIC Document.

Handegard, N.O., Buisson, L. du, Brehmer, P., Chalmers, S.J., Robertis, A., Huse, G., Kloser, R., Macaulay, G., Maury, O., Ressler, P.H., others, 2013. Towards an acoustic-based coupled observation and modelling system for monitoring and predicting ecosystem dynamics of the open ocean. Fish Fish. 14, 605–615.

Haralabous, J., Georgakarakos, S., 1996. Artificial neural networks as a tool for species identification of fish schools. ICES J. Mar. Sci. J. Cons. 53, 173–180. doi:10.1006/jmsc.1996.0019

Horne, J.K., 2000. Acoustic approaches to remote species identification: a review. Fish. Oceanogr. 9, 356–371.

Hothorn, T., Everitt, B.S., 2014. A handbook of statistical analyses using R. CRC press.

Hubert, L., Arabie, P., 1985. Comparing partitions. J. Classif. 2, 193–218. doi:10.1007/BF01908075

Huh, M.-H., Park, D.Y., 2008. Enhancing parallel coordinate plots. J. Korean Stat. Soc. 37, 129–133. doi:10.1016/j.jkss.2007.10.003

ICES, 2015. Report of the Workshop on scrutinisation procedures for pelagic ecosystem surveys (WKSCRUT). ICES CM 2015/SSGIEOM:18. 103 pp, Hamburg, Germany.

Kenchington, E., Murillo, F.J., Lirette, C., Sacau, M., Koen-Alonso, M., Kenny, A., Ollerhead, N., Wareham, V., Beazley, L., 2014. Kernel Density Surface Modelling as a Means to Identify Significant Concentrations of Vulnerable Marine Ecosystem Indicators. PLOS ONE 9, e109365. doi:10.1371/journal.pone.0109365

Kloser, R.J., Ryan, T., Sakov, P., Williams, A., Koslow, J.A., 2002. Species identification in deep water using multiple acoustic frequencies. Can. J. Fish. Aquat. Sci. 59, 1065–1077. doi:10.1139/f02-076

Kloser, R.J., Ryan, T.E., Macaulay, G.J., Lewis, M.E., 2011. In situ measurements of target strength with optical and model verification: a case study for blue grenadier, Macruronus novaezelandiae. ICES J. Mar. Sci. J. Cons. 68, 1986–1995.

Kloser, R.J., Ryan, T.E., Young, J.W., Lewis, M.E., 2009. Acoustic observations of micronekton fish on the scale of an ocean basin: potential and challenges. ICES J. Mar. Sci. J. Cons. fsp077.

Kondo, Y., Salibian-Barrera, M., Zamar, R., 2012a. A robust and sparse K-means clustering algorithm. ArXiv Prepr. ArXiv12016082.

Kondo, Y., Salibian-Barrera, M., Zamar, R., 2012b. A robust and sparse K-means clustering algorithm. ArXiv Prepr. ArXiv12016082.

Korneliussen, R.J., Diner, N., Ona, E., Berger, L., Fernandes, P.G., 2008. Proposals for the collection of multifrequency acoustic data. ICES J. Mar. Sci. J. Cons. 65, 982–994. doi:10.1093/icesjms/fsn052

Korneliussen, R.J., Heggelund, Y., Eliassen, I.K., Johansen, G.O., 2009a. Acoustic species identification of schooling fish. ICES J. Mar. Sci. J. Cons. 66, 1111–1118.

Korneliussen, R.J., Heggelund, Y., Eliassen, I.K., Øye, O.K., Knutsen, T., Dalen, J., 2009b. Combining multibeam-sonar and multifrequency-echosounder data: examples of the analysis and imaging of large euphausiid schools. ICES J. Mar. Sci. J. Cons. 66, 991–997. doi:10.1093/icesjms/fsp092

Korneliussen, R.J., Heggelund, Y., Macaulay, G.J., Patel, D., Johnsen, E., Eliassen, I.K., 2016. Acoustic identification of marine species using a feature library. Methods Oceanogr., Special section on Novel instrumentation in Oceanography: a dedication to Rob Pinkel 17, 187–205. doi:10.1016/j.mio.2016.09.002

Koslow, J.A., 2009. The role of acoustics in ecosystem-based fishery management. ICES J. Mar. Sci. J. Cons. fsp082.

Lawson, G.L., Barange, M., Fréon, P., 2001. Species identification of pelagic fish schools on the South African continental shelf using acoustic descriptors and ancillary information. ICES J. Mar. Sci. J. Cons. 58, 275–287.

Lazzari, M.A., Tupper, B., 2002. Importance of shallow water habitats for demersal fishes and decapod crustaceans in Penobscot Bay, Maine. Environ. Biol. Fishes 63, 57–66.

Lebart, L.M., Piron, A., Morineau, A., 2000. Statistique exploratoire multidimensionnelle. Dunod.

Legendre, P., Legendre, L.F.J., 2012. Numerical Ecology. Elsevier.

Lezama-Ochoa, A., Ballón, M., Woillez, M., Grados, D., Irigoien, X., Bertrand, A., 2011. Spatial patterns and scale-dependent relationships between macrozooplankton and fish in the Bay of Biscay: an acoustic study. Mar. Ecol. Prog. Ser. 439, 151–168. doi:10.3354/meps09318

Link, J.S., 2005. Translating ecosystem indicators into decision criteria. ICES J. Mar. Sci. 62, 569–576. doi:10.1016/j.icesjms.2004.12.015

Luckhurst, B.E., Luckhurst, K., 1978. Analysis of the influence of substrate variables on coral reef fish communities. Mar. Biol. 49, 317–323.

Maravelias, C.D., 1999. Habitat selection and clustering of a pelagic fish: effects of topography and bathymetry on species dynamics. Can. J. Fish. Aquat. Sci. 56, 437–450.

Massé, J., Koutsikopoulos, C., Patty, W., 1996. The structure and spatial distribution of pelagic fish schools in multispecies clusters: an acoustic study. ICES J. Mar. Sci. J. Cons. 53, 155–160.

Matheron, G., 1982. La déstructuration des hautes teneurs et le krigeage des indicatrices: Internal report N-761. Cent. Géostatistique Ecole Natl. Supér. Mines Paris Fontainebleau.

Melvin, G.D., Kloser, R., Honkalehto, T., 2016. The adaptation of acoustic data from commercial fishing vessels in resource assessment and ecosystem monitoring. Fish. Res. 178, 13–25.

Mitson, R., 2003. Causes and effects of underwater noise on fish abundance estimation. Aquat. Living Resour. 16, 255–263. doi:10.1016/S0990-7440(03)00021-4

Nelson, T.A., Boots, B., 2008. Detecting spatial hot spots in landscape ecology. Ecography 31, 556–566. doi:10.1111/j.0906-7590.2008.05548.x

Nicholson, M.D., Jennings, S., 2004. Testing candidate indicators to support ecosystem-based management: the power of monitoring surveys to detect temporal trends in fish community metrics. ICES J. Mar. Sci. 61, 35–42. doi:10.1016/j.icesjms.2003.09.004

Ona, E., Mitson, R.B., 1996. Acoustic sampling and signal processing near the seabed: the deadzone revisited. ICES J. Mar. Sci. 53, 677–690. doi:10.1006/jmsc.1996.0087

Peña, M., Calise, L., 2016. Use of SDWBA predictions for acoustic volume backscattering and the Self-Organizing Map to discern frequencies identifying Meganyctiphanes norvegica from mesopelagic fish species. Deep Sea Res. Part Oceanogr. Res. Pap. 110, 50–64. doi:10.1016/j.dsr.2016.01.006

Peña, M., Carbonell, A., Tor, A., Alvarez-Berastegui, D., Balbín, R., dos Santos, A., Alemany, F., 2015. Nonlinear ecological processes driving the distribution of marine decapod larvae. Deep Sea Res. Part Oceanogr. Res. Pap. 97, 92–106. doi:10.1016/j.dsr.2014.11.017

Petitgas, P., Woillez, M., Doray, M., Rivoirard, J., 2016. A Geostatistical Definition of Hotspots for Fish Spatial Distributions. Math. Geosci. 48, 65–77.

Pittman, S.J., Christensen, J.D., Caldow, C., Menza, C., Monaco, M.E., 2007. Predictive mapping of fish species richness across shallow-water seascapes in the Caribbean. Ecol. Model. 204, 9–21. doi:10.1016/j.ecolmodel.2006.12.017

Ressler, P.H., Fleischer, G.W., Wespestad, V.G., Harms, J., 2009. Developing acommercial-vessel-based stock assessment survey methodology formonitoring the US west coast widow rockfish (Sebastes entomelas) stock. Fish.Res. 99, 63–73.

Rivoirard, J., Demange, C., Freulon, X., Lécureuil, A., Bellot, N., 2013. A top-cut model for deposits with heavy-tailed grade distribution. Math. Geosci. 45, 967–982.

Rousseeuw, P.J., 1987. Silhouettes: A graphical aid to the interpretation and validation of cluster analysis. J. Comput. Appl. Math. 20, 53–65. doi:10.1016/0377-0427(87)90125-7

Ryan, T.E., Downie, R.A., Kloser, R.J., Keith, G., 2015. Reducing bias due to noise and attenuation in open-ocean echo integration data. ICES J. Mar. Sci. J. Cons. 72, 2482–2493. doi:10.1093/icesjms/fsv121

Ryan, T.E., Kloser, R.J., Macaulay, G.J., 2009. Measurement and visual verification of fish target strength using an acoustic-optical system attached to a trawlnet. ICES J. Mar. Sci. J. Cons. 66, 1238–1244. doi:10.1093/icesjms/fsp122

Schlosser, I.J., 1982. Fish Community Structure and Function along Two Habitat Gradients in a Headwater Stream. Ecol. Monogr. 52, 395–414. doi:10.2307/2937352

Simmonds, J., MacLennan, D.N., 2005. Fisheries acoustics: theory and practice. John Wiley & Sons.

Siwabessy, P.J., Tseng, Y., Gavrilov, A.N., 2004a. Seabed habitat mapping in coastal waters using a normal incident acoustic technique. Parameters 38, 198.864.

Siwabessy, P.J., Tseng, Y., Gavrilov, A.N., Roughness, E.B., Hardness, E.B., 2004b. Seabed habitat mapping in coastal waters using a normal incident acoustic technique. Parameters 38, 198.864.

Siwabessy, P.J.W., Penrose, J.D., Kloser, R.J., Fox, D.R., 1999. Seabed habitat classification, in: Proc. Int. Conf. High-Resolut. Surv. Shallow Water. pp. 1–9.

Soria, M., Fréon, P., Gerlotto, F., 1996. Analysis of vessel influence on spatial behaviour of fish schools using a multi-beam sonar and consequences for biomass estimates by echo-sounder. ICES J. Mar. Sci. J. Cons. 53, 453–458.

Tibshirani, R., 1996. Regression shrinkage and selection via the lasso. J. R. Stat. Soc. Ser. B Methodol. 267–288.

Trenkel, V., Ressler, P.H., Jech, M., Giannoulaki, M., Taylor, C., 2011. Underwater acoustics for ecosystem-based management: state of the science and proposals for ecosystem indicators. Mar. Ecol.-Prog. Ser. 442, 285–301.

Walker, B.K., Jordan, L.K.B., Spieler, R.E., 2009. Relationship of Reef Fish Assemblages and Topographic Complexity on Southeastern Florida Coral Reef Habitats. J. Coast. Res. 39–48. doi:10.2112/SI53-005.1

Weill, A., Scalabrin, C., Diner, N., 1993. MOVIES-B: an acoustic detection description software. Application to shoal species' classification. Aquat. Living Resour. 6, 255–267.

Witten, D.M., Tibshirani, R., 2010. A Framework for Feature Selection in Clustering. J. Am. Stat. Assoc. 105, 713–726. doi:10.1198/jasa.2010.tm09415

Woillez, M., Poulard, J.-C., Rivoirard, J., Petitgas, P., Bez, N., 2007. Indices for capturing spatial patterns and their evolution in time, with application to European hake (Merluccius

merluccius) in the Bay of Biscay. ICES J. Mar. Sci. J. Cons. 64, 537–550. doi:10.1093/icesjms/fsm025

Woillez, M., Ressler, P.H., Wilson, C.D., Horne, J.K., 2012. Multifrequency species classification of acoustic-trawl survey data using semi-supervised learning with class discovery. J. Acoust. Soc. Am. 131, EL184–EL190.

Woillez, M., Rivoirard, J., Petitgas, P., 2009. Notes on survey-based spatial indicators for monitoring fish populations. Aquat. Living Resour. 22, 155–164.

Zuur, A.F., Ieno, E.N., Smith, G.M., 2007. Principal component analysis and redundancy analysis. Anal. Ecol. Data 193–224.

Chapter 6

Discussion

The present thesis aimed at describing the marine ecosystem of selected fishing regions within the Northern Demersal Scalefish Fishery using opportunistically collected acoustic data. This was achieved through the completion of three main sub goals:

- The acoustic scattering properties of key species observed within the studied regions were described through a combination of empirical (*in situ* and *ex situ*) measurements and approximations through KRM modelling (Chapter 2, 3, 4, Gastauer *et al.* (2016, 2017c, 2017a).

- The distribution, abundance and biomass of key species groups and the associated estimates of variance were described through the application of geostatistical techniques to the acoustic data and catch information (Chapter 3, 4, Gastauer *et al.* (2017a, 2017c)).

- Habitat types and characteristics of acoustically observed fish schools were analysed using an unsupervised modelling approach (Chapter 5, Gastauer *et al.* (2017b).

As such, this thesis addresses some of the current key challenges in fisheries acoustic research, namely characterising the acoustic properties of some demersal fish species, using opportunistically collected acoustic data to derive species group specific biomass and abundance estimates and describing key characteristics of demersal fish schools, including habitats descriptors (Horne, 2000; Trenkel *et al.*, 2011; Barbeaux, 2012; Handegard *et al.*, 2013; Fässler *et al.*, 2016).

To the author's knowledge, this thesis represents the first attempt to describe a multispecies, tropical ecosystem using fisheries acoustics, solely based on data collected opportunistically aboard a fishing vessel during normal operation. Campanella et al. (2016)

presented one of the first attempts to describe a multispecies tropical environment using acoustic data in combination with an unsupervised clustering technique. The most significant difference between this study and that of Campanella et al. (2016) is the lack of dedicated alternative sampling and the data being collected aboard a commercially operating small fishing vessel without an underlying, designed survey. Campanella et al. (2016) were able to use optical techniques to gain further insights into the biological composition of the observed fish schools. Here, all data was collected during routine fishing operations, without additional directed sampling, which otherwise would have disrupted commercial fishing routines.

Fisheries acoustics have been identified as one of the most promising tools to satisfy information input into EBFM (Koslow, 2009; Trenkel *et al.*, 2011; Handegard *et al.*, 2013; Godø *et al.*, 2014). Trenkel et al. (2011) proposed three quality categories for acoustic data; 1) poor, 2) moderate and 3) good, based on its value for EBFM. At the beginning of the present study, all data available from fishing vessels in the NDSF would clearly have qualified as poor, with uncalibrated backscatter and unknown targets. As described by Trenkel et al. (2011), the data was coming from an uncalibrated vessel of opportunity with no complimentary sampling (other than information on the total number of commercially important species retained by the fisher), no or very limited information on the scattering properties of the target or similar species was available. Benoit-Bird *et al.* (2003) estimated *TS* for several Lutjanids. Such a dataset makes a robust classification of targets impossible and the data becomes almost unusable for developing indicators for EBFM (Petitgas *et al.*, 2009; Trenkel *et al.*, 2011). Through the development of methods to accurately and effectively monitor the catch of the commercially operating vessel (FishVid, described in Chapter 3, Gastauer *et al.* (2017c)), species-specific length frequencies for each pulled trap could be obtained and used as complimentary data. *TS-L* relationships were developed through *in situ* (Chapter 3, Gastauer *et al.*, 2017c) and *ex situ* measurements (Chapter 2, Gastauer *et al.*, 2016) as well as through modelling approaches (Chapter 2 and 4, Gastauer *et al.*, 2016, 2017a). Finally, through the application of geostatistical simulations, catch and acoustic information could be linked, and using geostatistical methods, estimates of sampling variance could be included.

The development and application of all methods described within the present thesis allowed the data collection program within the NDSF to be qualified as at least fair and for the case of the two established indicator species, red emperor and goldband snapper (Newman and Dunk, 2002, 2003; Newman *et al.*, 2004), as good. Calibrated acoustic was used in the classification of targets through application of robust methods with error estimates and *TS*

models for the most prevalent species. This alowed for the conversion of backscatter into ecologically relevant units (e.g. biomass or abundance estimates) (Chapter 3 and 4, Gastauer *et al.*, 2017a, 2017c). While data of sufficient quality was only available for 2014, within three fishing regions, a step towards the establishment of standardised indices has been provided.

In addition to abundance and biomass estimates of the two main indicator species, estimates for seven other species groups, commonly observed in trap catches have been derived (Chapter 4, Gastauer *et al.*, 2017a). This fulfils another recommendation for the use of fisheries acoustics for EBFM, formulated by Trenkel et al. (2011), i.e. consideration for collocated individuals of non-target species. Additionally, following up on the last recommendation made by Trenkel et al. (2011), the development of new indicators and reference points, which could be tested against changes in the ecosystem (e.g. climate change and fishing pressure), was achieved. The indices included; the description of the seabed habitats and associated indicator species and the description and clustering of fish school characteristics (energetic, geometric and environmental) in key fishing regions (Chapter 5, Gastauer *et al.*, 2017b). Further, a description of methods to quantitatively extract information on zooplankton has been applied (Ballón *et al.*, 2011; Lezama-Ochoa *et al.*, 2014; Gastauer *et al.*, 2017a, 2017b).

6.1 Description of the acoustic scattering properties of key species within the NDSF

Two of the most common indicators for EBFM, derived from acoustic information are abundance and biomass (Petitgas *et al.*, 2009; Trenkel *et al.*, 2011). To translate acoustic densities into fish biomass or abundance, a thorough understanding of the acoustic scattering properties of the target species are essential (Demer and Conti, 2005; Simmonds and MacLennan, 2005; Scoulding *et al.*, 2016). *TS* of many commercially exploited pelagic fish species are available (e.g. Foote and Traynor, 1988; Kloser and Horne, 2003; Fässler, 2010). However, given the sparsity of acoustic studies focusing on tropical demersal fish, there is a lack of information on the *TS* of species targeted in this study.

The modelling or observational technique used to obtain information about *TS* can influence the resulting *TS-L* relationship (Foote and Traynor, 1988; Foote and Francis, 2002; Simmonds and MacLennan, 2005; Jech *et al.*, 2015). Small changes in *TS* can have a significant effect on derived abundance or biomass estimates (Foote, 1980; Everson *et al.*, 1990;

McClatchie *et al.*, 1996; Scoulding *et al.*, 2016). Generally, empirical *in situ* observations of *TS* should deliver the most appropriate results, given they attempt to represent the natural behaviour of fish in the wild (Simmonds and MacLennan, 2005). In the case of the NDSF, where most fish occur in mixed schools, close to the bottom, *in situ TS* measurements are impracticable for the majority of the encountered situations (Sawada *et al.*, 1993; Gauthier and Rose, 2001; Sawada, 2002; Conti *et al.*, 2005). In situations where no *in situ* measurements are possible, *ex situ* experiments under controlled conditions can be conducted (Simmonds and MacLennan, 2005) or a modelling approach can be applied. Different models have different constraints and strengths, and may deliver similar or significantly different results, depending on characteristics of the analysed species and model input parameters (Macaulay *et al.*, 2013; Jech *et al.*, 2015). A major benefit of a modelling approach is that they allow for precise estimates of the influence of factors, such as tilt angle on *TS*. Together, a combination of empirical measurements and modelling estimates deliver the most complete understanding of the scattering properties of the analysed species (Jech *et al.*, 2015).

The only species observed to form loosely aggregated, single-species schools in the NDSF was goldband snapper. Therefore, goldband snapper were the only species suitable for *in situ TS* measurements within the present data collection program. *In situ TS* measurements require the availability of acoustically resolvable single targets in combination with length measurements from the same population (MacLennan and Menz, 1996; Sawada, 2002; Simmonds and MacLennan, 2005). Small trap fishing vessels are not an ideal sampling platform when it comes to *in situ TS* measurements. Given the small size of the vessels, they are heavily influenced by prevailing weather conditions and catch does not directly target specific schools. The orientation of the fish has a major impact on *TS* (Ona, 1990, 1999, 2001; Simmonds and MacLennan, 2005). Lacking information on the wave induced movement of the vessel (pitch and roll) during the time of recording and given the stochastic variability of *TS*, no information on the influence of tilt angle on the observed *TS* could be derived here.

While catch information from traps cannot be directly linked to specific schools, generally at least ten traps are located densely together (one line). Given the relatively small overall area of each selected fishing ground (33, 129 and 211 nmi^2, respectively) generally a high density of catch information could be obtained. To gain improved insights into the variability of *TS* a novel technique (Gastauer *et al.*, 2017c, Chapter 3), based on methods described by MacLennan and Menz (1996), allowed for the estimation of the *TS-L* equation with variance estimates of the slope and intercept. Methods described in Gastauer *et al.*

(2017c) could be used in many number of environments and situations, where loosely aggregated, single-species schools are being observed and could therefore contribute to an improved understanding of the scattering properties of marine organisms.

For red emperor, *ex situ TS* experiments were conducted. The main benefits of *ex situ* experiments are the guaranteed target discrimination and the execution of measurements in a more controlled environment (McClatchie *et al.*, 1996; Simmonds and MacLennan, 2005; Henderson and Horne, 2007). The experimental setup is likely to limit the movement of the fish as a very limited range of tilt angles was observed (80°-100°). To improve estimates of uncertainty surrounding these measurements, a modelling approach was taken (Kloser and Horne, 2003; Demer, 2004; Fässler *et al.*, 2009).A KRM model with Bayesian parameter estimation was applied. KRM was assumed to be a suitable model, given its ability to deal with complex shapes (unlike DWBA) and has been shown to deliver comparable results to the more complex BEM (Foote and Francis, 2002; Jech *et al.*, 2015). Bayesian parameter estimation used the outcomes of the *ex situ* experiments to calibrate the model parameters. This facilitated an assessment of uncertainty of unknown parameters or parameters that were difficult to estimate. It is noted, that the selected method might have introduced a bias due to prior selection (McAllister and Kirkwood, 1998) and the small sampling number (three modelled and three measured fish). In general, the modelled and measured *TS* showed reasonable agreement. Modelled *TS* at 38 kHz were on average −0.2 dB (SD ± 0.3 dB) lower than those estimated by the *ex situ* experiments. For 120 kHz, the shape of the fitted *TS* model relationship was very similar for both modelled and *ex situ* estimates, but were in general estimated to be stronger (mean 3.4 dB, s.d. ± 0.02 dB). A possible explanation for the differences between modelled and measured values could be the spread of tilt angles. Nonetheless the applied methods should be able to deliver robust *TS* estimates, suitable for the estimation of red emperor biomass or abundance estimates, based on acoustic recordings.

As one of the original objectives was to produce biomass and abundance estimates for seven species groups other than the two indicator species, *TS* estimates for those groups needed to be established. Based on biological and morphological similarities of the groups saddletail, other Lutjanids and red emperor, the *TS* for red emperor was assumed to hold validity for all of these groups. *TS* was established for spangled emperor, as representative for the lethrinids group; for rankin cod, representative of the rankin cod and cod groups and for triggerfishes. *TS* was modelled using a KRM model. While the methods employed are generally accepted as being robust (Gauthier and Horne, 2004; Macaulay *et al.*, 2013), producing results

comparable to empirical measurements (Hazen and Horne, 2003; Henderson and Horne, 2007; Peña and Foote, 2008; Gastauer *et al.*, 2016) and other modelling techniques (Foote and Francis, 2002; Jech *et al.*, 2015), the low sampling number and the retrieval of the specimens from great depths (mostly >100 m) might have biased the results. This is especially true for *TS* estimates of rankin cod, known to regularly suffer from barotrauma (Rudershausen *et al.*, 2007; Sadovy de Mitcheson *et al.*, 2013) and estimates based on deflated swimbladders. This might introduce a bias in the derived biomass and abundance estimates, but nonetheless provide first insights into otherwise unknown scattering properties of these previously acoustically unsurveyed species.

In conclusion, robust *TS* estimates could be established for the two main indicator species, based on data collected during routine fishing operations or through a combination of experimental and modelling approaches. Further insights into the *TS* of other species caught during routine commercial operations were provided. It is recommended that for species other than the two indicator species *TS* estimates with a higher number of samples of good quality should be repeated and where possible, *ex situ* or *in situ* measurements should be taken to contribute to the robustness of the estimates.

6.2 Classification of fish schools in a multi-species environment

Automated classification of acoustic fish traces has been described as the holy grail of fisheries acoustics (Horne, 2000). Challenges associated with the classification of fish schools detected by acoustics, in a multi-species environment have been raised by previous studies (e.g. Massé *et al.* (1996); Petitgas and Levenez (1996); Petitgas *et al.* (2003); Fablet *et al.* (2009). Given the dominance of temperate, pelagic environments in fisheries acoustic studies, focus has historically been mostly directed towards the classification of different single-species schools (Demer *et al.*, 2009; De Robertis *et al.*, 2010; Ballón *et al.*, 2011) or schools composed of few species with distinct acoustic scattering properties (Korneliussen *et al.*, 2016).

For most applications in temperate waters with large single species schools, empirical classification methods work well. These empirical methods heavily rely on either or both: differences in frequency response of the present species (Fässler *et al.*, 2007; Korneliussen *et al.*, 2008, 2016; De Robertis *et al.*, 2010; Korneliussen, 2010) and the availability of adequate alternative evidence (McClatchie *et al.*, 2000; Fernandes *et al.*, 2016). While detection algorithms based on a multifrequency approach are very useful when it comes to

distinguishing between coarse groups, such as gas-bearing and non-gas bearing organisms (Korneliussen, 2010; Ballón *et al.*, 2011), their applicability for mixed species environments with species of similar morphological and physiological features is very limited (Simmonds and MacLennan, 2005; Campanella and Taylor, 2016). This capability could be improved using the increasingly common broadband systems, which provide increased data resolution in respect to frequency dependent backscattering properties of targets (Reeder *et al.*, 2004; Stanton *et al.*, 2010; Andersen *et al.*, 2013; Bassett *et al.*, 2016; Kloser *et al.*, 2016). In the present thesis a simple empirical approach, as described in detail by Ballón et al. (2011) and Lezama-Ochoa *et al.*, (2014) was used to automatically extract fish schools and zooplankton aggregations from the echograms. While the inclusion of information on zooplankton distribution and its influence on the distribution of fish schools in the NDSF was beyond the scope of the present thesis, this could be an interesting future study point, especially with regards to effects of climate change and the general productivity of the ecosystem (Ballón *et al.*, 2011).

In environments where various species occur, classification techniques using a combination of different descriptors to identify species can be beneficial (Haralabous and Georgakarakos, 1996; Massé *et al.*, 1996; Cabreira *et al.*, 2009; Fernandes, 2009). In multi-species environments, dominated by small, mixed schools, such as the NDSF, currently available school descriptors generally deliver low success rates when it comes to species identification (Petitgas *et al.*, 2003). When operating in such a mixed, complex environment, it is useful to look at the structure of the acoustic and biological information. Gerlotto *et al.* (1990) and Gerlotto (1993) postulated the theory of acoustic populations. The underlying hypothesis is that fish do not occupy space randomly, but rather do so with some consistency which may change over time (Scalabrin and Massé, 1993). Gerlotto (1993) recognised that the underlying schooling structure for tropical fish can be determined by numerous factors (e.g. upwellings, bottom types, trophic systems, water temperatures, salinities or productivity). Gerlotto (1993) suggested that such a community gathers in constant species proportions for the time of a single survey. The acoustic echoes received from such a population are sufficiently permanent and typical that their synthesis can represent the community and should be scattering sound in a particular way, and therefore can be termed acoustic population (Gerlotto, 1993).

Combining acoustic bottom descriptors with geostatistically derived acoustic density hotspots (Petitgas *et al.*, 2016) allowed for the detection of different habitats in the analysed Regions 1 and 2 and 3 (Chapter 5, Gastauer *et al.* (2017b)). For all three habitat description

clusters, indicator species could be detected. Goldband snapper, was strongly associated with the first habitat cluster which was mainly characterised by greater depths. The chance of encountering goldband snapper within habitat Cluster 1, which covered the entire Region 1, was estimated to be 70%. The second habitat cluster, identified in approximately half the area of Region 2 and clearly dominating Region 3, was of a more mixed nature with respect to the indicator species. No highly significant indicator species could be detected within this region, but Lutjanids, Lethrinids and Cod remained indicators with a detection probability of approximately 50%. In habitat Cluster 3, mainly present in Region 2, the detection probability of Triggerfish was estimated to be approximately 50%. The extraction of indicator species in relation to selected habitats is relatively easy and could help to identify fluctuations in species distribution patterns. More detailed habitat information would increase the power of these indices.

Fish schools seemed to be more concentrated in more rugged environments, likely to represent coral reef patches (Luckhurst and Luckhurst, 1978, 1978; Friedlander and Parrish, 1998; Walker *et al.*, 2009). The classification of fish schools using an unsupervised clustering technique, using energetic, geometric and bathymetric input features of each detected fish school, facilitated the detection of clusters, driven predominantly by energetic features. Application of the Clest algorithm to determine the ideal number of clusters indicated high stability of the clustering results, which is indicative of the presence of clear patterns, potentially driven by biological patterns (Kondo *et al.*, 2012; Campanella and Taylor, 2016). Even though no clear relationship between species composition and acoustic school cluster could be detected, it could still be shown that there is some form of structural information contained with the acoustic reflection (Gerlotto, 1993; Scalabrin and Massé, 1993; Campanella and Taylor, 2016).

In cases where school descriptors can't be used to identify species to a satisfactory level, species proportions are generally attributed, according to alternative biological evidence (McClatchie *et al.*, 2000; Simmonds and MacLennan, 2005; Fernandes, 2009). In the case of the NDSF, this is not directly practical, given the temporal and spatial lag between the acoustic observations and the catch information, in combination with high variability of the catch composition. A direct link between the catch and the acoustically observed schools is not viable. While information extracted by traps might not represent individual schools very well, trap catch has been reported to be representative of species richness and composition in the NDSF (Newman *et al.*, 2004). Based on the theory of acoustic populations, Petitgas *et al.*

(2003) noted that in the situation where the observed schools are small and mixed in nature, it is not feasible to link catch to individual fish schools, but can be assumed to be representative for a distance range of several nautical miles (Massé *et al.*, 1996; Petitgas and Levenez, 1996; Petitgas *et al.*, 2003). This leads to the assumption that catch information used to derive species composition proportions for schools encountered in the surrounding area is valid. In the present study, geostatistical methods have been applied to facilitate the segregation of species groups within acoustic marks, based on catch proportions. One of the main benefits of such an approach is the possibility of including detailed variability estimates (Maravelias *et al.*, 1996; Woillez *et al.*, 2009, 2016; Scoulding *et al.*, 2016; Gastauer *et al.*, 2017c, 2017a). In Chapter 3, species allocation was based on kriged maps of catch proportions (Gastauer *et al.*, 2017c), weighted by fish weight derived from the measured length distributions, with the goal to derive goldband snapper abundance and biomass estimates with associated measurement and sampling error. In Chapter 4, geostatistical conditional simulations were used to produce 250 conditional representations of the acoustic information and 250 conditional representations of the catch proportions, based on which, combined species-group specific acoustic density estimates could be derived (Gastauer *et al.*, 2017a). The presented methods to derive biomass and precision estimates from acoustic data in combination with catch information could be applied to a variety of environments. This is especially valuable for data deficient ecosystems, where no dedicated scientific surveys can be conducted and available data lack an underlying design, restricting the applicability of more traditional methodology.

6.3 The use of small commercial vessels to derive indicators for EBFM

The main motivation of fishers to participate in any data collection program is the hope of contributing and taking part in fisheries data collection and the monitoring process for stock assessment. Involvement of stakeholders in the stock assessment process has potential to have a positive impact on the outcome, acceptance and implementation of integrated EBFM (Grimble and Wellard, 1997; Smith *et al.*, 1999; Reed, 2008; Fässler *et al.*, 2016). One possibility to include fishers in the process is through the collection of acoustic information, with the goal to derive indices which could be included in stock assessment models. Different indices could be considered and have been presented in this thesis, including indices of species or group specific biomass and abundance, indicator species related to habitats, extension and location of density hotspots, or species group specific length frequency distributions in selected regions. A prerequisite to make these indices useful for stock assessment would be

coverage of the same fishing regions over multiple seasons, allowing estimates of stability to be derived and to detect changes over time, through the generation of a time-series.

In recent years, several studies have analysed the scientific value of data collected aboard of commercial vessels. Major focus was given to large pelagic fishing vessels, which are similar to fisheries research vessels routinely used during AT surveys (Ressler *et al.*, 2009; Barbeaux, 2012; Fässler *et al.*, 2016; Melvin *et al.*, 2016). The present study is among the first to use a small commercial fishing vessel to opportunistically collect acoustic data in combination with detailed catch information, aiming at characterising the distribution and abundance of demersal species groups in key fishing regions.

A major difference between AT surveys and commercially operating fishing vessels is the underlying survey design (Simmonds and MacLennan, 2005; ICES, 2007; Barbeaux, 2012; Fässler *et al.*, 2016). Where AT surveys try to systematically cover the entire stock or population, fishing vessels direct their activities to find core aggregations or productive fishing grounds. This type of sampling 'design' has implications for data analysis. Data with selective sampling, is susceptible to spatial autocorrelation and incorporates the risk of double counting, especially if migrating species are observed, as is the case for many pelagic stocks (Fässler *et al.*, 2016). The risk of double counting in this study was assumed to be relatively low, given that mainly small, mixed schools were observed, and that they are not reported as migratory over the time of data collection. The data collection design of a trap fishing vessel during normal operation differs from that of pelagic fishing vessels. Pelagic fishing vessels generally try to find large aggregations and might decide to cover and target the school on multiple occasions (Fässler *et al.*, 2016). In the case of trap fishing vessels in the NDSF, fishers seek specific types of habitat, based on the hardness and roughness of the seabed and the availability of fish schools observed on the echogram, or a priori knowledge of site location by the fisher. Whether the fisher decides to target their efforts based on availability of schools or the availability of a suitable seabed, is sometimes in itself a stochastic relationship. Once a good location has been found, traps will be put into the water.

Geostatistics have been proposed to be the most suitable tool to analyse acoustic data from commercial fishing vessels, given their ability to account for spatial autocorrelation, not being reliable on the presence of an underlying regular grid (Rivoirard *et al.*, 2000; Barbeaux, 2012; Fässler *et al.*, 2016). A major benefit of the application of variogram analysis with kriging or geostatistical conditional simulations is the possibility to extract precision estimates (i.e.

sampling variance) (Rivoirard *et al.*, 2000; Gimona, 2003; Woillez *et al.*, 2009, 2016). Geostatistical methods have been successfully applied to the acoustic data in combination with catch information, allowing the extraction of estimates of abundance and biomass with estimates of variability within the selected three fishing regions. Abundance and biomass indices for the two indicator species as well as for seven other species groups were produced with varying degrees of sampling uncertainty. Total variance of the density, abundance and biomass estimates based on GCS were comparable (9.0 − 38.0%) to those reported for scientific surveys (e.g. 3.0 − 48%, Woillez *et al.* (2016)). A more detailed total CV was computed for goldband snapper, including CV for random error of acoustic data (13.8-22.7%), sampling variance (10.2 − 20.9%), signal to noise (0 − 0.1 %), *TS* variability due to fluctuations in the environmental conditions (0.5 - 1.15%), length estimates (1.2 − 2.0%) and catch proportions (2.5 − 3.7%), resulting in a total CV of 28.2 − 50.6%. The dominant contributor to the total CV was the random error contained within the zero-inflated acoustic data and the sampling variance due to the underlying survey design.

6.4 Outlook and conclusion

It has been shown that useful information can be extracted from opportunistically collected fisheries data. Such information would benefit largely from longer term data collection programs and the availability of data from multiple vessels, allowing for larger scale coverage, both on a temporal and spatial level. Collection of multiannual data of sufficient quality is needed to validate the true value of the data and to check its potential to track changes in the ecosystem. If multiannual data, collected at comparable locations in space and time become available, the described indices could be potentially used as calibration indices or as additional input variables in stock assessment models.

If data collection is to be continued, it is recommended that sounder settings are revised with the fisher and that calibration of the acoustic equipment is conducted on a regular basis. Indices developed here could be used to produce information on a regular basis if applied to data collected on a continual basis. Further, resulting indices could be used as additional information to improve the timing and survey design or strategies of dedicated scientific surveys currently executed.

Participation in various sea going commercial fishing trips strengthens the collaboration and mutual understanding between the fisher and scientists, as has been exemplified in this

thesis. Discussions about the fish resource and echograms provided novel insights to both, scientists and fishers aboard the vessel. If more data is to be collected, continuous communication and dialogue between fishers and scientists has to be maintained. For the involvement of stakeholders in data collection programs, it is crucial that all parties involved work on improved mutual understanding and meet each other with the needed respect. Improved dialogue between fishers and scientists in combination with shared data collection programs could greatly contribute to our understanding of the distribution and abundance of targeted and non-targeted marine organisms. Keeping in mind and improving the current performance on the above recommendations would help not only to further ameliorate our current understanding marine resources, but also work towards improved resource management, sustainable on a socio-economic and ecological level.

6.5 References

Andersen, L. N., Ona, E., and Macaulay, G. 2013. Measuring fish and zooplankton with a broadband split beam echo sounder. *In* OCEANS-Bergen, 2013 M*TS*/IEEE, pp. 1–4. IEEE. http://ieeexplore.ieee.org/abstract/document/6850133/ (Accessed 25 May 2017).

Ballón, M., Bertrand, A., Lebourges-Dhaussy, A., Gutiérrez, M., Ayón, P., Grados, D., and Gerlotto, F. 2011. Is there enough zooplankton to feed forage fish populations off Peru? An acoustic (positive) answer. Progress in Oceanography, 91: 360–381.

Barbeaux, S. J. 2012. Scientific acoustic data from commercial fishing vessels: Eastern Bering Sea walleye pollock (*Theragra chalcogramma*). University of Washington, United States -- Washington. 227 pp. http://search.proquest.com.dbgw.lis.curtin.edu.au/docview/1013759483/abstract/3E AE09E9E2FC462CPQ/1 (Accessed 6 September 2016).

Bassett, C., Weber, T. C., Wilson, C., and De Robertis, A. 2016. Potential for broadband acoustics to improve stock assessment surveys of midwater fishes. The Journal of the Acoustical Society of America, 140: 3242–3243.

Benoit-Bird, K. J., Au, W. W. L., and Kelley, C. D. 2003. Acoustic backscattering by Hawaiian lutjanid snappers. I. Target strength and swimbladder characteristics. The Journal of the Acoustical Society of America, 114: 2757–2766.

Cabreira, A. G., Tripode, M., and Madirolas, A. 2009. Artificial neural networks for fish-species identification. ICES Journal of Marine Science: Journal du Conseil, 66: 1119–1129.

Campanella, F., and Taylor, J. C. 2016. Investigating acoustic diversity of fish aggregations in coral reef ecosystems from multifrequency fishery sonar surveys. Fisheries Research, 181: 63–76.

Conti, S. G., Demer, D. A., Soule, M. A., and Conti, J. H. 2005. An improved multiple-frequency method for measuring in situ target strengths. ICES Journal of Marine Science: Journal du Conseil, 62: 1636–1646.

De Robertis, A., McKelvey, D. R., and Ressler, P. H. 2010. Development and application of an empirical multifrequency method for backscatter classification. Canadian Journal of Fisheries and Aquatic Sciences, 67: 1459–1474.

Demer, D. A. 2004. An estimate of error for the CCAMLR 2000 survey estimate of krill biomass. Deep Sea Research Part II: Topical Studies in Oceanography, 51: 1237–1251.

Demer, D. A., and Conti, S. G. 2005. New target-strength model indicates more krill in the Southern Ocean. ICES Journal of Marine Science: Journal du Conseil, 62: 25–32.

Demer, D. A., Cutter, G. R., Renfree, J. S., and Butler, J. L. 2009. A statistical-spectral method for echo classification. ICES Journal of Marine Science: Journal du Conseil, 66: 1081–1090.

Everson, I., Watkins, J. L., Bone, D. G., and Foote, K. G. 1990. Implications of a new acoustic target strength for abundance estimates of Antarctic krill. Nature, 345: 338–340.

Fablet, R., Lefort, R., Karoui, I., Berger, L., Massé, J., Scalabrin, C., and Boucher, J.-M. 2009. Classifying fish schools and estimating their species proportions in fishery-acoustic surveys. ICES Journal of Marine Science, 66: 1136–1142.

Fässler, S. M. 2010. Target strength variability in Atlantic herring (Clupea harengus) and its effect on acoustic abundance estimates. University of St Andrews. https://research-repository.st-andrews.ac.uk/handle/10023/1703 (Accessed 9 March 2017).

Fässler, S. M., Brunel, T., Gastauer, S., and Burggraaf, D. 2016. Acoustic data collected on pelagic fishing vessels throughout an annual cycle: Operational framework, interpretation of observations, and future perspectives. Fisheries Research, 178: 39–46.

Fässler, S. M. M., Santos, R., García-Núñez, N., and Fernandes, P. G. 2007. Multifrequency backscattering properties of Atlantic herring (Clupea harengus) and Norway pout (Trisopterus esmarkii). Canadian Journal of Fisheries and Aquatic Sciences, 64: 362–374.

Fässler, S. M. M., Brierley, A. S., and Fernandes, P. G. 2009. A Bayesian approach to estimating target strength. ICES Journal of Marine Science: Journal du Conseil. http://icesjms.oxfordjournals.org/content/early/2009/02/12/icesjms.fsp008 (Accessed 20 August 2015).

Fernandes, P. G. 2009. Classification trees for species identification of fish-school echotraces. ICES Journal of Marine Science: Journal du Conseil, 66: 1073–1080.

Fernandes, P. G., Copland, P., Garcia, R., Nicosevici, T., and Scoulding, B. 2016. Additional evidence for fisheries acoustics: small cameras and angling gear provide tilt angle distributions and other relevant data for mackerel surveys.

Foote, K. G. 1980. Averaging of fish target strength functions. The Journal of the Acoustical Society of America, 67: 504–515.

Foote, K. G., and Traynor, J. J. 1988. Comparison of walleye pollock target strength estimates determined from insitu measurements and calculations based on swimbladder form. The Journal of the Acoustical Society of America, 83: 9–17.

Foote, K. G., and Francis, D. T. 2002. Comparing Kirchhoff-approximation and boundary-element models for computing gadoid target strengths. The Journal of the Acoustical Society of America, 111: 1644–1654.

Friedlander, A. M., and Parrish, J. D. 1998. Habitat characteristics affecting fish assemblages on a Hawaiian coral reef. Journal of Experimental Marine Biology and Ecology, 224: 1–30.

Gastauer, S., Scoulding, B., Fässler, S. M., Benden, D. P., and Parsons, M. 2016. Target strength estimates of red emperor (Lutjanus sebae) with Bayesian parameter calibration. Aquatic Living Resources, 29: 301.

Gastauer, S., Scoulding, B., and Parsons, M. 2017a. Towards acoustic monitoring of a mixed demersal fishery based on commercial data: the case of the Northern Demersal Scalefish Fishery (Western Australia) - In Review Fisheries Research.

Gastauer, S., Scoulding, B., and Parsons, M. 2017b. An unsupervised acoustic description of fish schools and the seabed in three fishing regions within the Northern Demersal Scalefish Fishery (NDSF, Western Australia) - In Review Acosutic Australia.

Gastauer, S., Scoulding, B., and Parsons, M. 2017c. Estimates of variability of goldband snapper target strength and biomass in three fishing regions within the Northern Demersal Scalefish Fishery (Western Australia). Fisheries Research, 193: 250–262.

Gauthier, S., and Rose, G. A. 2001. Diagnostic tools for unbiased in situ target strength estimation. Canadian Journal of Fisheries and Aquatic Sciences, 58: 2149–2155.

Gauthier, S., and Horne, J. K. 2004. Acoustic characteristics of forage fish species in the Gulf of Alaska and Bering Sea based on Kirchhoff-approximation models. Canadian Journal of Fisheries and Aquatic Sciences, 61: 1839–1850.

Gerlotto, F., Marchal, E., and Réunion du Conseil International pour l'Exploitation de la Mer, Seattle (USA), 1987/06/22-26. 1990. The concept of acoustic populations : its use for analyzing the results of acoustic cruises. In <title>Collected reprints of the main contributed papers of EICHOANT program (Evaluation of Behaviour Influence on Fishery Biology and Acoustic Observations in Tropical Open Sea) presented during congresses from 1/1/87 to 4/30/90 = Compilation des principales communications du programme EICHOANT (Evaluation de l'Impact du Comportement en Halieutique et sur les Observations Acoustiques en Milieu Naturel Tropical) présentées à des congrès entre le 1/1/87 et le 30/4/90</title>. ORSTOM, Fort de France. http://www.documentation.ird.fr/hor/fdi:31201 (Accessed 25 May 2017).

Gerlotto, F. 1993. Identification and spatial stratification of tropical fish concentrations using acoustic populations. Aquatic Living Resources, 6: 243–254.

Gimona, A. 2003. A conditional simulation of acoustic survey data: advantages and potential pitfalls. Aquatic Living Resources, 16: 123–129.

Godø, O. R., Handegard, N. O., Browman, H. I., Macaulay, G. J., Kaartvedt, S., Giske, J., Ona, E., *et al.* 2014. Marine ecosystem acoustics (MEA): quantifying processes in the sea at the spatio-temporal scales on which they occur. ICES Journal of Marine Science: Journal du Conseil: fsu116.

Grimble, R., and Wellard, K. 1997. Stakeholder methodologies in natural resource management: a review of principles, contexts, experiences and opportunities. Agricultural systems, 55: 173–193.

Handegard, N. O., Buisson, L. du, Brehmer, P., Chalmers, S. J., Robertis, A., Huse, G., Kloser, R., *et al.* 2013. Towards an acoustic-based coupled observation and modelling system for monitoring and predicting ecosystem dynamics of the open ocean. Fish and Fisheries, 14: 605–615.

Haralabous, J., and Georgakarakos, S. 1996. Artificial neural networks as a tool for species identification of fish schools. ICES Journal of Marine Science: Journal du Conseil, 53: 173–180.

Hazen, E. L., and Horne, J. K. 2003. A method for evaluating the effects of biological factors on fish target strength. ICES Journal of Marine Science: Journal du Conseil, 60: 555–562.

Henderson, M. J., and Horne, J. K. 2007. Comparison of in situ, ex situ, and backscatter model estimates of Pacific hake (Merluccius productus) target strength. Canadian Journal of Fisheries and Aquatic Sciences, 64: 1781–1794.

Horne, J. K. 2000. Acoustic approaches to remote species identification: a review. Fisheries oceanography, 9: 356–371.

ICES. 2007. Collection of acoustic data from fishing vessels. ICES Cooperative Research Report No. 287. 83 pp. International Council for the Exploration of the Sea.

Jech, J. M., Horne, J. K., Chu, D., Demer, D. A., Francis, D. T., Gorska, N., Jones, B., *et al.* 2015. Comparisons among ten models of acoustic backscattering used in aquatic ecosystem research. The Journal of the Acoustical Society of America, 138: 3742–3764.

Kloser, R. J., and Horne, J. K. 2003. Characterizing uncertainty in target-strength measurements of a deepwater fish: orange roughy (Hoplostethus atlanticus). ICES Journal of Marine Science: Journal du Conseil, 60: 516–523.

Kloser, R. J., Ryan, T. E., Keith, G., and Gershwin, L. 2016. Deep-scattering layer, gas-bladder density, and size estimates using a two-frequency acoustic and optical probe. ICES Journal of Marine Science: Journal du Conseil, 73: 2037–2048.

Kondo, Y., Salibian-Barrera, M., and Zamar, R. 2012. A robust and sparse K-means clustering algorithm. arXiv preprint arXiv:1201.6082. http://arxiv.org/abs/1201.6082 (Accessed 16 August 2016).

Korneliussen, R. J., Diner, N., Ona, E., Berger, L., and Fernandes, P. G. 2008. Proposals for the collection of multifrequency acoustic data. ICES Journal of Marine Science: Journal du Conseil, 65: 982–994.

Korneliussen, R. J. 2010. The acoustic identification of Atlantic mackerel. ICES Journal of Marine Science: Journal du Conseil, 67: 1749–1758.

Korneliussen, R. J., Heggelund, Y., Macaulay, G. J., Patel, D., Johnsen, E., and Eliassen, I. K. 2016. Acoustic identification of marine species using a feature library. Methods in Oceanography, 17: 187–205.

Koslow, J. A. 2009. The role of acoustics in ecosystem-based fishery management. ICES Journal of Marine Science: Journal du Conseil: fsp082.

Lezama-Ochoa, A., Irigoien, X., Chaigneau, A., Quiroz, Z., Lebourges-Dhaussy, A., and Bertrand, A. 2014. Acoustics Reveals the Presence of a Macrozooplankton Biocline in the Bay of

Biscay in Response to Hydrological Conditions and Predator-Prey Relationships. PLoS ONE, 9: e88054.

Luckhurst, B. E., and Luckhurst, K. 1978. Analysis of the influence of substrate variables on coral reef fish communities. Marine Biology, 49: 317–323.

Macaulay, G. J., Peña, H., Fässler, S. M. M., Pedersen, G., and Ona, E. 2013. Accuracy of the Kirchhoff-Approximation and Kirchhoff-Ray-Mode Fish Swimbladder Acoustic Scattering Models. PLoS ONE, 8: e64055.

MacLennan, D. N., and Menz, A. 1996. Interpretation of in situ target-strength data. ICES Journal of Marine Science: Journal du Conseil, 53: 233–236.

Maravelias, C. D., Reid, D. G., Simmonds, E. J., and Haralabous, J. 1996. Spatial analysis and mapping of acoustic survey data in the presence of high local variability: geostatistical application to North Sea herring (Clupea harengus). Canadian Journal of Fisheries and Aquatic Sciences, 53: 1497–1505.

Massé, J., Koutsikopoulos, C., and Patty, W. 1996. The structure and spatial distribution of pelagic fish schools in multispecies clusters: an acoustic study. ICES Journal of Marine Science: Journal du Conseil, 53: 155–160.

McAllister, M. K., and Kirkwood, G. P. 1998. Bayesian stock assessment: a review and example application using the logistic model. ICES Journal of Marine Science: Journal du Conseil, 55: 1031–1060.

McClatchie, S., Alsop, J., and Coombs, R. F. 1996. A re-evaluation of relationships between fish size, acoustic frequency, and target strength. ICES Journal of Marine Science: Journal du Conseil, 53: 780–791.

McClatchie, S., Thorne, R. E., Grimes, P., and Hanchet, S. 2000. Ground truth and target identification for fisheries acoustics. Fisheries Research, 47: 173–191.

Melvin, G. D., Kloser, R., and Honkalehto, T. 2016. The adaptation of acoustic data from commercial fishing vessels in resource assessment and ecosystem monitoring. Fisheries Research, 178: 13–25.

Newman, S. J., and Dunk, I. J. 2002. Growth, Age Validation, Mortality, and other Population Characteristics of the Red Emperor Snapper, Lutjanus sebae (Cuvier, 1828), off the Kimberley Coast of North-Western Australia. Estuarine, Coastal and Shelf Science, 55: 67–80.

Newman, S. J., and Dunk, I. J. 2003. Age validation, growth, mortality, and additional population parameters of the goldband snapper (Pristipomoides multidens) off the Kimberley coast of northwestern Australia. Fishery Bulletin, 101: 116–128.

Newman, S. J., Young, G. C., and Potter, I. C. 2004. Characterisation of the inshore fish assemblages of the Pilbara and Kimberley coasts. http://researchrepository.murdoch.edu.au/19820/ (Accessed 6 September 2016).

Ona, E. 1990. Physiological factors causing natural variations in acoustic target strength of fish. Journal of the Marine Biological Association of the United Kingdom, 70: 107–127.

Ona, E. 1999. Methodology for target strength measurements. ICES Cooperative research report, 235: 59.

Ona, E. 2001. Herring tilt angles, measured through target tracking. http://brage.bibsys.no/xmlui/handle/11250/108201 (Accessed 9 August 2016).

Peña, H., and Foote, K. G. 2008. Modelling the target strength of Trachurus symmetricus murphyi based on high-resolution swimbladder morphometry using an MRI scanner. ICES Journal of Marine Science: Journal du Conseil, 65: 1751–1761.

Petitgas, P., and Levenez, J. J. 1996. Spatial organization of pelagic fish: echogram structure, spatio-temporal condition, and biomass in Senegalese waters. ICES Journal of Marine Science: Journal du Conseil, 53: 147–153.

Petitgas, P., Massé, J., Beillois, P., Lebarbier, E., and Cann, A. L. 2003. Sampling variance of species identification in fisheries acoustic surveys based on automated procedures

associating acoustic images and trawl hauls. ICES Journal of Marine Science: Journal du Conseil, 60: 437–445.

Petitgas, P., Cotter, J., Trenkel, V., and Mesnil, B. 2009. Fish stock assessments using surveys and indicators. Aquatic Living Resources, 22: 119–1.

Petitgas, P., Woillez, M., Doray, M., and Rivoirard, J. 2016. A Geostatistical Definition of Hotspots for Fish Spatial Distributions. Mathematical Geosciences, 48: 65–77.

Reed, M. S. 2008. Stakeholder participation for environmental management: a literature review. Biological conservation, 141: 2417–2431.

Reeder, D. B., Jech, J. M., and Stanton, T. K. 2004. Broadband acoustic backscatter and high-resolution morphology of fish: Measurement and modeling. The Journal of the Acoustical Society of America, 116: 747–761.

Ressler, P. H., Fleischer, G. W., Wespestad, V. G., and Harms, J. 2009. Developing acommercial-vessel-based stock assessment survey methodology formonitoring the US west coast widow rockfish (Sebastes entomelas) stock, 99: 63–73.

Rivoirard, J., Simmonds, J., Foote, K. G., Fernandes, P., and Bez, N. 2000. Geostatistics for Estimating Fish Abundance. Blackwell Science Ltd, Oxford. 216 pp.

Rudershausen, P. J., Buckel, J. A., and Williams, E. H. 2007. Discard composition and release fate in the snapper and grouper commercial hook-and-line fishery in North Carolina, USA. Fisheries Management and Ecology, 14: 103–113.

Sadovy de Mitcheson, Y., Craig, M. T., Bertoncini, A. A., Carpenter, K. E., Cheung, W. W. L., Choat, J. H., Cornish, A. S., et al. 2013. Fishing groupers towards extinction: a global assessment of threats and extinction risks in a billion dollar fishery. Fish and Fisheries, 14: 119–136.

Sawada, K., Furusawa, M., and Williamson, N. J. 1993. Conditions for the precise measurement of fish target strength <I>in situ</I>. The Journal of the Marine Acoustics Society of Japan, 20: 73–79.

Sawada, K. 2002. Study on the precise estimation of the target strength of fish. Bulletin of Fisheries Research Agency (Japan). http://agris.fao.org/agris-search/search.do?recordID=JP2002005603 (Accessed 18 May 2017).

Scalabrin, C., and Massé, J. 1993. Acoustic detection of the spatial and temporal distribution of fish shoals in the Bay of Biscay. Aquatic Living Resources, 6: 269–283.

Scoulding, B., Gastauer, S., MacLennan, D. N., Fässler, S. M. M., Copland, P., and Fernandes, P. G. 2016. Effects of variable mean target strength on estimates of abundance: the case of Atlantic mackerel (Scomber scombrus).

Simmonds, J., and MacLennan, D. N. 2005. Fisheries acoustics: theory and practice. John Wiley & Sons. https://books.google.nl/books?hl=en&lr=&id=ktUOvnfzB-QC&oi=fnd&pg=PR5&dq=simmonds+and+maclennan+2005+fisheries+acoustics&ots=KhFAju0IKm&sig=AqqX84hCs6CvysUa4fnhtcEgrc0 (Accessed 9 March 2017).

Smith, A. D. M., Sainsbury, K. J., and Stevens, R. A. 1999. Implementing effective fisheries-management systems–management strategy evaluation and the Australian partnership approach. ICES Journal of Marine Science: Journal du Conseil, 56: 967–979.

Stanton, T. K., Chu, D., Jech, J. M., and Irish, J. D. 2010. New broadband methods for resonance classification and high-resolution imagery of fish with swimbladders using a modified commercial broadband echosounder. ICES Journal of Marine Science: Journal du Conseil, 67: 365–378.

Trenkel, V., Ressler, P. H., Jech, M., Giannoulaki, M., and Taylor, C. 2011. Underwater acoustics for ecosystem-based management: state of the science and proposals for ecosystem indicators. Marine Ecology-Progress Series, 442: 285–301.

Walker, B. K., Jordan, L. K. B., and Spieler, R. E. 2009. Relationship of Reef Fish Assemblages and Topographic Complexity on Southeastern Florida Coral Reef Habitats. Journal of Coastal Research: 39–48.

Woillez, M., Rivoirard, J., and Fernandes, P. G. 2009. Evaluating the uncertainty of abundance estimates from acoustic surveys using geostatistical simulations. ICES Journal of Marine Science: Journal du Conseil: fsp137.

Woillez, M., Walline, P. D., Ianelli, J. N., Dorn, M. W., Wilson, C. D., and Punt, A. E. 2016. Evaluating total uncertainty for biomass-and abundance-at-age estimates from eastern Bering Sea walleye pollock acoustic-trawl surveys. ICES Journal of Marine Science: Journal du Conseil, 73: 2208–2226.

Appendix I Licence agreements

Chapter 2: Gastauer, S., Scoulding, B., Fässler, S.M., Benden, D.P., Parsons, M., 2016. Target strength estimates of red emperor (Lutjanus sebae) with Bayesian parameter calibration. Aquat. Living Resour. 29, 301. doi: 10.1051/alr/2016024

Dear Sir,

In answer to your request, we are pleased to inform you that you are authorized to reproduce:

"Target strength estimates of red emperor (Lutjanus sebae) with Bayesian parameter calibration" published in Aquatic Living Resources, 29(3), 301 (2016).

We kindly ask you to provide the references of the source: title, year, issue and the URL address of the journal.

Kind regards,

Permission Dept

edp sciences

17, av. du Hoggar - BP 112 - 91944 Les Ulis Cdx A, France
Tél. : +33 (0) 1 69 18 75 75 – Fax : +33 (0)1 69 28 84 91   Suivez-nous sur Twitter :
@EDPSciences   www.edpsciences.org   La Boutique EDP Sciences

Chapter 3: Gastauer, S., Scoulding, B., Parsons, M., 2017. Estimates of variability of goldband snapper target strength and biomass in three fishing regions within the Northern Demersal Scalefish Fishery (Western Australia). Fisheries Research 193, 250–262. doi:10.1016/j.fishres.2017.05.001

Estimated size (number of pages)
200
Elsevier VAT number
GB 494 6272 12
Requestor Location
Centre for Marine Science and Technology, Curtin University
GPO Box U1987

Perth, Western Australia WA 6845
Australia
Attn: Centre for Marine Science and Technology, Curtin University
Total
0.00 USD
Terms and Conditions

INTRODUCTION

1. The publisher for this copyrighted material is Elsevier. By clicking "accept" in connection with completing this licensing transaction, you agree that the following terms and conditions apply to this transaction (along with the Billing and Payment terms and conditions established by Copyright Clearance Center, Inc. ("CCC"), at the time that you opened your Rightslink account and that are available at any time at http://myaccount.copyright.com).

GENERAL TERMS

2. Elsevier hereby grants you permission to reproduce the aforementioned material subject to the terms and conditions indicated.

3. Acknowledgement: If any part of the material to be used (for example, figures) has appeared in our publication with credit or acknowledgement to another source, permission must also be sought from that source. If such permission is not obtained then that material may not be included in your publication/copies. Suitable acknowledgement to the source must be made, either as a footnote or in a reference list at the end of your publication, as follows: "Reprinted from Publication title, Vol /edition number, Author(s), Title of article / title of chapter, Pages No., Copyright (Year), with permission from Elsevier [OR APPLICABLE SOCIETY COPYRIGHT OWNER]." Also Lancet special credit - "Reprinted from The Lancet, Vol. number, Author(s), Title of article, Pages No., Copyright (Year), with permission from Elsevier."

4. Reproduction of this material is confined to the purpose and/or media for which permission is hereby given.

5. Altering/Modifying Material: Not Permitted. However figures and illustrations may be altered/adapted minimally to serve your work. Any other abbreviations, additions, deletions and/or any other alterations shall be made only with prior written authorization of Elsevier Ltd. (Please contact Elsevier at permissions@elsevier.com). No modifications can be made to any Lancet figures/tables and they must be reproduced in full.

6. If the permission fee for the requested use of our material is waived in this instance, please be advised that your future requests for Elsevier materials may attract a fee.

7. Reservation of Rights: Publisher reserves all rights not specifically granted in the combination of (i) the license details provided by you and accepted in the course of this licensing transaction, (ii) these terms and conditions and (iii) CCC's Billing and Payment terms and conditions.

8. License Contingent Upon Payment: While you may exercise the rights licensed immediately upon issuance of the license at the end of the licensing process for the transaction, provided that you have disclosed complete and accurate details of your proposed use, no license is finally effective unless and until full payment is received from you (either by publisher or by CCC) as provided in CCC's Billing and Payment terms and conditions. If full payment is not received on a timely basis, then any license preliminarily granted shall be deemed automatically revoked and shall be void as if never granted. Further, in the event that you

breach any of these terms and conditions or any of CCC's Billing and Payment terms and conditions, the license is automatically revoked and shall be void as if never granted. Use of materials as described in a revoked license, as well as any use of the materials beyond the scope of an unrevoked license, may constitute copyright infringement and publisher reserves the right to take any and all action to protect its copyright in the materials.

9. Warranties: Publisher makes no representations or warranties with respect to the licensed material.

10. Indemnity: You hereby indemnify and agree to hold harmless publisher and CCC, and their respective officers, directors, employees and agents, from and against any and all claims arising out of your use of the licensed material other than as specifically authorized pursuant to this license.

11. No Transfer of License: This license is personal to you and may not be sublicensed, assigned, or transferred by you to any other person without publisher's written permission.

12. No Amendment Except in Writing: This license may not be amended except in a writing signed by both parties (or, in the case of publisher, by CCC on publisher's behalf).

13. Objection to Contrary Terms: Publisher hereby objects to any terms contained in any purchase order, acknowledgment, check endorsement or other writing prepared by you, which terms are inconsistent with these terms and conditions or CCC's Billing and Payment terms and conditions. These terms and conditions, together with CCC's Billing and Payment terms and conditions (which are incorporated herein), comprise the entire agreement between you and publisher (and CCC) concerning this licensing transaction. In the event of any conflict between your obligations established by these terms and conditions and those established by CCC's Billing and Payment terms and conditions, these terms and conditions shall control.

14. Revocation: Elsevier or Copyright Clearance Center may deny the permissions described in this License at their sole discretion, for any reason or no reason, with a full refund payable to you. Notice of such denial will be made using the contact information provided by you. Failure to receive such notice will not alter or invalidate the denial. In no event will Elsevier or Copyright Clearance Center be responsible or liable for any costs, expenses or damage incurred by you as a result of a denial of your permission request, other than a refund of the amount(s) paid by you to Elsevier and/or Copyright Clearance Center for denied permissions.

LIMITED LICENSE

The following terms and conditions apply only to specific license types:

15. **Translation**: This permission is granted for non-exclusive world **English** rights only unless your license was granted for translation rights. If you licensed translation rights you may only translate this content into the languages you requested. A professional translator must perform all translations and reproduce the content word for word preserving the integrity of the article.

16. **Posting licensed content on any Website**: The following terms and conditions apply as follows: Licensing material from an Elsevier journal: All content posted to the web site must maintain the copyright information line on the bottom of each image; A hyper-text must be included to the Homepage of the journal from which you are licensing at http://www.sciencedirect.com/science/journal/xxxxx or the Elsevier homepage for books at http://www.elsevier.com; Central Storage: This license does not include permission for a scanned version of the material to be stored in a central repository such as that provided by Heron/XanEdu.

Licensing material from an Elsevier book: A hyper-text link must be included to the Elsevier homepage at http://www.elsevier.com . All content posted to the web site must maintain the copyright information line on the bottom of each image.

Posting licensed content on Electronic reserve: In addition to the above the following clauses are applicable: The web site must be password-protected and made available only to bona fide

students registered on a relevant course. This permission is granted for 1 year only. You may obtain a new license for future website posting.

17. **For journal authors:** the following clauses are applicable in addition to the above:

Preprints:

A preprint is an author's own write-up of research results and analysis, it has not been peer-reviewed, nor has it had any other value added to it by a publisher (such as formatting, copyright, technical enhancement etc.).

Authors can share their preprints anywhere at any time. Preprints should not be added to or enhanced in any way in order to appear more like, or to substitute for, the final versions of articles however authors can update their preprints on arXiv or RePEc with their Accepted Author Manuscript (see below).

If accepted for publication, we encourage authors to link from the preprint to their formal publication via its DOI. Millions of researchers have access to the formal publications on ScienceDirect, and so links will help users to find, access, cite and use the best available version. Please note that Cell Press, The Lancet and some society-owned have different preprint policies. Information on these policies is available on the journal homepage.

Accepted Author Manuscripts: An accepted author manuscript is the manuscript of an article that has been accepted for publication and which typically includes author-incorporated changes suggested during submission, peer review and editor-author communications.

Authors can share their accepted author manuscript:

- immediately
    - via their non-commercial person homepage or blog
    - by updating a preprint in arXiv or RePEc with the accepted manuscript
    - via their research institute or institutional repository for internal institutional uses or as part of an invitation-only research collaboration work-group
    - directly by providing copies to their students or to research collaborators for their personal use
    - for private scholarly sharing as part of an invitation-only work group on commercial sites with which Elsevier has an agreement
- After the embargo period
    - via non-commercial hosting platforms such as their institutional repository
    - via commercial sites with which Elsevier has an agreement

In all cases accepted manuscripts should:

- link to the formal publication via its DOI
- bear a CC-BY-NC-ND license - this is easy to do
- if aggregated with other manuscripts, for example in a repository or other site, be shared in alignment with our hosting policy not be added to or enhanced in any way to appear more like, or to substitute for, the published journal article.

Published journal article (JPA): A published journal article (PJA) is the definitive final record of published research that appears or will appear in the journal and embodies all value-adding publishing activities including peer review co-ordination, copy-editing, formatting, (if relevant) pagination and online enrichment.

Policies for sharing publishing journal articles differ for subscription and gold open access articles:

Subscription Articles: If you are an author, please share a link to your article rather than the full-text. Millions of researchers have access to the formal publications on ScienceDirect, and so links will help your users to find, access, cite, and use the best available version.

Theses and dissertations which contain embedded PJAs as part of the formal submission can be posted publicly by the awarding institution with DOI links back to the formal publications on ScienceDirect.

If you are affiliated with a library that subscribes to ScienceDirect you have additional private sharing rights for others' research accessed under that agreement. This includes use for classroom teaching and internal training at the institution (including use in course packs and courseware programs), and inclusion of the article for grant funding purposes.

Gold Open Access Articles: May be shared according to the author-selected end-user license and should contain a CrossMark logo, the end user license, and a DOI link to the formal publication on ScienceDirect.

Please refer to Elsevier's posting policy for further information.

18. **For book authors** the following clauses are applicable in addition to the above: Authors are permitted to place a brief summary of their work online only. You are not allowed to download and post the published electronic version of your chapter, nor may you scan the printed edition to create an electronic version. **Posting to a repository:** Authors are permitted to post a summary of their chapter only in their institution's repository.

19. **Thesis/Dissertation**: If your license is for use in a thesis/dissertation your thesis may be submitted to your institution in either print or electronic form. Should your thesis be published commercially, please reapply for permission. These requirements include permission for the Library and Archives of Canada to supply single copies, on demand, of the complete thesis and include permission for Proquest/UMI to supply single copies, on demand, of the complete thesis. Should your thesis be published commercially, please reapply for permission. Theses and dissertations which contain embedded PJAs as part of the formal submission can be posted publicly by the awarding institution with DOI links back to the formal publications on ScienceDirect.

Elsevier Open Access Terms and Conditions

You can publish open access with Elsevier in hundreds of open access journals or in nearly 2000 established subscription journals that support open access publishing. Permitted third party re-use of these open access articles is defined by the author's choice of Creative Commons user license. See our open access license policy for more information.

Terms & Conditions applicable to all Open Access articles published with Elsevier:

Any reuse of the article must not represent the author as endorsing the adaptation of the article nor should the article be modified in such a way as to damage the author's honour or reputation. If any changes have been made, such changes must be clearly indicated.

The author(s) must be appropriately credited and we ask that you include the end user license and a DOI link to the formal publication on ScienceDirect.

If any part of the material to be used (for example, figures) has appeared in our publication with credit or acknowledgement to another source it is the responsibility of the user to ensure their reuse complies with the terms and conditions determined by the rights holder.

Additional Terms & Conditions applicable to each Creative Commons user license:

CC BY: The CC-BY license allows users to copy, to create extracts, abstracts and new works from the Article, to alter and revise the Article and to make commercial use of the Article (including reuse and/or resale of the Article by commercial entities), provided the user gives appropriate credit (with a link to the formal publication through the relevant DOI), provides a link to the license, indicates if changes were made and the licensor is not represented as endorsing the use made of the work. The full details of the license are available at http://creativecommons.org/licenses/by/4.0.

CC BY NC SA: The CC BY-NC-SA license allows users to copy, to create extracts, abstracts and new works from the Article, to alter and revise the Article, provided this is not done for commercial purposes, and that the user gives appropriate credit (with a link to the formal publication through the relevant DOI), provides a link to the license, indicates if changes were made and the licensor is not represented as endorsing the use made of the work. Further, any new works must be made available on the same conditions. The full details of the license are available at http://creativecommons.org/licenses/by-nc-sa/4.0.

CC BY NC ND: The CC BY-NC-ND license allows users to copy and distribute the Article, provided this is not done for commercial purposes and further does not permit distribution of the Article if it is changed or edited in any way, and provided the user gives appropriate credit (with a link to the formal publication through the relevant DOI), provides a link to the license, and that the licensor is not represented as endorsing the use made of the work. The full details of the license are available at http://creativecommons.org/licenses/by-nc-nd/4.0. Any commercial reuse of Open Access articles published with a CC BY NC SA or CC BY NC ND license requires permission from Elsevier and will be subject to a fee.

Commercial reuse includes:

- Associating advertising with the full text of the Article
- Charging fees for document delivery or access
- Article aggregation
- Systematic distribution via e-mail lists or share buttons

Posting or linking by commercial companies for use by customers of those companies.

20. **Other Conditions**:

v1.9
Questions? customercare@copyright.com or +1-855-239-3415 (toll free in the US) or +1-978-646-2777.

Chapter 4: Gastauer, S., Scoulding, B. and Parsons, M., 2017. Towards acoustic monitoring of a mixed demersal fishery based on commercial data: The case of the Northern Demersal Scalefish Fishery (Western Australia). Fisheries Research, 195, pp.91-104. Doi:10.1016/j.fishres.2017.07.008

ELSEVIER LICENSE
TERMS AND CONDITIONS
Nov 08, 2017

This Agreement between Centre for Marine Science and Technology, Curtin University -- Sven Gastauer ("You") and Elsevier ("Elsevier") consists of your license details and the terms and conditions provided by Elsevier and Copyright Clearance Center.

License Number
4202850093533
License date
Oct 05, 2017
Licensed Content Publisher
Elsevier
Licensed Content Publication
Fisheries Research
Licensed Content Title
Towards acoustic monitoring of a mixed demersal fishery based on commercial data: The case of the Northern Demersal Scalefish Fishery (Western Australia)
Licensed Content Author
Sven Gastauer,Ben Scoulding,Miles Parsons
Licensed Content Date
Nov 1, 2017
Licensed Content Volume
195
Licensed Content Issue
n/a
Licensed Content Pages
14
Start Page
91
End Page
104
Type of Use
reuse in a thesis/dissertation
Intended publisher of new work
other
Portion
full article
Format
both print and electronic
Are you the author of this Elsevier article?
Yes
Will you be translating?
No
Title of your thesis/dissertation
An ecosystem approach, the acoustic assessment of the Northern Demersal Scalefish Fishery – Distribution, habitat and abundance
Expected completion date

Jun 2017
Estimated size (number of pages)
200
Requestor Location
Centre for Marine Science and Technology, Curtin University
GPO Box U1987

Perth, Western Australia WA 6845
Australia
Attn: Centre for Marine Science and Technology, Curtin University
Total
0.00 AUD
Terms and Conditions

<div align="center">

INTRODUCTION
</div>

1. The publisher for this copyrighted material is Elsevier. By clicking "accept" in connection with completing this licensing transaction, you agree that the following terms and conditions apply to this transaction (along with the Billing and Payment terms and conditions established by Copyright Clearance Center, Inc. ("CCC"), at the time that you opened your Rightslink account and that are available at any time at http://myaccount.copyright.com).

<div align="center">

GENERAL TERMS
</div>

2. Elsevier hereby grants you permission to reproduce the aforementioned material subject to the terms and conditions indicated.
3. Acknowledgement: If any part of the material to be used (for example, figures) has appeared in our publication with credit or acknowledgement to another source, permission must also be sought from that source. If such permission is not obtained then that material may not be included in your publication/copies. Suitable acknowledgement to the source must be made, either as a footnote or in a reference list at the end of your publication, as follows:
"Reprinted from Publication title, Vol /edition number, Author(s), Title of article / title of chapter, Pages No., Copyright (Year), with permission from Elsevier [OR APPLICABLE SOCIETY COPYRIGHT OWNER]." Also Lancet special credit - "Reprinted from The Lancet, Vol. number, Author(s), Title of article, Pages No., Copyright (Year), with permission from Elsevier."
4. Reproduction of this material is confined to the purpose and/or media for which permission is hereby given.
5. Altering/Modifying Material: Not Permitted. However figures and illustrations may be altered/adapted minimally to serve your work. Any other abbreviations, additions, deletions and/or any other alterations shall be made only with prior written authorization of Elsevier Ltd. (Please contact Elsevier at permissions@elsevier.com). No modifications can be made to any Lancet figures/tables and they must be reproduced in full.
6. If the permission fee for the requested use of our material is waived in this instance, please be advised that your future requests for Elsevier materials may attract a fee.
7. Reservation of Rights: Publisher reserves all rights not specifically granted in the combination of (i) the license details provided by you and accepted in the course of this licensing transaction, (ii) these terms and conditions and (iii) CCC's Billing and Payment terms and conditions.
8. License Contingent Upon Payment: While you may exercise the rights licensed immediately upon issuance of the license at the end of the licensing process for the transaction, provided that you have disclosed complete and accurate details of your proposed use, no license is finally effective unless and until full payment is received from you (either by publisher or by CCC) as provided in CCC's Billing and Payment terms and conditions. If full payment is not received on a timely basis, then any license preliminarily granted shall be deemed automatically revoked and shall be void as if

never granted. Further, in the event that you breach any of these terms and conditions or any of CCC's Billing and Payment terms and conditions, the license is automatically revoked and shall be void as if never granted. Use of materials as described in a revoked license, as well as any use of the materials beyond the scope of an unrevoked license, may constitute copyright infringement and publisher reserves the right to take any and all action to protect its copyright in the materials.

9. Warranties: Publisher makes no representations or warranties with respect to the licensed material.

10. Indemnity: You hereby indemnify and agree to hold harmless publisher and CCC, and their respective officers, directors, employees and agents, from and against any and all claims arising out of your use of the licensed material other than as specifically authorized pursuant to this license.

11. No Transfer of License: This license is personal to you and may not be sublicensed, assigned, or transferred by you to any other person without publisher's written permission.

12. No Amendment Except in Writing: This license may not be amended except in a writing signed by both parties (or, in the case of publisher, by CCC on publisher's behalf).

13. Objection to Contrary Terms: Publisher hereby objects to any terms contained in any purchase order, acknowledgment, check endorsement or other writing prepared by you, which terms are inconsistent with these terms and conditions or CCC's Billing and Payment terms and conditions. These terms and conditions, together with CCC's Billing and Payment terms and conditions (which are incorporated herein), comprise the entire agreement between you and publisher (and CCC) concerning this licensing transaction. In the event of any conflict between your obligations established by these terms and conditions and those established by CCC's Billing and Payment terms and conditions, these terms and conditions shall control.

14. Revocation: Elsevier or Copyright Clearance Center may deny the permissions described in this License at their sole discretion, for any reason or no reason, with a full refund payable to you. Notice of such denial will be made using the contact information provided by you. Failure to receive such notice will not alter or invalidate the denial. In no event will Elsevier or Copyright Clearance Center be responsible or liable for any costs, expenses or damage incurred by you as a result of a denial of your permission request, other than a refund of the amount(s) paid by you to Elsevier and/or Copyright Clearance Center for denied permissions.

LIMITED LICENSE

The following terms and conditions apply only to specific license types:

15. **Translation**: This permission is granted for non-exclusive world **English** rights only unless your license was granted for translation rights. If you licensed translation rights you may only translate this content into the languages you requested. A professional translator must perform all translations and reproduce the content word for word preserving the integrity of the article.

16. **Posting licensed content on any Website**: The following terms and conditions apply as follows: Licensing material from an Elsevier journal: All content posted to the web site must maintain the copyright information line on the bottom of each image; A hyper-text must be included to the Homepage of the journal from which you are licensing at http://www.sciencedirect.com/science/journal/xxxxx or the Elsevier homepage for books at http://www.elsevier.com; Central Storage: This license does not include permission for a scanned version of the material to be stored in a central repository such as that provided by Heron/XanEdu.

Licensing material from an Elsevier book: A hyper-text link must be included to the Elsevier homepage at http://www.elsevier.com . All content posted to the web site must maintain the copyright information line on the bottom of each image.

Posting licensed content on Electronic reserve: In addition to the above the following clauses are applicable: The web site must be password-protected and made available only to bona fide students registered on a relevant course. This permission is granted for 1 year only. You may obtain a new license for future website posting.

17. **For journal authors:** the following clauses are applicable in addition to the above:

Preprints:

A preprint is an author's own write-up of research results and analysis, it has not been peer-reviewed, nor has it had any other value added to it by a publisher (such as formatting, copyright, technical enhancement etc.).

Authors can share their preprints anywhere at any time. Preprints should not be added to or enhanced in any way in order to appear more like, or to substitute for, the final versions of articles however authors can update their preprints on arXiv or RePEc with their Accepted Author Manuscript (see below).

If accepted for publication, we encourage authors to link from the preprint to their formal publication via its DOI. Millions of researchers have access to the formal publications on ScienceDirect, and so links will help users to find, access, cite and use the best available version. Please note that Cell Press, The Lancet and some society-owned have different preprint policies. Information on these policies is available on the journal homepage.

Accepted Author Manuscripts: An accepted author manuscript is the manuscript of an article that has been accepted for publication and which typically includes author-incorporated changes suggested during submission, peer review and editor-author communications.

Authors can share their accepted author manuscript:

- immediately
    - via their non-commercial person homepage or blog
    - by updating a preprint in arXiv or RePEc with the accepted manuscript
    - via their research institute or institutional repository for internal institutional uses or as part of an invitation-only research collaboration work-group
    - directly by providing copies to their students or to research collaborators for their personal use
    - for private scholarly sharing as part of an invitation-only work group on commercial sites with which Elsevier has an agreement
- After the embargo period
    - via non-commercial hosting platforms such as their institutional repository
    - via commercial sites with which Elsevier has an agreement

In all cases accepted manuscripts should:

- link to the formal publication via its DOI
- bear a CC-BY-NC-ND license - this is easy to do
- if aggregated with other manuscripts, for example in a repository or other site, be shared in alignment with our hosting policy not be added to or enhanced in any way to appear more like, or to substitute for, the published journal article.

Published journal article (JPA): A published journal article (PJA) is the definitive final record of published research that appears or will appear in the journal and embodies all value-adding publishing activities including peer review co-ordination, copy-editing, formatting, (if relevant) pagination and online enrichment.

Policies for sharing publishing journal articles differ for subscription and gold open access articles:

<u>Subscription Articles:</u> If you are an author, please share a link to your article rather than the full-text. Millions of researchers have access to the formal publications on ScienceDirect, and so links will help your users to find, access, cite, and use the best available version.

Theses and dissertations which contain embedded PJAs as part of the formal submission can be posted publicly by the awarding institution with DOI links back to the formal publications on ScienceDirect.

If you are affiliated with a library that subscribes to ScienceDirect you have additional private sharing rights for others' research accessed under that agreement. This includes use for classroom teaching and internal training at the institution (including use in course packs and courseware programs), and inclusion of the article for grant funding purposes.

<u>Gold Open Access Articles:</u> May be shared according to the author-selected end-user license and should contain a CrossMark logo, the end user license, and a DOI link to the formal publication on ScienceDirect.

Please refer to Elsevier's posting policy for further information.

18. **For book authors** the following clauses are applicable in addition to the above: Authors are permitted to place a brief summary of their work online only. You are not allowed to download and post the published electronic version of your chapter, nor may you scan the printed edition to create an electronic version. **Posting to a repository:** Authors are permitted to post a summary of their chapter only in their institution's repository.

19. **Thesis/Dissertation**: If your license is for use in a thesis/dissertation your thesis may be submitted to your institution in either print or electronic form. Should your thesis be published commercially, please reapply for permission. These requirements include permission for the Library and Archives of Canada to supply single copies, on demand, of the complete thesis and include permission for Proquest/UMI to supply single copies, on demand, of the complete thesis. Should your thesis be published commercially, please reapply for permission. Theses and dissertations which contain embedded PJAs as part of the formal submission can be posted publicly by the awarding institution with DOI links back to the formal publications on ScienceDirect.

<u>Elsevier Open Access Terms and Conditions</u>

You can publish open access with Elsevier in hundreds of open access journals or in nearly 2000 established subscription journals that support open access publishing. Permitted third party re-use of these open access articles is defined by the author's choice of Creative Commons user license. See our open access license policy for more information.

Terms & Conditions applicable to all Open Access articles published with Elsevier:

Any reuse of the article must not represent the author as endorsing the adaptation of the article nor should the article be modified in such a way as to damage the author's honour or reputation. If any changes have been made, such changes must be clearly indicated.

The author(s) must be appropriately credited and we ask that you include the end user license and a DOI link to the formal publication on ScienceDirect.

If any part of the material to be used (for example, figures) has appeared in our publication with credit or acknowledgement to another source it is the responsibility of the user to ensure their reuse complies with the terms and conditions determined by the rights holder.

Additional Terms & Conditions applicable to each Creative Commons user license:

CC BY: The CC-BY license allows users to copy, to create extracts, abstracts and new works from the Article, to alter and revise the Article and to make commercial use of the Article (including reuse and/or resale of the Article by commercial entities), provided the user gives appropriate credit (with a link to the formal publication through the relevant DOI), provides a link to the license, indicates if changes were made and the licensor is not represented as endorsing the use made of the work. The full details of the license are available at http://creativecommons.org/licenses/by/4.0.

CC BY NC SA: The CC BY-NC-SA license allows users to copy, to create extracts, abstracts and new works from the Article, to alter and revise the Article, provided this is not done for commercial purposes, and that the user gives appropriate credit (with a link to the formal publication through the relevant DOI), provides a link to the license, indicates if changes were made and the licensor is not represented as endorsing the use made of the work. Further, any new works must be made available on the same conditions. The full details of the license are available at http://creativecommons.org/licenses/by-nc-sa/4.0.

CC BY NC ND: The CC BY-NC-ND license allows users to copy and distribute the Article, provided this is not done for commercial purposes and further does not permit distribution of the Article if it is changed or edited in any way, and provided the user gives appropriate credit (with a link to the formal publication through the relevant DOI), provides a link to the license, and that the licensor is not represented as endorsing the use made of the work. The full details of the license are available at http://creativecommons.org/licenses/by-nc-nd/4.0. Any commercial reuse of Open Access articles published with a CC BY NC SA or CC BY NC ND license requires permission from Elsevier and will be subject to a fee.

Commercial reuse includes:

- Associating advertising with the full text of the Article
- Charging fees for document delivery or access
- Article aggregation
- Systematic distribution via e-mail lists or share buttons

Posting or linking by commercial companies for use by customers of those companies.

20. **Other Conditions**:

v1.9

Questions? customercare@copyright.com or +1-855-239-3415 (toll free in the US) or +1-978-646-2777.

Chapter 5: Gastauer S, Scoulding B, Parsons M. An Unsupervised Acoustic Description of Fish Schools and the Seabed in Three Fishing Regions Within the Northern Demersal Scalefish Fishery (NDSF, Western Australia). Acoustics Australia. 2017:1-8. doi:10.1007/s40857-017-0100-0

Acoustics Australia
Order detail ID:70762515
Order License Id:4225010242430
ISSN:1839-2571
Publication Type:e-Journal
Volume:
Issue:
Start page:
Publisher: Australian Acoustical Society
Author/Editor: Australian Acoustical Society,

Permission Status: ✓ Granted

Permission type: Republish or display content
Type of use: Thesis/Dissertation
Hide details

○

Requestor type	Academic institution
Format	Print, Electronic
Portion	chapter/article
Number of pages in chapter/article	36
The requesting person/organization	Sven Gastauer
Title or numeric reference of the portion(s)	Chapter 5
Title of the article or chapter the portion is from	An Unsupervised Acoustic Description of Fish Schools and the Seabed in Three Fishing Regions Within the Northern Demersal Scalefish Fishery (NDSF, Western Australia)
Editor of portion(s)	N/A
Author of portion(s)	Sven Gastauer
Volume of serial or monograph	N/A
Page range of portion	120-155
Publication date of portion	17-08-2017
Rights for	Main product
Duration of use	Life of current edition
Creation of copies for the disabled	no
With minor editing privileges	yes
For distribution to	Worldwide
In the following language(s)	Original language of publication
With incidental promotional use	no
Lifetime unit quantity of new product	Up to 499
Title	An ecosystem approach, the acoustic assessment of the Northern Demersal Scalefish Fishery – Distribution, habitat and abundance
Instructor name	n/a
Institution name	n/a
Expected presentation date	Nov 2017

Note: This item will be invoiced or charged separately through CCC's **RightsLink** service. More info